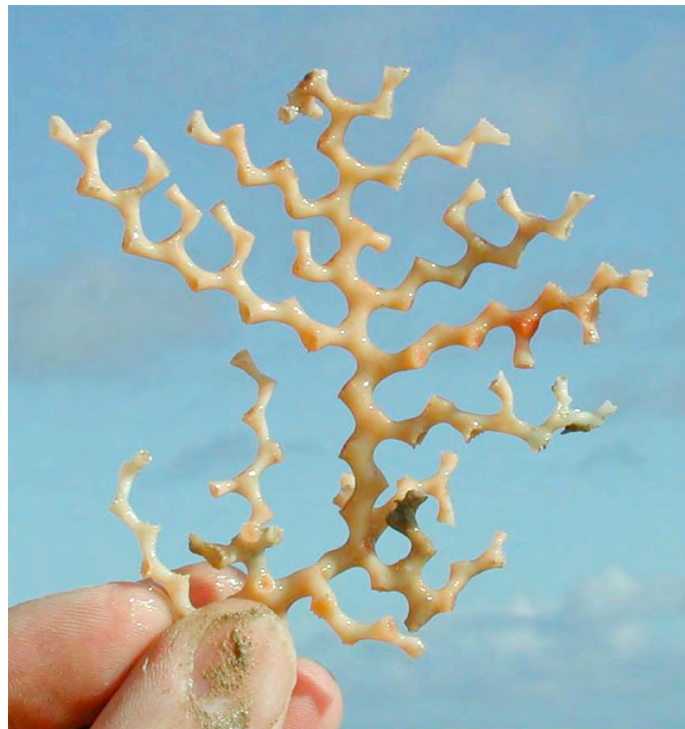


**ENVIRONMENTAL CONTROL ON GROWTH AND
DEVELOPMENT OF A DEEP-WATER CARBONATE MOUND
FROM THE PORCUPINE SEABIGHT**

UMWELTSTEUERENDE PROZESSE DES WACHSTUMS UND DER ENTWICKLUNG EINES
KALTWASSER-KARBONAT-HÜGELS IN DER PORCUPINE SEABIGHT

Kumulative Dissertation

Zur Erlangung des Doktorgrades
der Mathematisch-Naturwissenschaftlichen Fakultät
der Christian-Albrechts-Universität
zu Kiel



vorgelegt von

Andres Rüggeberg
geboren in
Jugenheim an der Bergstrasse

Kiel, 2003

Front cover: Deep-water coral *Madrepora oculata*, retrieved from 700 m water depth of the northern Porcupine Seabight during RV POSEIDON cruise POS265 in September 2000 (Photo: André Freiwald).

Referent: Prof. Dr. Wolf-Christian Dullo
Korreferent: Prof. Dr. Priska Schäfer
Tag der Disputation: Mittwoch, 29.10.2003, 13:15 Uhr
Zum Druck genehmigt, Kiel den 12.11.2003

.....
Der Dekan: Prof. Dr. Wulf Depmeier

*“Overhead the albatross hangs motionless upon the air
And deep beneath the rolling waves
In labyrinths of coral caves
The echo of a distant time
Comes willowing across the sand
And everything is green and submarine...”*

Echoes by Pink Floyd, 1971

ABSTRACT

Over the past decade large carbonate mound structures, situated in several provinces along the European continental margin have been discovered in 600 to 1200 m water depths. These structures appear as single, conical or ridge-like features, which are often colonised by a deep-water coral ecosystem. Cold-water corals *Lophelia pertusa* and *Madrepora oculata* dominate the coral community. Associated sessile and vagile fauna, like sponges, soft corals, bivalves, gastropods, crinoids, brachiopods, and fish make these bioherms as diverse as their tropical counterparts.

The objective of this study is to reconstruct past environmental settings locked in the sediments of a carbonate mound in the northern Porcupine Seabight, west off Ireland. Detailed investigations were concentrated on seven 3.5 to 6 m long sediment cores, retrieved from Propeller Mound and its closer vicinity. This mound is a ~150 m high structure within the Hovland Mound province, a cluster of several sea-floor protruding carbonate mounds.

A first detailed analysis on benthic foraminiferal assemblages in the vicinity of a carbonate mound was performed on two sediment cores, one located on top of the mound and a second one from an off-mound position further north as control site.

The **off-mound** samples reveal two different assemblages: (1) an *Interglacial group* dominated by infaunal species reflecting present-day environmental and oceanographic conditions with high nutrient flux to the sea-floor and low sediment accumulation under a strong hydrodynamic regime, and (2) a *Glacial group*, dominated

by cassidulinid species, which describe an influence of polar conditions with low nutrient supply and cold intermediate waters.

A single species, *Elphidium excavatum*, dominates the lower core section and is described here as a species displaced from shallow shelf areas. This removal of sediments from the shelf is related to a first advance of the Irish Ice Sheet onto the Irish Mainland shelf, inducing high sedimentation rates of ~28 cm/kyr with a coeval sea-level drop of ~50 m during Late Marine Isotope Stage (MIS) 3.

Due to an incomplete stratigraphic record in the **on-mound** core, the same species of the off-mound assemblages have been grouped in on-mound samples. The results indicate a dominance of the *Interglacial group*, whereas the *Glacial group* is less abundant throughout the entire core. This pattern indicates the lack of glacial time intervals in the on-mound core, which is coherent with stable oxygen isotope data and U/Th dates on coral fragments, presenting only interglacial/-stadial values and ages.

A third assemblage is abundant in samples of the on-mound core showing elevated epibenthic species not occurring in off-mound samples or only to a minor degree. This *Mound group* shows a great affinity to strong currents, high nutrient availability and is supposed to indicate Mediterranean Outflow Water in the northern Porcupine Seabight, as well as a higher coral cover on Propeller Mound in an earlier interglacial period. A Late Pleistocene decline in mound growth for Propeller Mound is suggested by a decrease of the *Mound group* towards the Holocene, which might face its complete

burial in the future as this already happened to the buried mounds of the Magellan Mound province further north.

Detailed information on off-mound sediment structures and contents from visual core description and the interpretation of Computer Tomographic images were used to evaluate sedimentary processes in glacial and interglacial periods. The sediments portray the depositional history of the past ~31 kyr BP, mainly controlled by sea-level fluctuations and the climate regime with the advance and retreat of the Irish Ice Sheet onto the Irish Mainland Shelf.

A first advance of glaciers is indicated by a turbiditic release slightly older than 31 kyr BP, coherent with Heinrich event 3. During MIS 3 and MIS 2 shelf erosion prevailed with abundant gravity flows and turbidity currents. A change from glaciomarine to hemipelagic contourite sedimentation during the onset of the Holocene indicates the establishment of the strong, present-day hydrodynamic regime at intermediate depths.

A general decrease in sediment accumulation with decreasing distance towards Propeller Mound was discovered throughout the entire core sections. This suggests that currents (turbidity currents, gravity flows, bottom currents) have had a strong impact on sediment accumulation at the mound base for the past ~31 kyr BP.

Finally, the reconstructed environmental setting deduced from sedimentary and micropaleontological analyses portrays the boundary conditions of the habitable range for the cold-water coral *Lophelia pertusa*. The growth of this ecosystem occurs during interglacial and interstadial periods, whereas a glacial retreat of corals is documented in the absence of glacial sediments in the on-mound core. These conclusions are summarised in a model – the *Mound Factory* – which efficiently accounts for the mound development covering the period of the Northern Hemisphere Glaciation (past 3.1–2.5 Ma).

KURZFASSUNG

Im Laufe der letzten 10 Jahre wurden große Karbonathügel-Strukturen, sogenannte carbonate mounds, entdeckt, die sich in einer Wassertiefe von 600 bis 1200 m entlang des europäischen Kontinentalhanges erstrecken. Diese Karbonathügel treten als einzelne, teils konische, teils langgestreckte Gebilde auf, die zumeist von Kaltwasserkorallen besiedelt sind. Neben den beiden dominierenden Kaltwasserkorallen *Lophelia pertusa* und *Madrepora oculata* sind zudem zahlreiche sessile und vagile marine Organismen vertreten: Schwämme, Weichkorallen, Muscheln, Schnecken, Seelilien, Brachiopoden und Fische. Zusammen bilden sie eine Gemeinschaft, die eine ähnlich hohe Diversität aufweist wie die weitaus bekannteren tropischen Korallenriffe.

Die vorliegende Arbeit hat sich zum Ziel gesetzt, die vergangenen Umweltbedingungen der nördlichen Porcupine Seabight (westlich von Irland) anhand von Sedimentkernen zu rekonstruieren. Die Kerne wurden vom Propeller Mound gewonnen, der mit 150 m einen der größten und meistbeprobtesten Karbonathügel innerhalb der Hovland Mound Provinz im Norden der Porcupine Seabight darstellt.

Die Vergesellschaftung von benthischen Foraminiferen wurde an zwei Sedimentkernen untersucht: ein Kern vom Propeller Mound (on-mound) und ein zweiter, weiter nördlich gelegener Referenzkern (off-mound).

Die Untersuchungen des **off-mound** Kernes lassen zwei unterschiedliche Vergesellschaftungen erkennen: (1) eine interglaziale, von endobenthischen Foraminiferen dominierte Gruppe, die den heutigen

Umweltbedingungen (rezentes Strömungsmuster mit erhöhten Nährstofffluß zum Meeresboden, niedrige Sedimentakkumulation aufgrund starker Strömungen) angepaßt ist, und (2) eine glaziale, von cassidulinoiden dominierte Gruppe, die die Situation unter polaren Bedingungen (kalte Zwischenwassermasse und geringes Nährstoffangebot) widerspiegelt.

Desweiteren wurde im älteren Kernabschnitt des späten Marinen Isotopen Stadiums 3 (MIS 3, ~31000–24000 Jahre vor Heute; J.v.H.) die Art *Elphidium excavatum* identifiziert, die eine vom Schelf exportierte Flachwasserart darstellt. Diese weist auf eine erhöhte Schelferosion hin, zurückzuführen auf den Vorstoß der Irischen Eismasse auf den Schelf und einem kohärenten Meeresspiegelrückgang von ~50 m.

Aufgrund einer unvollständigen Stratigraphie in den **on-mound** Sedimenten, wurden die off-mound identifizierten Vergesellschaftungen auf den on-mound Kern übertragen. Diese Untersuchung zeigt eine Dominanz der *Interglazialen Gruppe* und weist auf das Fehlen von glazialen Intervallen im on-mound Kern hin. Diese Beobachtung wird von den stabilen Sauerstoffisotopen und den U/Th Datierungen unterstützt.

Desweiteren zeigt der on-mound Kern ein erhöhtes Auftreten von epibenthischen Arten, die in den off-mound Sedimenten einen höchstens sehr geringen Anteil ausmachen und deshalb zu der *Mound Gruppe* zusammengefasst wurden. Diese Gruppe ist abhängig von starken Strömungen und einem hohen Nährstoffangebot und zeigt möglicherweise das Auftreten von Mediterranem Ausstrom-

wasser an. Da die Arten dieser Gruppe an erhöhtes Substrat gebunden sind, das die Korallen ermöglichen, können sie als Indiz für eine höhere Korallenbedeckung während eines früheren Interglazials angesehen werden. Eine generelle Abnahme der *Mound Gruppe* zum Holozän weist auf einen möglichen Rückgang des Moundwachstums während des späten Quartärs hin.

Um die Sedimentationsprozesse innerhalb glazialer und interglazialer Abschnitte von off-mound Kernen zu untersuchen, wurden neben Kernbeschreibungen auch computer-tomographische Aufnahmen genutzt. Diese Sedimente zeigen die Sedimentationsgeschichte der vergangenen ~31000 Jahre, welche hauptsächlich durch Meeresspiegelschwankungen und den Vorstoß bzw. Rückzug des Irischen Eisschildes auf den Schelf kontrolliert wurde.

Einen Hinweis auf einen ersten Vorstoß der Gletscher gibt ein Turbiditereignis in zeitlicher Übereinstimmung mit dem Heinrich Ereignis 3 (>31000 J.v.H.). Anhaltende Dichte- und Turbiditströme führten zur Schelferosion während der MIS

3 und 2. Ein Wechsel von glazialer zu hemipelagischer Sedimentation zu Beginn des Holozän weist auf das Einsetzen des heutigen, starken Strömungsregimes in mittleren Tiefen hin.

Alle untersuchten off-mound Kerne zeigen zunehmende Sedimentationsraten mit größer werdender Distanz vom Propeller Mound und deuten auf einen erhöhten Einfluß der Strömung auf den Fuß des Propeller Mounds hin.

Abschliessend können mit Hilfe der Rekonstruktion von Umweltbedingungen Aussagen über die Verbreitung der Kaltwasserkoralle *Lophelia pertusa* gemacht werden. Während sich diese in interglazialen und interstadialen Phasen ausbreitete und somit zum Moundwachstum führte, läßt das Fehlen von glazialen Sedimenten in dem on-mound Kern auf den Rückzug ihrer Verbreitungsgrenze im Glazial schliessen. Diese Rückschlüsse sind in einem Modell – dem sogenannten *Mound Factory* – zusammengefasst, das wesentlich zum Verständnis der Moundentwicklung während der Nordhemisphären-Vereisung (3,1-2,5 Millionen Jahre) beiträgt.

ACKNOWLEDGEMENTS

First of all I would like to thank my supervisor Prof. Dr. Wolf-Christian Dullo for providing me with an excellent working place at GEOMAR and within the ECOMOUND project. He supported my research with the participation of several cruises, project meetings throughout Europe's nicest places, and gave me the opportunity to join scientific conferences to present my results. I appreciate his support and look forward to future collaboration.

I am also thankful to Prof. Dr. Priska Schäfer (Christian-Albrechts-University of Kiel) for co-correcting this thesis.

A close collaboration with my colleagues from University of Bremen led to intense discussions, especially regarding the difficult interpretation of on-mound stratigraphy. Therefore, I thank my PhD companion Boris Dorschel and his supervisor PD Dr. Dierk Hebbeln for the nice atmosphere during several visits with neverending discussions, posing new questions, which finally took a step forward to solve the *Mystery of Propeller Mound*. I am looking forward to future co-operation.

I am very grateful to all members of ECOMOUND, GEOMOUND and ACES projects for very nice meetings, presentations, discussions, and good collaboration. It was a pleasure participating this international cluster of projects during the past three years.

Participating scientific cruises was one "bonbon" of my research. Therefore, I would like to thank additionally to my supervisor: Prof. Dr. André Freiwald (University of Erlangen), Bjørn Lindberg (Univer-

sity of Tromsø) and the captains and crews of RV POSEIDON (cruise POS265 and 292) and RV JAN MAYEN (Nov. 2001).

The discussion and exchange of ideas with my colleagues of the Department of Paleoceanology and the Carbonate Sedimentology Group at GEOMAR are greatly acknowledged, especially PD Dr. John J. G. Reijmer, Dr. Sibylle Noe, Dr. Miriam Pfeiffer, Dr. Jens Zinke, Lars Reuning, Thorsten Bauch, and last, but not least, my room- and UT-mate Dr. Sven Roth.

All colleagues of GEOMAR are thanked for a good working environment. Special thanks go to Dr. Volker Liebetrau for performing U/Th dates on *Lophelia* corals and the discussions and interpretations together with Prof. Dr. Anton Eisenhauer. Anke Bleyer and Bettina Domeyer are thanked for analysing TOC and TCN on the sediments. M. Segl is acknowledged for the stable isotope analyses at the Isotope Lab Bremen University.

Prof. Dr. Piet Grootes (Christian-Albrechts-University of Kiel) is thanked for providing AMS ^{14}C dates of the sediments and fruitful discussions.

Prof. Dr. Heller and Dr. Morvain from the Department of Radiology, Universitätsklinikum Kiel, are greatly acknowledged for performing Computer Tomographic analyses on the sediment cores.

Prof. Dr. W. Kuhnt (Christian-Albrechts-University of Kiel) is thanked for providing the Lutze-collection of benthic foraminifera at the Institute of Micropalaeontology.

The administrative and technical staff of GEOMAR are thanked for their efficient project management, support with the laboratory work and good working atmosphere.

Jenny Lezius (University of Stuttgart) is thanked for the assistance in the laboratory.

For the improvement of my English, as well as comments and suggestions of earlier versions of this thesis, I would like to send my sincere thanks to Dr. Joachim Schönfeld (GEOMAR), Alexandra Jurkiw (University of Bremen), Dr. Stefan Rehm, Dr. Sven

Roth, PD Dr. John J. G. Reijmer, and Lars Reuning.

Finally, I am very grateful to my family for their support during my academic career. My warmest and sincere gratitude goes to Henrike Schünemann, for her love and support during the past years. I am looking forward to a long future co-operation (;-).

This study is part of the OMARC project ECOMOUND funded by EU during the course of 5th Framework Programme (Contract n°. EVK3-CT-1999-00013).

September 2003,

Andres

CONTENTS

Abstract/Kurzfassung	I
Acknowledgements	V

Chapter 1 Introduction

1.1 Aim of study and structure of thesis	1
1.2 General notes on <i>Lophelia pertusa</i> and its distribution in the NE Atlantic	2
1.2.1 <i>Lophelia pertusa</i> (Linné 1758)	2
1.2.2 Deep-water coral structures	5
1.2.3 Geological record of <i>Lophelia</i>	6
1.3 Study area: the Porcupine Seabight	6
1.3.1 Regional setting and geological history	6
1.3.2 Carbonate mound in the Porcupine Seabight	8
1.3.3 The Propeller Mound	10
1.4 Glacial setting of the Porcupine Seabight	12
1.4.1 Surface water, seasonal sea ice and intermediate glacial water mass distribution	12
1.4.2 British Irish Ice Sheet variability	14
1.5. Present-day oceanographic setting	15
1.5.1 Water mass distribution and general circulation	15
1.5.2 Slope current and current strength intensities	16
1.5.3 Primary productivity and downslope transport of organic matter	17

Chapter 2	Materials and Methods	
2.1	Sediment core analyses	19
2.1.1	Computer tomographic analysis	19
2.1.2	Opening procedure of cores	20
2.1.3	Visual core description	20
2.1.4	Colour determination	20
2.1.5	Sampling	21
2.2	Sample analyses	21
2.2.1	Micropaleontological analysis	21
2.2.2	Grain size analysis	21
2.2.3	Total carbon and organic carbon measurements	22
2.2.4	Stable isotope analysis	22
2.2.5	Radiocarbon measurements	23
2.2.6	U/Th dating on coral fragments	23
Chapter 3	Benthic foraminiferal assemblages from Propeller Mound, Northern Porcupine Seabight	27
Chapter 4	Sedimentary pattern during the last glacial/interglacial cycle around a carbonate mound in the Hovland Mound province, Porcupine Seabight	47
Chapter 5	Environmental changes and growth history of a cold-water carbonate mound (Propeller Mound, Porcupine Seabight)	69

Chapter 6	Conclusions and Perspectives	85
References		87
Appendix		
Appendix 1	Faunal reference list of identified benthic foraminifera	A 1
Appendix 2	Relative abundance of benthic foraminifera	A 9
Appendix 2.1	Off-mound core GeoB 6725-1	A 9
Appendix 2.2	On-mound core GeoB 6730-1	A 15
Appendix 3	Grain size data	A 19
Appendix 3.1	Sand, silt and clay content	A 19
Appendix 3.2	Silt fraction	A 21
Appendix 4	Total carbon and total organic carbon	A 39
Appendix 5	Stable isotope data	A 41
Appendix 6	Computer tomographic images	A 43
Appendix 7		
	B. Dorschel, D. Hebbeln, A. Rüggeberg, C. Dullo (subm. to <i>Modern Carbonate Mound Systems: A Window to Earth History</i>)	
	Carbonate budget of a cold-water coral carbonate mound: Propeller Mound, Porcupine Seabight	A 57
Appendix 8		
	B. Dorschel, D. Hebbeln, A. Rüggeberg, W.-Chr. Dullo, A. Freiwald (subm. to <i>Nature</i>)	
	Deglacial sweeping of a deep-water carbonate mound	A 73
Vita and Publication List		A 83

CHAPTER 1

INTRODUCTION

1.1 Aim of study and structure of thesis

Carbonate mounds situated along the European continental margin have been studied in detail during the past decade within several projects. This thesis originated from the OMARC project ECOMOUND funded by EU 5th Framework Programme during the years 2000–2003. The aim of this project was to investigate the external oceanographic control and forcing mechanisms on carbonate mound and carbonate build up formation. Target areas of ECOMOUND were the Porcupine Seabight (PSB) margins, along the Rockall Trough, and sites in the very north offshore Norway, where clusters of carbonate mounds occur, densely settled by cold-water coral ecosystem.

These deep-water coral reefs are dominated by scleractinian corals *Lophelia pertusa* and *Madrepora oculata*, and to a minor degree by *Desmophyllum cristagalli*. The research history of the dominating *L. pertusa* is subject of Chapter 1.2 including its geographical distribution along the European continental margin and the geological record of this coral.

Major research object of this thesis is the Propeller Mound, a carbonate mound in the Hovland mound province of the northern PSB (Chapter 1.3.3). A regional overview of the Sea Bight with a brief description of its evolution during Paleozoic and Cenozoic times is presented in Chapter 1.3.1.

The carbonate mounds are not randomly distributed but occur in high densities in

distinct provinces of the PSB. These mound provinces show similarities but also differences in size, morphology and the settlement of benthic species, which is given in a detailed summary of Chapter 1.3.2. Recent studies on *L. pertusa* indicate that the corals occur only during interglacial/-stadial times along the European continental margin (see Chapter 3). To determine limiting factors of coral and mound growth, it is necessary to obtain a detailed knowledge of the glacial setting and oceanography west off Ireland, which is exemplarily reviewed for the last glacial stage covering Marine Isotope Stages (MIS) 2 to 4 (Chapter 1.4). The present-day distribution of water masses, their hydrodynamic regime and the general environmental setting within the PSB are summarised in Chapter 1.5.

Several sediment cores have been retrieved from Propeller Mound and the surrounding area (Chapter 2.1). All analyses, summarised in Chapter 2.1 and 2.2, were used to differentiate between ‘on-mound’ cores (sediment cores containing coral fragments) and ‘off-mound’ cores (‘normal’ hemipelagic sediment cores).

The off-mound sediments provide information on environmental changes during the last glacial-interglacial cycle. These sediments have been compared to on-mound sediments from the top of Propeller Mound. Their differences are used to define controlling or limiting factors of mound growth and evolution of Propeller Mound for the past 200,000 years.

Chapter 3 presents a manuscript in which a detailed investigation on benthic fora-

miniferal assemblages from on- and off-mound cores characterises varieties of the two different settings. The study presents the first down core results of faunal analysis in the northern PSB.

Chapter 4 is dedicated to the sedimentary setting around the Propeller Mound indicating changing current strength intensities and the influence of the nearby British Irish Ice Sheet covering most of Ireland during peak glacial times. These studies have been reported from areas further south or north, but not within the PSB.

The combination of all results and their interpretation with respect to environmental changes in the course of glacial-interglacial times finally results into the growth history of Propeller Mound (Chapter 5). This manu-

script presents first insights of a detailed stratigraphic record of a carbonate mound and shows for the first time, how such a carbonate mound developed through time.

Chapter 6 summarises main conclusions in a model describing the growth and evolution of Propeller Mound and other mounds of the northern PSB. The development of Propeller Mound, which is entirely forced by environmental conditions for the investigated time scale, is compared with other carbonate mounds along the European continental margin.

Finally, this thesis focuses on objectives of ECOMOUND project and presents additional knowledge and understanding of carbonate mounds and their evolution through Late Pleistocene time.

1.2 General notes on *Lophelia pertusa* and its distribution in the NE Atlantic

1.2.1 *Lophelia pertusa* (Linné 1758)

L. pertusa is the most abundant deep-sea coral in the NE Atlantic. Carl von Linné already described this species in 1758 in the 10th edition of *Systema naturae –Tomus I: Regnum animale*. Early scientific publications of the 19th century reported on deep-water reef structures in Norwegian waters (e.g. Sars, 1865). These were subject of detailed investigation in the early 20th century. Numerous scientific publications describe both living and dead coral banks along the Norwegian coast (summarised in Dons, 1944), but also of coral patches along the western European continental margin (Joubin, 1922). Teichert (1958) presented detailed maps showing the distribution of living and sub-fossil coral banks along the Norwegian coast and of coral patches along

the slopes off France and Ireland (Fig. 1-1). He broadly summarised some environmental aspects on coral banks and patches like (1) the high benthic diversity at these sites, (2) the temperature as a limiting factor for coral distribution, and (3) special oceanographic conditions for the development of ahermatypic coral banks. But these interpretations remained sketchily.

Teichert (1958) also described first human impacts on deep-water coral banks as these occurrences have long been known to Norwegian and French fishermen, while fish are plentiful in the vicinity of these coral banks. The coral reefs, however, are also destructive to their fishing gear. Nowadays, the interpretation of the destructive behaviour of coral banks to fishing gear is nowadays better described reversed, as the deep-fishing trawlers actually damage the coral reefs ecosystem (Hall-Spencer et al., 2001). As these coral reef ecosystems are

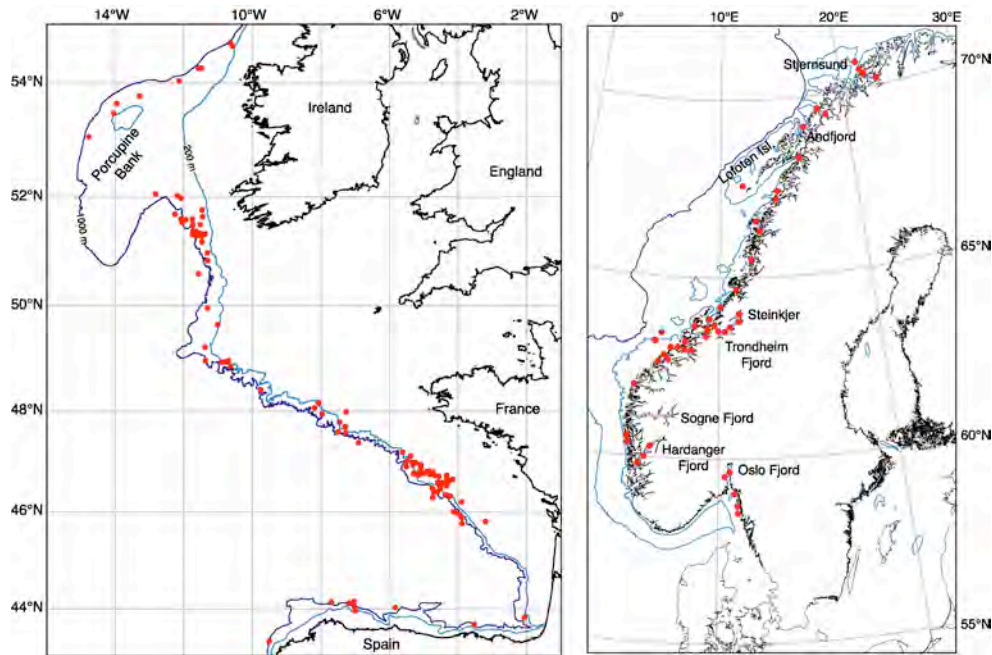


Figure 1-1. Distribution of deep-sea coral banks and patches along the European continental shelf as reported from early to middle 20th century (from Teichert, 1958).

known to be very important for fish recruitment and therefore necessary for fish populations to recover, a series of campaigns started in the past years to actively save these unique reef structures (e.g. OSPAR Commission, www.ospar.org).

The deep-sea coral *L. pertusa* belongs to the scleractinia (stone coral) and lacks photosymbionts in its endodermal tissue (azooxanthellate coral). A wide variety of different morphotypes of *L. pertusa* is reported (Freiwald, 1998). Intraspecific variations are described such as the branching pattern (zig zag; Fig. 1-2; or dendroid), the shape and thickness of corallites, and the soft tissue colouration (white, yellowish, orange-reddish to pink: Fig. 1-2). *Lophelia* species often occur together with *Madrepora oculata* and *Desmophyllum* species, but the latter is never found alone in a coral framework and is less abundant (Frederiksen et al., 1992; Rogers, 1999).

Azooxanthellate corals are globally found in a wide bathymetric range (0-6200 m), bathing in temperatures between 1° to

29°C (Stanley and Cairns, 1988). Only 25 % of azooxanthellate corals are colonial or pseudocolonial. Pseudocolonial corals produce their skeleton by clonal reproduction of polyps, which live as individuals without



Figure 1-2. Zig-zag branching *Lophelia pertusa* from (Photo: A. Freiwald)

any interconnected neural network (Freiwald, 1998). *L. pertusa* is one of the few pseudocolonial species able to create a rigid

framework (Fig. 1-3). It requires a hard substrate to settle on, normally in an environmental setting with low sediment deposition (Freiwald, 1998). These hard substrates can be of various origins: out

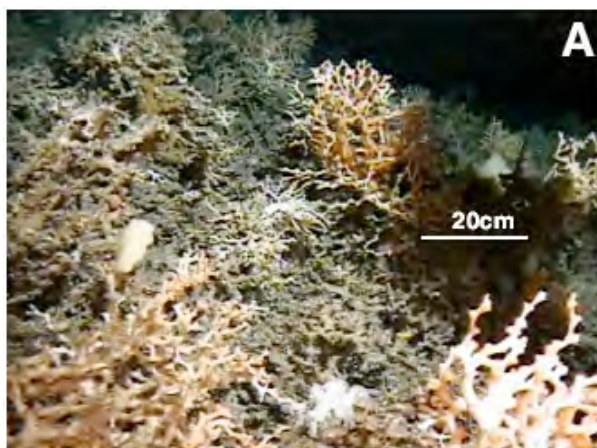


Figure 1-3. Underwater photo of life and dead corals from top of a carbonate mound, NW Porcupine Bank (Freiwald and Shipboard Party, 2002).

cropping rocks, moraine boulders, iceberg released dropstones, levees created by ploughing icebergs, biogenic hardgrounds or even artificial substrates (wrecks, fishing gear, cables, oil rigs). Compared to other deep-sea corals, *Lophelia* is reported in a smaller temperature range of 4° to 12°C and shallower waters of 250 m to 1200 m along the margin from Norway to Portugal (e.g. Freiwald, 2002). Until now, the full extent of geographic distribution of *L. pertusa* is unknown. About 95 % of *Lophelia*'s global documented occurrence appears in the N Atlantic region (Wheeler et al., subm.; Fig. 1-4). The remaining 5 % correspond to occurrences in the Caribbean, the S Atlantic, and the Indian and Pacific Oceans. However, this distribution mirrors the intense investigation by scientists, military and oil industry along the N Atlantic shelves.

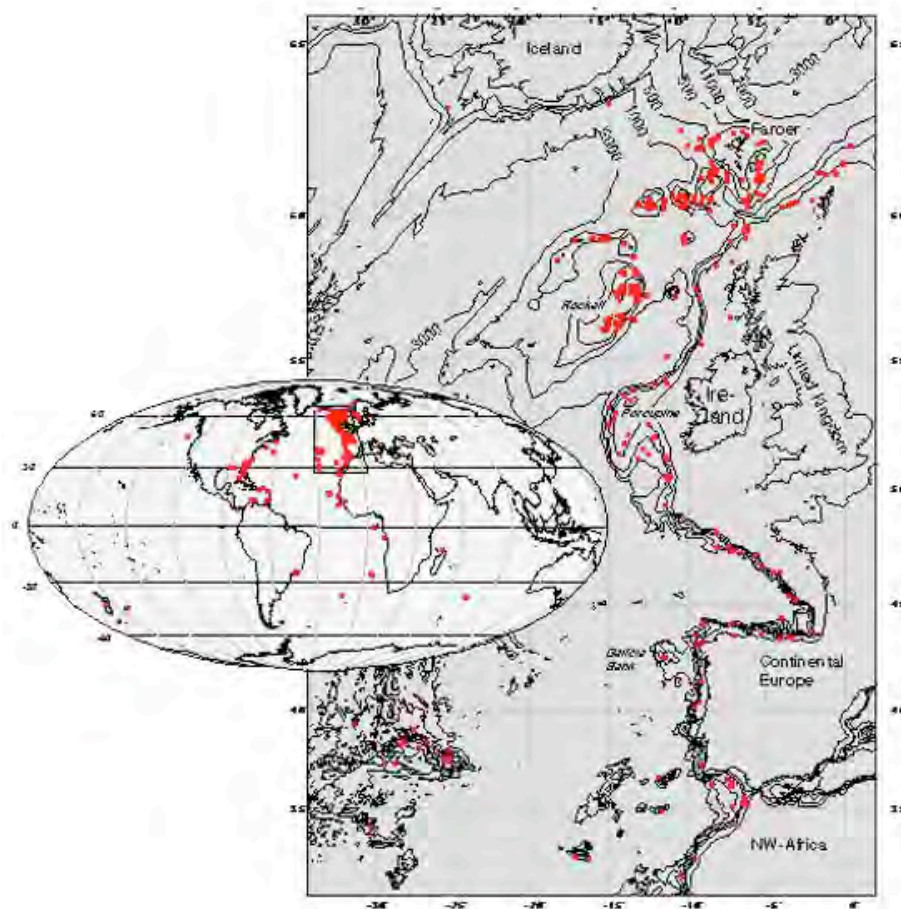


Figure 1-4. Present-day documented distribution of *L. pertusa* (from Freiwald, 2002; data source: see Rogers, 1999).

1.2.2 Deep-water coral structures

Until now, several different terminologies of deep-water coral structures appear in the literature, such as coral patches, coral thickets, coral banks, coral reefs, coral reef mounds, coral mounds, carbonate mounds or bioherms (see review of Freiwald, 2002 and references therein).

Lophelia larvae settle on elevated hard substrates and start to grow, when strong currents prevent the deposition of fine-grained deposits. Under ideal conditions, the coral starts to grow to form a colony (Freiwald, 2002). Further development is characterised by an outer ring of younger satellite colonies, which can reach a maximum height of 1 m and a width of 1.5 to 2 m, typically as cauliflower-like structures (Freiwald, 1998). With increasing size of *Lophelia* colonies, the lower, initial part gets vulnerable to infestation of boring organisms. Mechanical breakdown (bioerosion) is the result, which produces a coral rubble layer around the colony, while the satellite colonies continue to grow. The coral rubble zone serves as new substrate for larvae to settle. Wilson (1979) describes this stage as coral thickets, rarely exceeding 6–8 m in diameter. Continuing growth of these thickets to a size of 10 to 50 m across and an elevation of 1.5 m above the surrounding sea-floor have been described on Rockall Bank as coral patches (Wilson, 1979).

Coral banks (Teichert, 1958) or coral reefs (Rogers, 1999) represent the final evolutionary step in the formation of a deep-water coral buildup (Freiwald, 2002). A coral bank is principally characterised by a cap of living coral colonies usually on the top and on its upper flanks (Mortensen et al., 1995). The living corals rest on a dead coral framework, which itself overlies a zone of dead coral debris within hemipelagic sedi-

ments. High-elevated mounds with living coral ecosystem on their top and upper flanks have been subject of intense research during the past decade. The discovery of these mounds in distinct provinces along the slopes of Rockall Trough (Fig. 1-5) and Porcupine Seabight started the ongoing debate about their origin and genesis. A number of studies positively correlate the environmental controls of distinct oceanographic and hydrographic factors to the distribution of *Lophelia* reefs (Teichert, 1958; Frederiksen et al., 1992; Freiwald et al., 1997; Freiwald, 1998; 2002; Rogers, 1999).

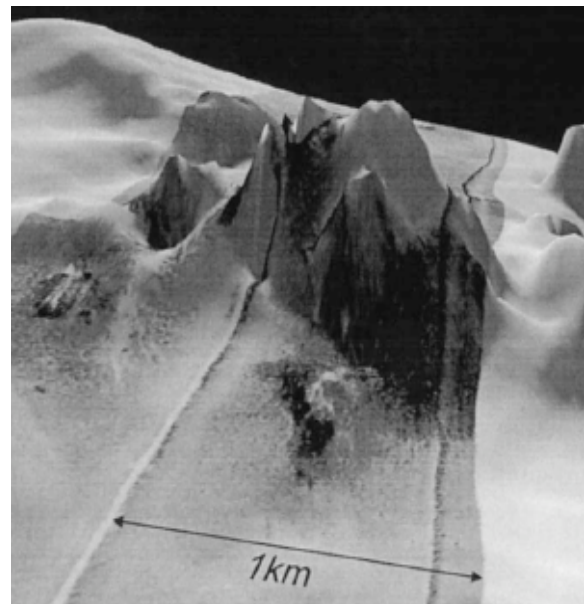


Figure 1-5. A high elevated carbonate mound from the northern Porcupine Bank margin, vertical exaggeration is 1:10 (from Kenyon et al., 2003).

Another theory relates the occurrence of *Lophelia* to an endogenous control through gas seepage (methane) from sediments below (Hovland, 1990). This theory probably plays an important role for initial mound growth (substrate stage) on authigenic carbonate crusts or microbially induced biogenic crusts (Hovland et al., 1994; Henriot et al., 1998; 2002). To solve this problem, a deep drilling survey is necessary to obtain information from the mound base.

1.2.3 Geological record of *Lophelia*

First fossil occurrence of *Lophelia* is documented from the Paleocene of Seymour Island, Antarctica (Filkorn, 1994). Squires (1957) reported of occurrences of *Lophelia* from Eocene sediments in the Gulf Coast and later of a preserved *Lophelia* buildup from a Late Miocene deposit on southeastern New Zealand's North Island (Squires, 1964). Nearby the Late Miocene build-ups, *Lophelia* thickets of similar dimension are described from mudstones of Late Pliocene age (Vella, 1964).

First appearance of *Lophelia pertusa* in the N Atlantic region has been found in several outcrops of Pliocene age along the Messina Strait, Mediterranean Sea (Freiwald, 2002). Further east, Late Pliocene to Early Pleistocene *Lophelia* thickets have

been reported from Rhodes (Hanken et al., 1996) preserved as *in situ* colonies or coral rubble in limestone marl. At this time (Late Pliocene) the appearance of *Lophelia* increased rapidly in the Mediterranean area. Abundant *Lophelia* deposits often coincide with glacial periods during the Pleistocene (Delibrias and Taviani, 1985), whereas today only a few places in the Mediterranean Sea are known, where life *Lophelia* exists. De Mol et al. (2002) have suggested that Mediterranean Outflow Water has transported larvae of deep-water corals from the Mediterranean Sea into the NE Atlantic to initiate the formation of various mound provinces in different geological times. This hypothesis has yet to be tested through deep drilling of these mounds.

1.3 Study Area: the Porcupine Seabight

1.3.1 Regional setting and geological history of the Porcupine Seabight

The study area is located in the Porcupine Seabight (PSB), which is a N-S oriented, amphitheatre like embayment located in the NE Atlantic Ocean west off Ireland between 50° to 54°N and 10° to 15°W (Fig. 1-6). It is surrounded by the Irish Mainland shelf to the east, the Slyne Ridge to the north, the Porcupine Bank and Ridge to the NW-W and widens to the south into the Porcupine Abyssal Plain. The water depth increases from >200 m of the shallow shelf areas to >3000 m in the southwest. The slopes at the eastern and western flank of the PSB are generally steep with 2–3°, but decrease in the northern part. To the southeast, the Gollum channels cut into the slope and the deeper Porcupine Basin as indicated by deep E-W oriented canyons (Fig. 1-6).

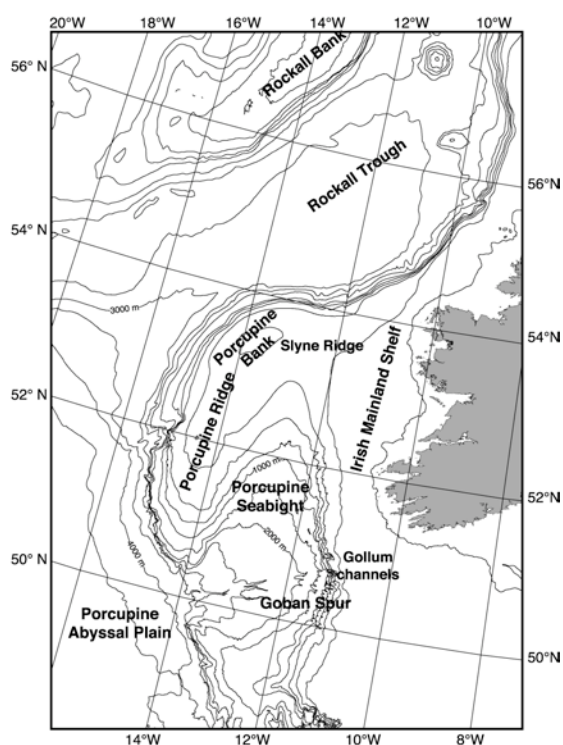


Figure 1-6. Bathymetric map of the Porcupine Seabight, NE Atlantic Ocean (GEBCO, 1997).

The origin and evolution of the PSB is complex influenced by several episodes of rifting, sea-floor spreading dynamics of the N Atlantic, basin wide thermal subsidence and the Alpine orogenesis (McCann et al., 1995). Possible minor rifting occurred already during the Late Triassic (~220 Million years ago (Ma)), followed by intrabasinal uplift of the Porcupine Basin during the Middle Jurassic (~160 Ma; Doré et al., 1999).

The most significant phase of crustal extension is reported for the period of Late Jurassic to Early Cretaceous, 150–100 Ma (McDonnell and Shannon, 2001), when the Atlantic sea-floor spreading propagated northwards from the central Atlantic region (Johnston et al., 2001). Faulting was extensive during this main rift phase (McCann et al., 1995).

Basin flank uplift in the Aptian and Albian (120–100 Ma) is thought to be the response to regional extension and sea-floor spreading between the Bay of Biscay and Newfoundland (Knott et al., 1993). This subsequent lithospheric response resulted in a phase dominated by passive thermal subsidence, which created the accommodation space for the Late Cretaceous and Tertiary sedimentary fill in the basin (McDonnell and Shannon, 2001).

The Tertiary sedimentary record in the Porcupine Basin is divided by four regional unconformity surfaces C40, C30, C20 and C10 (McDonnell and Shannon, 2001; Stoker et al., 2001). Every single surface marks a distinct change in sedimentary patterns in response to sea-level fluctuations.

A change from carbonate to clastic deposits is described at the Paleocene regional unconformity C40, around 60 Ma, coherent with a sea-level fall (McDonnell and Shannon, 2001). The sediments of Late Palaeo-

cene and Eocene are characterised by clastic and deltaic deposits in the shallow parts, and submarine fan deposits in the deeper parts of the Porcupine Basin. Main Eocene sediment transport direction was from the north and west (McDonnell and Shannon, 2001). The second basin-wide unconformity developed in the latest Eocene (~34 Ma) and correlates with the designated C30 event of the Rockall Trough (Stoker et al., 2001).

After the C30 unconformity fine-grained deep-sea sediments with occasional limestone intercalations dominate the overall Oligocene to Recent succession in the Porcupine Basin. Around 20 to 15 Ma several closely spaced unconformities have been identified in the basin, which correlate to the C20 unconformity of the Rockall Trough stratigraphy (Stoker et al., 2001). These latest Early Miocene markers, indicated by erosional scouring, probably correspond to a relative sea-level fall and intensifying bottom current activity as noted elsewhere in the North Atlantic (Stoker, 1997). Post C20 sequence of the Porcupine Basin is dominated by parallel reflections of shale-dominated sediments, indicating a relative sea-level rise through Miocene to Recent times (McDonnell and Shannon, 2001).

The final unconformity C10 indicates an erosional horizon, recently dated by Stoker et al. (2001) as of intra Early Pliocene age. This horizon may represent the stratigraphic response to the latest Cenozoic exhumation of Britain and Ireland (Japsen, 1997), and the subsequent effects of glacial abrasion and unloading (McDonnell and Shannon, 2001). The sediment sequence overlying C10 experienced the present-day ocean circulation regime, which commenced after the closure of the Isthmus of Panama around 4.6 Ma (Haug et al., 2001). During the Pleistocene, the sedimentary system of the Sea Bight was influenced by glacial and

interglacial cycles with completely different settings for glacials (see Chapter 1.4) and interglacials (Chapter 1.5 for the Holocene).

1.3.2 Carbonate mounds in the Porcupine Seabight

Within the setting of the PSB three different provinces occur, where mound structures have been identified: the **Belgica Mound province** at the eastern slope of the PSB, the **Hovland Mound province** in the north, which is separated from the **Magellan Mound province** further north (Fig. 1-7). These mound features are described in literature as carbonate knolls (Hovland et al., 1994), bioherms (Henriet et al., 1998) or coral banks (De Mol et al., 2002).

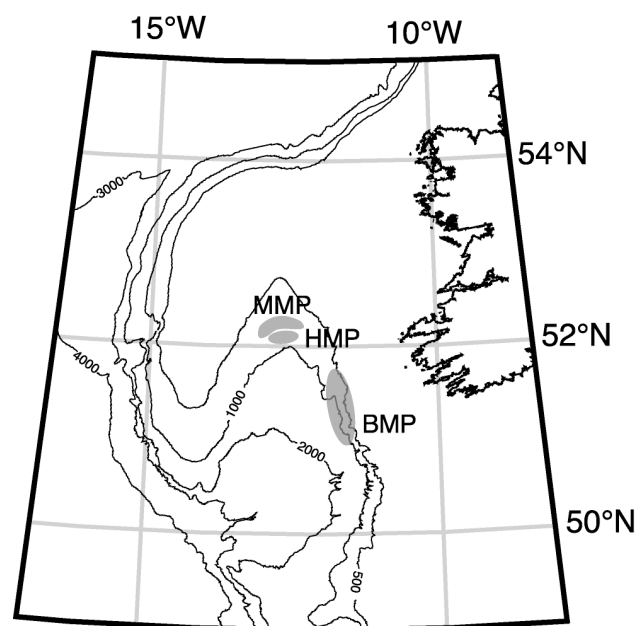


Figure 1-7. Three mound provinces within the PSB (MMP = Magellan Mound Province, HMP = Hovland Mound Province, BMP = Belgica Mound Province). Bathymetric contours in metres (GEBCO, 1997).

The **Belgica Mound province** is located between 51°10' to 51°35'N and 11°30' to 11°45'W. It is named after the Belgian research vessel, which discovered the mounds

in 1997 (Henriet et al., 1998). The mounds are placed along the steep eastern slope in water depth of 600-900 m over a distance of 20 km. Both exposed and buried mounds occur in this province. The exposed mounds appear in 750-850 m water depth while the buried features have been identified on seismic lines further upslope (De Mol et al., 2002; Van Rooij et al., 2003; Fig. 1-8). The mounds appear conical on seismic profiles (Fig. 1-9). Their eastern flanks are ponded with sediment, while the western flanks remain exposed with average slopes of 10°–15° (De Mol et al., 2002). Large mounds merge into ridge-like structures with a NNE-SSW direction. Rough sea-floor and sand waves in between the mounds indicate a strong, northerly-flowing hydrodynamic regime (De Mol et al., 2002).

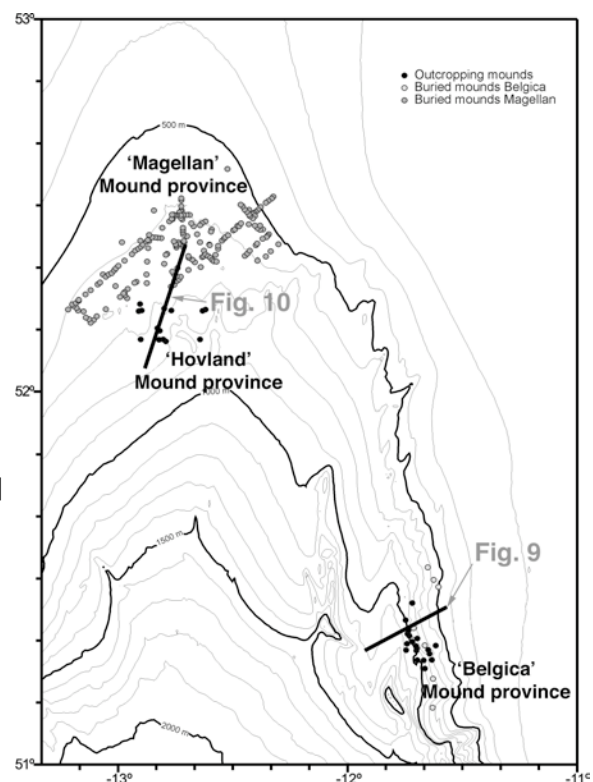


Figure 1-8. Exposed (black dots) and buried mounds (grey dots) of the three mound provinces in the PSB (after De Mol et al., 2002). Indicated seismic lines across the slope of Belgica and Hovland/Magellan Mound provinces are shown in Fig. 1-9 and 1-10.

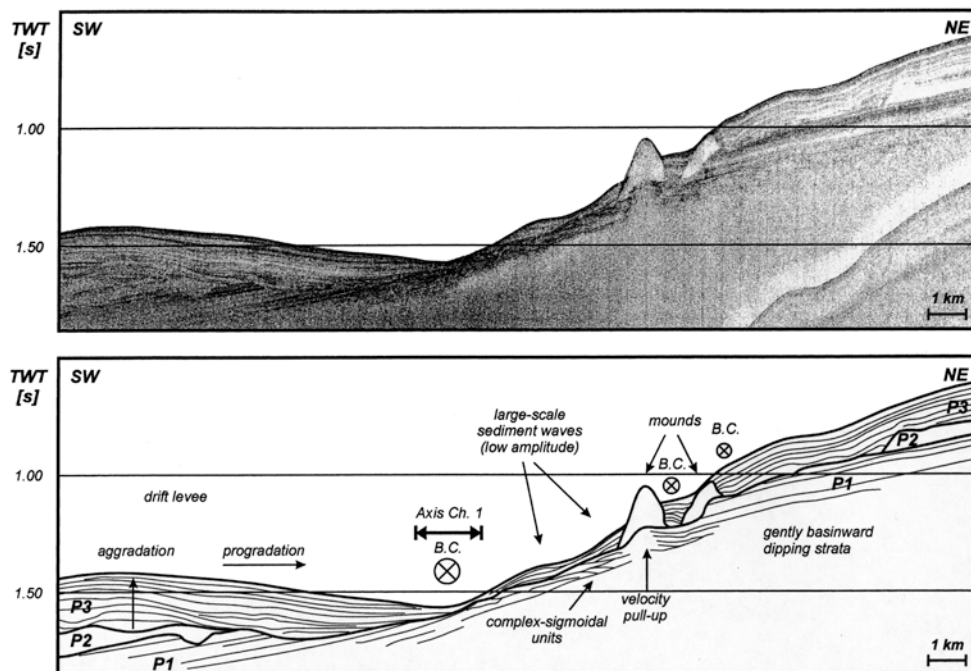


Figure 1-9. Overview of seismic features along indicated line in Fig. 1-8 at eastern slope of PSB (from Van Rooij et al., 2003). B.C. = bottom current, P1-P3 = seismic units, TWT = Two-way travel time in seconds.

Other erosional features like moats around the mound foot are not well developed. The base of the Belgica mounds is formed by a continuous erosional surface between seismic units P1/P3 or P2/P3 (Fig. 1-9). This unconformity is probably of Miocene age (De Mol et al., 2002) implying a possibly earlier origin for the Belgica mounds compared to the other mounds in the northern PSB (see below).

The **Magellan Mound province** consists of numerous (up to 1500) buried mounds in the area between 52°12' to 52°38'N and 12°22' to 12°08'W (De Mol et al., 2002, Fig. 1-8). Only a few mounds protrude the sea-floor at the western boundary of the province. They have been discovered on industrial 2D site survey seismic data obtained in 1996 by MV Svitzer Magellan in water depth of 450–700 m. The mounds occur as a crescent shaped province with a surface area of ~1500 km². They are abundant at some depth below the seabed

(Huvenne et al., 2002). These mounds are small at shallower sites and become larger towards the SE, where sediment drape on the mounds is thinnest (De Mol et al., 2002).

The buried mounds are acoustically transparent (Fig. 1-10), have an average height of 80 m and a cross section at their basis of 300-800 m. In contrast to the conical Belgica mounds, the Magellan mounds are predominantly vertical, stock-like features with an often wider top (De Mol et al., 2002). Some mounds occur in symmetric or asymmetric twin patterns, which may suggest sections through a ring structure (Henriet et al., 1998). At the mound-basis the Magellan mounds are often associated with moats (average of 34 m deep), indicating erosion and strong currents during their genesis (De Mol et al., 2002).

The **Hovland Mound province** is separated from the Magellan mounds by a 4 to 10 km wide zone, which lacks any indication of mound structures (De Mol et al.,

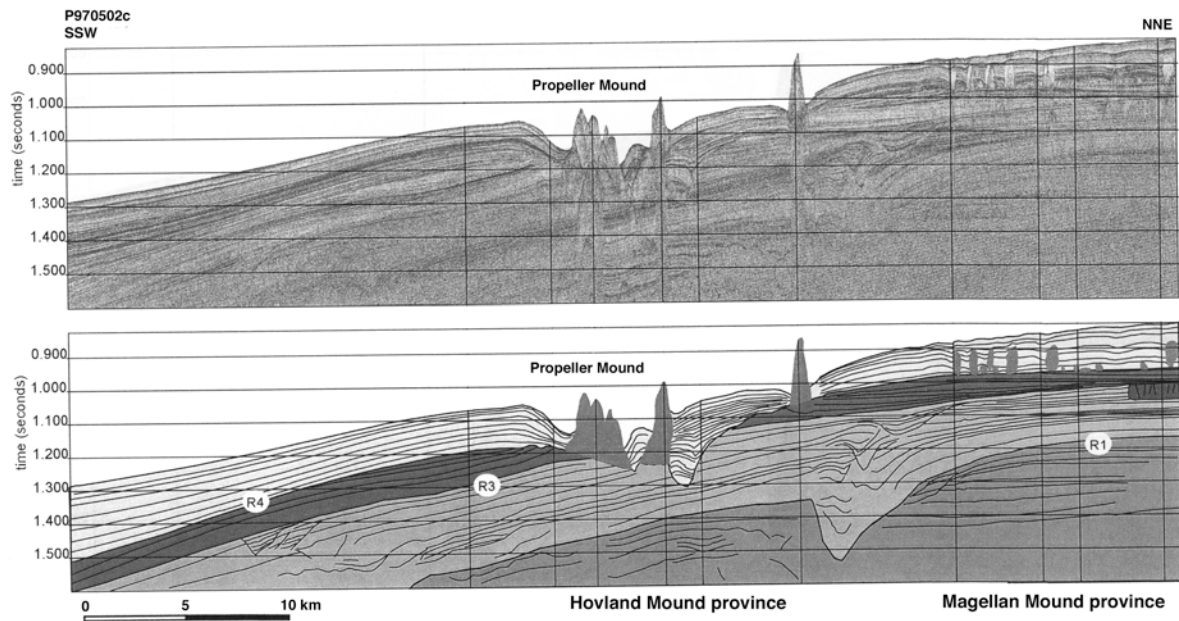


Figure 1-10. Seismic line as indicated in Fig. 1-8 crossing the Magellan (NNE) and Hovland Mound provinces (modified after De Mol, 2002). Acoustically transparent and buried Magellan mounds occur to the NNE of the profile, outcropping Hovland mounds, like Propeller Mound, appear in the centre of the seismic line. The mound base is indicated by Facies boundary R4, probably corresponding to pré-Late Pliocene age (De Mol et al., 2002).

2002). The Hovland mounds occur between 52° and $52^{\circ}30'N$ and 12 to $13^{\circ}W$, bathing in water depths ranging between 725 to 900 m (Fig. 1-8). They are associated with N-S trending sea-floor depressions. The mounds appear as large conical shaped structures or elongate mound ridges, which are flanked by deep moats incising into the sea-floor (De Mol et al., 2002). These mounds are named after the first author of publication by Hovland et al. (1994), who recognised and characterised the mounds in this part of the PSB. The authors relate their possible origin to gas hydrate dissociation or hydrocarbon leakage from deeper seabed below. A typical single mound is 100 m high, 1 km in diameter and has slopes of average 10° . The mounds are flanked on the seabed by erosional moats, most likely formed by scouring through topographically enhanced bottom currents. These moats are elongated, show a length of 1 to 3 km, and are much

deeper (20–150 m) than these from Magellan mounds. The mound basis of Hovland and Magellan mounds is described by an erosional unconformity between seismic units P1 and P3 (R4 in Fig. 1-10). Based on uncalibrated interpretation of seismic units draping the mounds, an age of pré-Late Pliocene is suggested (De Mol, 2002), which is probably coherent with NE Atlantic unconformity C10 (Chapter 1.3.1).

1.3.3 Propeller Mound

The Propeller Mound is object of detailed investigation (Fig. 1-11). It was mapped and sampled during RV POSEIDON cruise POS 265 and 292 (Freiwald et al., 2000; Freiwald and Shipboard Party, 2002). The mound forms an exposed 140 m high structure and shows a N-S elongation with a combination of three ridges connected in the central part. The summit of the mound lies at $52^{\circ}09.80'N$

and 12°46.40'W in ~670 m water depth. The shape of this mound is very peculiar due to three merged spurs resembling a three-bladed propeller. These spurs point to NE, NW and S direction. The overall extension of Propeller Mound is ~2.5 km in N-S and 1.5 km in E-W direction, thinning out to ~400 m at the southern tip. The slope inclination varies between 8–10° over the long-axis of the three spurs, increasing to generally 12° to 20°, but reaches a maximum of up to >45° at the eastern and western flanks (Freiwald and Shipboard Party, 2002). The mound foot is at 800 m water depth along the western flank and 900 m at its eastern flank. Moats occur at the base of the eastern and western flank of the mound.

Investigation with the remotely operated vehicle (ROV) CHEROKEE from Bremen University during RV POSEIDON cruise POS 292 (Freiwald and Shipboard Party, 2002) clearly separates different sea-floor characteristics of Propeller Mound. The off-mound area is formed by the characteristic sandy mud drape of the northern PSB (Fig. 1-11a). At the foot of the mound the slope gets steeper and IRD boulders and hardgrounds occur with predominantly dead coral rubble (Fig. 1-11b). In this area, the currents are strongest. Further upslope, an increasingly higher abundance of coral thickets are present along very steep flanks (up to 60°, Fig. 1-11c). These thickets provide shelter and a highly structured habitat for numerous sessile and vagile organisms. The summit of Propeller Mound is narrow and flat and shows a less dense cover of living corals. The currents are much weaker at the upper slope and top mound area compared to the mound foot.

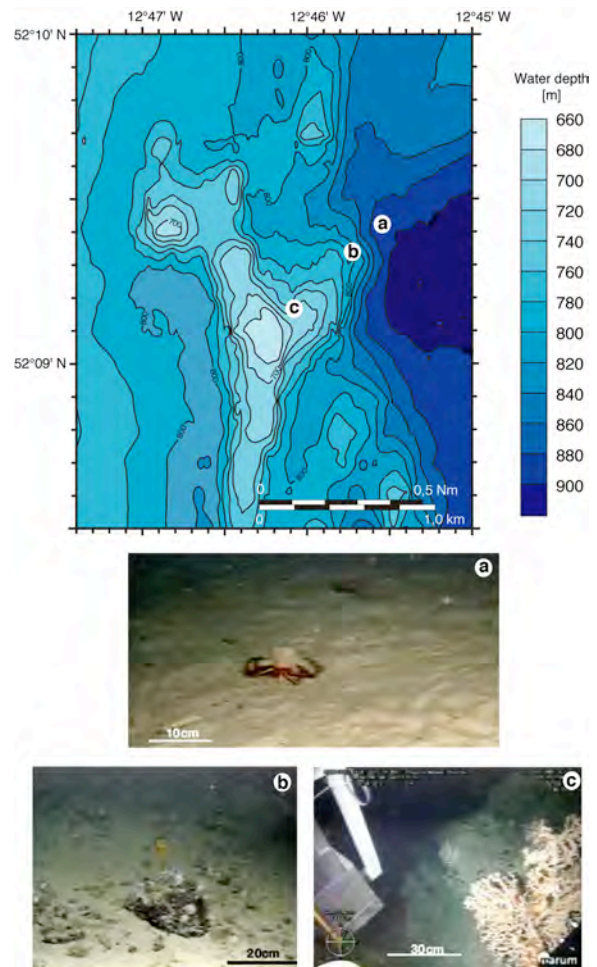


Figure 1-11. Bathymetry of Propeller Mound, southern Hovland Mound province. (a) Off-mound sediments with anemone overgrown hermit crab, (b) IRD boulders at mound foot, (c) dense coral thickets on upper slope with steep inclination of up to 60° (Freiwald and Shipboard Party, 2002).

To demonstrate the extension of Propeller Mound, a comparison with Germany's only offshore island Helgoland is performed (Fig. 1-12). Propeller Mound has a comparable extension like Helgoland's main island, where about 1700 inhabitants live. Despite the up to 60 m high cliffs at the western side of Helgoland, the cross sections of both structures illustrates nicely, that Propeller Mound is more than twice as high as Helgoland.

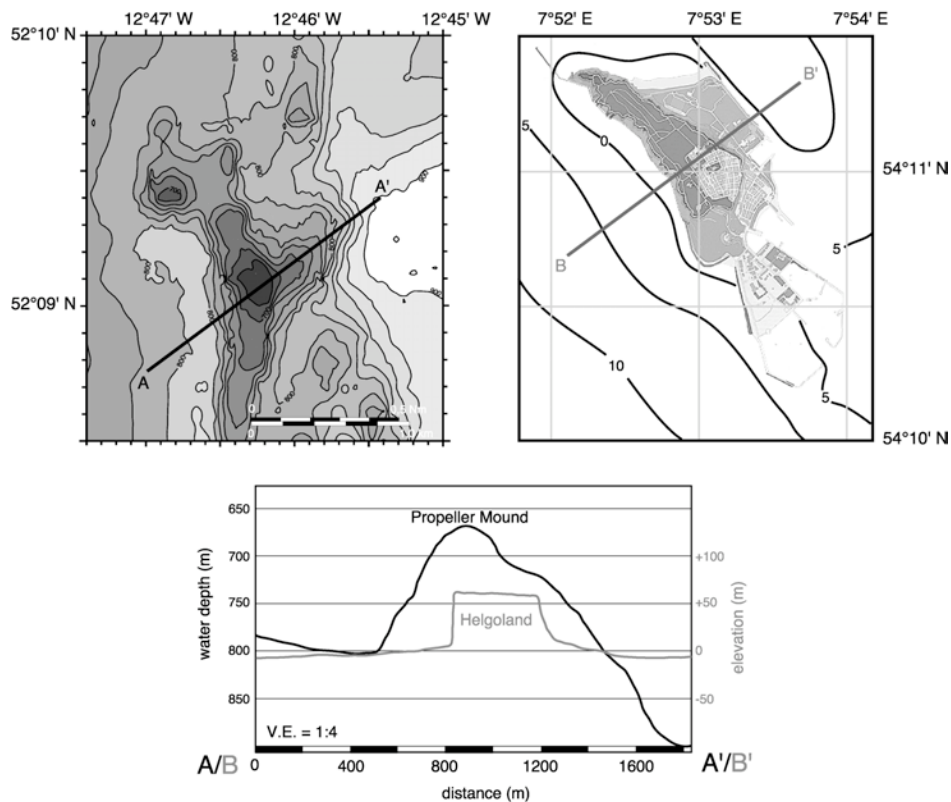


Figure 1-12. Comparison of Propeller Mound and Helgoland, Germany's only offshore island. Cross sections from Propeller Mound and Helgoland follow indicated lines A-A' and B-B', both about 1.8 km long. Propeller Mound is more than twice as high as the similar-sized main island of Helgoland. Note: vertical exaggeration is 1:4. Helgoland map from <http://www.helgoland.de>, bathymetry from sea chart "Deutsche Bucht", 50 INT 1045, Bundesamt für Seeschifffahrt und Hydrographie, Hamburg.

1.4 Glacial setting of the Porcupine Seabight

The carbonate mounds originated during the Late Tertiary and experienced during their further development the northern hemisphere glaciation and the resulting glacial-interglacial cycles. During peak glacials, the Polar Front of the North Atlantic was situated as far south as 40° to 45°N offshore Portugal (Ruddiman and McIntyre, 1981), which led to polar conditions on Ireland and the surrounding shelf environment. This chapter summarises the oceanographic setting of the PSB and the land ice extension on Ireland for the last glacial period.

1.4.1 Surface water, seasonal sea-ice and intermediate glacial water mass distribution

Surface water moved southward as a coastal current (Sarnthein et al., 1995), transporting cold waters from the North Atlantic along the Irish coast (Fig. 1-13). Sea surface temperatures were low during glacial summers with around 5°C, which decrease to 0–1°C during glacial winters (Sarnthein et al., 1995; Bowen et al., 2002; Sarnthein et al., 2003). These chilling surface waters in glacial winters support the extent of sea-ice covering the entire PSB and Rockall Bank (Sarnthein et al., 2003; Fig. 1-13). During glacial summer months, warmer waters entered the NE Atlantic as far north as Spitsbergen, which led to a retreat of sea-ice

in the PSB onto the Irish shelf. Sea-ice cover is probably the most influential environmental factor in present-day high-latitude environments with strong control on biological and physical processes (e.g. Weinelt et al., 2001). Biological primary productivity strongly depends on the duration of sea-ice cover, which is low during ice cover and high at the summer ice edge (Hebbeln and Wefer, 1991).

The intermediate oceanographic setting of the PSB is not well studied. Glacial North Atlantic Intermediate Water (GNAIW) is reported in water depths below surface waters down to 1700–2000 m in areas further west (Manighetti and McCave, 1995). They describe a flow from the north via the Wyville-Thomson Ridge and through the Rockall Trough to the south.

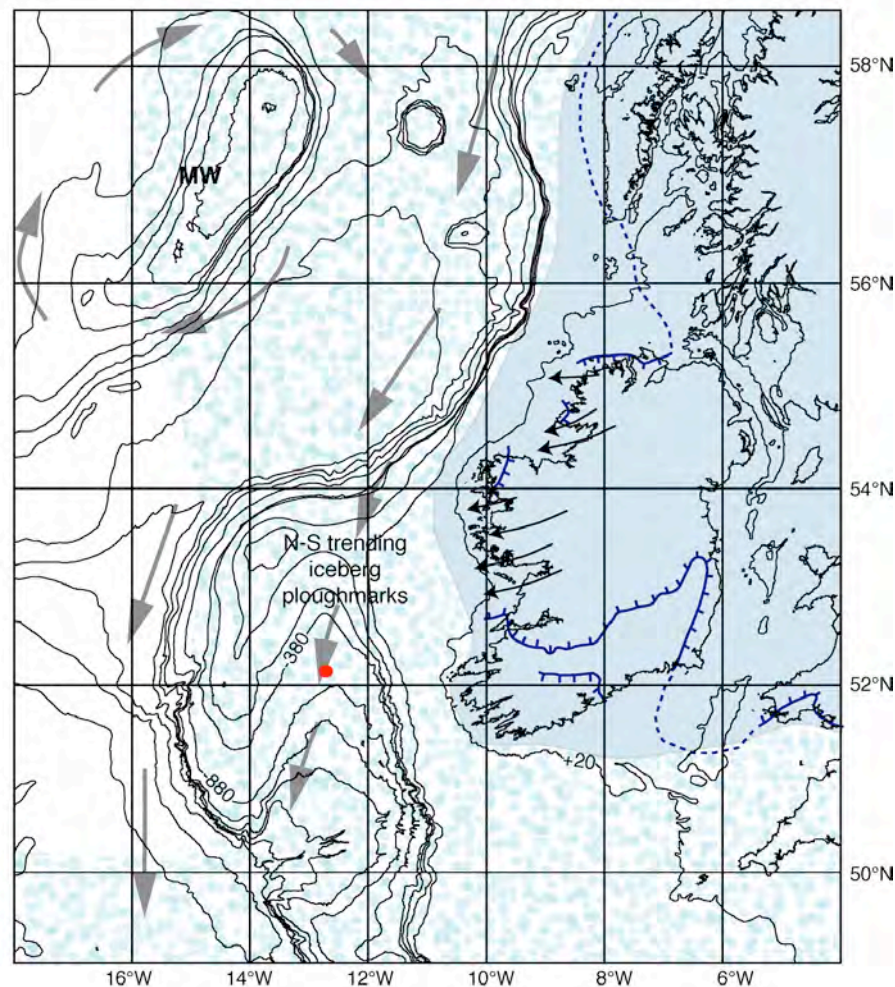


Figure 1-13. General map of Ireland during glacial intervals. Indicated are ice limits (dark blue) and general ice flow (black arrows) for Marine Isotope Stage (MIS) 2 (after Eyles and McCabe, 1989; Jones and Keen, 1993), maximum land-ice extent (light blue) for MIS 4 (after Bowen et al., 2002), surface circulation (grey arrows) and melt water intrusion (MW) resulting in a weak anticyclonic circulation around Rockall Bank for MIS 2 (after Sarnthein et al., 1995), and sea-ice cover (light blue dots) covering entire PSB during peak glacial winters (Sarnthein et al., 2003). N-S trending iceberg ploughmarks are reported on Slyne Ridge (after Games, 2001). Glacial bathymetry corresponds to present-day water depth minus 120 m. Red dot marks the position of Propeller Mound.

According to Duplessy et al. (1988) and Oppo and Lehman (1993) the term GNAIW is used for mid-depth waters of uncertain origin. Veum et al. (1992) reported of production in the Norwegian Sea at least during MIS 2 via a mechanism strongly influenced by sea-ice formation, but the composition of GNAIW may have changed during the glacial time with differing sources. GNAIW is characterised as a moderate water mass with respect to current speed for the Last Glacial Maximum. It expands to greater depth during deglaciation and becomes more vigorous (Manighetti and McCave, 1995). The influence of the very cold GNAIW on the PSB is not reported due to limited investigations in that area. But an influence is assumed, as very cold waters occurred west of the Porcupine Bank, indicated by benthic oxygen isotope data (e.g. Lehman and Keigwin, 1992; Sarnthein et al., 1994). Mediterranean Outflow Water (MOW) had a great influence within intermediate depths of the PSB during the Holocene (see Chapter 1.5). Schönfeld and Zahn (2000) described a main glacial MOW flow up to 800 m deeper than today, due to an increased density induced by a distinct higher salinity. In addition, the glacial flow pattern indicates no northward flow of MOW along the European continental margin, which results into a homogenous intermediate water column for the PSB.

1.4.2 British Irish Ice Sheet variability

In the North Atlantic region the British Irish Ice Sheet (BIIS) was probably the most sensitive and earliest amplifier of climatic change because of its extreme maritime position at the southern limit of the last glaciation in NW Europe (Eyles and McCabe, 1989; Knutz et al., 2001). A maximum land ice extend of the BIIS

probably reaching offshore W Ireland to the present 200 m isobath is reported by Bowen et al. (2002) for MIS 4 (Fig. 1-13). During MIS 3 the Polar Front was mainly north of the British Isles. Ireland was covered with treeless, tundra-like vegetation with small ice caps covering most of Ulster in the north of Ireland (Jones and Keen, 1993). An advance of land ice took place around 30 ka BP, covering most of Ireland. Only a narrow band remained ice-free (Knutz et al., 2001). This advance of BIIS around the transition of MIS 3 and 2 is synchronous with a sea-level drop of around 50 m (Lambeck et al., 2002). Eyles and McCabe (1989) indicated ice flows from central Ireland to the Galway Bay onto the Irish Mainland Shelf.

Sedimentary processes closely related to glacial conditions are not well studied in the PSB. However, the southward flowing surface waters, land ice extension and calving of icebergs from Irish mainland as documented by iceberg plough marks on Slyne Ridge (Games, 2001), as well as the sea-level lowering suggest an enormous increase in terrigenous sediment supply into the PSB. An abrupt increase in basaltic IRD at 30 thousand years before present (kyr BP) from a core recovered at Barra Fan north of the PSB indicates a change from hemipelagic to glaciomarine sedimentation (Knutz et al., 2001). Glaciers carried eroded material and reached the shelf edge releasing gravity flows leading to increased sediment supply from the shelf and to subsequent high glaciomarine sedimentation on the slope and deeper basin. Along the Western Approaches to the south of the PSB similar indications of enormous sediment supply induced by progressing glaciers onto the shelf have been found (e.g. Auffret et al., 2002).

1.5 Present-day oceanographic setting

Within the PSB the present-day hydrodynamic regime is quite complex. Several processes interact with the general northward flowing water masses, like tidal currents, vertical mixing, eddies, cascading, internal tidal waves and the effect of the sea-floor morphology on currents and flows. All these processes play an important role on the exchange of nutrients and sediments between the shallow shelves and the deeper basin. They are important for marine biota within the Sea Bight, especially for the deep-water coral ecosystem in the distinct depth range of 500 to 1000 m.

The PSB falls in between the two main circulation systems of the North Atlantic, the sub polar and sub tropical gyre. The main branch of the North Atlantic Current (NAC) shows a division into one branch flowing NW of Rockall Bank, and a southern branch flowing SE into the Bay of Biscay to form part of the subtropical gyre (Pingree, 1993). NAC carries relatively warm and salty waters into the NE Atlantic.

1.5.1 Water mass distribution and general circulation

In the PSB, 14–16°C warm and relatively salty (35.5) surface water occurs during summer months down to 40–50 m water depth, where a decrease in temperature, oxygen concentration and salinity indicates the seasonal thermocline (Fig. 1-14). During winters, the upper water column is characterised by a homogeneously stratified water mass.

The dominant water mass below the thermocline down to 600–700 m water depth is the Eastern North Atlantic Water

(ENAW, Fig. 1-14). The source of ENAW lies in the Bay of Biscay further south of the PSB, where it is formed as a winter mode water by strong cooling at the sea surface (Pollard et al., 1996). ENAW flows northward along the European continental margin (Pingree and LeCann, 1989; Huthnance, 1986) and enters the PSB (Mohn, 2000), where it circulates as a slope current topographically steered within the Sea Bight (Ellet et al., 1986). In the northern PSB the water mass flow turns southward and flows around the Porcupine Bank (White, *subm.*; Fig. 1-15).

The Shelf Edge Current (SEC) carries a significant portion of ENAW and is marked by high salinity cells in 150–400 m water depth (Hill and Mitchelson-Jacob, 1993; Fig. 1-14). It plays an important role in physical exchange processes at the shelf break and hence cross-shelf fluxes (Huthnance, 1995). This water mass is found below the summer thermocline but reaches the sea surface during winter.

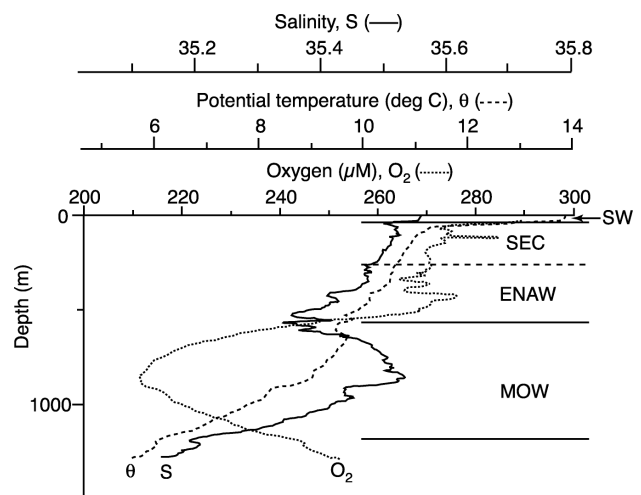


Figure 1-14. Hydrographic parameters and characteristic water masses of the upper 1500 m from outer Goban Spur (see Fig. 1-6). SW = Surface waters, SEC = Shelf Edge Current, which is part of ENAW = Eastern North Atlantic Water, MOW = Mediterranean Outflow Water (from McCave et al., 2001).

Below 600 m water depth salinity increases again, but dissolved oxygen is depleted, which indicates the contribution of the underlying Mediterranean Outflow Water (MOW; Fig. 1-14). MOW is a warm but very salty water mass due to high evaporation in the Mediterranean area. It flows out over the sill at the Straits of Gibraltar, where it enters the Atlantic Ocean. The main MOW flow follows a narrow advection path 100–150 km wide along the western Iberian continental slope at depths between 600 and 1500 m. The MOW is separated into an upper and lower core layer displaying distinctive temperature maxima of $>11^{\circ}\text{C}$ at 750 m and salinity maxima of >36.6 at 1250 m (Schönfeld and Zahn, 2000). The upper core layer underlies ENAW and shows a similar circulation like ENAW and SEC along the continental slope (Fig. 1-15) with mean current velocities of around 12 cm s^{-1} (Zenk, 1971; 1975; Zenk and Armi, 1990; Zenk et al., 1992). This upper core layer of MOW occupies the whole Porcupine basin between 800 and 1200 m water depth (White, *subm.*; Fig. 1-14).

1.5.2 Slope current and current strength intensities

The generally poleward flow of waters along the eastern boundary of the N Atlantic (Smith, 1989) is theoretically driven by the poleward decline in sea surface height, which is caused by increasing water density with latitude. Along the continental margin the slope current has been measured at many locations.

Directly measured mean circulation near the seabed in the water depth of carbonate mounds is reported from the PSB (White, *subm.*). The predominant circulation in the Sea Bight is essentially cyclonic (Fig. 1-15) with a poleward flow along the Irish Shelf

and the eastern Sea Bight margin. Current speeds are generally strong where mounds are located and exceed 15 cm s^{-1} for nearly 49 % of the measured period at the Belgica mound province. At the northern PSB, where the flow turns from northerly into more southwesterly direction, only 7 to 15 % of the measurement period shows currents exceeding 15 cm s^{-1} (White, *subm.*). During spring, the measurements indicate weaker currents. Pingree and LeCann (1989; 1990) describe for the slope current a so-called SOMA (Sept-Oct-Mar-Apr) seasonality response, which White (*subm.*) also identified in measurements near the carbonate mounds. Rough topography as generated by the carbonate mounds also has a great impact on inducing localised strong currents and mixing processes (White, *subm.*).

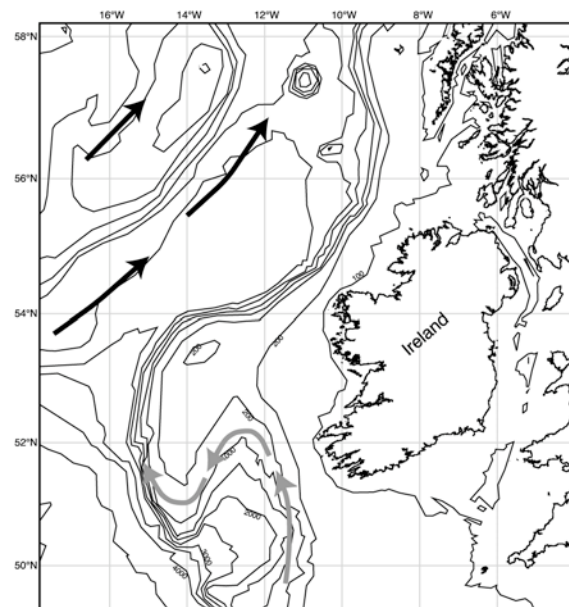


Figure 1-15. General circulation within the PSB. NAC = black arrows, intermediate water masses (SEC, ENAW, MOW) = grey arrows.

Other processes exist that generate localised strong currents at specific depths. Internal waves occur at the interface of two water masses (e.g. ENAW-MOW) and be-

come periodically unstable, which results into pressure gradients causing internal wave motion. Tidal flow across the shelf edge is a known mechanism for generating internal motions, with subsequent propagation of the internal tidal energy on and off the shelf (Pingree and New, 1991). Other external forces are changes in density, in vertical component of barotropic currents or changes in topography (Wunsch, 1975). Rice et al. (1990) suggested that reflecting internal waves cause enhanced currents along the eastern PSB, but not along the northern margin, where the Hovland and Magellan mounds are situated. The data set of White (subm.) confirms this theoretical argument of Rice et al. (1990), but he notes that the cause of strong currents may not be entirely due to internal wave interactions but may result from more than one dynamic process.

1.5.3 Primary productivity and down-slope transport of organic matter

The NE Atlantic is a highly productive region and it is estimated that there is a large flux of organic material to the lower continental slope. Figure 1-16 shows an example of a true-colour MODIS image of the Porcupine Seabight illustrating the regional biological characteristics. This image, taken in May 2001, shows high chlorophyll levels along (1) the Irish shelf edge region following the 200 m bathymetric contour and (2) on the relatively shallow Porcupine Bank. Measurements in the nearby region of the Goban Spur at the mouth of the PSB (50°N, 12°W, see Fig. 1-16) are typically high for this shelf environment with $\sim 160 \text{ g C m}^{-2} \text{ yr}^{-1}$, as presented by Joint et al. (2001). They estimated about $60 \text{ g C m}^{-2} \text{ yr}^{-1}$ available for the export to intermediate and off-shelf waters. Several mechanisms exist

transporting organic material downslope into greater depth. A cold-water dome with enhanced phytoplankton productivity is reported over the Porcupine Bank (White et al., 1998; Mohn et al., 2002). The combination of high productivity over this bank and the downslope transport off the bank (Ekman drainage flows, cascading) provides a highly efficient way of delivering food to the slope flanks (White et al., subm.).

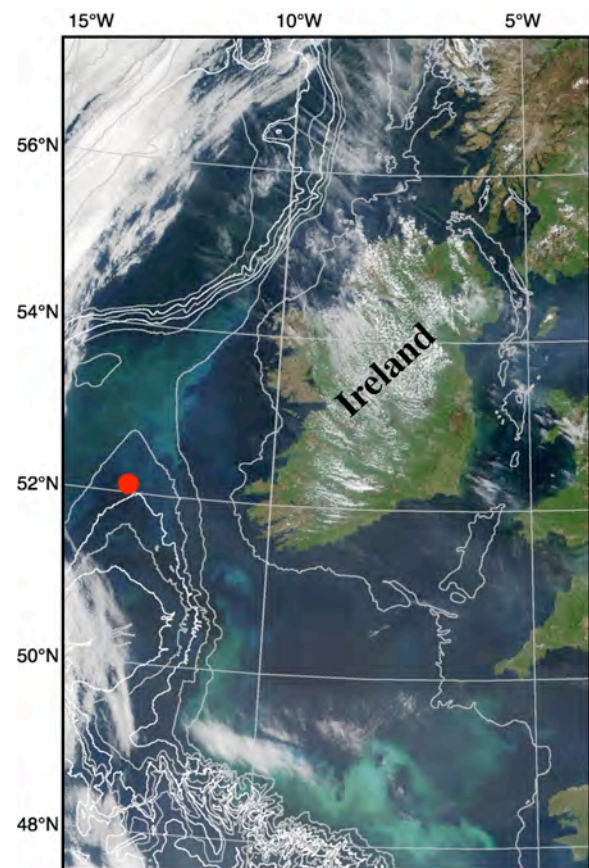


Figure 1-16. True-colour MODIS image made from data collected by satellite Terra on May 22, 2001. Phytoplankton blooms appear as blue-green swirls to the west and south of Ireland (Credits: J. Descloitres, MODIS Land Rapid Response Team, NASA/GSFC, <http://visibleearth.nasa.gov/cgi-bin/viewrecord?10019>). Bathymetric contours correspond to 100, 200, 500, 1000, 1500, 2000, etc from shallow to deep (GEBCO 1997). Red dot marks position of Propeller Mound.

Well-developed Bottom Nepheloid Layers (BNLs) are reported for the slope area at the Goban Spur (McCave et al., 2001) and for slopes at Porcupine Bank (McCave, 2002; White et al., *subm.*). These layers develop through mixing processes on the slope and may collapse due to the reflection of internal waves (eastern PSB, see above). This leads to the formation of Intermediate Nepheloid Layers (INLs), which have been detected by Thorpe and White (1988) out to a distance of 16 km from the slope. The combination of intermittent resuspension under internal waves and slope currents, plus strong meddy-driven basinward transport accounts for most features of the INL field recorded at depth of 700–1400 m at Goban Spur (McCave et al., 2001; Fig 1-17). At this site, INLs show a seasonal

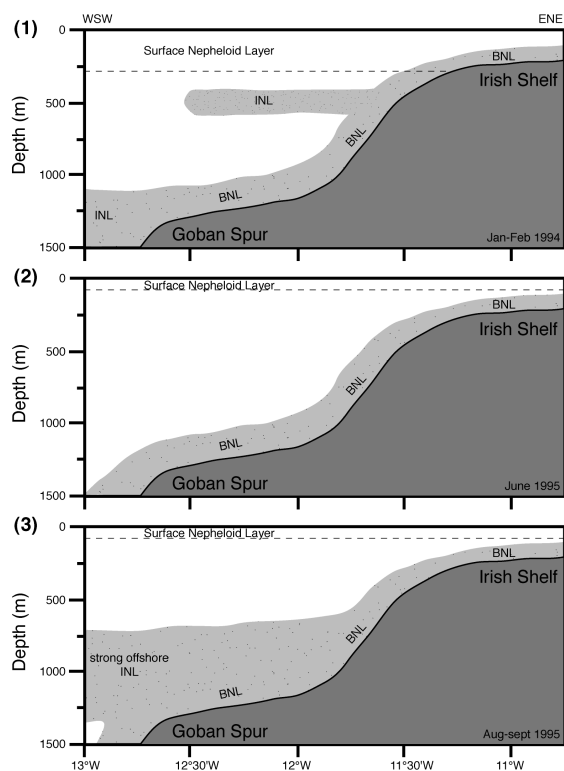


Fig. 1-17: Bottom and Intermediate Nepheloid Layers (BNLs, INLs) along Goban Spur ($\sim 49^\circ\text{N}$) for (1) winter, (2) summer and (3) autumn (simplified after McCave et al., 2001). Strong offshore INL occurs during autumn in water depth of MOW.

variability: (1) a series of INLs are present between 400–600 m during winter and a distinct INL between 1000–1500 m with a weak offshore signal, (2) INLs with a top at ~ 600 m are apparent during summer 55 km further south of the transect shown in Fig. 1-17, but are lacking here, and (3) a return to strong offshore INLs occurs during autumn with a strong, single INL between 700–970 m (McCave et al., 2001). The distribution of strong offshore INLs suggests a correlation with the presence of MOW and the water mass boundaries of ENAW and MOW (Fig. 1-17). Due to a strong gradient in density at this water mass interface, organic material persists at this level for a longer time. In addition, it is also transported laterally within the PSB. The combination of internal waves and northward oriented slope currents suggests a similar distribution of BNLs and INLs within the PSB, possibly decreasing towards the north with respect to water depth.

The combination of above mentioned processes enables the material to remain in suspension, supporting the filter-feeding corals on top of the carbonate mounds, but also other benthic organisms in intermediate to greater depths. It seems obvious that water mass variations during glacial and interglacial cycles, when major differences of the oceanographic setting existed (compare Chapter 1.4 with 1.5), had a great impact on coral growth and distribution. In this thesis to point out these environmental changes will be discussed with respect to glacial and interglacial cycles at the close neighbourhood of Propeller Mound.

CHAPTER 2

MATERIALS AND METHODS

2.1 Sediment core analyses

This thesis is based on analyses of seven gravity cores from Propeller Mound and adjacent areas collected during cruise POS265 with the German Research vessel POSEIDON (Freiwald et al., 2000). Sediment cores were retrieved from an area of 1.5 km² (Fig. 2-1) and range in length from 350 to 600 cm (Table 2-1). All cores were cut into 1 m sections, stored at 4°C for further treatment and finally archived in Bremen.

2.1.1 Computer tomographic analysis

Before sampling and splitting of sediment cores, a computer tomographic analysis was performed at the Universitätsklinikum Kiel, Department of Radiology by Dr. Morvain. Still closed core sections were investigated for their contents and sediment structures using a Phillips Tomoscan LX. The CT radiographs have been scanned and visually evaluated (Chapter 4, Appendix 6). This analysis divided the gravity cores into

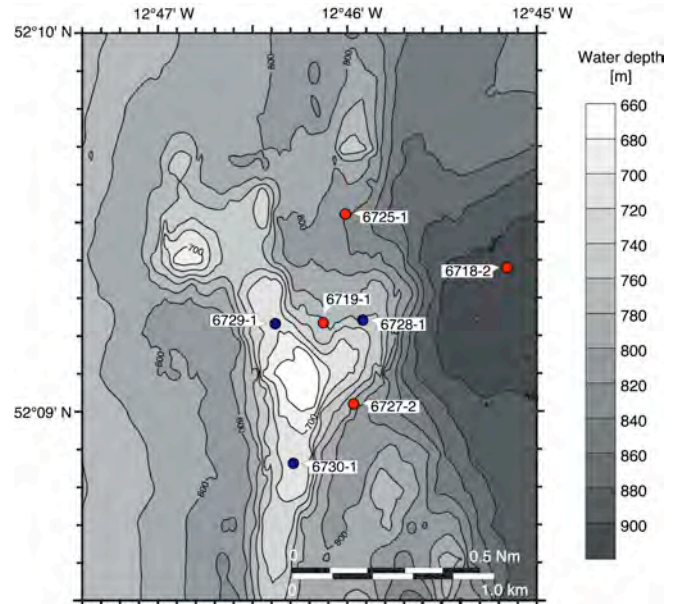


Figure 2-1. Locations of on- (blue) and off-mound cores (red) on Propeller Mound, recovered during RV POSEIDON cruise POS265 (Freiwald et al., 2000).

‘on-mound’ and ‘off-mound’ cores with on-mound cores containing large coral fragments (up to 30 cm in length), whereas off-mound cores represent coral rubble free, ‘normal’ sediment cores.

Table 2-1. Overview of gravity cores from Propeller Mound used in this study.

Core number	Latitude N	Longitude E	Water depth (m)	Recovery (cm)	Content	Core type
GeoB 6718-2	52°09.379'	12°45.158'	900	450	hemipelagic sediments	off-mound
GeoB 6719-1	52°09.233'	12°46.127'	758	580	hemipelagic sediments	off-mound
GeoB 6725-1	52°09.520'	12°46.010'	820	450	hemipelagic sediments	off-mound
GeoB 6727-2	52°08.017'	12°45.970'	794	470	hemipelagic sediments	off-mound
GeoB 6728-1	52°09.240'	12°45.920'	749	590	corals in fine grained matrix	on-mound
GeoB 6729-1	52°09.231'	12°45.380'	711	460	corals in fine grained matrix	on-mound
GeoB 6730-1	52°08.861'	12°46.282'	704	360	corals in fine grained matrix	on-mound

2.1.2 Opening procedure of cores

After the first results from CT analysis, the off-mound cores have been opened at University Bremen using conventional opening procedures. However, these failed on on-mound cores, as the coral fragments would have disturbed the sediment matrix and associated sedimentary features. Therefore, the cores were first frozen at -18°C for at least 72 hours. The frozen cores were then split using a diamond bladed circular saw. After cutting, the frozen cutting fluid and the upper surface of the cores were immediately removed with a spatula or knife. It was essential for retaining a good surface to perform the cleaning procedure on still frozen surfaces of the core halves. Serious damage to sedimentology structures has not been observed.

2.1.3 Visual core description

After splitting of the cores into working and archive halves and cleaning of their surfaces, all sections were visually described.

On-mound cores contain significant amounts of coral fragments of *L. pertusa* and *M. oculata*, and shells of associated benthic biota (echinodermata, molluscs, gastropods, brachiopods, and bryozoans) throughout the entire core sections. The coral density varies within the cores and is embedded in finer sediments consisting of foraminiferal tests, sponge spiculae, re-worked coral material, coccoliths and terrigenous material. The preservation state of larger coral fragments varies from living corals at the core top to heavily bioeroded and partly dissolved fragments in deeper parts.

Hemipelagic sediments dominate off-mound cores, which lack any indications of large coral fragments. Glacial sediments

contain numerous drop stones embedded in sandy silty clays. Silty sand represents interglacial sediments and is dominated by both planktonic and benthic foraminiferal tests. Those off-mound cores contain information of background sedimentation around Propeller Mound. They are used in this thesis for the determination of environmental condition of glacial and Holocene intervals, which then are compared to on-mound sediments.

2.1.4 Colour determination

Within less than an hour after opening, a spectral photometer (Minolta CM 2002) was used to achieve optical data of the sediment in the wavelength range of visible light. To protect the camera from pollution by sediment, the core surfaces were covered by transparent plastic foil. The measurement area of the spectrophotometer is 8 mm in diameter. To achieve the highest possible resolution, a sampling interval of 1 cm was chosen throughout the core. The camera was calibrated with black and white standards before every new core section measurement. The CM 2002 is equipped with a pulsed xenon arc lamp, which illuminates the integrating sphere of the spectrophotometer. Diffusely backscattered, the light hits the target, becomes reflected, and is focused on a silicon photodiode. The reflectance-intensity of a wavelength range of 400 nm to 700 nm (in 10 nm increments) and L^* (lightness), a^* (red-green shift), b^* (blue-yellow shift) values are detected by this sensor.

2.1.5 Sampling

Each working halve was sampled using 10 cm³ syringes at 5 cm intervals. All samples were weighed and then freeze dried at –50°C. With known sediment volume, the dry bulk density, porosity and water content were calculated from weight loss during freeze-drying. One set of samples was wet sieved through a 63 µm sieve and the sus-

pended fine fraction (<63 µm) was collected in 5-litre jars for fine fraction analysis (II.2.2). The coarse fraction (>63 µm) was oven dried at 50°C and weighed afterwards. To separate the grain size fractions, the coarse fraction was dry sieved through a sieve set with 125 µm, 250 µm, 500µm and 1000 µm mesh widths. All samples were weighed thereafter.

2.2 Sample analyses

2.2.1 Micropaleontological analysis

Biotic composition of benthic foraminifera was performed on samples of off-mound core GeoB 6725-1 and on-mound core GeoB 6730-1. At least 300 benthic specimens of foraminifera were identified on species level and counted in the fractions >125 µm. However, less than 300 specimens per sample could be identified in the off-mound core due to low numbers of foraminifera in glaciomarine sediments.

The concentration of benthic foraminifera was calculated into specimens per gram of sediment dry weight and percentages of total number of foraminiferal tests per sample. To determine the diversity of benthic foraminiferal assemblages (1) the species diversity expressed in numbers of species corrected to an equal size of 100 specimens (Lutze, 1980) and (2) the diversity index H(S) (Murray, 1991) was calculated. The designation of epibenthic and attached epibenthic species follows the observations and results of Murray (1991) and Schönfeld (1997; 2002a; 2002b). A taxonomic list of determined species is given in Appendix 1. Relative abundance of benthic foraminifera is given in Appendix 2-1 for off-mound core GeoB 6725-1

and in Appendix 2-2 for on-mound core GeoB 6730-1.

2.2.2 Grain size analysis

The collected fine fraction (<63 µm) was used to determine grain-size distribution of the silt-sized fraction (2–63 µm) and the sortable silt spectrum (10–63 µm, McCave et al., 1995). Therefore, a Micromeritics Sedigraph 5100 was used, which measures the concentration of the suspension by the attenuation of an X-Ray beam. Samples were separated from water, filled with Sodium polyphosphate (0.05 %) to avoid hindered settling. The samples were homogenised on a rotating carousel overnight (at least 15 hours) and sonified for 10 seconds before analysis. The grain size analysis was performed for on- and off-mound cores with a density setting of calcite (2.71 g/cm³) on a constant temperature of 35°C and with an analysis range of 1 to 63.1 µm. To evaluate the difference of bulk and carbonate-free grain-size distribution, organic material and CaCO₃ was removed from off-mound samples of core GeoB 6718-2 using H₂O₂ (35 %) and acetic acid (6 %). These samples

were measured with the density setting of quartz (2.65 g/cm³).

Sedigraph 5100 gives data output as cumulative curve and as mass frequency curves. Both were used to calculate mean silt and mean sortable silt distribution, as well as size frequency distribution. The data were converted into weight percentages (wt.-%) and are given in Appendix 3.

Principles of measurement, technical information, and comparisons to other grain size determination instruments can be found in Bianchi et al. (1999), McCave et al. (1995), and Konert and Vandenberghe (1997).

2.2.3 Total carbon and organic carbon measurements

Total carbon (TC) and total organic carbon (TOC) were analysed on on- and off-mound samples using Carlo Erba NA-1500-CNS at GEOMAR, Kiel (Appendix 4). The analytical method is based on the complete and instantaneous oxidation of the sample by „flash combustion“ at 1050°C, which converts all organic and inorganic substances into combustion products. The resulting combustion gases pass through a reduction furnace and are swept into the chromatographic column by the carrier gas (helium). The gases are separated in the column and detected by the thermal conductivity detector (TCD), which gives an output signal proportional to the concentration of the individual components of the mixture.

The freeze-dried samples were grinded in an agate mortar. Depending of the C/N/S concentration, 10 mg of sample is weighed into a tin cup (TC) and 7-9 mg into silver cup for the TOC measurements. Organic carbon is determined after removing car-

bonate carbon by acidification with 0.01N hydrochloric acid. Calibration standards for TC and TOC were Acetanilid (N=10.36 %, C=71.09 %) and SOIL Standard BSTD1 (N=0.216 %, C=3.5 %). Standard deviation of continuously analysed standards was better than 2 %. Carbonate contents of the sediments were finally calculated according to their atomic weight ratios:

$$\text{CaCO}_3 (\%) = 8.33 \cdot (\text{C}_{\text{total}} - \text{C}_{\text{org}})$$

2.2.4 Stable isotope analysis

Stable oxygen and carbon isotope analysis was carried out at Isotope Lab Bremen University. 3 to 5 individuals of benthic foraminifera *Cibicidoides wuellerstorfi* or *Cibicidoides kullenbergi* were selected from fraction 250–500 µm of on- and off-mound cores (Appendix 5). *C. wuellerstorfi* was rare in most of the samples, especially within the glaciomarine sediments. Therefore, the two species have been analysed in samples, where both occur. $\delta^{18}\text{O}$ values for both benthic species are comparable, but show an offset in $\delta^{13}\text{C}$, which is known from literature (e.g. Hodell et al., 2001) and related to the apparently infaunal life style of *C. kullenbergi*. Therefore, $\delta^{13}\text{C}$ data will not be considered within this thesis. Samples from the top 130 cm of off-mound core GeoB 6725-1 were additionally analysed for the stable isotope composition of planktonic foraminifera. For these analyses 15 specimens of *Globigerina bulloides* were collected from fraction 250–315 µm.

Isotopic composition of the foraminiferal tests was determined on the CO₂ gas evolved by treatment with phosphoric acid at a constant temperature of 75°C. Working standard (Burgbrohl CO₂ gas) was used for all stable isotope measurements. $\delta^{18}\text{O}$ and $\delta^{13}\text{C}$ data have been calibrated against PDB

by using the NBS 18, 19 and 20 standards and are given relative to the PDB standard. Analytical standard deviation is about ± 0.07 ‰ PDB.

2.2.5 Radiocarbon measurements

Radiocarbon dating (AMS ^{14}C) using mono-species samples (~ 10 mg) of planktonic foraminifera *Neogloboquadrina pachyderma* (either dextral or sinistral) from fraction 125–250 μm were analysed at the Leibniz Laboratory for Age Determinations and Isotope Research at the University of Kiel (Table 2-2; Nadeau et al., 1997). The data were corrected for ^{13}C and the calibration to calendar years was performed with CALIB 4.3 program (Stuiver and Reimer, 1993) using the marine data set of Stuiver et al. (1998) and a reservoir age of 400 years. All ages are given in 1000 calendar years before present (kyr BP; Table 2-2). Ages greater 21 kyr BP were calibrated using the method of Voelker et al. (1998).

2.2.6 U/Th dating on coral fragments

In several depth intervals of cores GeoB 6728-1, 6729-1 and 6730-1 some coral

fragments of *L. pertusa* were used to determine additional absolute ages using the U/Th ratio of the aragonite skeleton. All samples were first ultrasonically cleaned and scrubbed with dental tools to remove exterior contaminants (iron-manganese crusts and coatings) from the fossil coral fragments as described in Cheng et al. (2000a). When the coral appeared clean under the binocular, a first run was performed on samples of cores GeoB 6728-1, 6729-1 and 6730-1. The samples were measured by V. Liebetrau using a Finnigan MAT 262 RPQ2+ Thermal Ionisation Mass Spectrometer (TIMS) at GEOMAR, Kiel. Uranium and Thorium concentrations and activities are given in Table 2-3. The dating method using U/Th ratios requires several conditions for reliable datings: (1) a closed system decay of U and Th, without any exchange between carbonate and water mass, (2) no additional U or Th through detrital contamination, and (3) no ^{230}Th within the carbonate during formation. The latter requirement has to be assumed, as it is not possible to determine initial ^{230}Th ratios, which normally originates exclusively by ^{234}U decay within the carbonate.

Table 2-2. AMS ^{14}C dates of core GeoB 6719-1, GeoB 6725-1 and GeoB 6730-1.

Laboratory number	core depth (cm)	^{14}C AMS age (yr BP)	\pm err. (yr)	Calibrated age (kyr BP)
Core GeoB 6719-1				
KIA 17091	18	6200	35	6640
KIA 19092	98	16100	70	18630
KIA 17093	163	21670	110	25420
KIA 17094	273	26780	180	30830
Core GeoB 6725-1				
KIA 16206	68	7135	45	7600
KIA 16202	168	20360	140	23530
Core GeoB 6730-1				
KIA 16201	23	4370	35	4500
KIA 16200	93	42700	+2090/-1660	44770
KIA 16198	143	>45070	-	-
KIA 16197	208	45010	+2820/-2080	46510
KIA 16196	243	>44350	-	-

Table 2-3. U/Th dates of on-mound cores GeoB 6728-1, GeoB 6729-1 and GeoB 6730-1

Core #	Core depth (cm)	$^{234}\text{U}/^{238}\text{U}$ (%)	^{238}U (dpm/g)	^{230}Th (dpm/g)	^{232}Th (dpm/g)	$^{230}\text{Th}/^{232}\text{Th}$ (dpm/g)	$^{230}\text{Th}/^{234}\text{Th}$ (dpm/g)	age (kyr BP)	error (kyr)
GeoB 6728-1									
	3 ^a	86 ±2	2.251 ±0.002	1.825 ±0.008	0.01621 ±0.00002	112.6 ±0.5	0.741 ±0.003	143	1.3
	83	82 ±3	2.549 ±0.003	2.263 ±0.004	0.00533 ±0.00001	424.6 ±0.9	0.818 ±0.002	178	1.0
	218 ^a	72 ±2	2.495 ±0.003	2.323 ±0.009	0.01473 ±0.00003	157.7 ±0.7	0.865 ±0.004	207	2.6
	368	60 ±3	2.574 ±0.004	2.531 ±0.008	0.00929 ±0.00002	272.3 ±1.0	0.924 ±0.003	261	3.6
GeoB 6729-1									
	23	113 ±3	3.086 ±0.003	1.332 ±0.006	0.02022 ±0.00030	66.8 ±0.3	0.388 ±0.002	53	0.3
	73	80 ±3	2.416 ±0.003	2.095 ±0.007	0.01395 ±0.00002	151.0 ±0.5	0.802 ±0.003	170	1.4
	143 ^a	33 ±3	1.966 ±0.002	1.887 ±0.031	0.00976 ±0.00013	194.2 ±4.0	0.929 ±0.015	275	20
	268 ^a	44 ±2	2.630 ±0.003	2.607 ±0.006	0.00678 ±0.00001	385.5 ±1.0	0.949 ±0.003	300	4.1
GeoB 6730-1									
	88	107 ±2	3.294 ±0.003	2.122 ±0.003	0.01370 ±0.00003	155.8 ±0.4	0.582 ±0.001	93	0.3
	158	109 ±4	1.994 ±0.003	1.526 ±0.006	0.03068 ±0.00004	50.6 ±0.2	0.690 ±0.003	124	1.0
	188 ^a	77 ±2	2.906 ±0.003	2.552 ±0.043	0.00744 ±0.00005	343.1 ±6.3	0.813 ±0.014	176	7.3
	268	82 ±7	2.673 ±0.008	2.357 ±0.007	0.01040 ±0.00001	226.5 ±0.7	0.815 ±0.003	176	1.8
	358 ^a	62 ±3	3.184 ±0.005	2.891 ±0.011	0.02652 ±0.00004	109.9 ±0.5	0.855 ±0.003	207	2.5

Remarks: ^a samples below radioactive decay of initial ^{234}U of seawater. Half-lives of ^{234}U and ^{230}Th used in the calculations are 245,250 ±490 yr and 75,690 ± 230 yr respectively (Cheng et al., 2000b). The decay constant for ^{238}U is 1.551 x 10⁻¹⁰ yr⁻¹ (Jaffey et al., 1971). All errors are 2 σ .

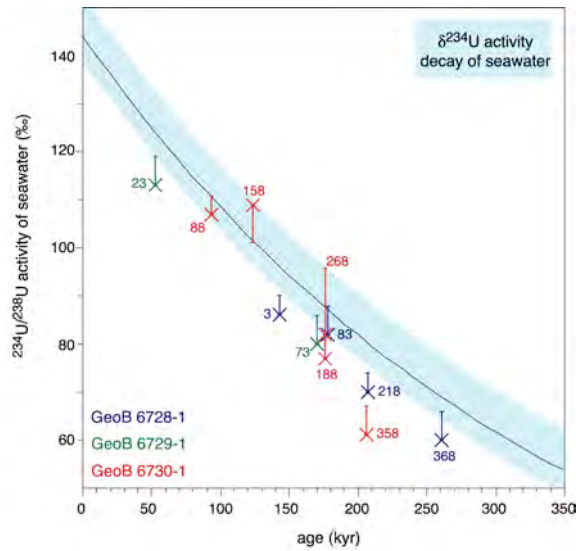


Figure 2-2. ^{234}U activity of coral fragment from on-mound cores according to time. Shaded blue area indicates the decay of initial seawater ($^{234}\text{U}=140\text{--}155\text{‰}$). Samples, which fall out of range are marked in Tab. 2-3.

The initial activity ratio of $^{234}\text{U}/^{238}\text{U}$ (^{234}U) of the samples follows the evolution curve starting with the activity ratio of seawater ($^{234}\text{U} = 155\text{--}140\text{‰}$), which is illustrated in Figure 2-2 and determines the reliability of dating. Towards older ages, the samples show an increase in deviation from the ^{234}U decay of seawater. These samples tend to lighter ^{234}U values, which are indicated in Table 2-3.

In a second run, all samples were additionally bathed after the macro- and microscopic cleaning in a 50/50 mixture of 30 % peroxide and 1M NaOH for 15 minutes with ultrasonification. This procedure removed organic stains left on the coral and up to 50 % of the inner and outer coral skeleton. Cheng et al. (2000a) described another step, where the samples are submerged afterwards in a 50/50 mixture of 30 % peroxide and 1 % HClO_4 . This step of the cleaning procedure was skipped, otherwise no material would have been left. The samples were additionally checked for the

cleanness of the aragonite. A little part of three samples was cut off before and after the chemical cleaning procedure and was analysed using X-ray diffraction (XRD), to evaluate the chemical composition (Fig. 2-3). The results of XRD analysis show that the coral skeletons consist of >95 % of aragonite and to a minor degree of calcite and quartz as contamination. After the cleaning procedure up to 100 % aragonite had been measured, indicating pure aragonite skeletons of fossil coral fragments also in deeper core sections.

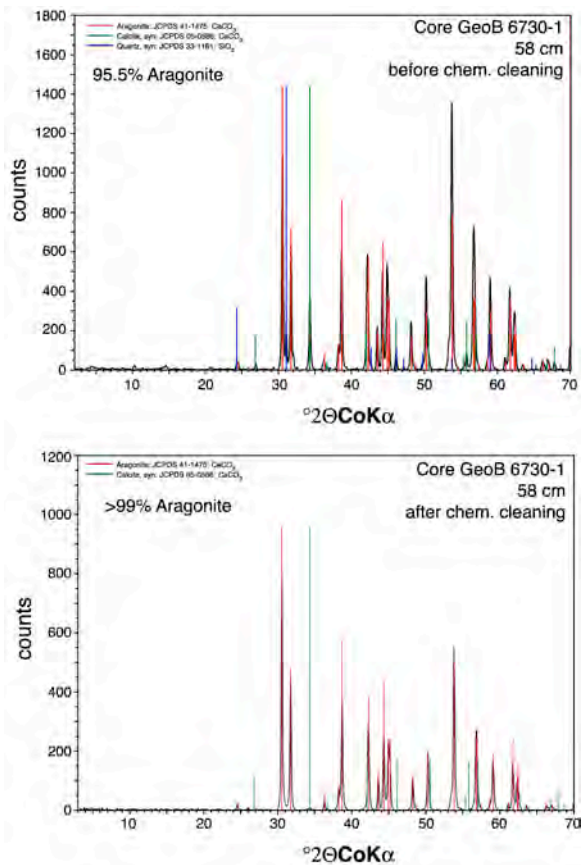


Figure 2-3. XRD analysis of coral fragment before and after chemical cleaning. Before the cleaning procedure, intensity peaks indicate the sample consisting of aragonite, calcite and quartz. After the cleaning, >99 % aragonite of the same sample describes all major peaks. Calcite occurs accessorially whether as contamination of coccoliths and foraminiferal test fragments or as recrystallisation of the primary aragonite. Quartz was removed completely.

CHAPTER 3

BENTHIC FORAMINIFERAL ASSEMBLAGES FROM PROPELLER MOUND, NORTHERN PORCUPINE SEABIGHT

Andres Rüggeberg¹, Boris Dorschel², Wolf-Christian Dullo¹, and Dierk Hebbeln²

¹ GEOMAR Research Center for Marine Geosciences, Wischhofstr. 1-3, D-24148 Kiel; Germany

² Department of Geology, University of Bremen, Postbox 330440, D-28334 Bremen, Germany

submitted to

Marine Micropaleontology

Abstract

The benthic environment in the vicinity of a carbonate mound at the northern Porcupine Seabight was studied on two sediment cores: one from top of the Propeller Mound, a 150 m high carbonate mound densely colonised by a deep-water coral ecosystem on the upper flanks, and a second one from an off-mound position further north as control site. At the off-mound position faunal analysis of dead benthic foraminifera reveals two assemblages. The *Interglacial group* contains infaunal species reflecting present-day environmental and oceanographic conditions with high nutrient flux to the sea-floor and low sediment accumulation under a strong hydrodynamic regime. The *Glacial group*, dominated by cassidulinid species, describes an influence under polar conditions with low nutrient supply and cold intermediate waters. *Elphidium excavatum* is described here as a species displaced from shallow shelf areas under the influence of the glacial ice cap on Ireland, which advanced towards the shelf, inducing high sedimentation rates of ~30 cm/kyr with a coeval sea-level drop of ~50 m.

The off-mound identified assemblages have been transferred to the on-mound core and show that the *Glacial group* is less abundant throughout the entire core. This pattern indicates the lack of glacial time intervals in the on-mound core. A third assemblage is abundant in samples of the on-mound core showing elevated epibenthic species not described in off-mound samples or only to a minor degree. This *Mound group* shows a great affinity to strong currents, high nutrient availability and is supposed to indicate Mediterranean Outflow Water in the northern Porcupine Seabight and a higher amount of substrates (i.e. corals) to settle.

Keywords: benthic foraminifera; carbonate mounds; environmental reconstruction; Porcupine Seabight; NE Atlantic Ocean

3.1 Introduction

3.1.1 Benthic foraminiferal study in the Porcupine Seabight

Benthic foraminiferal faunas contain information on oceanic deep environments and are therefore a good tool to reconstruct paleoenvironments. Several studies deal with recent distributions of living benthic foraminifera, which prove the relationship between abundances of distinct species and the nutrient flux to the sea-floor (e.g. Loubere, 1991; Mackensen et al., 1993; Kaiho, 1994; Altenbach et al., 1999), the ambient bottom waters oxygen content (Kaiho, 1994; Alve, 1995; Brüchert et al., 2000; Seidenkrantz et al., 2000) or other levels of environmental stress like water turbulence (Pujos, 1971; Schönfeld, 1997; 2002a; 2002b; Schönfeld and Zahn, 2000). The understanding of faunal abundances mirroring present-day environmental conditions can be helpful for the reconstruction of fossil assemblages in relation to changes of water mass physics and chemistry, nutrient availability, microhabitat colonisation structures or reworking of sediments.

Studies on benthic foraminiferal assemblages from sediments of the Porcupine Seabight (PSB) have been confined on analyses of surface samples. Weston (1985) presents both, living and dead benthic foraminiferal assemblages from surface samples south of 51°50'N in the PSB and found extremely good zonations of foraminiferal faunas with respect to depth, dominated by *Trifarina angulosa*, *Gavelinopsis lobatulus* and *Uvigerina pygmaea*. Other studies (e.g. Gooday, 1986; Lamshead and Gooday, 1990) focussed their analyses on spatial distribution of living epibenthic and shallow infaunal species and their response to sea-

sonally deposited phytodetritus within the northern part of the Sea Bight.

However, little is known about benthic foraminiferal assemblages and their variations over the past glacial-interglacial cycle(s) for the PSB. Such studies are reported from areas further offshore in the Rockall Trough (e.g. Rasmussen et al., 2002a; 2002b; Thomas et al., 1995), to the north of the Sea Bight, offshore Scotland (Austin and Kroon, 1996) or in areas of the Western Approaches to the south of the PSB (Caralp, 1985).

Carbonate mounds occur in a distinct depth range of the PSB and are densely settled by cold-water corals, mainly *Lophelia pertusa* (Freiwald, 2002). Studies on faunal abundances of benthic foraminifera from these carbonate mounds are extremely limited. Only Coles et al. (1996) described species in relation to carbonate mounds of the northern PSB. Their study only presents analysis of sediment samples from core top and core base with varying sample size, which is insufficient to interpret faunal changes through time. However, the authors give a first overview about benthic foraminifera in relation to carbonate mounds.

The aim of this study is to present first results of a detailed study of benthic foraminifera from two sediment cores (off-mound core GeoB 6725-1 and on-mound core GeoB 6730-1, Fig. 3-1) from the northern PSB. The distribution and abundance of the dominant and subdominant species is described in detail and has been related to oceanographic and environmental conditions. Furthermore the identified assemblages of the off-mound core are compared to the samples from the on-mound position to reveal similarities and differences of the two different environments.

3.1.2 Study area and hydrography

The PSB is an amphitheatre-like embayment widening to the southeast. It is bound by the Irish mainland shelf to the east, the Slyne Ridge to the north, and the Porcupine Bank to the west (Fig. 3-1). The shallowest parts (<200 m) are represented by the shelf and occur in the northern PSB, deepening gradually towards the south, where a depth of >4000 m is reached (Porcupine Abyssal Plain). The shallow shelf is predominantly covered by fine to coarse sand and varying

carbonate contents of 25 to >75 %. Below ~500 m depth the mud content as well as the number of abundant pebbles and boulders increases and the carbonate content is generally >50 % (Scoffin and Bowes, 1988). This environment is under the influence of the Eastern North Atlantic Water (ENAW) extending from the seasonal thermocline (~50 m) down to about 600 m depth (White, *subm.*).

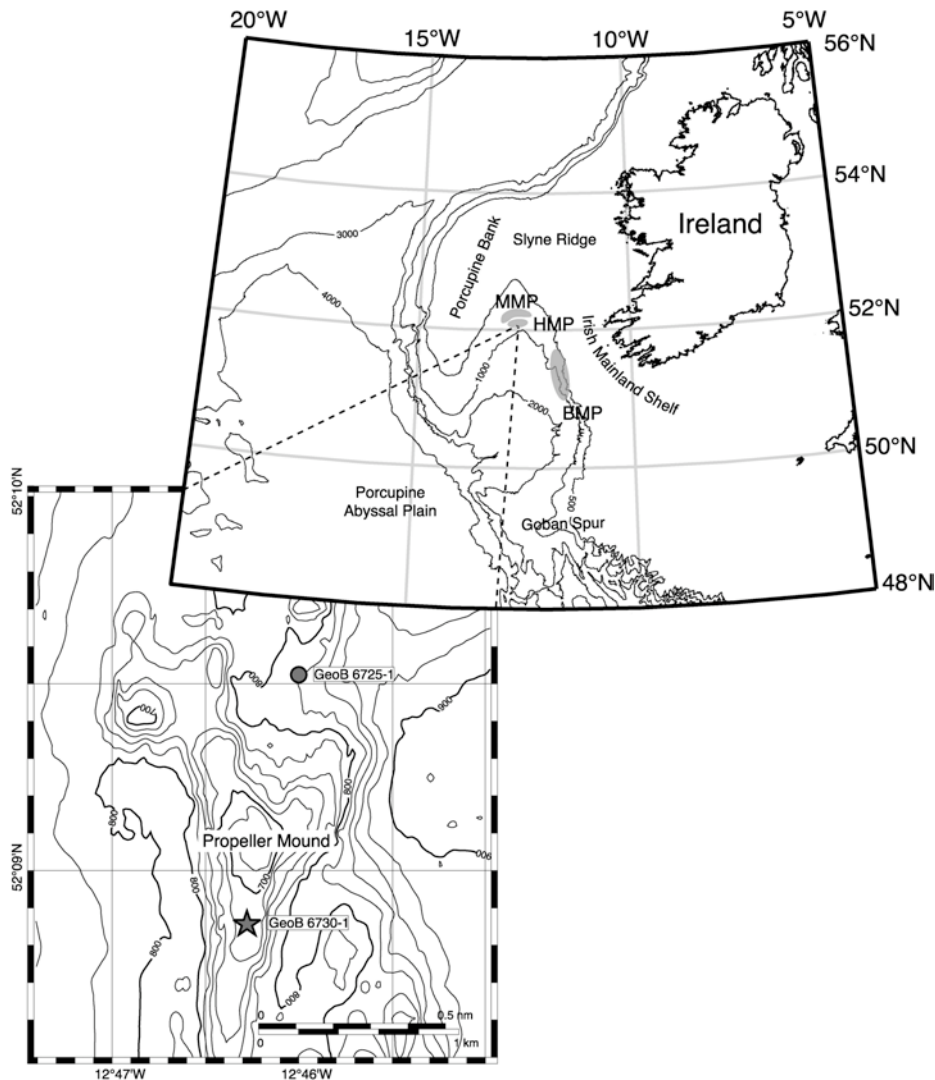


Figure 3-1. Location of Propeller Mound within the Hovland Mound province (HMP), northern Porcupine Seabight (MMP = Magellan Mound province, BMP = Belgica Mound province). Indicated are the locations of the investigated on-mound core GeoB 6730-1 (star) and off-mound core GeoB 6725-1 (circle).

The ENAW originates in the Bay of Biscay, produced by deep convection during wintertime. This water mass flows poleward along and adjacent to the NE Atlantic margin (Pollard et al., 1996), enters the PSB and turns cyclonically in the northern PSB to flow topographically steered around the Porcupine Bank into the Rockall Trough (Mohn, 2000). A similar flow pattern is described for the Mediterranean Outflow Water (MOW) underlying the ENAW in 800–1000 m depth. Increasing salinity and decreasing oxygen content below 600 m indicates the mixing-zone of ENAW and MOW (McCave et al., 2001; White, 2001; White, *subm*; Fig. 3-2).

In this water depth (600–1000 m) three carbonate mound provinces are described (Fig. 3-1): (1) the Belgica Mound province (BMP) along the eastern slope with high elevated structures, (2) the Hovland Mound

province (HMP) located at the northern PSB, which is bound by (3) the Magellan Mound province (MMP) further northwest with mounds already buried by a Pleistocene sediment cover as indicated through seismic investigations (Henriet et al., 1998; Freiwald et al., 2000; 2002; De Mol et al., 2002; Van Rooij et al., 2003).

These mounds are densely settled with cold-water corals on the tops and flanks (Freiwald, 2002) and are elevated up to 200 m above the surrounding sea-floor. Strong currents are reported from the Belgica Mound province (mean flow of 10 cm s^{-1} , Pingree and LeCann, 1990). These current speeds decrease to mean flows of $2\text{--}5 \text{ cm s}^{-1}$ for the Hovland-Magellan Mound provinces as a result of a changing current regime, which turns from northern to southern directions (White, *subm*).

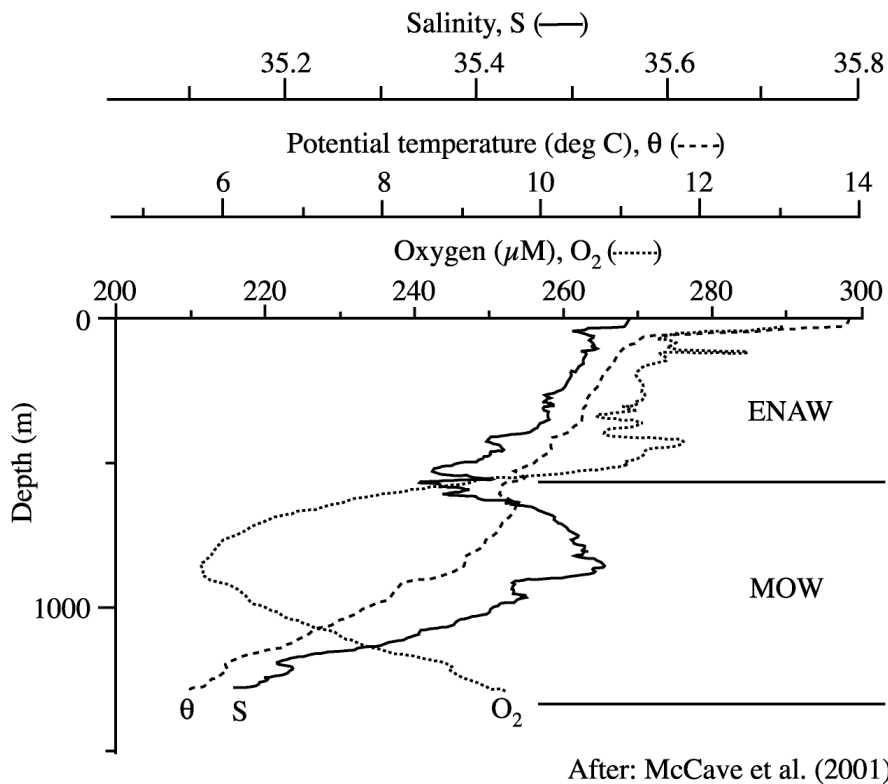


Figure 3-2. Hydrographic parameters and characteristic water masses of the upper 1500 m from outer Goban Spur (from McCave et al. 2001). ENAW: Eastern North Atlantic Water, MOW: Mediterranean Outflow Water.

Internal wave reflections forced by the dominant tidal period additionally contribute to enhanced currents for the eastern Sea Bight, but not along the northern margin of the Hovland and Magellan mounds (White, *subm.*).

The Propeller Mound is situated at the southern edge of the Hovland Mound province. Its morphology describes a N-S extension with three spurs pointing towards the NE, NW and S (Fig. 3-1). Moats occur around the foot of the mound and the steepest flanks of up to 45° are at the western side. These features strongly correlate with the hydrodynamic regime, in this case with

strong bottom currents flowing from northerly directions to the south with mean velocities of up to 5 cm s⁻¹ (White, 2001). Nowadays, cold-water corals cover the upper flanks of Propeller Mound, whereas the top and the deeper flanks mainly consist of dead coral fragments embedded in hemipelagic sediments. At core site GeoB 6730-1 only patches of coral growth are present as reported by underwater investigations using ROV CHEROKEE of RCOM, University of Bremen (Freiwald and Shipboard Party., 2002).

3.2 Materials and Methods

Two sediment cores from the Propeller Mound region, GeoB 6725-1 (52°09.52' N, 12°46.01' W; water depth 820 m; 450 cm core length) and GeoB 6730-1 (52°08.86' N, 12°46.28' W; water depth 704 m; 360 cm core length; see Fig. 3-1) were investigated. Both cores were recovered during RV POSEIDON cruise POS 265 in September 2000 (Freiwald et al., 2000). Core GeoB 6730-1 bears fragments of predominantly cold-water coral *L. pertusa* and is hereafter referred to as “on-mound core”, whereas “off-mound core” GeoB 6725-1 is composed of hemipelagic sediments. Both cores were sampled at 5 cm intervals using 10 ml syringes. Each sample was weighed, carefully washed over 63 µm sieves, dried at 50°C and weighed again. For faunal analysis all samples were dry sieved through a sieve set into fractions 63–125 µm, 125–250 µm, 250–500 µm, 500–1000 µm and >1000 µm.

3.2.1 Foraminifera analyses

To determine faunal composition of both cores a minimum of 300 benthic specimens of foraminifera from the >125 µm fraction were identified on species level and counted in each sample. Due to low numbers of foraminifera in glacial sediments, less than 300 specimens per sample were counted in the off-mound core. The concentration of benthic foraminifera was calculated as individuals per gram of sediment dry weight (ind/g) and percentages of total number of foraminiferal tests per sample (%). To determine the diversity of benthic foraminiferal assemblages (1) the species diversity expressed in numbers of species corrected to an equal size of 100 specimens (Lutze, 1980) and (2) the diversity index H(S) (Murray 1991) was calculated. The designation of epibenthic and attached epibenthic species follows the observations and results of Murray (1991) and Schönfeld (1997; 2002a; 2002b). A taxonomic list of the dominant (>10 % of total abundance) and subdominant (5–10 %), as well as some minor (<5 %) species of benthic foraminifera

fera described in this study is given in Appendix 1. Relative abundances of benthic foraminifera are given in Appendix 2 for off-mound core GeoB 6725-1 and in Appendix 3 for on-mound core GeoB 6730-1.

3.2.2 Stratigraphic analyses

The age models for cores GeoB 6725-1 and GeoB 6730-1 are based on accelerator mass spectrometry (AMS) ^{14}C dates, stable oxygen isotope data and U/Th dates for the on-mound core (Table 3-1).

Stable oxygen isotope composition of shells of benthic foraminifera *Cibicidoides kullenbergi* or *Cibicidoides wuellerstorfi* (3–5 specimens of fraction 250–500 μm) and planktic foraminifera *Globigerina bulloides* (15 specimens of fraction 250–315 μm) were measured with a Finni-

gan MAT 251 mass spectrometer at Isotope Lab Bremen University.

The isotopic composition of the carbonate sample was measured on the CO_2 gas evolved by treatment with phosphoric acid at a constant temperature of 75°C. For all stable isotope measurements a working standard (Burgbrohl CO_2 gas) was used, which has been calibrated against PDB using NBS 18, 19 and 20 standards. Consequently, all $\delta^{18}\text{O}$ data given here are relative to the PDB standard. Analytical standard deviation is about ± 0.07 ‰ PDB. AMS ^{14}C dates on *Neogloboquadrina pachyderma* (either dextral or sinistral, fraction 125–250 μm , ~10 mg) were analysed at Leibniz Laboratory for Age Determinations and Isotope Research, University Kiel (Nadeau et al., 1997). Calibration to calendar years was performed using Calib 4.3 software

Table 3-1. AMS ^{14}C dates, U/Th dates and age control points of cores GeoB 6725-1 and GeoB 6730-1.

Laboratory number ^a	Core depth (cm)	AMS ^{14}C age (yr BP)	\pm Err. (yr)	Calibrated age (cal yr BP)
Core GeoB 6725-1				
KIA 16206	68	7135	45	7600
KIA 16202	168	20360	140	23530
	368			30830 ^b
Core GeoB 6730-1				
KIA 16201	23	4370	35	4500
	88		300	93000 ^c
KIA 16200	93	42700	+2090/-1660	> 45000
	158		1000	124000 ^c
	188		7300	176000 ^d
KIA 16196	208	45010	+2820/-2080	> 45000
	268		1800	176000 ^c
	358		2500	207000 ^c

The ^{14}C ages were corrected for a reservoir effect of 400 yr and calibrated using the Calib 4.3 software of Stuiver and Reimer (1993).

^a KIA, Leibniz Laboratory, University of Kiel, Germany.

^b Inter-core correlation to off-mound cores GeoB 6719-1 and GeoB 6718-2 (Appendix 7).

^c U/Th dates performed by V. Liebetrau, GEOMAR Kiel, Germany. Detailed ratios published in Appendix 7.

^d U/Th ratios: $^{234}\text{U}/^{238}\text{U} = 77 \pm 2$ ‰; $^{238}\text{U} = 2.906 \pm 0.003$ dpm/g; $^{230}\text{Th} = 2.546 \pm 0.043$ dpm/g; $^{232}\text{Th} = 0.00744 \pm 0.00005$ dpm/g; $^{230}\text{Th}/^{232}\text{Th} = 343.1 \pm 6.3$ dpm/g; $^{230}\text{Th}/^{234}\text{U} = 0.813 \pm 0.014$ dpm/g.

(Stuiver and Reimer, 1993) and marine data set of Stuiver et al. (1998) with a reservoir age of 400 yr. All ages are given as 10^3 calendar years before present (kyr BP).

Fragments of cold-water coral *Lophelia pertusa*, which occur throughout the entire on-mound core, were used for determination of the U/Th ratio of the aragonite skeleton.

The coral fragments were physically cleaned to remove secondary Mn- and Fe-coatings following the standard procedure described in Cheng et al. (2000a). Sample measurements using a Finnigan MAT 262 RPQ2+ Thermal Ionisation Mass Spectrometer (TIMS) were performed at GEOMAR, Kiel. All absolute ages are given in Table 3-1.

3.3 Stratigraphy

Off-mound core GeoB 6725-1 comprises the marine isotopic stages (MIS) 1, 2 and Late 3 (Fig. 3-3a). The evaluation of the stratigraphy is based on (1) AMS ^{14}C dates, (2) stable isotope measurements on *C. kullenbergi*, *C. wuellerstorfi* and *G. bulloides* (for top 120 cm, which corresponds to the last 20 kyr BP) and (3) inter-core correlation with off-mound cores GeoB 6718-2 and GeoB 6719-1 (Appendix 7).

The lower core part is characterised by reworked material (not shown). Correlation to other off-mound records reveals an age of >31 kyr BP for this turbidite event. Late MIS 3 is characterised by high benthic $\delta^{18}\text{O}$ values of 3–3.5 ‰ increasing slightly towards MIS 2 to >3.5 ‰. An AMS ^{14}C date indicates an age of 23.5 kyr BP after the transition of MIS 3 to 2 (Appendix 7). MIS 2 shows high benthic and planktonic $\delta^{18}\text{O}$ values. At around 14 kyr BP the planktonic stable oxygen isotopes reaches much lighter values. Visual core description indicates a large burrow consisting of coarse and carbonate-rich sediments. An additional AMS ^{14}C date within this section indicates an age of 7.65 kyr BP, indicating an interval of bioturbated sediments. Again, light planktonic $\delta^{18}\text{O}$ values occur in the Holocene section as illustrated in Figure 3-3a, whereas the benthic $\delta^{18}\text{O}$ values remain very high

most certainly due to bioturbation by transferring the dominant glacial foraminifera *C. kullenbergi* into the Holocene sequence. Sedimentation rates vary between 2–3 cm/kyr for the Holocene, ~10 cm/kyr for MIS 2 and ~30 cm/kyr for late MIS 3. Similar values are also reported in other near shelf studies of the NE Atlantic (e.g. Rasmussen et al., 2002b; Auffret et al., 2002; De Mol et al., 2002).

The classification into marine isotope stages is still insufficient for on-mound core GeoB 6730-1 (Fig. 3-3b). The benthic oxygen isotope values show a higher variability than those of the off-mound record. The stable oxygen isotope record of the lower core part (60–360 cm) fluctuates between 1.8 and 3.2 ‰ suggesting that the peak glacial sediments, which show $\delta^{18}\text{O}$ values of >3.5 ‰ in the off-mound record, but also peak interglacial sediments (<1.8 ‰, Fig. 3-3b) had been removed from the mound (Appendix 8). U/Th dates support the assumption that no glacial sediments occur in the on-mound record (Fig. 3-3b). Dorschel et al. (Appendix 8) point out several hiatuses characterised by distinct peaks of coarse lithic grains, which occur mostly at abrupt shifts in stable oxygen isotopes (Fig. 3-3b). They relate these concentrations of coarse grains to ice rafted detritus

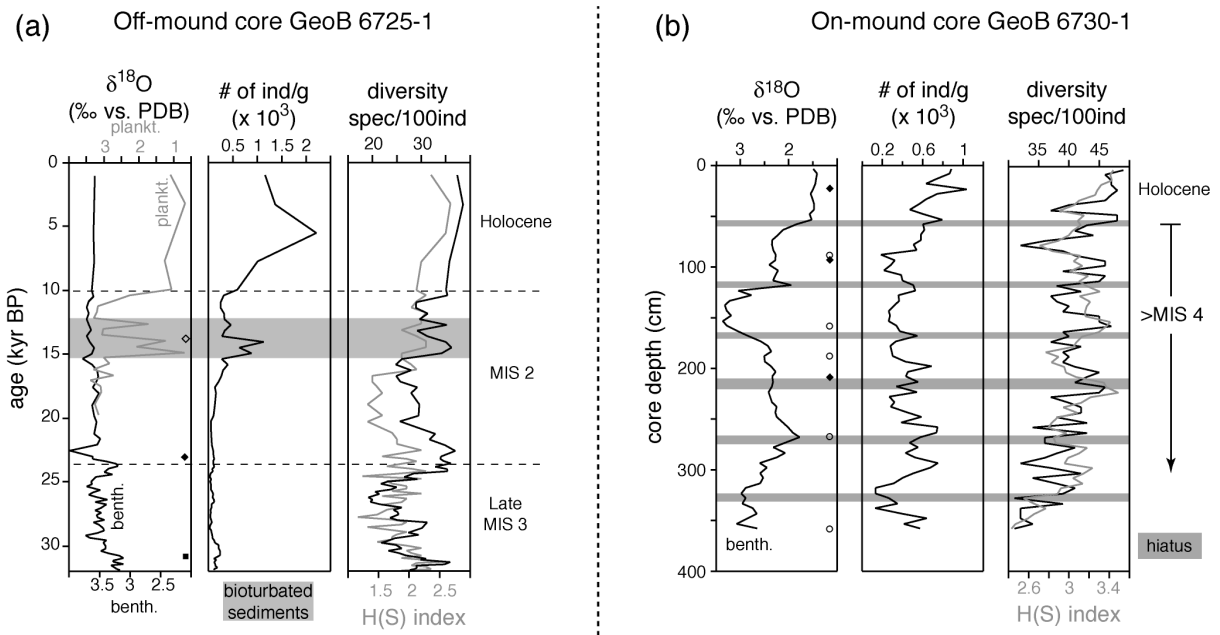


Figure 3-3. Stable isotopes, absolute abundance of benthic foraminifera in numbers of individuals per gram dry weight sediment (ind/g) and benthic diversity indices (spec/100ind) of (a) off-mound core GeoB 6725-1 and (b) on-mound core GeoB 6730-1. Light grey areas indicate bioturbated sediments within the off-mound core (a) and removal of glacial sediments (hiatuses) for the on-mound core (b), respectively (hiatuses from Appendix 8). AMS ^{14}C dates (filled diamond, open diamond = bioturbated age), date revealed from inter-core correlation (square) and U/Th dates (open circles) are listed in Table 3-1.

deposited during glacials and winnowed during terminations, where the current regime is enhanced. These results suggest a division into several sections, which may be related to interglacial or interstadial periods (Fig. 3-3b). Low $\delta^{18}O$ values of ~ 1.5 ‰ and an AMS date of 4.5 kyr BP at 23 cm clearly characterise a Holocene cover of 50–60 cm.

3.4 Benthic foraminiferal species and assemblages in off-mound sediments

In core GeoB 6725-1, a total of 97 identified species belonging to 57 genera of benthic foraminifera have been found. Absolute abundance of benthic species is low in sediments comprising MIS 3 rarely exceed-

ing 200 ind/g, but increasing abruptly to >2000 ind/g during the Holocene (Fig. 3-3a). The normalised species diversity and diversity index $H(S)$ decrease from around 30 species ($H(S) \approx 2.5$) during late MIS 3 to 20 species ($H(S) \approx 2$) for MIS 2 and exceed values of 30 species ($H(S) > 2.6$) in the Holocene (Fig. 3-3a).

Classification into dominant, subdominant and minor species reduces the total number of 97 species to fourteen most abundant species, which represent on average 76.6 % of the total assemblage. Two distinct assemblages have been determined (Fig. 3-4). One assemblage depicts high relative abundance of 60–80 % during MIS 3 and 2, referred to as *Glacial group*. Species of the second assemblage dominate samples with >60 % during the Holocene

and therefore is referred to as *Interglacial group*. Dominant relative abundance of the single species *Elphidium excavatum* exceeding 50 % during late MIS 3 is coherent with high sediment supply and indicates that this species is considered as a displaced one and is therefore not contributing to the fossil community.

3.4.1 Special conditions for *Elphidium excavatum*

E. excavatum shows high relative abundance of >50 % in the lower core part of GeoB 6725-1 (Fig. 3-5). According to Seidenkrantz et al. (2000) it belongs to the epi-

phytic taxa, but Murray (1991) described non-keeled species of the family *Elphidiidae* as infaunal, living free in the sediment of the inner shelf. *E. excavatum* is extremely tolerant to and adaptable of large variations in temperature, salinity and food supply (Linke and Lutze, 1993), which is profitable for surviving in near glacial environments (Nagy, 1965; Hald et al., 1994). It occurs in shallow polar seas (Hald et al., 1994; Schröder-Adams et al., 1990), in the proximity of river estuaries in the Barents and Kara Sea, in areas with heaviest ice cover (Steinsund and Hald, 1994) and in ice-rafted sediments in the Norwegian Sea (Hald and Vorren, 1987).

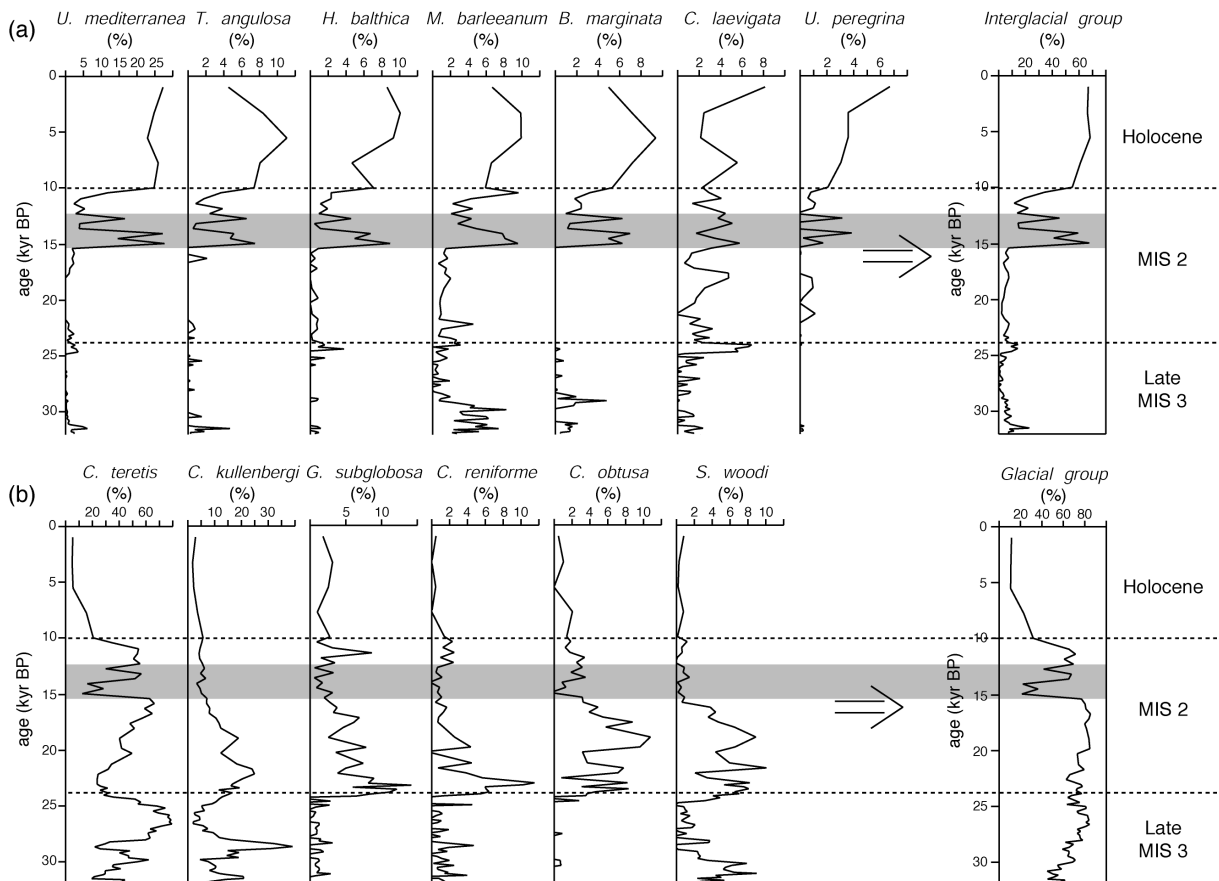


Figure 3-4. Relative abundance of dominant and subdominant benthic foraminifera of off-mound core GeoB 6725-1. (a) Species with highest abundance during the Holocene. (b) Species with highest abundance during MIS 2 and 3. Light grey = bioturbation. Note: Species *E. excavatum* is not considered within calculation of relative abundance of illustrated species (see text).

The depth range of *E. excavatum* is discussed controversially in the literature. Seidenkrantz et al. (2000) reported this species to live in shallow shelf areas generally above 200 m, but it has been reported to survive, even if passively transported to greater depth (Bergsten, 1994; Corliss, 1991). At the Faeroe-Shetland Ridge in water depths >1000 m, Rasmussen et al. (1996) concluded that this species is most important for transitional cooling events. A study on glacial sediments from Ireland's east coast and the Irish Sea describes very high abundance of 80 to 95 % of *E. excavatum* in marine mud beds below and interbedded with ice-contact outwash (McCabe and Clark, 1998). They relate the occurrence of this species to areas vacated by tidewater glaciers, as reported from contemporary Arctic-subarctic areas. According to Struck (1992),

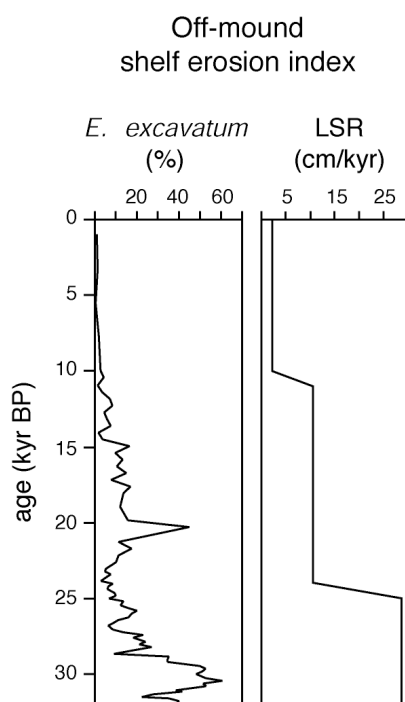


Figure 3-5. Relative abundance of *Elphidium excavatum* and Linear Sedimentation Rate (LSR) of the off-mound core. Both records show a strong correlation, which determines *E. excavatum* to be considered as a displaced species.

the abundance of *E. excavatum* is considered to be an indication of erosional processes from shallow shelf areas and therefore is not part of the fossil community.

3.4.2 The Glacial group

The *Glacial group* is dominated by *Cassidulina teretis*, *Globocassidulina subglobosa*, *Cassidulina reniforme*, *Cibicidoides kullenbergi*, and the subdominant species *Cassidulina obtusa* and *Sigmoilopsis woodi*. This assemblage depicts high relative abundance for MIS 3 (>50 %) and increases to values up to 80 % for late MIS 3 and MIS 2 (Fig. 3-4b).

C. teretis is the most abundant species in this assemblage. It increases from 20 % to maximum of 70 % during late MIS 3, shows lower relative abundance of 23 % for the onset of MIS 2 and increases again to 60 % within peak glaciation (Fig. 3-4b). *C. teretis* is reported to live shallow infaunal (Murray, 1991) but also as epifaunal on sponge needles (Altenbach, 1992). It feeds on organic debris at the surface or in the uppermost layer of the sediment (Korsun and Polyak, 1989). Mackensen and Hald (1988) described *C. teretis* as a continental slope species thriving in cold bottom waters (-1°C) from the Norwegian shelf and slope, preferring fine-grained, organic-rich, terrigenous mud. In the Barents and Kara Sea, Steinsund and Hald (1994) observed this species following chilled Atlantic waters.

In sections with lower abundance of *C. teretis* (onset of MIS 2, around 23–24 kyr BP and in late MIS 3 at 28.5 and 31 kyr BP), *G. subglobosa*, *C. reniforme*, *C. kullenbergi*, *C. obtusa* and *S. woodi* show their maximum relative abundances (Fig. 3-4b). *C. reniforme* seems to prefer similar conditions as *C. teretis* and is fre-

quent in glaciomarine environments (Elverhøi and Bomstad, 1980; Østeby and Nagy, 1982). This suggests that *C. teretis* and *C. reniforme* are opportunistic species taking advantage of generally unfavourable environments (Steinsund and Hald, 1994) with respect to low temperatures and zones of oxygen depletion (Kaiho, 1994; Mullins et al., 1985). *C. obtusa* has been found on the Norwegian shelf mainly in troughs where sandy mud facies occur (Hald and Vorren, 1984). *G. subglobosa* is an infaunal form (Murray, 1991) preferentially living at higher oxygen levels of the sediment pore water (Kaiho, 1994), but also tolerating high environmental stress (Seidenkrantz et al., 2000). Rasmussen et al. (1996) reported of increasing abundances of *C. obtusa* and *G. subglobosa* in sediments of deglaciation and Holocene from the Faeroe-Shetland Gateway. *C. kullenbergi* is described as epibenthic species, but also lives shallow endobenthic and is therefore not considered to belong to the ‘Attached Epibenthos Group’ (Schönfeld, pers. comm.).

3.4.3 The Interglacial group

The Holocene interval is dominated by *Uvigerina mediterranea* and *Trifarina angulosa*. Subdominant species are *Melonis barleeanum*, *Hyalinea balthica*, *Bulimina marginata*, *Cassidulina laevigata* and *Uvigerina peregrina* (Fig. 3-4a). All species show similar distribution throughout the entire core with maximum values during the Holocene and the bioturbated section. Only *C. laevigata* presents slightly higher relative abundance during MIS 2 and at the transition between MIS 2 and 3. *M. barleeanum* also shows higher values during late MIS 3 with a decreasing trend towards MIS 2 (Fig. 3-4a). The combined relative abundance of all species of the *Interglacial*

group reaches a maximum of 68 % for the past 10 kyr but rarely exceed 10 % during MIS 2 and 3 (Fig. 3-4a).

U. mediterranea, *T. angulosa*, *M. barleeanum*, *B. marginata* and *U. peregrina* are reported as infaunal species living in muddy to fine sandy sediments (Murray, 1991), whereas *T. angulosa* is associated with coarser sediments under the influence of stronger bottom currents (Mackensen et al., 1995; Rasmussen et al., 2002a). Except *T. angulosa*, these species show a great affinity to high and continuous flux of organic material to the sea-floor (e.g. Loubere, 1991; Mackensen et al., 1993; Kaiho, 1994), which is most important for the recent distribution of *Uvigerina* species (Thomas et al., 1995; Altenbach et al., 1999). *M. barleeanum* shows special demands on quality and concentration of food (Caralp, 1989) and is migrating upward in sediment during times of starvation (Linke and Lutze, 1993).

All infaunal species are tolerant with respect to reduced oxygen concentration in the pore water (Kaiho, 1994; Brüchert et al., 2000; Seidenkrantz et al., 2000). *C. laevigata* is an epifaunal species and is, similar to *Epistominella exigua*, characteristic of areas with seasonal food supply to the sea bottom (Gooday 1986, 1988). The latter species show high relative abundances in NE Atlantic regions further offshore (e.g. Thomas et al., 1995; Smart and Gooday, 1997; Rasmussen et al., 2002a; 2002b), but occurs only as a minor species (<3 %) in the Holocene succession of core GeoB 6725-1. Weston (1985) showed that *E. exigua* is highly abundant in water depth >2400 m in the PSB. *H. balthica* is an epibenthic species (Murray 1991) very common in upper slope environments in the PSB (Coles et al 1996).

3.5 Paleooceanography of the Porcupine Seabight

3.5.1 Shelf erosion during Late MIS 3

In off-mound core GeoB 6725-1 the abundance of *E. excavatum* strongly correlates with the sedimentation rate. During late MIS 3 sedimentation rate was very high (>30 cm/kyr) and *E. excavatum* exceeds 50 % of the relative abundance. The abundance and the sedimentation rate decrease towards MIS 2 to around 15 % and to around 10 cm/kyr, respectively (Fig. 3-5). This relation suggests that *E. excavatum* is transported passively from the surrounding shallow shelves into the PSB. Therefore, the abundance of this species is considered to be an indicator for shelf erosion and high sediment shedding into the PSB.

During Late MIS 3, polar conditions and near-glacial environments influenced the PSB and Ireland. This is indicated by high numbers of *E. excavatum* (Fig. 3-5), which nowadays occurs in near-glacial environments. The British Irish Ice Sheet (BIIS) covered almost complete Ireland during MIS 2 to 4, interrupted by occasional retreat and advance of glaciers. Knutz et al. (2001) described a progression of glaciers reaching the edge of the shelf north of the Sea Bight at the Barra Fan, indicated by an abrupt increase of basaltic ice rafted debris into marine sediment around 30 kyr BP. Increased terrigenous sediment supply and the abrupt increase of *E. excavatum* probably indicate the advance of BIIS onto the Irish Mainland shelf ~31 kyr BP. A sea-level drop of 50 m during Late MIS 3 (Lambeck et al., 2002) most certainly forced sediment erosion from the shelf, which decreased towards MIS 2 indicated in decreasing abundance of *E. excavatum* (Fig. 3-5).

3.5.2 Glacial setting

The *Glacial group* strongly reflects the influence of polar conditions in the northern PSB. Absolute abundance of benthic foraminifera is very low during MIS 2 and 3 (Fig. 3-4a). However, the high sedimentation rate suggests dilution of faunas. The Polar Front was situated south of 50°N, which led to seasonal sea-ice cover over the PSB and Bank during glacial winter, as indicated by paleotemperature reconstruction of <1°C for paleo-surface waters (Sarnthein et al., 2003). Glacial summer sea surface temperature of 4°C caused the retreat of sea-ice cover.

Dominant abundance of *C. teretis* and associated fauna of the *Glacial group* indicate the influence of a cold water mass. As *C. teretis* is found in present water temperatures down to -1 to 2°C (Mackensen and Hald, 1988; Wollenburg and Mackensen, 1998), a similar glacial intermediate water temperature most certainly occurred taking the dominance of this species into account. *C. teretis* and *C. reniforme* are associated with nutrient-poor bottom water conditions and slow benthic currents speeds (Belanger and Streeter, 1980; Sejrup et al., 1981; Mackensen et al., 1985; Rasmussen et al., 2002b). A weak glacial hydrodynamic regime is also indicated by the deposition of fine-grained terrigenous sediments (Chapter 4, Appendix 8). Moreover, Schönfeld and Zahn (2000) reported about a glacial MOW flow up to 800 m deeper than today due to increased density (i.e. higher salinity) and found no indication of a northward transport. Instead, Glacial North Atlantic Water (GNAIW) dominated the water column down to 1700–2000 m. These observations

indicate that no comparable water mass boundary at intermediate water depth during glacial times was present as it occurs today with strong hydrodynamic regime and high nutrient concentration.

According to Duplessy et al. (1988) and Oppo and Lehman (1993) the term GNAIW is used for mid-depth waters of uncertain origin. Manighetti and McCave (1995) reported GNAIW production to occur in the North Atlantic flowing southward via the Wyville-Thomson Ridge and the Rockall Trough. This is supported by Veum et al. (1992) suggesting GNAIW production in the Norwegian Sea through a mechanism strongly influenced by sea-ice formation. They also mentioned that the composition of GNAIW may have changed during glacial time due to differing sources. Sarnthein et al (2001; 2003) discussed a production area of Upper North Atlantic Deep Water west off Rockall Bank at least during glacial winters. Different source of glacial intermediate waters is probably indicated by changing abundances of *Glacial group* species (*G. subglobosa*, *C. obtusa*, *C. kullenbergi*, *S. woodi*, Fig. 3-4b). *G. subglobosa* and *C. obtusa* show increasing abundance during the time of deglaciation and the Holocene in cores south of the Faeroe-Shetland Gateway (Rasmussen et al., 2002b). These species probably indicate a slight increase in bottom water temperature and/or enhanced ventilation (higher oxygen concentrations) as a result of a different source of GNAIW during early MIS 2.

3.5.3 Holocene setting

The transition from MIS 2 to the Holocene is marked by a sharp shift in faunal assemblages. The abundance of the *Glacial group* decreases from >60 % to around 10 %,

while the Holocene group increases from around 10 % to >60 % (Fig. 3-4a). This distinct change indicates the replacement of the glacial setting by present-day oceanographic and environmental conditions. The Polar Front moved northward to its modern position crossing the PSB. Warm and saline waters of the North Atlantic Drift entered the North Atlantic carrying higher temperatures and thus providing more moisture to the North Atlantic realm. During the retreat of the BIIS from Ireland, the sea-level increased by 120 m from its maximum lowstand at ~18–20 kyr BP to its present level at ~6 kyr BP (Siddall et al., 2003; Clark et al., 1999; Lambeck et al., 2002).

Low sedimentation rate during the Holocene inhibits the detection of small-scale variations within the course of the past 10 kyr. Thus, the period will be described as a whole, reflecting present-day conditions. The assemblage of the *Interglacial group* strongly correlates with the recent environmental conditions and oceanographic setting of the northern Porcupine Seabight. The domination of infaunal species (*U. mediterranea*, *M. barleeanum*, *U. peregrina*, *B. marginata*) during this period indicates that the bottom environment was characterised by a high amount of organic material in the sea-floor sediment. Strong and continuous flux of organic material to the sea-floor occurs due to enhanced surface primary productivity on the shelf and bank.

Present-day primary production of 160 g C m⁻² yr⁻¹ is a typically value for the shelf environment measured in the nearby region of the Goban Spur at the mouth of the PSB (Joint et al., 2001). They estimate about 60 g C m⁻² yr⁻¹ available for export to intermediate and off-shelf water. White et al. (subm.) described several mechanisms driving enhanced downslope transport of

organic material, such as off-slope Ekman transport, cascading and benthic nepheloid layers. Nowadays, bottom nepheloid layers and intermittently present intermediate nepheloid layers in water depth of 700 m to 1400 m are reported at the Goban Spur area (McCave et al., 2001). The distribution of intermediate nepheloid layers strongly correlates with water mass boundary of ENAW and MOW. The combined effect of internal waves and northward oriented slope currents suggests a similar distribution of these nepheloid layers within the PSB. Species of the *Interglacial group* benefit from this high and rapid down-slope deposition of nutrients, their resuspension in greater depths and transport into the Sea Bight and thus dominate the benthic assemblage of the past 10 kyr.

All endobenthic species of the *Interglacial group* are associated with lower oxygen concentrations in the sediment pore water (Murray, 1991; Kaiho, 1994; Brüchert et al., 2000; Seidenkrantz et al., 2000), probably

indicating low-level oxygen concentration of the overlying water mass. In water depths of 600 to 800 m the mixing of ENAW and MOW controls the present-day oceanography. MOW is characterised by high salinity and low oxygen content as indicated in Figure 3-2 (McCave et al., 2001). Thus, the *Interglacial Group* probably portrays this mixing process and the influence of MOW in the northern PSB.

Recent current meter measurements in the PSB show the influence of strong bottom currents along the slope of the PSB in water depths of carbonate mound provinces (White, 2001; White et al., *subm.*). Coarser sediments in the Holocene samples indicate the stronger hydrodynamic regime during this period, supported by fine fraction analysis from off-mound sediment cores (Chapter 4; Appendix 8). *T. angulosa* is associated with coarse-grained sediments (Mackensen et al., 1993; 1995; Rasmussen et al., 2002a) and higher abundances indicate the influence of stronger currents.

3.6 Occurrence of benthic foraminiferal assemblages in on-mound sediments

In contrast to the off-mound core, 114 species belonging to 74 genera of benthic foraminifera have been identified in on-mound core GeoB 6730-1. Absolute abundances are generally higher in on-mound samples ranging between 200 and 800 ind/g, reaching maximum abundances of 1000 ind/g in the Holocene (Fig. 3-3b). The normalised species diversity and diversity index $H(S)$ indicate a higher diversity of benthic foraminifera on-mound. The numbers range between 31 species ($H(S) = 2.4$) at the core base and 49 species ($H(S) = 3.4$) at the core top (Fig. 3-3b).

To evaluate how on-mound sediments differ from samples of the off-mound core, we grouped the off-mound identified species of the *Interglacial* and *Glacial group* in samples of on-mound core GeoB 6730-1 (Fig. 3-6). This method additionally helped to determine glacial or interglacial sections, as the age model is incomplete due to the assumingly preferred loss of glacial sediments (Appendix 8). Both assemblages show lower relative abundance in on-mound samples ranging between 20 and 60 % for the *Interglacial group* and 10 to 45 % for the *Glacial group*. Additionally, a third as-

semblage dominated by epibenthic species has been identified and is described by species rarely found in off-mound samples and therefore termed as *Mound group*. This group presents high values of 40 % in the lower core part and decreases towards core top to ~10 % (Fig. 3-6). All species of the three assemblages describe the core with mean 73.1 %.

3.6.1 The *Interglacial group* in on-mound sediments

Species belonging to the *Interglacial group* show different distributions throughout the on-mound record (Fig. 3-6). *U. mediterranea*, *H. balthica* and *U. peregrina* have lower maximum abundances compared to off-mound site, showing maximum abundances during the Holocene. Also higher abundant during the Holocene are *M. barleeanum* (exceeding 15 %) and *C. laevigata* (>10 %). Both species are more dominant than in off-mound samples, whereas *T. angulosa* and *B. marginata* show considerably higher occurrences below 60 cm (Fig. 3-6). The combined stack of the *Interglacial group* does not present comparable low off-mound glacial values of around 10 %. Only at ~180 cm and ~315 cm the values fall below 20 %. Similar off-mound Holocene values are reached between 70 and 90 cm, but the record decreases to around 45 % for the Holocene.

The combined stack of *Interglacial group* species demonstrates that this group generally describes >20 % of the faunal assemblage with similar Holocene values as in the off-mound core around 70 cm. During the Holocene the group reaches values of ~45 %, approximately 20 % lower than in the off-mound core. This suggests additional

species being abundant in Holocene off-mound samples (i.e. the *Mound group*, see below).

3.6.2 The *Glacial group* in on-mound sediments

Glacial species *C. obtusa*, *C. reniforme* and *S. woodi* are less abundant in sediment core GeoB 6730-1 (Fig. 3-6). *C. kullenbergi* reaches maximum abundance of 9 % at 150 cm and 70 cm, and *C. teretis* exceed 20 % only at 313 cm. The only species higher in abundance, compared to the glacial off-mound samples, is *G. subglobosa*, showing elevated values in two distinct intervals within the 180-260 cm core section (Fig. 3-4 and 3-6). With values around 12 % the combined record of the *Glacial group* presents comparable values to those species of the off-mound Holocene succession. Only four sections with relative abundance exceeding 20 % are visible, but the maximum of 40 % is by far too small to describe comparable glacial values, as in the off-mound core (Fig. 3-4).

Both the *Interglacial group* and *Glacial group* clearly demonstrate a generally lower abundance compared to the off-mound core. Only four specific sections (123–153 cm, 173–208 cm, 233–268 cm, 308–323 cm) show slightly higher values with respect to the *Glacial group* giving evidence for glacial conditions during deposition.

3.6.3 The *Mound group*

Dominant species of the *Mound group* are *Discanomalina coronata* and *Gavelinopsis translucens*. Both species show high relative abundances in the lower core part and decrease towards the core top (Fig. 3-6).

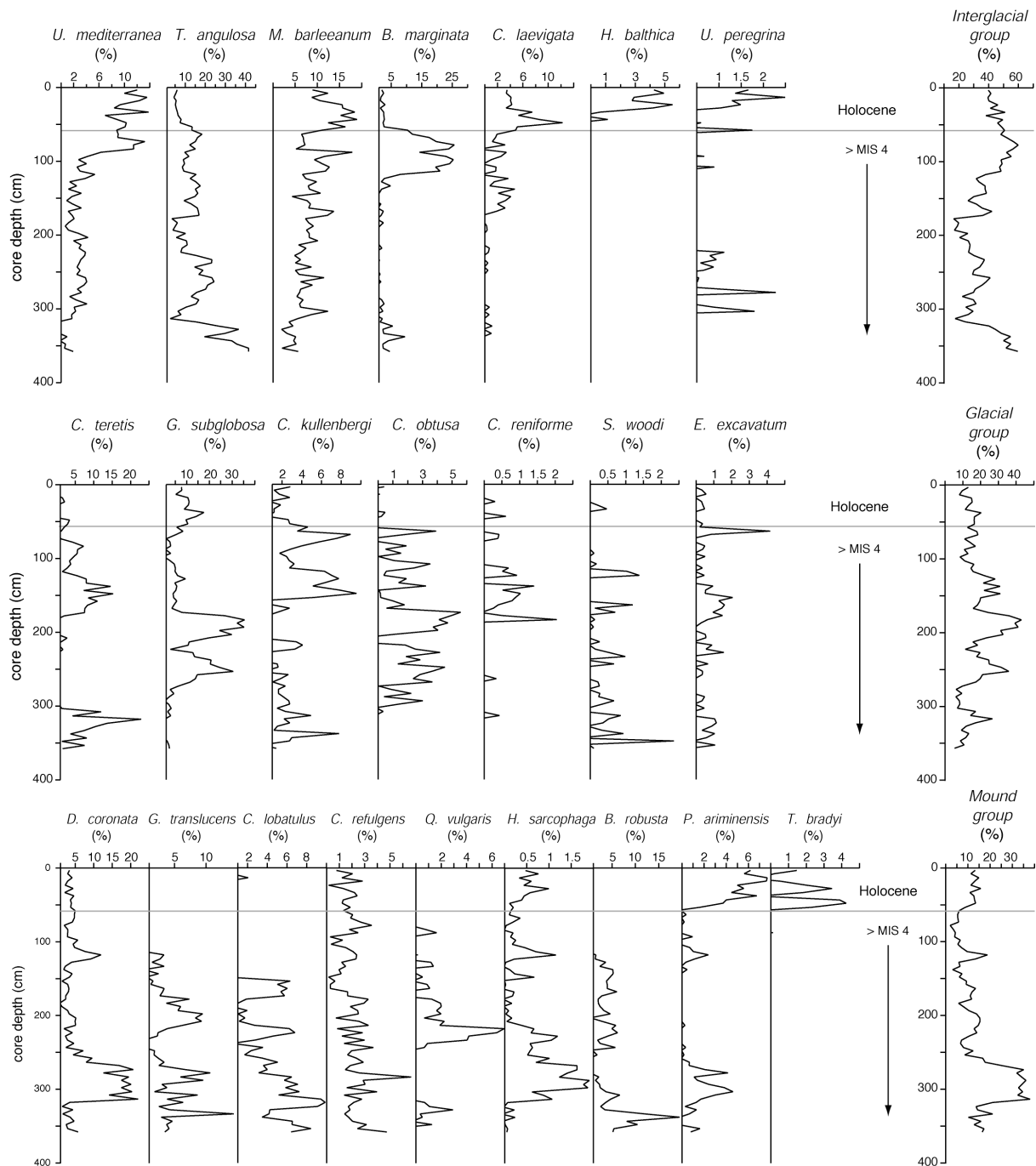


Figure 3-6. Relative abundance of benthic foraminifera of on-mound core GeoB 6730-1. Top panel: Species identified as *Interglacial group* in off-mound core. Centre panel: Species identified as *Glacial group* (MIS 2 and 3) in off-mound core. Bottom panel: dominant, subdominant and minor benthic foraminifera of the *Mound group* identified in on-mound core, which are not abundant or only to a minor degree in the off-mound core.

This is also the case for the subdominant (*Cibicides lobatulus*, *Cibicides refulgens*, *Quinqueloculina vulgaris*, *Bolivina robusta*) and minor species (*Hyrrokkin sarcophaga*). *Planulina ariminensis* and *Trifarina bradyi*

have high abundance during the Holocene, suggesting a connection to the *Interglacial group*. However, as they are largely suppressed or even lacking in off-mound samples, they contribute to the *Mound group*.

All species are reported to be epifaunal, except *B. robusta*, which was found to live also shallow infaunal (Murray, 1991). *D. coronata*, *G. translucens*, *C. lobatulus*, *C. refulgens* and *P. ariminensis* favour environments with high bottom currents and coarse sediments (e.g. Pujos, 1971; Hald and Vorren, 1984; Murray, 1991) living attached to elevated substrates (Schönfeld, 1997; Schönfeld and Zahn, 2000; Schönfeld, 2002a; 2002b). *H. sarcophaga* contributes to a minor content to this assemblage. It lives attached to *L. pertusa* and shows a parasitic life style (Freiwald and Schönfeld, 1996). Some individuals of *H. sarcophaga* have been counted still attached to fragments of *L. pertusa* in fraction >1000 μm , but it is generally rarely found in the samples.

3.6.4 Impact of the hydrodynamic regime and the influence of MOW in the PSB

An additional indication for changing current-strength intensities is described by Schönfeld (2002b). High abundance of opportunistic epibenthic species, which are specialised to catch particles from streaming water (Lutze and Thiel, 1989; Linke and Lutze, 1993), is associated to intensified benthic currents (Schönfeld, 1997; 2002a; 2002b). The author reported of a benthic foraminiferal assemblage dominated by *C. lobatulus*, *C. wuellerstorfi*, *D. coronata*, *P. ariminensis*, and *Vulvulina pennatula*, living directly on the lateral particle flow of MOW at the Portuguese Margin. The strategy to live attached on elevated substrates provides these species with a competitive advantage over others, resulting in higher abundances in both, living and dead assemblages (Schönfeld, 1997). Similar epibenthic

assemblages have also been reported in areas presently affected by MOW advection along the European continental margin, e.g. in the Bay of Biscay (Pujos, 1971), at the Western Approaches and in the Porcupine Seabight (Weston, 1985).

The *Mound group* comprises most of the identified benthic foraminifera with an attached epibenthic life style. This group is similar to the ‘Attached Epibenthos Group’ described by other studies along the European continental margin. According to observations of Murray (1991) and Schönfeld (1997; 2002a; 2002b) *Cibicidoides wuellerstorfi*, *Gaudryna nitida* and *Patellina corrugata* were attributed to the *Mound group* to form the ‘Attached Epibenthos Group’ (Fig. 3-7).

With species living attached to elevated substrates, high abundance of ‘Attached Epibenthos Group’ species from on-mound core most certainly imply periods with elevated substrates (i.e. corals) and higher amounts of nutrients, transported by intensified bottom currents. This suggests a link between this group and the occurrence of MOW, as it portrays similar present-day conditions. Surprisingly, the ‘Attached Epibenthos Group’ indicates much lower abundances during the Holocene than in section 260–320 cm (Fig 3-7). As Schönfeld (2002a) postulated that a co-occurrence of the ‘Attached Epibenthos Group’ could serve as indicator of a near-bottom flow regime, higher benthic currents on Propeller Mound may have occurred during the period described by section 260–320 cm - or - much more elevated substrates have been provided by a much higher coral growth density on the mound (Chapter 5).

The ‘Attached Epibenthos Group’ consists mainly of species of the *Mound group*, therefore, its occurrence in off-mound sam-

ples is very low. It only reach maximum abundance of 5 % during the Holocene and possibly reflects the influence of MOW in conjunction with an intensified hydrody-

namic regime (Fig. 3-7). Another explanation of slightly higher abundance of these species at the off-mound site is that they have been transported from the mound.

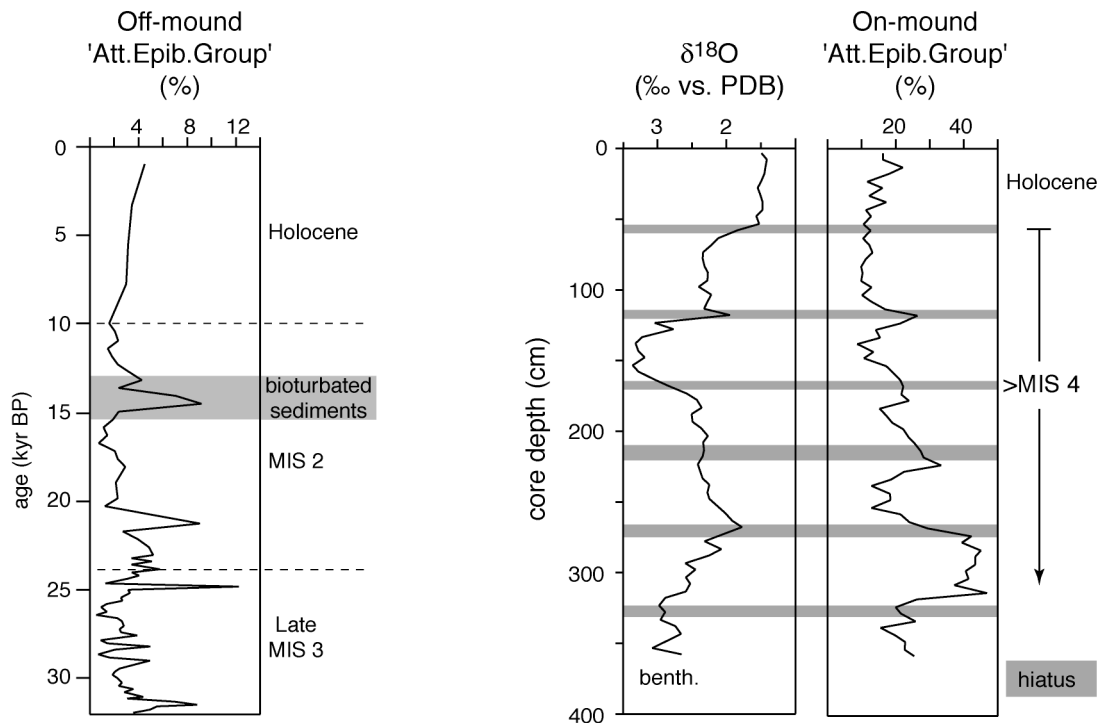


Figure 3-7. ‘Attached Ebibenthos Group’, which is mainly described by the *Mound group*, of off- and on-mound cores. Their abundance probably indicates the influence of MOW in the PSB and enhanced bottom current regime.

3.7 Summary and conclusions

Faunal analysis of dead benthic foraminifera from a carbonate mound and an off-mound position in the northern PSB reveals three different assemblages. The *Interglacial* and *Glacial group* identified in off-mound samples clearly reflect the oceanographic and environmental conditions for the Holocene, MIS 2 and Late MIS 3, summarised in Table 3-2. During Late MIS 3 high abundance of the displaced species *E. excavatum* indicates strong shelf erosional processes related to the advance of the British Irish Ice Sheet onto the Irish Mainland shelf with a coeval sea-level drop of around 50 m.

The *Glacial group* is typical for present-day polar regions and its dominant species *C. teretis*, *C. kullenbergi*, *G. subglobosa*, *C. reniforme*, *C. obtusa* and *S. woodi* describe the influence of a very cold intermediate water mass, as well as low nutrient availability. High sedimentation rate of predominantly terrigenous material and low current velocities must have prevailed during this time.

The *Interglacial group* is described by high abundance of *U. mediterranea*, *T. angulosa*, *H. balthica*, *M. barleeaanum*, *B. marginata*, and *C. laevigata*. They indi-

cate a warm intermediate water mass and a high nutrient supply to the sea bottom. The environmental setting is described by the mixing of ENAW and MOW, leading to a strong hydrodynamic regime, which reduces Holocene sedimentation rate.

The distribution of the off-mound identified assemblages in the on-mound core shows that no clear glacial conditions are preserved in on-mound sediments, whereas the *Interglacial group* is relative abundant throughout the complete core, and shows lower abundance than in the off-mound core. As the on-mound core is marked by several hiatuses, a removal of nearly all glacial sediments is suggested.

The third assemblage is found in the on-mound core, dominated by attached epibenthic species *D. coronata*, *G. translucens*, *C. lobatulus*, *C. refulgens*, *Q. vulgaris*, *H. sarcophaga*, *B. robusta*, *P. ariminensis* and *T. brady*. These species live preferably attached to elevated substrates, such as the cold-water coral *L. pertusa* and do not or to a minor degree occur in off-mound sediments. The *Mound group* or ‘Attached Epibenthos Group’ is related to the occurrence of MOW in the northern PSB and indicate comparable conditions like today with strong currents and a high nutrient availability.

Table 3-2. Faunal summary and paleoenvironmental interpretation of foraminiferal assemblages of the off-mound core.

Age	core depth (cm)	Assemblage	Benthic species	Paleoenvironment
Holocene (0-10 kyr BP)	0–23 cm	<i>Interglacial group</i>	<i>U. mediterranea</i> , <i>T. angulosa</i> , <i>H. balthica</i> , <i>M. barleeaanum</i> , <i>B. marginata</i> , <i>C. laevigata</i>	warm (>8°C) bottom waters, strong currents, high nutrient supply, influence of MOW
MIS 2 (10-24 kyr BP)	23–178 cm	<i>Glacial group</i>	<i>C. teretis</i> , <i>C. kullenbergi</i> , <i>G. subglobosa</i> , <i>C. reniforme</i> , <i>C. obtusa</i> , <i>S. woodi</i>	cold (< 2°C) bottom waters, glacial marine, high sedimentation rate, weak currents, low nutrient availability, homogenous intermediate water mass, lowered salinity?
Late MIS 3 (24-31 kyr BP)	178–403 cm	displaced species	<i>E. excavatum</i>	cold, near glacial environment, shelf erosion, very high sedimentation rate

Acknowledgements

This study is part of the OMARC project ECOMOUND funded by the EU during the course of 5th Framework Programme (Contract n°. EVK3-CT-1999-00013). We greatly thank Dr. V. Liebetrau from GEOMAR, Kiel for his support on U/Th measurements. Additionally, we wish to thank the captains, crew and scientific shipboard parties of POSEIDON cruises POS 265 and 292. A.R. especially wishes to thank A. Freiwald and P. Floyd for intensive night-

shifts during the latter cruise. Dr. J. Schönfeld from GEOMAR, Kiel is acknowledged for his comments and suggestions on an earlier version of this manuscript. Dr. S. Roth, PD Dr. J.J.G. Reijmer are acknowledged for improving the language. Finally, all colleagues from ECOMOUND and the twin projects ACES and GEOMOUND are thanked for help and good co-operation during the past three years.

CHAPTER 4

SEDIMENTARY PATTERNS IN THE VICINITY OF A CARBONATE MOUND IN THE HOVLAND MOUND PROVINCE, NORTHERN PORCUPINE SEABIGHT

A. Rüggeberg^{1*}, B. Dorschel², W.-Chr. Dullo¹, D. Hebbeln²

¹ GEOMAR – Research Center for Marine Geosciences, Wischhofstr. 1-3, D-24114 Kiel, Germany

² Fachbereich 5 Geowissenschaften, Universität Bremen, Postfach 330440, 28334 Bremen, Germany

* Corresponding author. Fax: +49-431-6002941. E-mail address: arueggeberg@geomar.de

submitted to

Marine Geology

Abstract

Large carbonate mound structures have been discovered in the northern Porcupine Seabight (Northeast Atlantic) at depths between 600 and 1000 m. These mounds are associated with the growth of deep-sea corals *Lophelia pertusa* and *Madrepora oculata*. In this study, three sediment cores have been analysed. They are from locations close to Propeller Mound, a 150 m high ridge-like feature covered with a cold-water coral ecosystem at its upper flanks. The investigations are concentrated on grain size analyses, carbon measurements and on the visual description of the cores and Computer Tomographic images, to evaluate sediment content and structure.

The cores portray the depositional history of the past ~31 kyr BP, mainly controlled by sea-level fluctuations and the climate regime with the advance and retreat of the Irish Ice Sheet onto the Irish Mainland Shelf. A first advance of glaciers is indicated by a turbiditic release slightly older than 31 kyr BP, coherent with Heinrich event 3 deposition. During Late Marine Isotope Stage 3 (MIS 3) and MIS 2 shelf erosion prevailed with abundant gravity flows and turbidity currents. A change from glaciomarine to hemipelagic contourite sedimentation during the onset of the Holocene indicates the establishment of the strong, present-day hydrodynamic regime at intermediate depths.

The general decrease in accumulation of sediments with decreasing distance towards Propeller Mound suggests that currents (turbidity currents, gravity flows, bottom currents) had a generally stronger impact on the sediment accumulation at the mound base for the past ~31 kyr BP, respectively.

4.1 Introduction

Carbonate mounds along the European continental margin have been the subject of detailed investigation by several campaigns during the past decade (OMARC projects of the 5th Framework Programme, EU). Within the Porcupine Seabight (PSB), several mounds clustered in three distinct provinces have been identified from high-resolution seismic profiles (e.g. De Mol et al., 2002; Van Rooij et al., 2003) and side-scan sonar images (e.g. Huvenne et al., 2002; Kenyon et al., 2003; Masson et al., 2003), and were intensively sampled during cruises between 1997 and 2003 (e.g. Freiwald et al., 2000; Freiwald and Shipboard Party, 2002). The Hovland Mound province in the north of the PSB (Fig. 4-1) is bound by the Magellan Mound province further northwest, which mainly consists of already buried mounds under a Pleistocene sediment cover. The sea-floor protruding Hovland mounds reach a height of up to 200 m and occur as single, conical features or ridge-like structures with several summits (De Mol et al., 2002). These mound structures are constructed by the framework builder *Lophelia pertusa* and associated fauna (Freiwald, 1998; Rogers, 1999; Hovland and Mortensen, 1999), which baffle fine-grained sediment and form those large topographic features. The occurrence of deep-water carbonate mounds in a distinct depth range of 600 m to 900 m is closely related to oceanographic conditions favourable for azooxanthellate corals, of which high nutrient supply, strong current activity, temperatures between 4–12°C, and slow sedimentation rate seem most important (Teichert, 1958; Frederiksen et al., 1992; Freiwald et al., 1999; De Mol et al., 2002).

Intermediate-water circulation along the European continental margin and within the

PSB has an important role in sediment distribution and downslope transport of terrigenous and biogenic material (e.g. Joint et al., 2001; McCave et al., 2001). The influence of currents is known to be an important factor in mound initiation, growth and decay (Freiwald and Wilson, 1998; De Mol et al., 2002). Sand sheets and sand waves suggest the present-day sea-floor is swept by relatively strong bottom currents at the Belgica Mound province (Akhmetzhanov et al., 2001), which are reduced in the Hovland Mound province (Huvenne et al., 2002) but still exceed 15 cm s⁻¹ (White, *subm.*). Thus, strong current strength intensities prevent the burial of the carbonate mounds.

High sedimentation rates are one limiting factor of carbonate mound development, as can be seen from the already buried Magellan mounds (Huvenne et al., 2002). The Holocene sedimentation rate within the PSB is generally low with 1–8 cm/kyr, which is the result of strong benthic currents removing fine-grained material. However, sediment deposition was about 3 to 10 times higher during the last glacial period, comparable to results of other studies from the Celtic margin to the south or the Hebridean continental slope to the north of the PSB (Auffret et al., 2002; Knutz et al., 2001). Generally, Quaternary sediment deposition in near shelf areas is essentially controlled by the climate regime and sea-level variability. Both factors control the weathering of soils, the transport capacity of rivers, ice sheet dynamics, the annual coverage of sea ice, and the prevailing wind and current regimes (McCave, 2002; Auffret et al., 2002). Continental margins are preferentially sites of terrigenous sediment deposition eroded from land and exported to the ocean essentially through transport by rivers. However, present-day riverine influx

of terrigenous sediments into the PSB is low. During peak glacials, the maximum lowering of the sea-level was 120–130 m below present level (Labeyrie et al., 1987; Fairbanks, 1989). This degree of lowering uncovers effectively the Irish Mainland shelf and sediments were discharged directly into the Porcupine Basin with much reduced trapping in coastal plains. Additionally, shelf-protruding glaciers overrode the uncovered shelves leading to strong glacial erosion and high supply of reworked sediments into the basin.

The aim of this study is to describe the sedimentary setting and processes in the northern Porcupine Seabight around a carbonate mound. It is based on the description of sediments in three gravity cores revealed

from visual core description and Computer Tomographic (CT) images, analyses on grain size distribution, contents, carbon measurements, and stable isotopes data. The variability of sediments is controlled by the hydrodynamic setting and the climate regime with the advance and retreat of the British-Irish Ice Sheet (BIIS) controlling the sediment flux from Ireland and the Irish shelves into the Sea Bight. Surface morphology of carbonate mounds and adjacent areas have been analysed in detail (e.g. Huvette et al., 2002; Masson et al., 2003; De Mol et al., 2002). However, here we present a first detailed study on the sedimentary downcore variability within the closer vicinity of a carbonate mound.

4.2 Regional setting

4.2.1 *The Porcupine Seabight*

The Porcupine Seabight is an embayment in the Atlantic Irish shelf, located southwest of Ireland. It has an extension of about 200 km in N-S direction and widens from 65 km in the north to 100 km in the south. The Sea Bight is surrounded by shallow shelves and ridges to the west, north and east (Porcupine Ridge and Bank, Slyne Ridge and Irish Mainland shelf) and deepens gradually to the south into the Porcupine Abyssal Plain (Fig. 4-1). The study area is Propeller Mound and its surrounding sea-floor, which was mapped during RV POSEIDON cruise 265 in September 2000 (Freiwald et al., 2000). This mound is part of a cluster of high relief mounds of the Hovland Mound province in a water depth between 650 and 1000 m (52°06'–52°22'N and 11°53'–

12°45'W, Hovland et al., 1994; De Mol et al., 2002). The Propeller Mound is elevated up to 150 m above the surrounding sea-floor, possesses a N-S elongation of about 3 km and a maximum extension of 1.5 km in EW direction (Fig. 4-1). The base of the triangular-shaped mound lies in water depths of around 800 m to the west and 900 m to the east. Smaller mounds appear further NE and NW of Propeller Mound. Its morphology clearly indicates a relation to strong currents running in N-S direction. At the northern, eastern and western flanks of the mound little depressions or moats occur, which are generated by scouring of turbulence currents around the mound (De Mol, 2002). Drift bodies further off mound also indicate the erosive hydrodynamic regime.

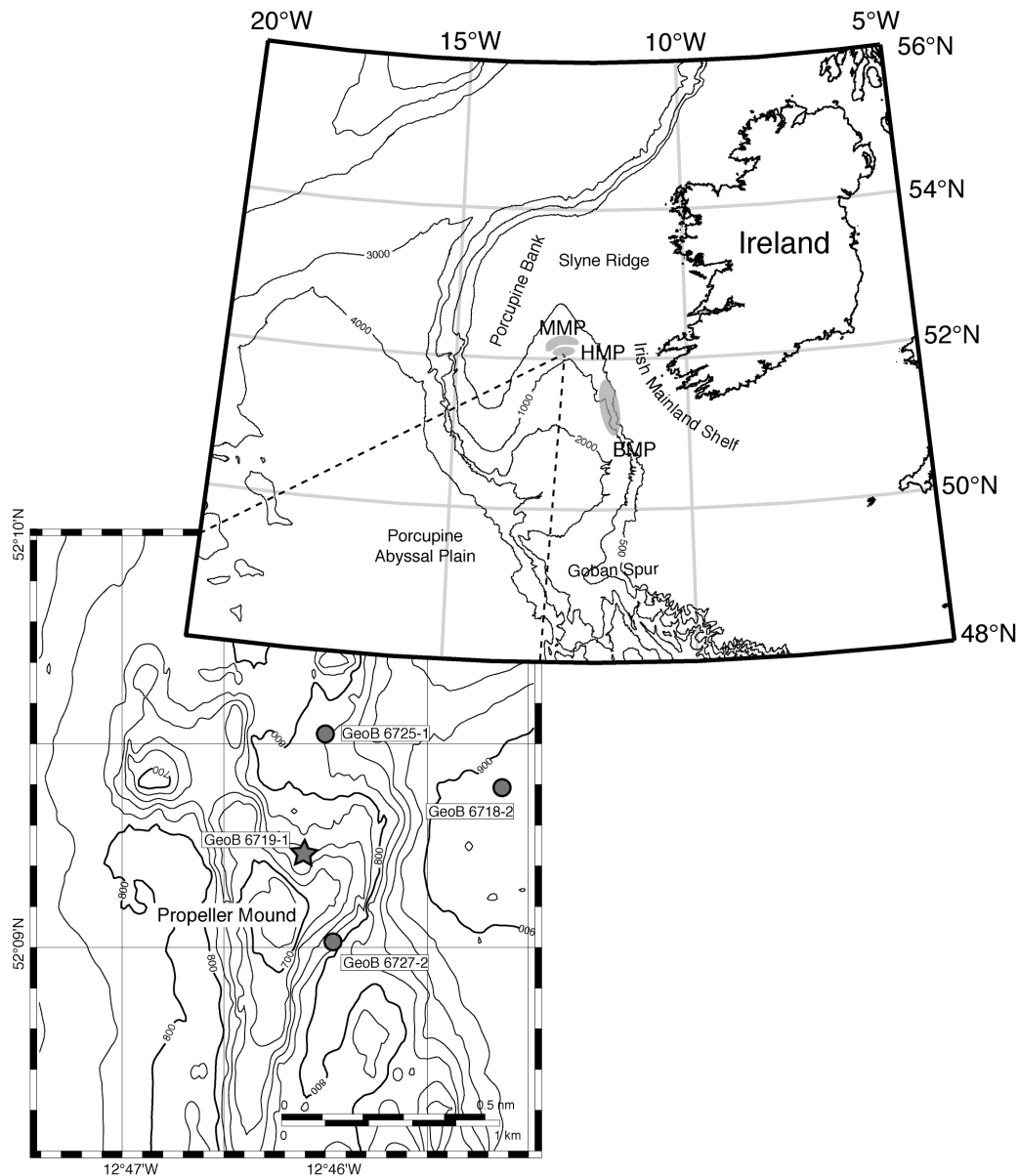


Figure 4-1. Bathymetric setting of the Porcupine Seabight west off Ireland. Propeller Mound is located at the southern margin of the Hovland Mound province and was mapped during RV POSEIDON cruise POS 265 in September 2000 (Freiwald et al., 2000). Indicated are the positions of investigated gravity cores (core GeoB 6719-1 (star) was only used for stratigraphic correlation). MMP = Magellan Mound province, HMP = Hovland Mound province, BMP = Belgica Mound province.

4.2.2 Recent hydrography

The general hydrography along the East Atlantic Margin is dominated by northward along-slope currents flowing from the Iberian Margin to the Norwegian Sea (Huthnance and Gould, 1989; Pingree and LeCann, 1989; 1990). Within the PSB, the Eastern North Atlantic Water (ENAW), a

winter mode water formed by strong cooling of waters northwest of Spain, is found to a water depth of about 750 m. It flows along the continental margin of the Bay of Biscay into the Porcupine Seabight (Pollard et al., 1996; van Aken, 2000; White, *subm.*). Between 150 and 400 m, ENAW can be

divided into an upper and lower core of the Shelf Edge Current (SEC), expressed in salinity maxima (Hill and Mitchelson-Jacob, 1993; White and Bowyer, 1997). SEC plays an important role in physical exchange processes at the shelf break and hence cross-shelf fluxes (Huthnance, 1995). Mediterranean Outflow Water (MOW) is underlying ENAW, characterised by a salinity maximum and an oxygen minimum at a depth of about 950 m (Pollard et al., 1996). A mixing between ENAW and MOW occurs between 600 and 700 m water depth.

The general flow pattern in the Porcupine Seabight is characterized by poleward flowing currents at all depth levels along the eastern slope. Direct measurements of benthic currents indicate mean velocities of 5 cm s^{-1} , exceeding 15 cm s^{-1} for 15 % of the measured period (White, *subm.*). There is evidence of topographic steering of the mean flow at the northern end of the PSB. Currents become weaker ($1\text{--}5 \text{ cm s}^{-1}$) and flow cyclonically around the slope leading to a southward flow at the western slope of the Sea Bight (White, *subm.*).

4.3 Materials and methods

Sediment cores GeoB 6718-2, GeoB 6719-1, GeoB 6725-1, and GeoB 6727-2 were recovered during RV POSEIDON cruise POS 265 close to Propeller Mound (Freiwald et al., 2000, Table 4-1). Before sampling and splitting of sediment cores, computer tomographic analysis was performed at the Universitätsklinikum Kiel, Department of Radiology by Dr. Morvain. Still closed core sections were investigated for their content and sedimentary structures using a Phillips Tomoscan LX. The CT radiographs have been scanned and visually described and were compared with core description of split core halves.

Each core was sampled using 10 cm^3 syringes at 5 cm intervals. All samples were weighed and then freeze-dried at -50°C .

With known sediment volume and weight loss during freeze-drying, the dry bulk density, porosity and water content were calculated. One set of samples was wet sieved through a $63 \mu\text{m}$ sieve and the suspended fine fraction ($<63 \mu\text{m}$) was collected in 5-litre jars for fine fraction analysis. The coarse fraction ($>63 \mu\text{m}$) was oven dried at 50°C and weighed afterwards. To separate the sample into grain size fractions, the coarse fraction was dry sieved through a sieve set with $125 \mu\text{m}$, $250 \mu\text{m}$, $500 \mu\text{m}$ and $1000 \mu\text{m}$ mesh widths. All samples were weighed thereafter.

Stable oxygen isotope analysis was carried out at Isotope Lab Bremen University. 3 to 5 individuals of benthic foraminifera *Cibicidoides wuellerstorfi* or

Table 4-1. Sediment core information

Core number	Latitude N	Longitude W	Water depth (m)	Recovery (cm)
GeoB 6718-2	$52^\circ09.379'$	$12^\circ45.158'$	900	450
GeoB 6719-1	$52^\circ09.233'$	$12^\circ46.127'$	758	580
GeoB 6725-1	$52^\circ09.520'$	$12^\circ46.010'$	820	450
GeoB 6727-2	$52^\circ08.017'$	$12^\circ45.970'$	794	470

Cibicidoides kullenbergi were selected from fraction 250-500 μm . *C. wuellerstorfi* was rare in most of the samples, especially within the glaciomarine sediments. Therefore, the two species were analysed in some samples, where both occur, which revealed comparable $\delta^{18}\text{O}$ values for both benthic species. The isotopic composition of foraminiferal tests was determined on the CO_2 gas evolved by treatment with phosphoric acid at a constant temperature of 75°C . Working standard (Burgbrohl CO_2 gas) was used for all stable isotope measurements. $\delta^{18}\text{O}$ data have been calibrated against PDB by using the NBS 18, 19 and 20 standards and are given here relative to the PDB standard. Analytical standard deviation is about $\pm 0.07\text{‰}$ PDB.

Radiocarbon dating (AMS ^{14}C) using mono-species samples (~ 10 mg) of planktonic foraminifera *Neogloboquadrina pachyderma* (either dextral or sinistral) from fraction 125-250 μm were analysed at the Leibniz Laboratory for Age Determinations and Isotope Research at the University of Kiel (Nadeau et al., 1997). The data were corrected for ^{13}C and the calibration to calendar years was performed using Calib 4.3 program (Stuiver and Reimer, 1993) and the marine data set of Stuiver et al. (1998) with

a reservoir age of 400 years. All ages are given in 1000 calendar years before present (kyr BP; Table 4-2). Ages greater 21 kyr BP were calibrated using the method of Voelker et al. (1998).

The collected fine fraction ($< 63\ \mu\text{m}$) of cores GeoB 6718-2, GeoB 6725-1 and GeoB 6727-2 was used to determine grain-size distribution of the silt-sized fraction (2-63 μm) and the sortable silt spectrum (10-63 μm , McCave et al., 1995). For this, Micromeritics Sedigraph 5100 was used. It measures the concentration of the suspension by the attenuation of an X-Ray beam. The water of the samples was replaced by Sodium polyphosphate (0.05 %) to avoid hindered settling. The samples were homogenised on a rotating carousel overnight (at least 15 hours) and sonified for 10 seconds before analysis. The grain size analysis was performed with a density setting of calcite ($2.71\ \text{g/cm}^3$) at a constant water temperature of 35°C and with an analysis range from 1 to 63.1 μm . In a second step, organic material and CaCO_3 was removed on samples from off-mound core GeoB 6718-2 using H_2O_2 (35%) and acetic acid (6%) to evaluate the difference of bulk and carbonate-free grain-size distribution.

Table 4-2. AMS ^{14}C dates of cores GeoB 6719-1 and GeoB 6725-1.

Core number	sample depth (cm)	AMS ^{14}C age (\pm err.) (kyr BP)	calibrated age (kyr BP)	Remarks
GeoB 6719-1	18	6.2 (0.035)	6.64	KIA 17091 ^a
	98	16.1 (0.07)	18.6	KIA 17092 ^a
	163	21.7 (0.11)	25.4	KIA 17093 ^a
	273	26.8 (0.18)	30.8	KIA 17094 ^a
GeoB 6725-1	68	7.1 (0.045)	7.6	KIA 16206 ^a
	168	20.4 (0.14)	23.5	KIA 16206 ^a

AMS ^{14}C ages were corrected for a reservoir effect of 400 yr and calibrated using the Calib 4.3 software of Stuiver and Reimer (1993). ^aKIA laboratory number, Leibniz Laboratory, University of Kiel, Germany.

Those samples were measured with the density setting of quartz (2.65 g/cm³). Cumulative and mass frequency data output were used to calculate mean silt and mean sortable silt distribution, as well as size frequency distribution. The data were converted into weight percentages (wt.-%).

Another set of samples was ground in an agate mortar after freeze-drying. About 10 mg was weighed into a tin cup for analysing total carbon (TC) using Carlo Erba NA-1500-CNS at GEOMAR, Kiel. Calibration standards for TC were Acetanilid (N = 10.36 %, C = 71.09 %) and SOIL Standard BSTD1 (N = 0.216 %, C = 3.5 %).

Standard deviation of continuously analysed standards was better than 2 %. Carbonate contents of sediments were finally calculated according to their atomic weight ratios:

$$\text{CaCO}_3 (\%) = 8.33 \cdot (\text{C}_{\text{total}} - \text{C}_{\text{org}}).$$

In addition to the discrete carbonate analysis, high-resolution calcium determinations were performed with CORTEX-XRF scanner (Jansen et al., 1998) at University of Bremen. The resulting data are element intensities in counts per second (cps). Correlation of calcium data and carbonate content of the analysed sediment cores presents a linear regression with $R^2 = 0.77$ (Appendix 7).

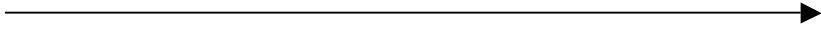
4.4 Stratigraphy

The stratigraphic framework of the investigated cores is primarily based on AMS ¹⁴C ages and benthic stable oxygen isotopes. Additional evidence is derived from calibrated Ca corescanner data (Appendix 7), tracing glacial-interglacial fluctuations of calcium carbonate. Core GeoB 6719-1 is used here for stratigraphic correlation to the other cores, as four AMS ¹⁴C dates have been performed (Table 4-3). All cores present a rather continuous record

reaching back to Late MIS 3 (Fig. 4-2). The correlation of the lower core section of GeoB 6727-2 (>280 cm) and GeoB 6719-1 (>420 cm) remains questionable, as very small numbers of benthic and planktonic foraminifera in fraction >125 μm prevent stable isotope and AMS ¹⁴C analyses. However, low carbonate content of <20 % suggests comparable conditions as during MIS 2 and/or dilution of sediment by a high supply of terrigenous material.

Table 4-3. Sedimentation rates of investigated cores.

	GeoB 6727-2 (cm/kyr)	GeoB 6719-1 (cm/kyr)	GeoB 6725-1 (cm/kyr)	GeoB 6718-2 (cm/kyr)
Holocene	1.70	2.50	2.00	7.30
MIS 2	5.50	8.33	15.67	20.42
Late MIS 3	17.86	20.86	27.86	–



 Increasing distance from Propeller Mound

The records of GeoB 6727-2, GeoB 6719-1 and GeoB 6725-1 are marked by a major horizon of reworked sediment (dark grey area in Fig. 4-2). This event seems to be slightly older than 31 kyr BP according to an AMS ^{14}C date in core GeoB 6719-1 at 273 cm (Fig. 4-2, Table 4-3). The thickness of this horizon varies between 60 cm (GeoB 6725-1) and 130 cm (GeoB 6719-1). Due to higher sedimentation rates in core GeoB 6718-2 the level of reworked sediments is not reached. An additional tie point is indicated by a characteristic double peak in records of XRF Calcium counts (Fig. 4-2; Appendix 7). This peak corresponds to an age of around 25 kyr BP, related to Heinrich

event 2 (HE 2) and its European precursor event (Grousset et al., 2000) at the stage boundary of MIS 2 and 3. A significant increase in the carbonate content close to the core top indicates Termination Ia (12 kyr BP) and Ib (10 kyr BP), the onset of the Holocene (Martinson et al., 1987). The latter CaCO_3 increase is coherent with a decrease of benthic $\delta^{18}\text{O}$ values in cores GeoB 6718-2 and GeoB 6727-2. However, $\delta^{18}\text{O}$ values of core GeoB 6725-1 and GeoB 6719-1 remain at high level most certainly due to bioturbation. The resulting sedimentation rate decreases from Late MIS 3 towards the Holocene and increases with increasing distance from Propeller Mound (Table 4-3).

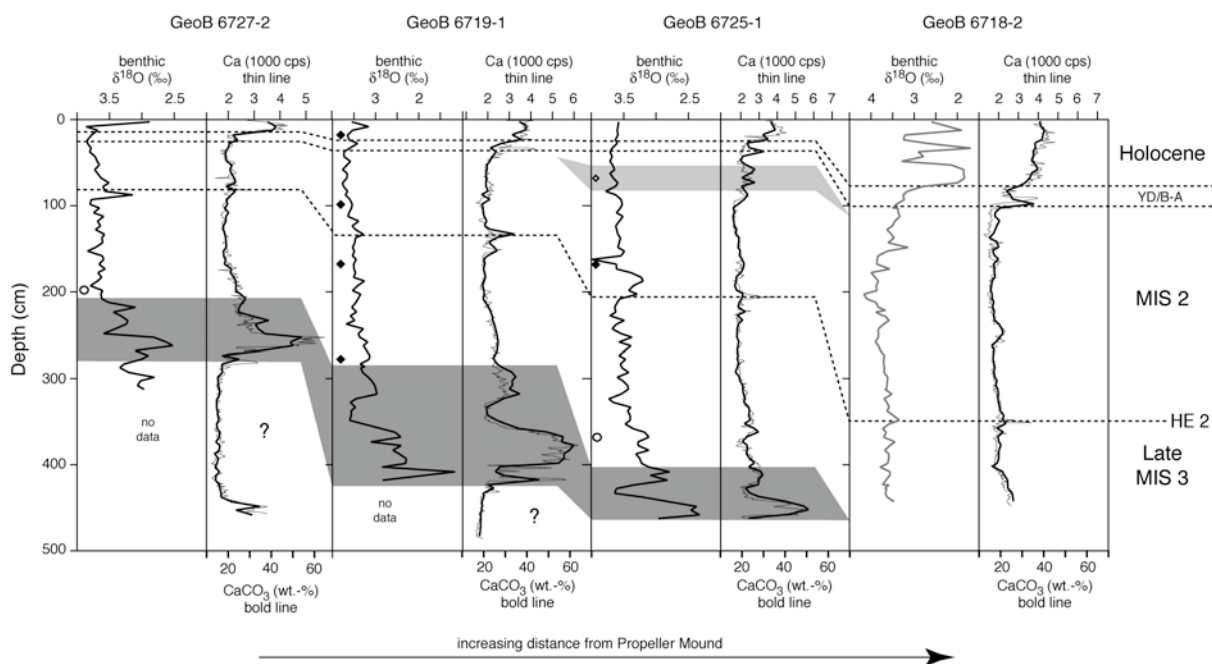


Figure 4-2. Benthic stable oxygen isotope data and CaCO_3 content, as well as XRF Ca-counts of sediment cores GeoB 6718-2, GeoB 6719-1, GeoB 6725-1, and GeoB 6727-2. The cores follow the increasing distance from Propeller Mound (from left to right). Stratigraphy is indicated to the right. Dashed lines indicate stratigraphic boundaries between marine isotope stages 1, 2 and 3, based on calibrated scanner data (Appendix 7), rectangles = AMS ^{14}C dates, open rectangle = bioturbated AMS ^{14}C age, open circle = age determination from inter core correlation (Appendix 7), light grey area = bioturbated sediments, dark grey = reworked sediments (turbidite). Surface of turbidite seems to be slightly older than 31 kyr BP. Below turbidite, no foraminifera were available for stable isotope measurements and AMS ^{14}C dating.

4.5 Results

4.5.1 Sedimentology of sediment cores around Propeller Mound

The sediments of the three investigated cores GeoB 6718-2, GeoB 6725-1 and GeoB 6727-2 are dominated by dark greyish brown silty clay and olive grey to greyish brown sandy silt (Fig. 4-3). Greyish brown silty sands occur at the core tops representing Holocene sediments, and at the core base of GeoB 6725-1 and within a section at around 250 cm of core GeoB 6727-2 (Fig. 4-3). The latter two sections are composed of reworked material with high amounts of coarse lithic grains, drop stones, deep-water coral fragments (mainly *Lophelia pertusa* and *Madrepora oculata*), and shells of molluscs, gastropods, bryozoans, echinodermata, and brachiopods, comprising the associated fauna of the deep-water coral reef ecosystem. The carbonate content of the reworked sediments is much higher reaching 60 %, compared to the Holocene sections (Fig. 4-2). Between 300-400 cm of core GeoB 6725-1, high numbers of coral fragments indicate a supply of sediments from the nearby mound.

The sedimentary structure revealed from CT images varies from sections dominated by silty and clayey laminae, diffuse structures with no clear lineation, to heavily disorganised sediments. Indications of burrows and bioturbation occur within the coarser sediments of the Holocene, but are also present in the glaciomarine sediments, especially between 50 and 80 cm of core GeoB 6725-1 (Fig. 4-3). Fining upward cycles describe the turbidite section of core GeoB 6727-2 and GeoB 6725-1.

4.5.2 Sediment facies

From the visual examination of cores, computed tomographic imaging, grain size analysis, and calcium carbonate content, six sediment facies types have been distinguished in the studied cores (Fig. 4-4). CT images allow identifying different sediment structures and composition. Bright (white) structures occur, when the density is high (e.g. lithic grains, coral fragments), whereas dark sections correspond to lower densities (clayey to silty matrix, higher porosity).

Facies 1: homogenous, structureless hemipelagic sandy silt

Facies 1 appears on CT images as homogenous, bioturbated sediment (Fig. 4-4). It is composed of olive grey to greyish brown sandy silt with relatively high concentrations of foraminifera. The CaCO₃ content is around 40 % (Fig. 4-2). Silt is the dominating fraction of this sediment (62 wt.-%), while clay and sand have an similar contribution (22 wt.-% and 16 wt.-%). This facies is observed within the late Holocene of core GeoB 6718-2 (top ~70 cm, Fig. 4-5) and is interpreted as hemipelagic drape sediment, as this sediment has been reported from different sites within the PSB (Coles et al., 1996; Huvenne et al., 2002; De Mol et al., 2002;).

Facies 2: diffuse structured silty sand

Facies 2 describes a diffuse structured silty sand, consisting of strongly bioturbated, hemipelagic silty sand (Fig. 4-4). The carbonate content varies between 35 % and 45 % (Fig. 4-2). Sand reaches maximum content of 50 wt.-%, whereas clay is generally below 20 wt.-%. This facies describes the top section of cores GeoB 6727-2 (top

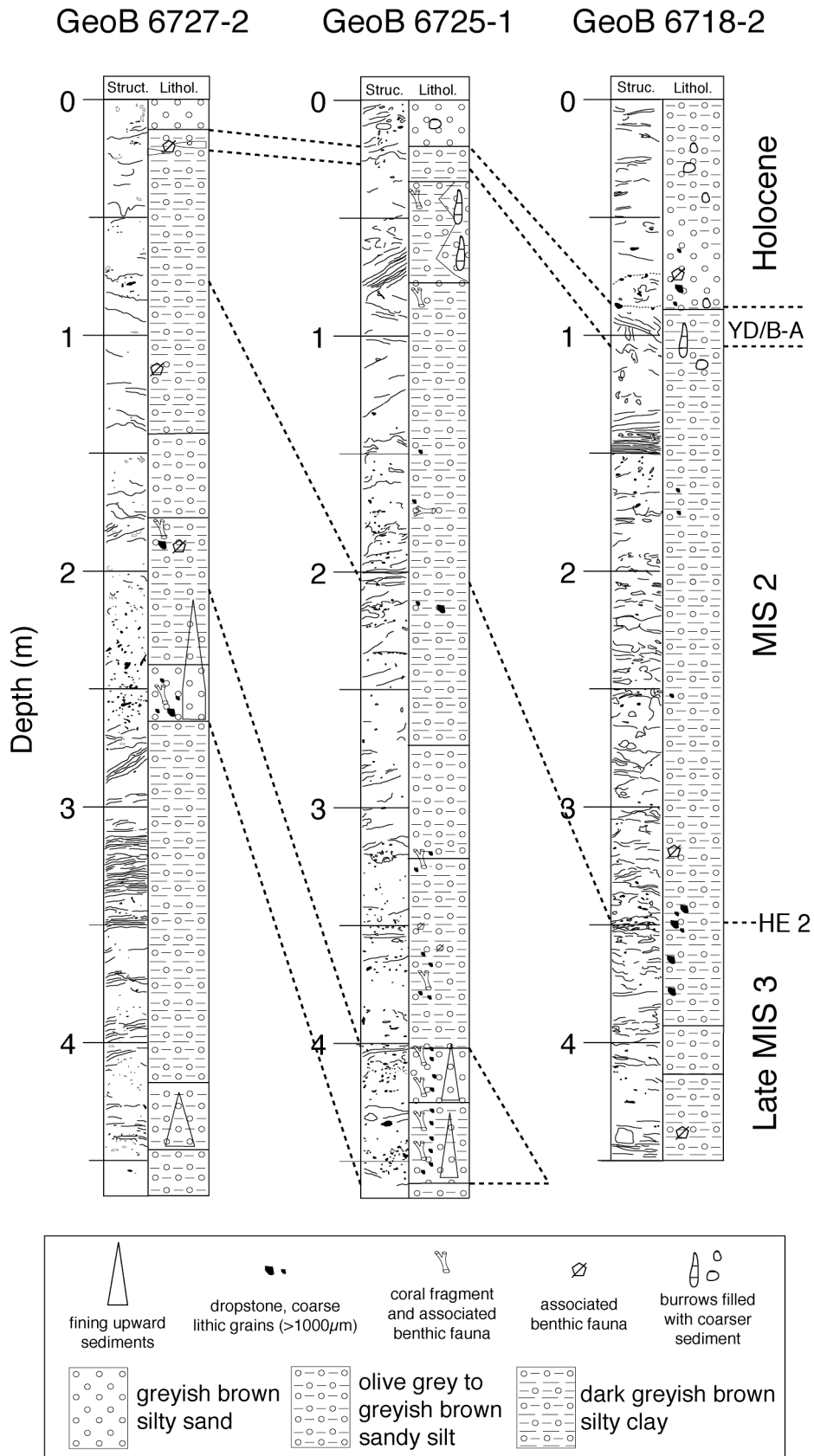


Figure 4-3. Lithology and sediment structure of cores GeoB 6727-2, GeoB 6725-1 and GeoB 6718-2 from visual core description, CT images, carbonate content and grain size analyses.

15 cm) and GeoB 6725-1 (top 25 cm), and early Holocene section of core GeoB 6718-2 (~70–85 cm, Fig. 4-5). It is interpreted as a hemipelagic contourite sediment, which was probably deposited under a stronger current regime.

Facies 3: diffuse laminated to disorganised silty clay

Facies 3 consists of intervals with varying thickness (10–120 cm) of diffuse laminated to chaotic, disorganised silty clay (Fig. 4-4). The carbonate content rarely exceeds 20 % (Fig. 4-2). The clay content is generally >40 wt.-%, while the sand content lies below 20 wt.-%. Due to its diffuse and disorganised structure, Facies 3 is interpreted as a result from mass transport of fine-grained sediments (slump, debris flow,

strong turbidity currents), whether from the shelf or from the mounds. It describes most of MIS 2 and Late MIS 3 (Fig. 4-5).

Facies 4: structureless silty clay

Facies 4 is a structureless silty clay (Fig. 4-4), dominated by terrigenous material (CaCO₃ content <20 %, Fig. 4-2). It consists of dark greyish brown clay (40 to 50 wt.-%) with low sand content of <20 wt.-%. In some areas, this facies contains black dots. In deeper environments black coloured bandings occur usually due to the presence of black hydrotroilite (Nelson et al., 1992; Zaragosi et al., 2000) and represent enhanced preservation of organic material due to high sedimentation rate and/or anoxic bottom water conditions (Stow et al., 1996).

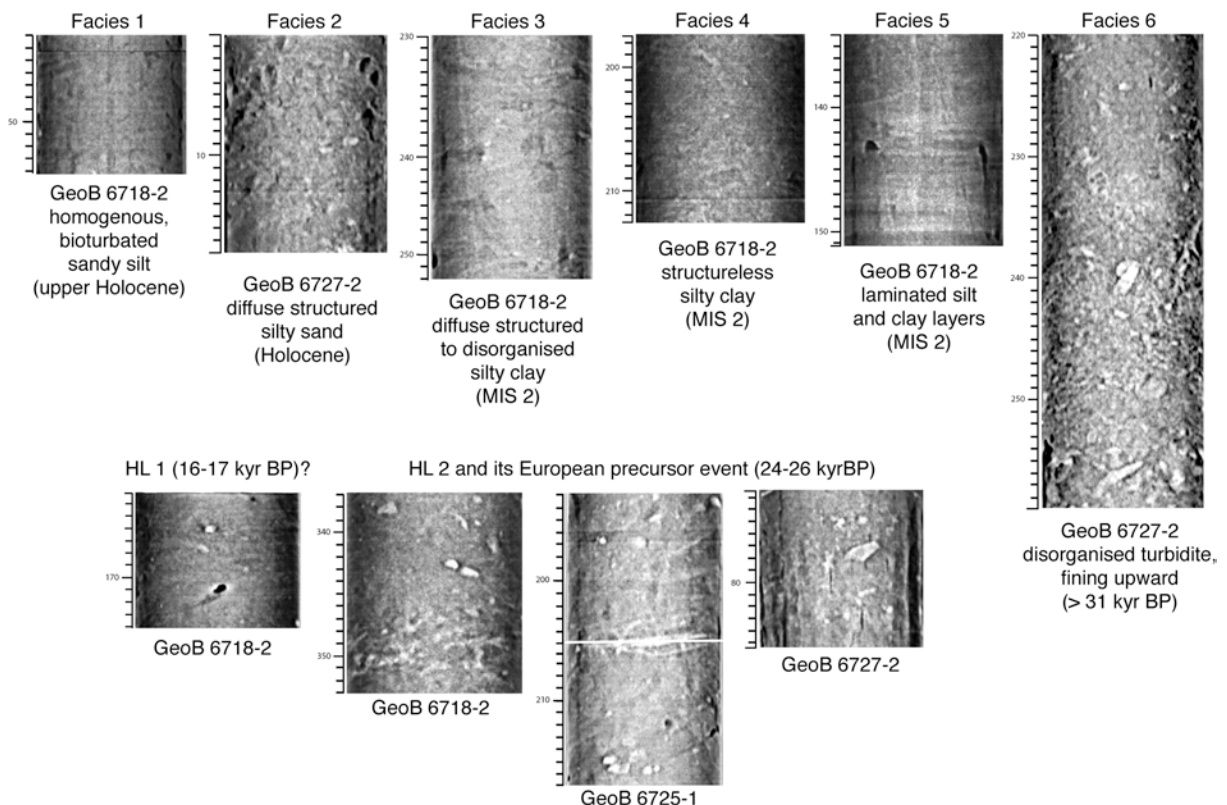


Figure 4-4. Sediment facies identified from CT images and visual core description. Within Facies 3 and 4, sections with ice rafted gravel and debris have been identified, corresponding to Heinrich layer 1 and 2 (HL 1 and 2). Scale to the left of CT images is in cm and corresponds to the core depth.

Facies 4 occurs during MIS 2 and Late MIS 3 and represents the high deposition rate under calm hydrodynamic condition.

Facies 5: laminated silt and clay

At the base of core GeoB 6718-2 and in 150 cm core depth (~14 kyr BP), CT images clearly present laminated sediments

(Fig. 4-4). The carbonate content below 20 % is similar to Facies 3 and 4. These alternating silt and clay laminae have a sharp contact at the base and gradually change into Facies 4. Facies 5 sequences are observed in core GeoB 6718-2 during MIS 2 and 3 and below the turbidite in core GeoB 6727-2.

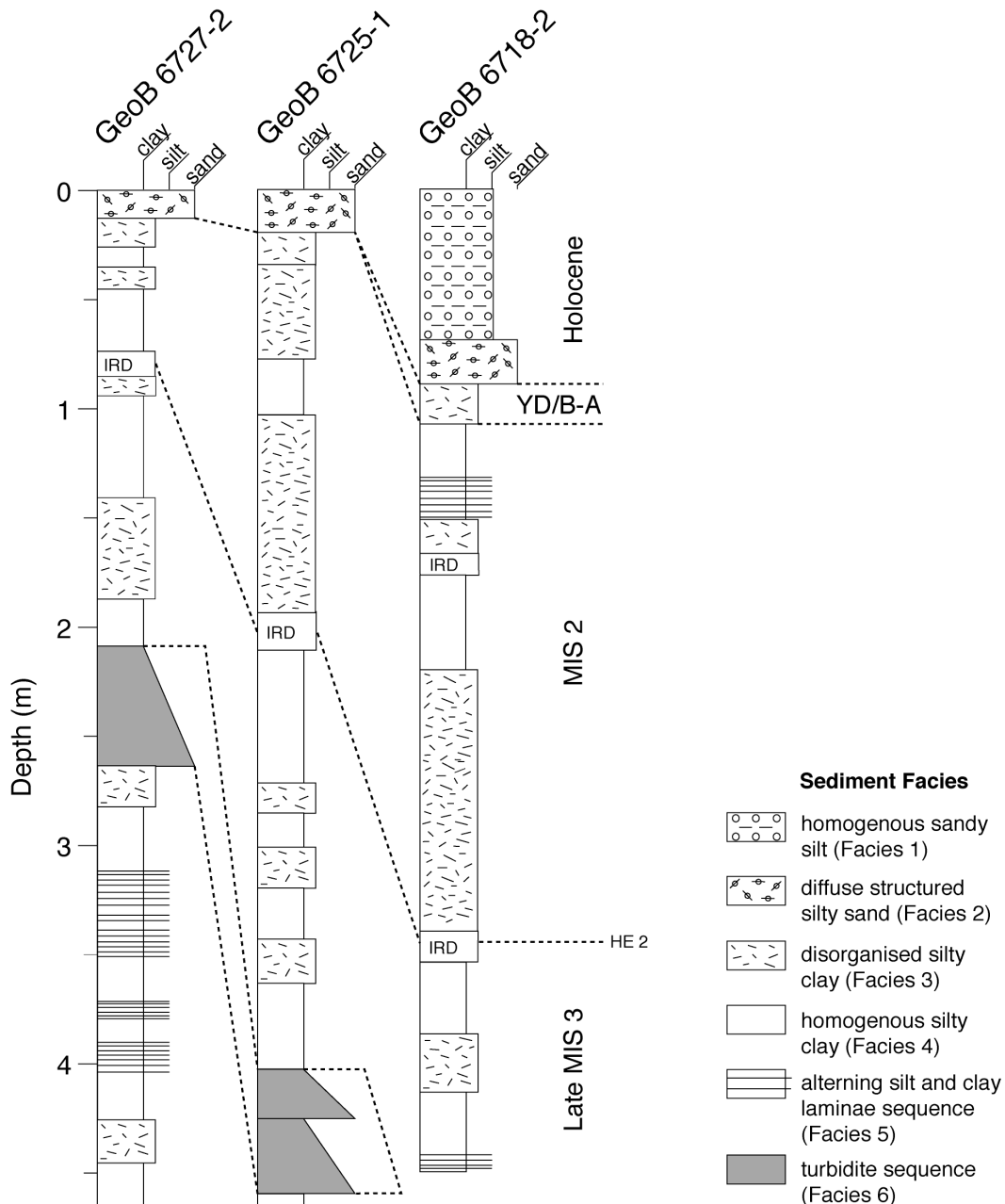


Figure 4-5. Downcore record of identified sediment facies 1-6. The Holocene succession is characterised by Facies 1 and 2. Facies 3 and 4 dominate MIS 2 and Late MIS 3. Alternating silt and clay laminae only occur in core GeoB 6718-2 and below the turbidite (Facies 6) of core GeoB 6727-2.

The altering silt and clay laminae have also been reported from the Celtic margin south of the PSB and probably also indicate a fine-grained turbidite facies being deposited by low-density turbidity currents (Zaragosi et al., 2000).

Facies 6: disorganised turbidite sequence

Facies 6 consists of disorganised, coarse-grained sediments (sand content up to 50 wt.-%) with high amounts of coral fragments and shells from bivalves, gastropods and echinodermata, but also of dropstones and coarse lithic grains (Fig. 4-3 and 4-4). The abundance of fragments and pebbles decreases towards the top of the turbidite, where the sediment gradually turns into Facies 4. The carbonate content is 50 % high at the base and decreases towards the top of the turbidite section to reach similar low values as in Facies 4 (Fig. 4-2). This facies is interpreted as being deposited by high-density turbidity currents and/or as resulting from mass transport deposits (slump or debris flow). Facies 6 is present in cores GeoB 6727-2 and GeoB 6725-1 (Fig. 4-5). Due to the stratigraphic correlation to other sediment cores, the turbidite is suggested to be slightly older than 31 kyr BP and possibly comprises Ice Rafted Detritus (IRD) of HE 3 (32.5 to 29.6 kyr BP) as reported from the Celtic margin (Auffret et al., 2002).

Ice rafted detritus layer

Within Facies 3 and 4, CT images show gravel sized drop stones at the transition from MIS 2 to 3 (24–26 kyr BP, Fig. 4-3 to 4-5), which most certainly corresponds to HE 2 and the European precursor event (Grousset et al., 2000). High sand content is coherent with the IRD layer of core GeoB 6718-2, but is absent in the other cores. At

~170 cm of core GeoB 6718-2, another horizon containing coarse lithic grains is visible from CT images (Fig. 4-4). Sand content increases slightly from 10 to 20 wt.-%. According to the stratigraphy, this IRD layer may be related to HE 1, but does not occur in the cores located closer to Propeller Mound (Fig. 4-5).

4.5.3 Silt fraction analysis

Grain size analysis on fine sediment size (<63 μm) of carbonate-free samples has been proposed to indicate paleocurrent strength intensities (McCave et al., 1995). Sortable silt describes the grain size range of fraction 10–63 μm , which behaves dominantly noncohesively, whereas grains smaller than 10 μm show a cohesive behavior. Thus, silt coarser than 10 μm displays size sorting in response to hydrodynamic processes and its properties are used to infer current speed.

On samples of core GeoB 6718-2 grain-size analyses were performed on bulk and carbonate-free samples of fraction <63 μm (Fig. 4-6). The results indicate a similar downcore record for both bulk and lithogenic samples. Differences only occur with respect to their intensity, especially of fraction <10 μm and at the core top in fraction 20–40 μm , which is the result of dissolution of coccoliths and foraminiferal test fragments. However, correlation of both bulk and lithogenic mean sortable silt records present a correlation coefficient of $R^2 = 0.87$ and the records display similar downcore variability (Fig. 4-6). This pattern is also suggested for cores GeoB 6725-1 and GeoB 6727-2, as they display comparable sediments with similar carbonate contents (Fig. 4-2 and 4-3). Therefore, all cores will be discussed with respect to their bulk fine

fraction distribution, representing sorting of sediment dependent on changes of current strength intensity.

Sedimentary processes may vary from strongly erosive, transport dominated to accumulative, and control the rate of sedimentation. Höppner and Henrich (1999) characterised different sediment types, each related to a different hydrodynamic setting. Type I is characterised by relatively coarse sediments and shows a unimodal distribution within the silt range (Fig. 4-7). Relatively strong currents remove fine-grained material from the sediment surface and leave behind this sorted, residual sediment. Within the marine milieu, contour currents often produce these sediments.

Type II portrays a polymodal distribution, formed under strongly variable bottom current velocities. Decreasing current intensity reduces the ability of water to keep larger particles in suspension, which results into the accumulation of fine material (Type III). Sediment Type III is here divided into Type IIIa and IIIb (Fig. 4-7). Both show generally fine material of fine-silt spectrum (2–10 μm) and describe accumulated sediments, caused by weak currents. However, Type IIIa has a stronger affinity to slightly coarser sediments, indicating transitional sediments between Type II and Type IIIb. This sediment type is related to in- or decreasing current activity (Fig. 4-7).

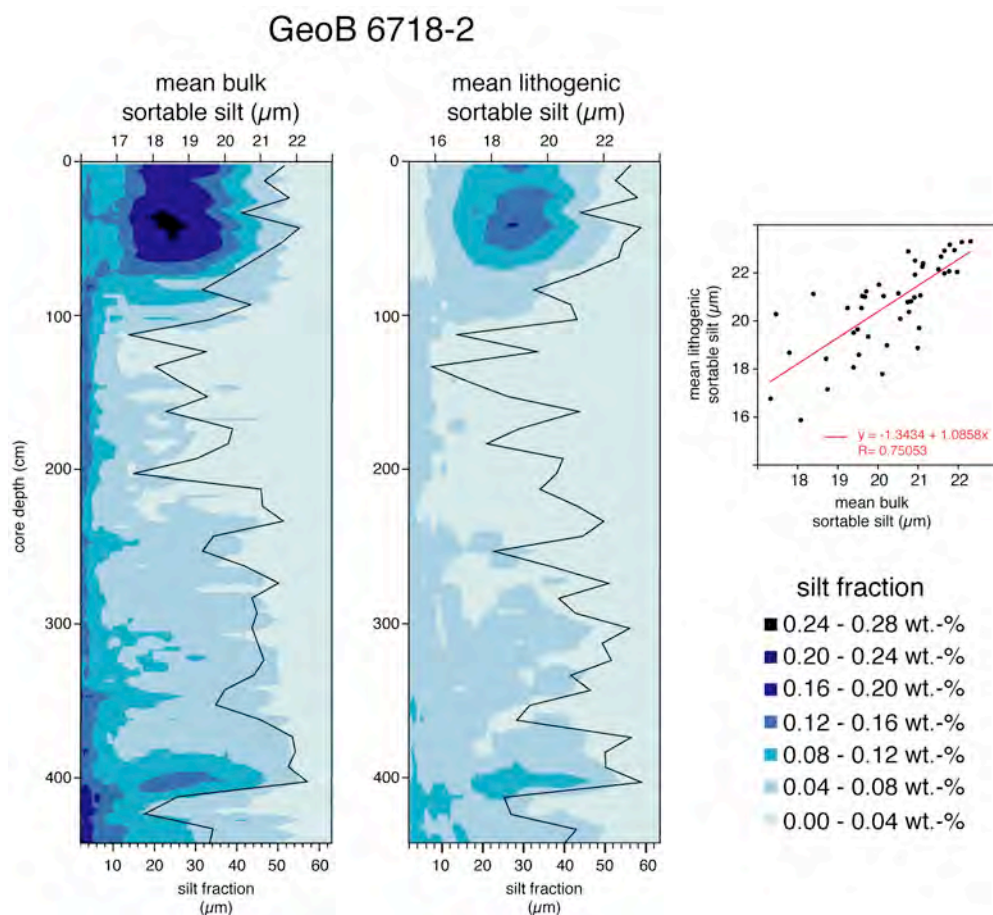


Figure 4-6. Comparison of bulk and lithogenic silt fraction analysis of core GeoB 6718-2. Silt spectrum and mean sortable silt present good correlation with $R^2 = 0.87$. Changes in intensity of silt spectrum are the result of removal of CaCO_3 (shell fragments of foraminifera and coccoliths).

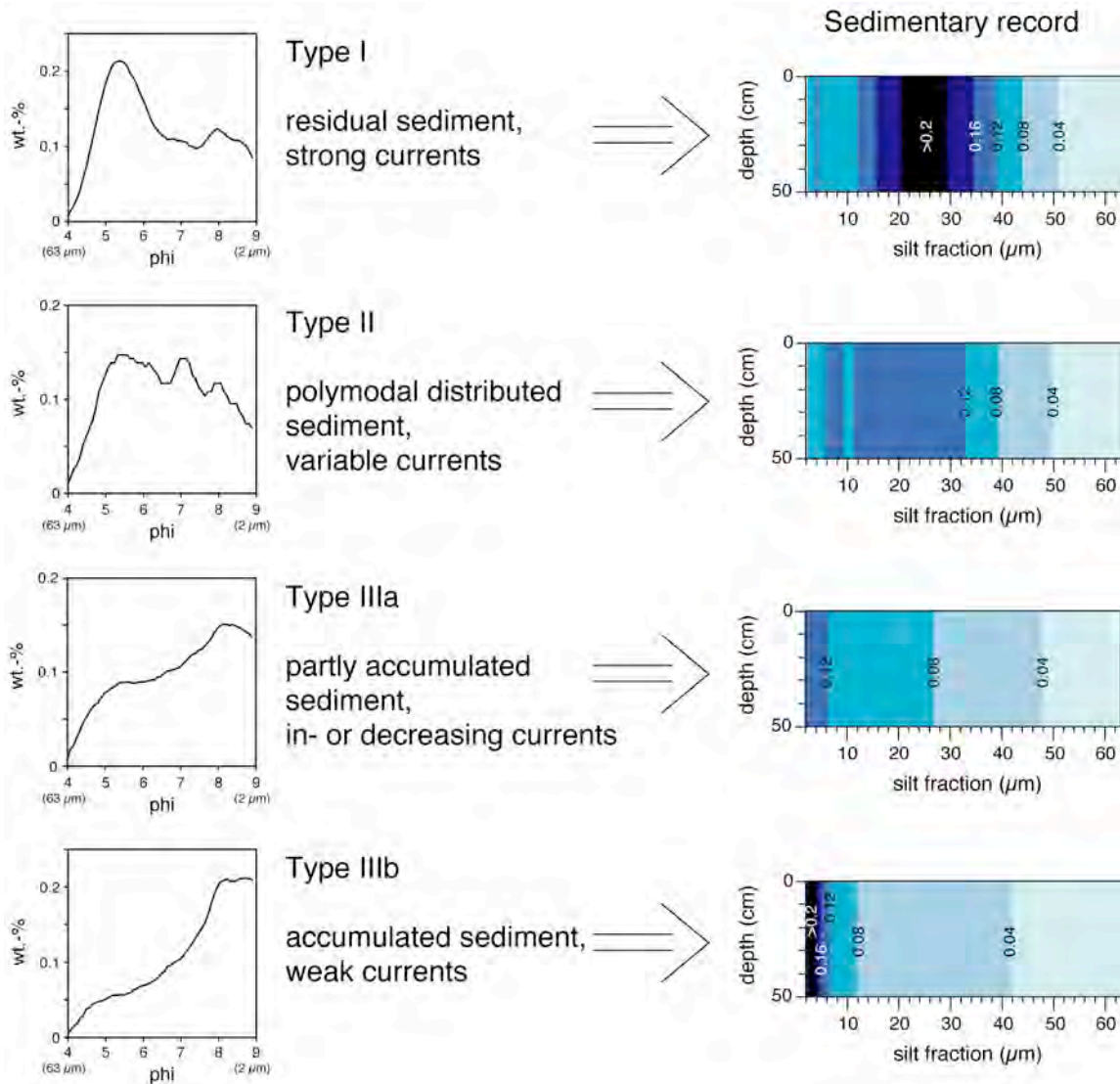


Figure 4-7. Characterised sediment types of silt fraction analyses after Höppner and Henrich (1999) and their sedimentary record to the right. The phi-scale corresponds to the negative logarithm to the base 2 of the grain size (in mm). Values in sedimentary record are in wt.-%.

The downcore record of the classified sediment Types I to III is illustrated in Figure 4-8. The base of the turbidite is described by polymodal distributed silt spectrum (Type II), fining upward to accumulated sediments (Type IIIb). The period of Late MIS 3 (31–24 kyr BP) is dominated by accumulation of sediments (Type IIIa and b). An increase towards coarser sediments (sorted and residual, Type I and II) occurs at around 28–29 kyr BP

(GeoB 6727-2: 140–180 cm, GeoB 6725-1: 275–315 cm), indicating an increase of the generally weak current regime (Fig. 4-8). Accumulated sediments dominate MIS 2 implying a weak hydrodynamic regime. A trend to finer sediments occurs at around 18 kyr BP in core GeoB 6718-2 (~220 cm) and GeoB 6725-1 (~130 cm), illustrated by a gradual change from sediment Type IIIa to IIIb. However, this feature is not visible in core GeoB 6727-2 (Fig. 4-8).

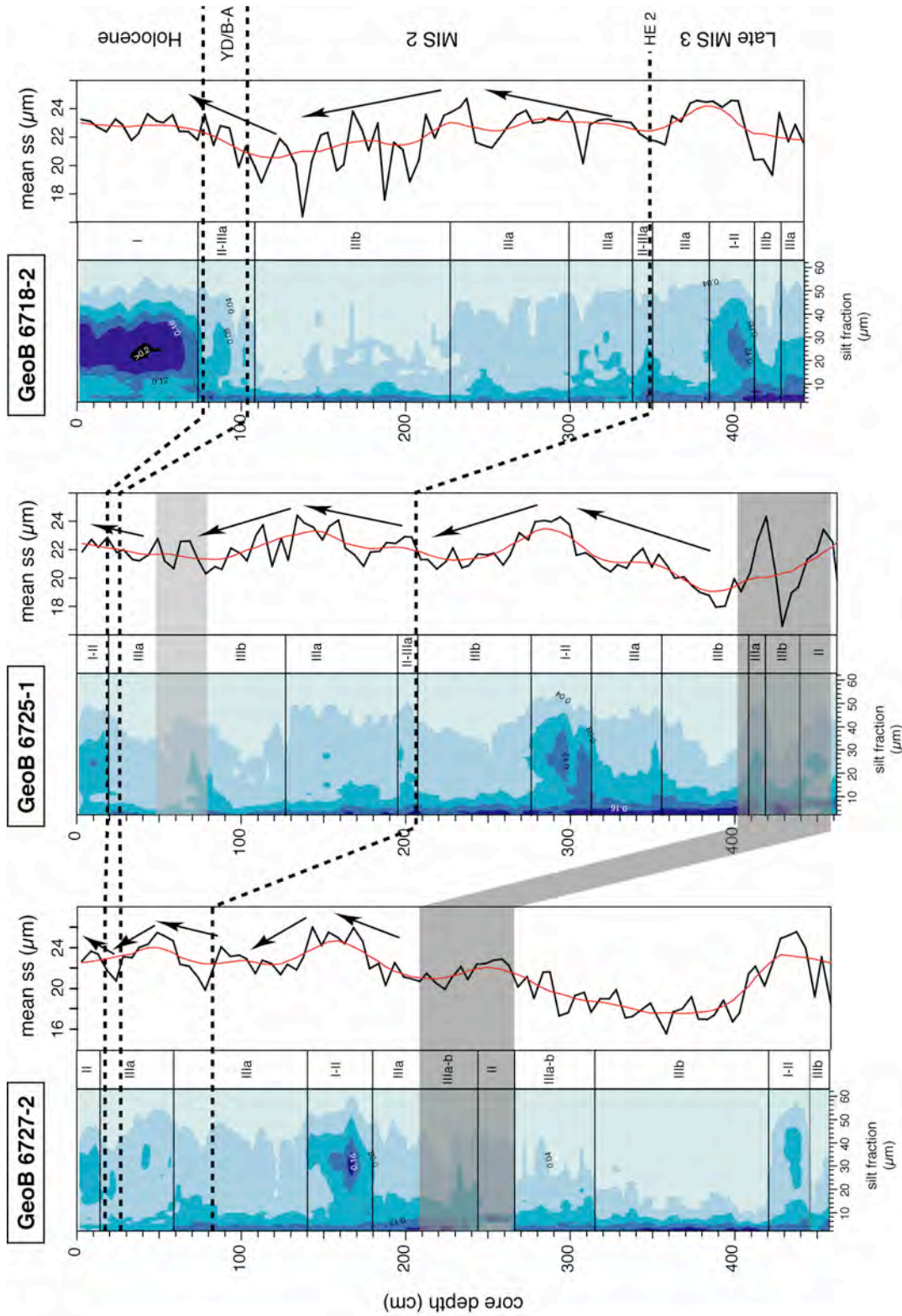


Figure 4-8. Downcore record of silt fraction (in wt.-%; see Fig. 4-7) and the corresponding Types I – III (after Höppner and Henrich, 1999). Mean sortable silt (black curve) and the weighted mean (20 %, red curve) indicate an in- or decrease in current strength intensity (arrows). Dark grey area = tubidite, light grey = bioturbation, stratigraphic units are illustrated to the right.

A slight increase from Type IIIb to IIIa at around 80 cm in core Geob 6725-1 defines the transition to the bioturbated section. The abrupt change from accumulated sediments to polymodally distributed and residual sediments at Termination Ia is clearly visible in core GeoB 6718-2, indicating an intensified current regime, which persists for the whole Holocene period (Fig. 4-8).

The mean sortable silt record generally follows the change between accumulated and polymodally distributed to residual sediments with an increasing or decreasing signature between 16 and 25 μm (Fig. 4-8). In all three cores the mean sortable silt record displays similar variability:

- (1) an increase from the top of the turbidite to maximum values of $\sim 24 \mu\text{m}$ at 140–180 cm (GeoB 6727-2), and 275 to 305 cm (GeoB 6725-1), corresponding to ~ 28 – 29 kyr BP,
- (2) a decrease towards the stage boundary MIS 2/3 (GeoB 6727-1, GeoB 6725-1),
- (3) an increase to a maximum of 24 – $25 \mu\text{m}$ at ~ 18 kyr BP (GeoB 6727-2: ~ 50 cm, GeoB 6725-1: ~ 130 cm, GeoB 6718-2: 230 cm),
- (4) a decrease towards the Younger Dryas/Bølling-Allerød,
- (5) and finally an increase towards the Holocene, where the values remain at one level (e.g. GeoB 6718-1: top 80 cm).

4.6 Discussion

4.6.1 Irish ice sheet advance and shelf erosion during Late MIS 3

Coarse-grained turbidites have been suggested as being derived from an ice-proximal glaciomarine environment and are possibly associated with high discharges of subglacial meltwater. They are reported from the Hebrides Shelf (Knutz et al., 2001) and from the Celtic margin (Zaragosi et al., 2000; Auffret et al., 2002). Their presence may thus indicate periods when glacial ice was grounded on the shelf margins.

Before 30 kyr BP, Ireland was largely ice-free and interstadial conditions prevailed (Jones and Keen, 1993). Glaciers may have existed in western Scotland and Northern Ireland (Bowen, 1999) but were probably grounded above the marine limit. However, Knutz et al. (2001) reported variable deposition of quartz-rich IRD between 45 and 30 kyr BP suggesting glaciomarine

conditions were intermittently established along the NW British margin. According to McCabe (1987), Irish inland ice was rapidly advancing after 30 ^{14}C kyr BP (~ 33.5 kyr BP), coherent with subarctic, tundra-like, open vegetation of the Derryvree cold phase (30–35 ^{14}C kyr; Jones and Keen, 1993). A sea-level decrease and worsened climatic conditions are reported for the western margin of Ireland during Late MIS 3 (Auffret et al., 2002).

The turbidite section in core GeoB 6725-1 and GeoB 6727-2 probably indicates a first advance of the BIIS. High carbonate contents ($>50\%$) of the reworked material implies the deposition of interglacial sediments, which is also suggested by high abundance of benthic foraminifera representing an interglacial assemblage (Chapter 5). These sediments must have been eroded from (a) the exposed shallow shelves due to the low sea-level stand and a first advance of the glaciers onto the shelf,

or (b) from the nearby Propeller Mound. The occurrence of coral fragments within the turbidite section accounts for a sediment source from the mound. However, epibenthic foraminifera typical for the deep-water coral ecosystem are scarce and the assemblage is similar to species describing the Holocene section of core GeoB 6725-1 (Chapter 3).

High abundance of IRD within the turbidite may correspond to HE 3 (32.5 to 29.6 kyr BP). Isotopic analysis of the coarse lithic fraction from the Celtic margin indicates a presumably European origin of HE 3 deposits along the western margin of the British Isles (Auffret et al., 2002). The general ice flow on Ireland accounts for high terrigenous fluxes from Ireland, across Galway Bay and into the PSB (Fig. 4-9, Eyles and McCabe, 1989; Jones and Keen, 1993). Hence both IRD and reworked interglacial sediments indicate that glaciers had reached the western margin of the Irish shelf at a time that correlates with HE 3. Therefore, the turbidite represents a release of eroded sediments (mass wasting) by a first advance of glaciers onto the shelf. However, the occurrence of coral fragments in the turbidite layer suggests, that strong turbidity currents also had an effect on the elevated mounds with a removal of sediments from them (Fig. 4-9). It seems, that this turbidite facies is a result of mass waste from both, the elevated mounds and the Irish Mainland shelf.

The glaciomarine environment was established after the first advance of the Irish ice sheet onto the Irish shelf. Sediments covering the period of Late MIS 3 (~31–24 kyr BP) are described by homogenous to laminated and disorganised silty clays (Facies 3–5) indicating a weak benthic current regime interrupted by phases

of fine-grained debris flow or turbidity currents (Fig. 4-5). The substantial high sedimentation rate further indicates an enormous sediment supply from the shelf into the PSB. During this period, sea-level was decreasing and the climatic conditions worsened (Auffret et al., 2002), while the BIIS propagated to its maximum extent between 24 and 20 ¹⁴C kyr BP (McCabe, 1987). Additional information supporting strong shelf erosional processes is indicated by displaced benthic foraminiferal species preferably living in an estuarine and near-glacial shelf environment (Chapter 3).

Towards the transition between MIS 3 and 2, the double peak in XRF Ca-records (Fig. 4-2), as well as abundant IRD (Fig. 4-4) indicate the deposition related to HE 2 and its European precursor event (Grousset et al., 2002; Richter et al., 2001). The abundant IRD is related to the calving of icebergs from Irish glaciers, which started significantly at ~25 kyr BP (Siegert and Dowdeswell, 2002; Auffret et al., 2002). Richter et al. (2001) reported of increased supply of detrital carbonates during HE 2 and MIS 2 at Feni Drift in the Rockall Trough and argued that this site was dominantly effected by British-Irish detrital IRD input, eroded from the Carboniferous limestone formations of Ireland. An increased input of detrital carbonates of Irish origin is assumed for the PSB, indicated by peaks in the Ca counts (Fig. 4-3).

4.6.2 Redistribution of glacial sediments during MIS 2

After HE 2, the sediments around Propeller Mound are dominated by disorganised silty clays (Facies 3, Fig. 4-5) indicating abundant gravity flows and turbidity currents during early MIS 2. The sedi-

mentation rate decreased from 17 to 28 cm/kyr for Late MIS 3 to 5–20 cm/kyr during MIS 2 (Table 4-3). According to McCabe (1987), the maximum expansion of the BIIS was reached between 24–20 ^{14}C kyr BP, coherent with the onset of iceberg calving from British glaciers at ~ 25 kyr BP (Fig. 4-9; Siegert and Dowdeswell, 2002). The final position of the BIIS without any indications of a further advance to the

southwest resulted in an abrupt decrease of sediments supplied into the PSB. Sea-level was still decreasing to its maximum lowstand of 120 m below present level at ~ 17 –18 kyr BP (Labeyrie et al., 1987; Fairbanks, 1989; Auffret et al., 2002), while the Irish ice sheet margin retreated markedly from 21–18 kyr BP (McCabe and Clark, 1998).

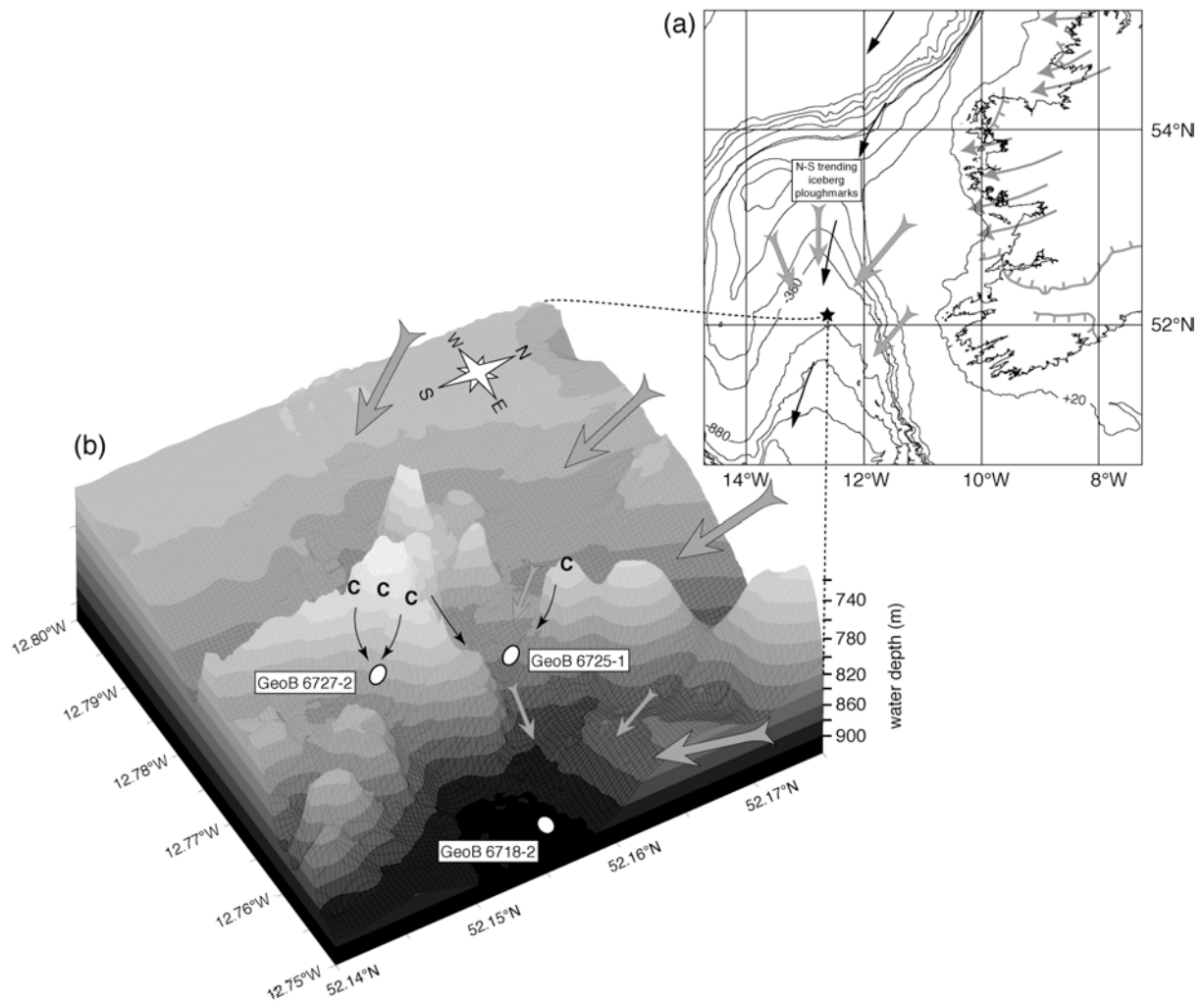


Figure 4-9. (a) Map of the Porcupine Seabight for the last glacial stage. Ice limits on Ireland (grey lines on Ireland) and general ice flow across the Galway Bay (thin grey arrows) are from Eyles and McCabe (1989) and Jones and Keen (1993). The general southward flow of surface waters is indicated with black arrows (Sarnthein et al., 1995). Big grey arrows correspond to sediment transport (shelf erosion, turbidity currents).

(b) Propeller Mound, viewed from the SE, with indicated core sites, flow path of turbidity currents and gravity flows (grey arrows) and the erosion paths from the mound contributing coral fragments to the off-mound sites. V.E. $\approx 1:3$.

As a consequence, glacial material had been exposed to erosion, documented in an important phase of shelf sediment erosion at the Celtic Margin (Auffret et al., 2002). The sediment cores off Propeller Mound show an increase in mean sortable silt to approx. 18–19 kyr BP, which portrays the increase in abundant turbidity currents (Fig. 4-8). A change to fine-grained, accumulated sediments (Facies 4, Type IIIb) indicates a decline in sediment erosion from the shelf and/or mound (decreasing currents) at the sea-level lowstand, when the glaciers on SW Ireland were already above the marine limit (Eyles and McCabe, 1989).

The period of deglaciation is expressed in decreasing terrigenous fluxes along the Celtic Margin (16.7–11 kyr BP; Auffret et al., 2002), whereas Knutz et al. (2001) reported of a readvance of the western sector of British Ice Sheet further north with renewed gravity flow sedimentation and a clearly defined IRD horizon, corresponding to HE 1 (16–17 kyr BP). Only in core GeoB 6718-2 a layer with IRD occurs at ~170 cm (Fig. 4-5), indicating a release of terrigenous material by icebergs, probably indicating HE 1 deposits. However, an advance of glaciers onto the Irish shelf is not reported after 19 kyr BP (Eyles and McCabe, 1989). The low abundance of *E. excavatum* supports this indication by an absence of a near-glacial environment along the Irish Mainland shelf (Chapter 3) Therefore, the IRD layer in core GeoB 6718-2 seems to be a result of the southward transported of IRD by icebergs, as indicated by N-S trending iceberg plough marks on Slyne Ridge (Fig. 4-9; Games, 2001).

Late MIS 2 deposition around Propeller Mound is described by the renewed

establishment of turbiditic supply (Facies 3 and 5; Fig. 4-5), indicating the reworking of shelf sediments by the rising sea-level. This sea-level rise started at ~18 kyr BP and reached its highstand at ~6 kyr BP (Clark et al., 1999; Siddall et al., 2003). However, the shelf erosion during late MIS 2 was probably not as high as for Late MIS 3, as shallow shelf dwelling benthic foraminifera have low abundance during MIS 2 (Chapter 3).

4.6.3 Holocene and present-day sedimentary setting around Propeller Mound

During Termination I, a change from glaciomarine to hemipelagic deposition is indicated by an increase of the sediment grain-size (Facies 3 (IIIa) to Facies 2 (I–II), Fig. 4-5 and 4-8), an increase in the carbonate content (Fig. 4-3), as well as a change towards stronger currents, expressed in an increase of the mean sortable silt record (Fig. 4-8). The oceanographic setting changed remarkably with the establishment of the present-day hydrodynamic regime. The Polar Front moved northward across the PSB (Jones and Keen, 1993) and intermediate water masses with a southern source (ENAW, MOW) entered the PSB. The decrease in sedimentation rate from 5–20 cm/kyr during MIS 2 to 1.7–7.3 cm/kyr for the Holocene (Table 4-3), portrays the strong current regime at intermediate depths (White, subm.) with the deposition of polymodally distributed to residual silty sands (Facies 1 and 2; Fig. 4-5).

In core GeoB 6718-2, Facies 2 probably indicates the reintroduction of ENAW and MOW during the onset of MIS 1 (Fig 4-5). The top 70 cm of this core is described by

Facies 1, which is composed of slightly finer material. Masson et al. (2003) described a similar sediment in areas of depressions in the vicinity of the Darwin Mound, NE Rockall Trough. With sea-floor photographs they confirmed that this sediment accumulates in areas where bottom currents are weak and generally lack bedforms typical in areas of strong current activity. GeoB 6718-2 is situated in a small basin further off the mound (Fig. 4-9), where the sea-floor is also characterised by heavily bioturbated sediments (Fig. 1-11a, Chapter 1). Towards the foot of Propeller Mound, the Holocene cover thins out and the sediments become coarser (Fig. 4-3 to 4-5, 4-8). According to

White (subm.), the carbonate mounds themselves generate a rough topography that induces localised strong currents. Indeed, observations using the ROV CHEROKEE during RV POSEIDON cruise 292 indicated strongest currents occurring at the foot of the mound, with increased abundance of IRD boulders and outcropping hardgrounds (Freiwald et al., 2002). Therefore, the ~20 cm Holocene cover of GeoB 6725-1 and GeoB 6727-2 indicates the influence of generally stronger currents near the mound, generating this contourite sand sheet. A similar Holocene layer is described by Masson et al. (2003) indicating maximum velocities of $>25\text{--}30\text{ cm s}^{-1}$.

4.7 Conclusion

Sea-level evolution and climatic conditions have been the main controls on the sedimentary system at the northern Porcupine Seabight during the past ~31 kyr BP, which are summarised in Table 4-4. A first advance of the Irish Ice Sheet onto the Irish Mainland shelf led to the deposition of thick turbidite layer of reworked interglacial sediments. This event also had an erosional impact on the carbonate mounds, as abundant coral fragments are embedded within the turbidite layer. IRD probably indicates the conjunction with HE 3.

Late MIS 3 and MIS 2 deposition is essentially controlled by sea-level fluctuations and the further advance of the BIIS, inducing shelf erosion and releasing turbidity currents and gravity flows. During the terminations and the onset of the Holocene the sedimentation had a pronounced current induced signature, indicating the introduction of the present-day strong hydrodynamic regime at

intermediate depths. The decreasing trend of sedimentation rate towards the Propeller Mound for the last glacial period and the Holocene suggests that currents (turbidity currents, gravity flows, bottom currents) had a generally stronger impact on the sediment accumulation at the mound base.

Acknowledgements

This study is part of the FP5-OMARC project ECOMOUND funded by the EU (Contract n°. EVK3-CT-1999-00013). We wish to thank the captains, crews and scientific shipboard parties of RV POSEIDON cruises POS 265 and 292. A. Jurkiw (University of Bremen) is acknowledged for revising the manuscript. Finally, all colleagues from ECOMOUND, GEOMOUND and ACES are thanked for good co-operation during the past three years.

Table 4-4. Summary of the Paleoenvironmental setting in the northern Porcupine Seabight.

Period	Age*	“What do we see?”	“Why do we see it?”
Holocene	0-10	Silty sands (Facies 1 and 2), low sedimentation rate (1.7–7.3 cm/kyr)	Present-day oceanographic setting with a strong hydrodynamic regime
Younger Dryas/ Bølling-Allerød	10-12	Change from glaciomarine to hemipelagic deposition, increase in mean sortable silt, grain-size and change from accumulated to current-induced sedimentation	Polar Front moved across PSB, introduction of ENAW and MOW with strong hydrodynamic signature at intermediate depths, sea-level increase
MIS 2	12-17 17-18 18-24	IRD deposit (GeoB 6718-2, HE 1?), increasing turbidity currents Quiet sedimentary pattern (Facies 4) High sedimentation rate (5–20cm/kyr) of abundant gravity flow and turbidity current deposition (Facies 3)	Increasing sea-level during deglaciation of BIIS Maximum sea-level lowstand (-120 m) Decreasing sea-level, erosion of shelf and/or mound sediments, retreat of Irish Ice Sheet above marine limit
Late MIS 3	24-31 >31	very high sedimentation rates (17 to 28 cm/kyr) with abundant gravity flows and turbidity currents (Facies 3 and 4), establishment of glaciomarine environment release of turbidite (Facies 6) with eroded (interglacial) sediments and abundant coral fragments	Further advance of Irish Ice Sheet to maximum extent at ~25 kyr BP, coherent with onset of iceberg calving and HE 2 deposition, decreasing sea-level, strong shelf erosion First advance of the Irish Ice Sheet onto the shelf, turbidity currents remove sediments from mounds

* in kyr BP; References within text.

CHAPTER 5

ENVIRONMENTAL CHANGES AND GROWTH HISTORY OF A COLD-WATER CARBONATE MOUND (PROPELLER MOUND, PORCUPINE SEABIGHT)

Andres Rüggeberg¹, Christian Dullo¹, Boris Dorschel², Dierk Hebbeln²

¹ GEOMAR Research Centre for Marine Geosciences, Wischhofstraße 1-3, D-24148 Kiel, Germany

² Department of Geology, University of Bremen, Postbox 330440, D-28334 Bremen, Germany

submitted to

Modern Carbonate Mound Systems: A Window to Earth History

eds. J.-P. Henriot and W.-Chr. Dullo

Abstract

On- and off-mound sediment cores from Propeller Mound (Hovland Mound province, Porcupine Seabight) were analysed to better understand the evolution of a carbonate mound. The evaluation of benthic foraminiferal assemblages and sedimentary aspects from an off-mound position helps to determine the changes of the environmental controls of Propeller Mound for glacial and interglacial times. Their variability is related to changes in oceanographic conditions, surface productivity, the waxing and waning of the British Irish Ice Sheet (BIIS) and variations of the sea-level during the past ~31 000 years. The multi-proxy data-set portrays the boundary conditions of the habitable range for the cold-water coral *Lophelia pertusa*, which dominates the deep-water reefal ecosystem on the upper flanks of Propeller Mound. The growth of this ecosystem occurs during interglacial and interstadial periods, whereas a retreat of corals is documented in the absence of glacial sediments in an on-mound core. Glacial conditions with cold intermediate waters, a weak current regime and high sedimentation rates portray an unfavourable environmental setting for *Lophelia* corals to grow. A Late Pleistocene decrease is observed in the mound growth for Propeller Mound, which might face its complete burial in the future as it already happened to the buried mounds of the Magellan Mound province further north.

5.1 Introduction

5.1.1 Regional setting

Carbonate mounds along the European continental margin have been the subject of intense research during the past decade. In this paper we want to discuss the environmental setting of a carbonate mound in the Porcupine Sea Bight (PSB), which has been intensively sampled and studied during several cruises within the period of 2000 to 2002 (Freiwald et al., 2000; Freiwald and Shipboard Party, 2002; De Mol, 2002; De Mol et al., 2002; Chapter 3 and 4). The object of

interest is the Propeller Mound, which is part of a cluster of highly elevated mounds (up to 150 m) in the Hovland Mound province (Fig. 5-1).

North of this region, seismic surveys detected a cluster of buried mounds – the Magellan Mound province (Huvenne et al., 2002; De Mol, 2002), indicating sediment transport from the surrounding shallower shelf areas. The Belgica Mound province is located at the eastern slope of the PSB to the

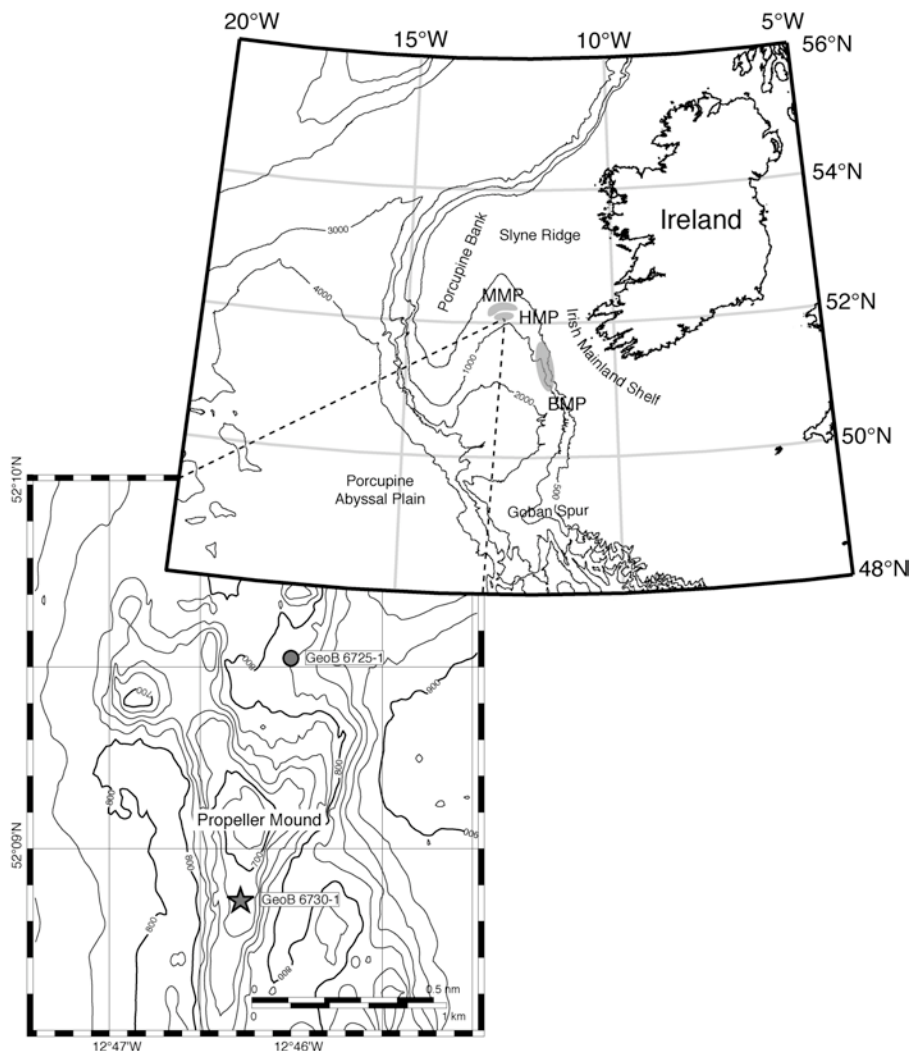


Figure 5-1. Location map of Propeller Mound with sediment core sites analysed within this study. Star = on-mound core GeoB 6730-1, circle = off-mound core GeoB 6725-1. MMP = Magellan Mound province, HMP = Hovland Mound province, BMP = Belgica Mound province.

SE of the Hovland and Magellan Mounds (Fig. 5-1, Henriët et al., 1998; De Mol et al., 2002).

Propeller Mound shows strongly current induced features, such as its N-S elongation, its steep flanks ($>45^\circ$) and the moats around the foot of the mound (De Mol, 2002; Freiwald, 2002). Underwater investigations using the ROV CHEROKEE of Bremen university (Freiwald and Shipboard Party, 2002) clearly show the sediment distribution on the mound. It is mainly covered by dead coral debris in a sandy silty matrix. Recent coral growth is restricted to the upper flank of the mound (690–710 m water depth), where a dense living coral ecosystem occurs. However, close to the studied on-mound core GeoB 6730-1 (Fig. 5-1) only patches of corals have been observed. The reefs on Propeller Mound are mainly built up by cold-water corals *Lophelia pertusa*, *Madrepora oculata* and to a minor degree by *Desmophyllum cristagalli* (Freiwald, 2002).

5.1.2 Recent oceanographic setting

The recent mound growth is strongly controlled by the present oceanographic setting, which is described in detail by White (subm.). A generally northward transport of water masses west of Ireland is documented at the surface and in mid water depths (<1000 m). At 600–800 m, the depth of recent coral growth in the Hovland Mound province, a water mass boundary occurs between the Eastern North Atlantic Water (ENAW) and the Mediterranean Outflow Water (MOW). A branch of ENAW and MOW enters the PSB (Mohn, 2000) and flows topographically steered cyclonically around the slope within the PSB (Ellet et al., 1986). At the northern end of the PSB, where the Hovland and Magellan Mounds

are situated, the currents are relatively weaker ($1\text{--}5\text{ cm s}^{-1}$) and turn into a southward flow (White, 2001). It has been suggested that MOW does not penetrate to any large degree further poleward in the Rockall Trough north of Porcupine Bank (New et al., 2001; McCartney and Mauritzen, 2001; White, subm.). During RV POSEIDON cruise POS265 in 2000, several CTD profiles overlying the Propeller Mound show an increase in salinity below 600 m (De Mol, 2002). Due to a strong gradient in density at this water mass interface, organic material from the sea surface persists at this level to a longer time. In addition, it is also transported laterally within the PSB by currents generally flowing at around 5 cm s^{-1} with maximum velocities up to 40 cm s^{-1} (White, 2001; White, subm.). The corals benefit from this enrichment of food particles. It is obvious that water mass variations during glacial-interglacial cycles, where major differences of the oceanographic setting exist, have a great impact on coral growth and distribution.

5.1.3 Glacial oceanographic setting

The glacial oceanographical setting is not well studied in the PSB. The North Atlantic Polar Front was situated south during most of last glacial stages (Jones and Keen, 1993). Surface water movement was reversed during glacials, flowing southward as a coastal current west off Ireland (Fig. 5-2; Sarnthein et al., 1995), leading to summer Sea Surface Temperatures (SST) of 5°C for the Last Glacial Maximum (LGM) and winter SST of $0\text{--}1^\circ\text{C}$ (Sarnthein et al., 1995; Bowen et al., 2002). Glacial North Atlantic Intermediate Water (GNAIW) occurs in water depths down to 1700–2000 m (Manighetti and McCave, 1995) and flows from the north via the Wyville-Thomson

Ridge and through the Rockall Trough to the south. According to Duplessy et al. (1988) and Oppo and Lehman (1993) the term GNAIW is used for mid-depth waters of uncertain origin. Its production occurs in the Norwegian Sea at least during MIS 2 via a mechanism strongly influenced by sea ice formation (Veum et al., 1992), but the composition of GNAIW may have changed during the glacial time with differing sources. An influence of the very cold GNAIW on the PSB is assumed. Schönfeld and Zahn (2000) describe a main glacial

MOW flow up to 800 m deeper than today, due to an increased density induced by a much higher salinity. In addition, the glacial flow pattern indicates no northward flow of MOW along the European continental margin and therefore no boundary between the glacial intermediate water mass and MOW existed in the PSB.

A maximum land ice extend of the BIIS probably reaching offshore W Ireland to the present 200 m isobath is reported by Bowen et al. (2002) for MIS 4 (Fig. 5-2).

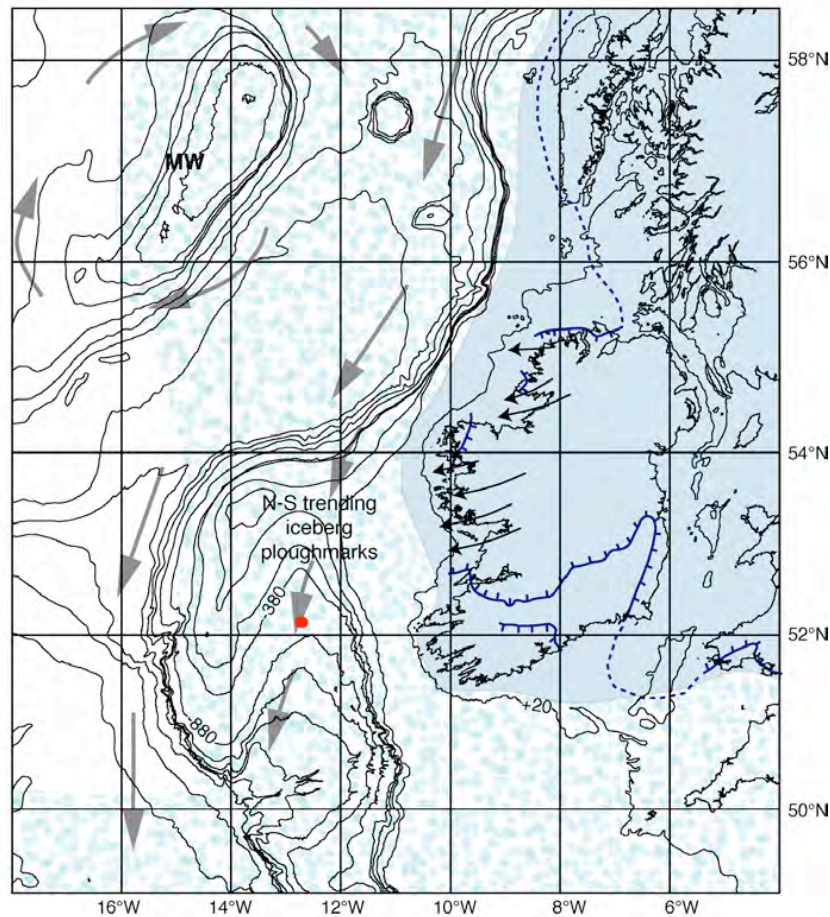


Figure 5-2. General map of Ireland during glacial intervals. Indicated are ice limits (dark blue) and general ice flow (black arrows) for MIS 2 (after Eyles and McCabe, 1989; Jones and Keen, 1993), maximum land-ice extend (light blue) for MIS 4 (after Bowen et al., 2002), surface circulation (gray arrows) and melt water intrusion (MW) resulting in a weak anticyclonic circulation around Rockall Bank for MIS 2 (after Sarnthein et al., 1995). N-S trending iceberg ploughmarks are reported on Slyne Ridge (after Games, 2001). Sea-ice (light blue dots) covered entire PSB during peak glacial winters (Sarnthein et al., 2003). Glacial bathymetry corresponds to present-day water depth minus 120 m. Red dot marks the position of Propeller Mound.

During MIS 3 Ireland was covered with treeless, tundra-like vegetation (Jones and Keen, 1993). An advance of land ice occurred around 30 ka BP, covering most of Ireland (Knutz et al., 2001) synchronous with a sea-level lowering of around 50 m (Lambeck et al., 2002). The southward flowing surface waters, land ice extension and calving of icebergs from Irish mainland as documented by ice berg plough marks on Slyne Ridge (Games, 2001), as well as the sea-level lowering suggest an enormous increase in terrigenous sediment supply to the PSB (e.g. Auffret et al., 2002).

5.1.4 Aim of study

The objective of this study is the reconstruction of the environmental setting of Propeller Mound for glacial and interglacial period, which will be discussed with respect to the environmental control on the Late Pleistocene development of Propeller Mound. Therefore we have produced stable oxygen isotope data, AMS ^{14}C and U/Th datings, total and organic carbon measurements, and use the evaluation of benthic foraminiferal assemblages, as well as the sedimentary results from an off- (core GeoB 6725-1) and an on-mound (core GeoB 6730-1) location (Chapter 3 and 4).

5.2 Material and methods

Two sediment cores from the Propeller Mound region, GeoB 6725-1 (off-mound position 52°09.52'N, 12°46.01'W; water depth 820 m) and GeoB 6730-1 (on-mound position 52°08.86'N, 12°46.28'W; water depth 704 m; see Fig. 5-1) were investigated. Both cores were sampled every 5 cm using 10 ml syringes. Each sample was weighed, carefully washed over 63 μm sieves, dried at 50°C and weighed again. Thereafter all samples were dry sieved into fractions 63–125 μm , 125–250 μm , 250–500 μm , 500–1000 μm and >1000 μm . Fractions >125 μm were used for faunal analysis (Chapter 3). A taxonomic list of benthic foraminiferal species discussed in this study is given in Appendix 1. Species diversity is expressed in numbers of species corrected to an equal size of 100 specimens (Lutze, 1980; see Appendix 2).

For the analysis of organic carbon (TOC) and total carbon (TC) the samples were measured using a Carlo Erba NA-1500-CNS analyser at GEOMAR, Kiel. Organic carbon is determined after removing carbonate car-

bon by acidification with 0.01N hydrochloric acid. Inorganic carbon was derived from the difference between total and organic carbon. Percent carbonate was calculated according to their atomic weight ratios as $\text{CaCO}_3 (\%) = 8.33 \cdot (\text{TC} - \text{TOC})$.

Stable oxygen isotopes ($\delta^{18}\text{O}$) were measured on 3–5 specimens of either the benthic foraminifera *Cibicidoides kullenbergi* or *Cibicidoides wuellerstorfi* (fraction 250–500 μm) for both investigated cores. Additionally, 15 specimens per sample of planktic foraminifera *Globigerina bulloides* (fraction 250–315 μm) have been analysed for their $\delta^{18}\text{O}$ composition for the top 120 cm of the off-mound core GeoB 6725-1. The isotopic composition of the samples was carried out with a Finnigan MAT 251 mass spectrometer at the Isotope Lab Bremen University. A working standard (Burgbrohl CO_2 gas) was applied, which has been calibrated against PDB by using the NBS 18, 19 and 20 standards. All $\delta^{18}\text{O}$ data given here are relative to the PDB standard. Analytical standard deviation is about $\pm 0.07 \text{‰}$.

Age estimations in both cores are based on AMS ^{14}C datings using mono-species samples of planktic foraminifera species *Neogloboquadrina pachyderma* (either dextral or sinistral) from the fraction 125 to 250 μm . Approximately 10 mg of foraminiferal carbonate were analysed at the Leibniz Laboratory for Age Determinations and Isotope Research at the University of Kiel (Nadeau et al., 1997). After the correction for $\delta^{13}\text{C}$, the ^{14}C ages were calibrated to the calendar year scale by the Calib 4.3 program (Stuiver and Reimer, 1993) using the marine data set of Stuiver et al. (1998) and a reservoir age of 400 years. Ages greater than 21 kyr BP were corrected using the method of Voelker et al. (1998) (see Tables in Chapter 3, 4 and Appendix 7).

In several depth intervals of core GeoB 6730-1 some coral fragments of *L. pertusa* were used to determine additional absolute ages using the U/Th ratio of the aragonite skeleton (see Tables in Chapter 3, 4 and Appendix 7). All samples were first ultrasonically cleaned and scrubbed with dental tools to remove exterior contaminants (iron-

manganese crusts and coatings) from the fossil coral fragments as described in Cheng et al. (2000a). When the coral looked clean under the binocular, each sample was bathed in 50/50 mixture of 30 % peroxide and 1M NaOH for 15 minutes with ultrasonification to remove organic stains left on the coral. This step already removed up to 50 % of the inner and outer coral skeleton. Therefore, the last step of the cleaning procedure described by Cheng et al. (2000a), where the samples were submerged in a 50/50 mixture of 30 % peroxide and 1 % HClO_4 was omitted, otherwise no material would have been left. Before the measurements using a Finnigan MAT 262 RPQ2+ Thermal Ionisation Mass Spectrometer (TIMS) at GEOMAR Kiel, all samples were checked for the cleanness of the aragonite. Therefore a little part of the samples was cut off before and after the chemical and physical cleaning and was analysed using X-ray diffraction (XRD), to evaluate the chemical composition primarily of the aragonite skeleton after the whole procedure (100 % aragonite in all samples).

5.3 Results

5.3.1 Stratigraphy

Off-mound

Benthic and planktonic oxygen isotope data and carbon measurements of core GeoB 6725-1 are illustrated in Figure 5-3a. The base of the core is disturbed by turbidites indicated by two sequences of upward fining sediments. Above this sequence the benthic $\delta^{18}\text{O}$ record shows low variability with values around 3.5 ‰ PDB. Planktic $\delta^{18}\text{O}$ measurements within the top 120 cm present higher variability with values ranging between 0.7 and 3.3 ‰ PDB. Lower $\delta^{18}\text{O}$ values of *G. bulloides* are synchronous with

higher carbonate content of 35 weight percent (wt.-%) of the foraminifera bearing silty sand, whereas persistently low values of carbonate (20 wt.-%) were found in fine-grained, terrigenous sediments. The mean carbonate content of the off-mound core is 22.5 wt.-%. Organic carbon contents (0.2–0.4 wt.-%) are low throughout the core, again with the highest values recorded at the core top.

These data suggest a distribution into the youngest three marine isotope stages. Inter-

core correlation of different off-mound cores (GeoB 6718-2, 6719-1, GeoB 6727-2; Chapter 4; Appendix 7) indicate, that (1) a stratigraphic tie point, indicated by a characteristic double peak in the carbonate record, is probably related to Heinrich event 2 (HE 2) and its European precursor event, both dated to 23.7–25.6 cal kyr BP (Bond and Lotti, 1995; Grousset et al., 2000; Bowen et al., 2002), and (2) that the turbidite sequence below 404 cm seems to be slightly older than 31 kyr BP. The sedimentation rate decreases from ~28 cm/kyr for the late MIS 3 to 15 cm/kyr for MIS 2, comparable to other near-shelf studies (e.g. Rasmussen et al., 2002b; Auffret et al., 2002; De Mol et al., 2002). The Holocene layer (top 23 cm) is indicated by lower $\delta^{18}\text{O}$ values of *G. bulloides*, which results in a sedimentation rate of 2.3 cm/kyr assuming the core top reflects the present-day surface sediment. An additional AMS ^{14}C date at 68 cm represents an age of 7.65 kyr BP, indicating an interval of heavily bioturbated sediments.

On-mound

Figure 5-3b presents benthic oxygen isotope data and carbon measurements of on-mound core GeoB 6730-1. The $\delta^{18}\text{O}$ record is highly variable compared to the off-mound core, showing values between 1.4 and 3.4 ‰ PDB. In general, the carbonate content follows the $\delta^{18}\text{O}$ record with higher values during sections with low $\delta^{18}\text{O}$ values and vice versa. The carbonate content is more than twice as high as in the off-mound core (24–70 wt.-%, mean = 50 wt.-%), whereas organic carbon is generally less abundant with values ranging between 0.1 and 0.4 wt.-%.

The low benthic $\delta^{18}\text{O}$ values within the top 60 cm of the on-mound core GeoB 6730-1 as well as an AMS ^{14}C date of 4.5 kyr BP at 23 cm correspond to the Holocene interval (Fig. 5-3b). Below the Holocene cover, the stable isotope record and several U/Th dates on coral fragments of *L. pertusa* indicate that the on-mound core is marked by numerous hiatuses with almost

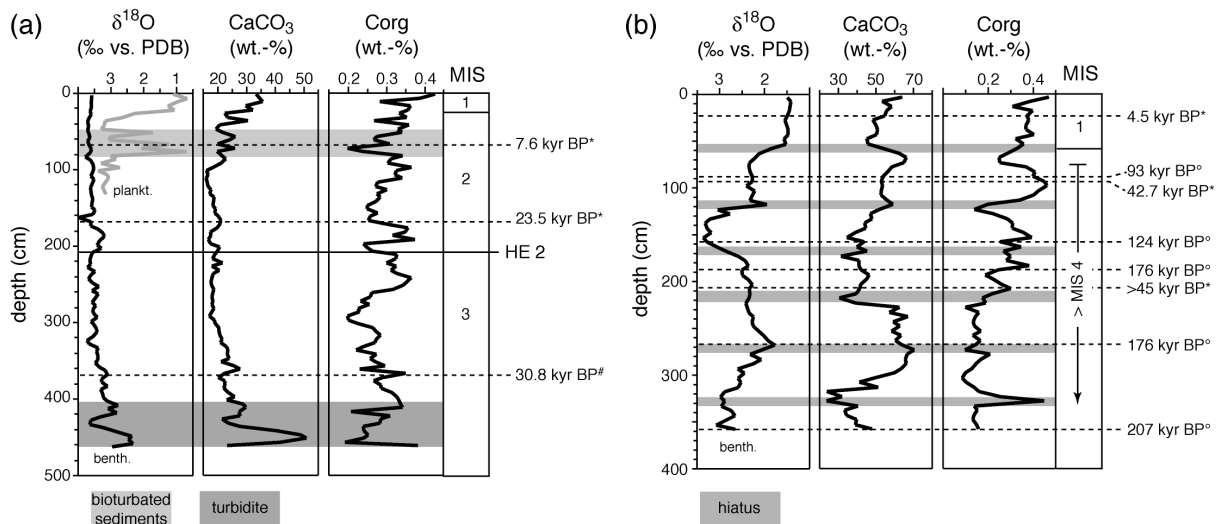


Figure 5-3. Established stratigraphy and carbon measurements of (a) off-mound core GeoB 6725-1 from benthic and planktonic oxygen isotope data, *AMS ^{14}C dates, and $^{\circ}$ inter-core correlation (Chapter 4, Appendix 7) and of (b) on-mound core GeoB 6730-1 from benthic oxygen isotope data, *AMS ^{14}C and $^{\circ}$ U/Th dates. Differences between U/Th and ^{14}C dates may be the result of bioturbation.

no fully interglacial sediments (expected $\delta^{18}\text{O}$ values of around 1.5 ‰ PDB), nor glacial sediments (expected $\delta^{18}\text{O}$ values of >3.5 ‰ PDB) being preserved. Most likely erosional processes on elevated mound areas with removal of nearly all glacial and interglacial sediments during phases of enhanced current intensity may have caused the hiatuses (Appendix 8). Therefore core GeoB 6730-1 can only be divided into a Holocene cover and older sediments below.

5.3.2 Off-mound environmental setting

Benthic foraminiferal assemblages and the sediment distribution in off-mound samples of core GeoB 6725-1 clearly portray the environmental setting of glacial (Late MIS 3 and MIS 2) and interglacial (Holocene) times.

Glacial (Late MIS 3 and MIS 2) setting

The glacial sediments consist of fine-grained, terrigenous mud with carbonate contents rarely exceeding 20 %. The sediment structure indicates abundant gravity flows or turbidity currents with a high sediment supply from the shallow shelves, leading to high sedimentation rates of up to 28 cm/kyr. The accumulation of this reworked material is controlled by sea-level fluctuations and the first advance of the Irish Ice Sheet onto the Irish Mainland shelf slightly before 31 kyr BP (Chapter 4).

Elphidium excavatum is highly abundant in the lower core section of off-mound core GeoB 6725-1 right after the turbidite (<31 kyr BP), where it exceeds 50 % of total abundance (Fig. 5-4). This species is reported to live in shallow shelf areas generally above 200 m (Seidenkrantz et al., 2000) and is associated with near glacial environments in areas with heaviest ice cover

(Nagy, 1965; Hald et al., 1994; Steinsund and Hald, 1994). High numbers of *E. excavatum* and a very high sedimentation rate of ~28 cm/kyr indicates that this species was displaced by erosional processes from shallow shelf areas shortly after the first advance of the Irish Ice Sheet (Chapter 4). Therefore, it forms not a part of the fossil community (Struck, 1992) and is not considered in the calculation of the relative abundance of the *Glacial* and *Interglacial* group.

Shelf erosional processes continued between 31 and 24 kyr BP, simultaneously with a sea-level lowering of around 50 m (Lambeck et al., 2002) and the extension of the BIIS. The occurrence of coral fragments in off-mound core GeoB 6725-1 during late MIS 3 (red stars in Fig. 5-4) also suggests that turbidity currents and gravity flows had a great impact on the elevated mound, contributing sediments to the off-mound location. Towards MIS 2 shelf erosion decreases, expressed in decreasing numbers of *E. excavatum* (increasing abundance of the *Glacial* group) but probably still persisted to a less amount during MIS 2 (Fig. 5-4).

Several foraminiferal species dominate the benthic fauna within the terrigenous muds comprising Late MIS 3 and MIS 2. *Cassidulina teretis*, *Globocassidulina subglobosa*, *Cassidulina reniforme*, *Cibicides kullenbergi* and subdominant species *Cassidulina obtusa* and *Sigmoilopsis woodi* describe the *Glacial* group. The relative abundance of this assemblage increases continuously from ~40 % during late MIS 3 to values >80 % during MIS 2 (Fig. 5-4) with *C. teretis* being the most abundant species. These continental slope species thrives in cold bottom waters (–1°C; Mackensen and Hald, 1988) and are associated with nutrient-poor bottom water conditions and

slow benthic current speeds (Chapter 4). Thus, the *Glacial group* is related to indicate polar conditions (Korsun and Hald, 2000) with the occurrence of the cold and nutrient-poor GNAIW, which is described as the prominent water mass present in the glacial North Atlantic down to 1700–2000 m (Manighetti and McCave, 1995). Its composition may have changed through the glacial time due to different sources, but a contribution of MOW can be excluded as its glacial flow pattern predominantly occurred towards the west (Schönfeld and Zahn, 2000).

The glacial environment in the northern PSB was controlled by a homogenous water mass with water temperatures below 2°C

and a low nutrient availability at intermediate depths. A weak hydrodynamic regime and strong shelf-erosional processes led to a very high sediment accumulation. The temperature range, where *L. pertusa* is reported to live along the European continental margin, is given by Freiwald (2002) with 4 to 12.5°C. The lower temperature limit corresponds to the occurrence of reefs offshore Norway. Minimum temperatures of *L. pertusa* within the PSB show slightly higher values of 7.5°C. As low glacial temperatures and high sediment supply prevailed at intermediate depths, it is evident that the glacial oceanographic setting in the PSB is below the habitable limits of *L. pertusa*.

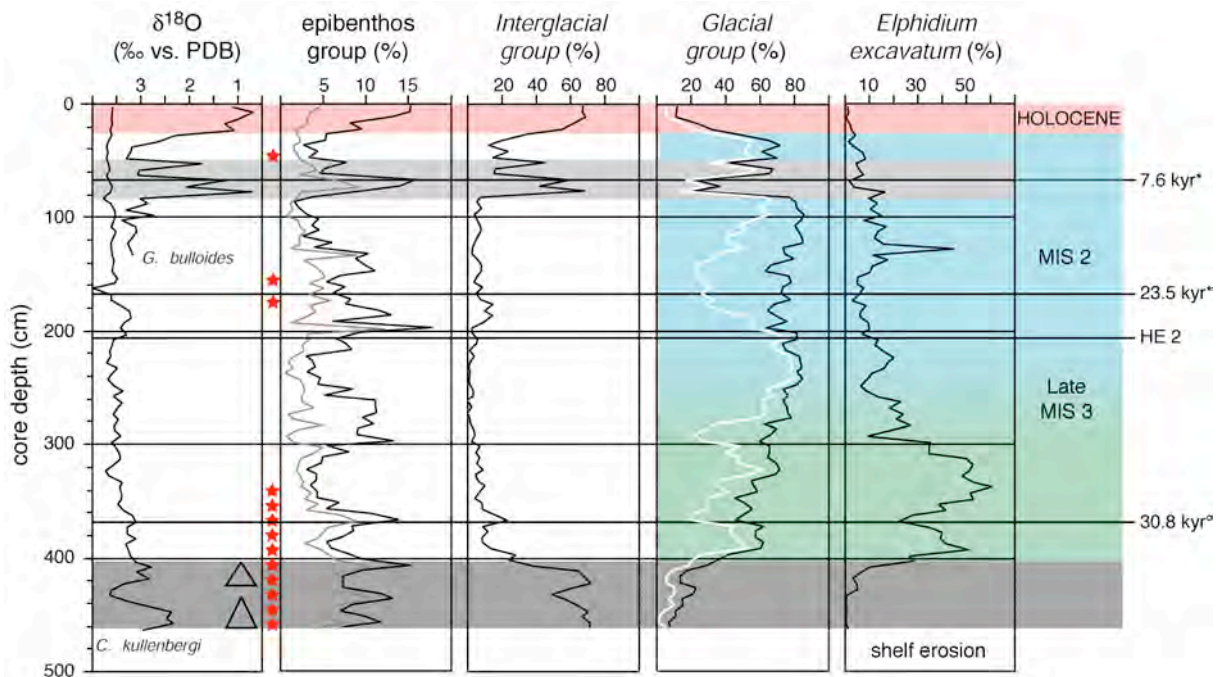


Figure 5-4. Relative abundance of the *Interglacial group* (*U. mediterranea*, *T. angulosa*, *M. barleeianum*, *H. balthica*, *B. robusta*, *B. marginata*, *C. laevigata*, *U. peregrina*), the *Glacial group* in black (*C. teretis* (in white), *G. subglobosa*, *C. reniforme*, *C. kullenbergi*, *C. obtusa*, *S. woodi*) and the dominance of *E. excavatum* for late MIS 3 of core GeoB 6725-1. Epibenthic (black) and attached epibenthic species (gray) are according to Murray (1991) and Schönfeld (1997; 2002a). Red stars mark intervals with occurrence of coral fragments and other shell fragments, triangles show upward fining sediment, *AMS ^{14}C dates, °inter-core correlation (Chapter 4, Appendix 7). Note: Relative abundance of *Interglacial group*, *Glacial group* and *C. teretis* are calculated without consideration of *E. excavatum* to the total assemblage.

Interglacial (Holocene) setting

The Holocene interval is described by a coarse-grained, carbonate-rich, contourite sediment, which reflects the strong hydrodynamic regime at the foot of Propeller Mound (Chapter 4).

Within this sediment analysis on benthic foraminifera revealed an assemblage, dominated by infaunal species: *Uvigerina mediterranea*, *Trifarina angulosa*, *Melonis barleeanum*, *Hyalinea balthica*, *Bulimina marginata*, *Uvigerina peregrina* and *Cassidulina laevigata*. This assemblage is described as the *Interglacial group*, and presents a maximum relative abundance of 68 % during the past 10 kyr, but rarely exceeds 20 % during the glacial period (Fig. 5-4). In the bioturbated interval the Holocene group presents a comparable behaviour as the $\delta^{18}\text{O}$ record of *G. bulloides*, determining the existence of this heavily bioturbated section.

The interglacial benthic foraminiferal assemblage strongly reflects the present-day environmental conditions and oceanographic setting. They indicate a great affinity to a high and continuous flux of organic material to the sea floor (e.g. Loubere, 1991;

Mackensen et al., 1993; Schönfeld and Zahn, 2000) and show an association with lower oxygen concentrations in the sediment pore water (Kaiho, 1994; Brüchert et al., 2000; Seidenkrantz et al., 2000). A generally higher amount of organic material in sediments may be related to higher surface productivity during the Holocene interval, but a correlation between organic carbon content (TOC) in the sediment with species of the Holocene group does not exist (Fig. 5-3a and 5-4). The mixing of ENAW and MOW controls the present-day oceanography in 600 to 800 m water depth, with the MOW being characterised by lower oxygen and higher salinity concentrations. The endobenthic species of the *Interglacial group* probably indicate this mixing process and the influence of MOW in the northern PSB during the Holocene.

This environment with a higher surface productivity, a water mass boundary and therefore higher nutrient availability in the depth of recent coral growth, as well as strong current intensities, appears to be the controlling factor not only for the cold-water coral ecosystem, but also for the high abundance of the *Interglacial group*.

5.4 Discussion

5.4.1 Which setting is locked in sediments from Propeller Mound?

The age model of on-mound core GeoB 6730-1 is insufficient to resolve glacial, interglacial or interstadial periods (Fig. 5-3b). Below the Holocene layer (top ~60 cm) several hiatuses were identified, which indicate a sediment removal off the mound (Appendix 8). Therefore, we use the off-mound benthic foraminiferal assemblages describing interglacial and glacial conditions and grouped the relative abundance of the same

species in on-mound samples to become an idea of their distribution and variability (Fig. 5-5).

Species of the *Interglacial group* are less abundant in on-mound Holocene sediments than in core GeoB 6725-1 with mean values of around 45 % (Fig. 5-5). Maximum abundance (>40 %) of this group occurs within the top 118 cm and the section 323–358 cm at the core base, but its abundance generally

describes >20 % throughout the entire core. The *Glacial group* is generally less abundant in the on-mound compared to the off-mound setting (Fig. 5-5). During the Holocene this group presents a similar relative abundance as in the off-mound core with values between 10–20%. However, it exceeds 20 % only within four sections between 120–320 cm, with a maximum of 43 % at 183 cm (Fig. 5-5). Only these four sections show higher contributions of the *Glacial group*.

As species of the *Interglacial group* represent a high and more continuous flux of organic material to the sea-floor within lower oxygen concentrated waters (see above), most of the sediments of the on-mound core can be related to indicate warmer periods (interglacials or at least interstadials). This is supported by the low abundance of the *Glacial group*, which does not describe comparable polar conditions as in core GeoB 6725-1, where ~80 % portray fully glacial conditions (Fig. 5-4). Additionally, the range of the benthic oxygen isotope record (2–3.2 ‰), as well as U/Th dates, indicating only interglacial and interstadial ages, confirms the conclusion that only interglacial/-stadial sediments are preserved in the on-mound record below the Holocene layer (see also Appendix 8). However, neither the *Glacial group* nor the *Interglacial group* have a comparable high relative abundance as documented in core GeoB 6725-1, which suggests, that an additional group contributes the assemblage on Propeller Mound.

5.4.2 The *Mound group*

The faunal diversity of the on-mound benthic foraminifera is much higher compared to core GeoB 6725-1, indicating that the

coral ecosystem offers a habitable life for much more different species with both an infaunal and epifaunal lifestyle. Several species have been described in on-mound samples, which do not occur in the off-mound core or only show accessory contribution (<1 %) to the total assemblage (Chapter 3). These species (*Discanomalina coronata*, *Gavelinopsis translucens*, *Planulina ariminensis*, *Cibicides lobatulus*, *Trifarina bradyi* and minor species (<5 %) *Cibicides refulgens* and *Hyrrokkin sarcophaga*) are also common elsewhere in the NE Atlantic, but as they are not recorded in off-mound samples, they are considered as another assemblage, referred to as *Mound group*. The record of this *Mound group* varies between 2 and 38 % of the total assemblage showing maximum values downcore between 278–323 cm. It is dominated by epibenthic and attached epibenthic species (Fig. 5-5).

Schönfeld (2002b) describes a similar group in the Gulf of Cadiz, where he found coherence between this elevated epibenthos and the current intensity of the upper MOW flow. As a similar group of species is described here, the path flow MOW with a higher current intensity seem to be one controlling factor for the species of the *Mound group*. However, as the *Mound group* is described by attached epibenthic species, they additionally indicate a higher availability of elevated substrates to settle. The deep-water coral ecosystem provides high amounts of elevated substrates. Therefore, high abundances of the *Mound group* are related to portray the occurrence of a dense coral ecosystem on Propeller Mound.

During the Holocene the *Mound group* only contributes 13 % to the total assemblage, which is related to the restricted coverage of corals on the upper flanks of the mound. In an earlier period of the Late

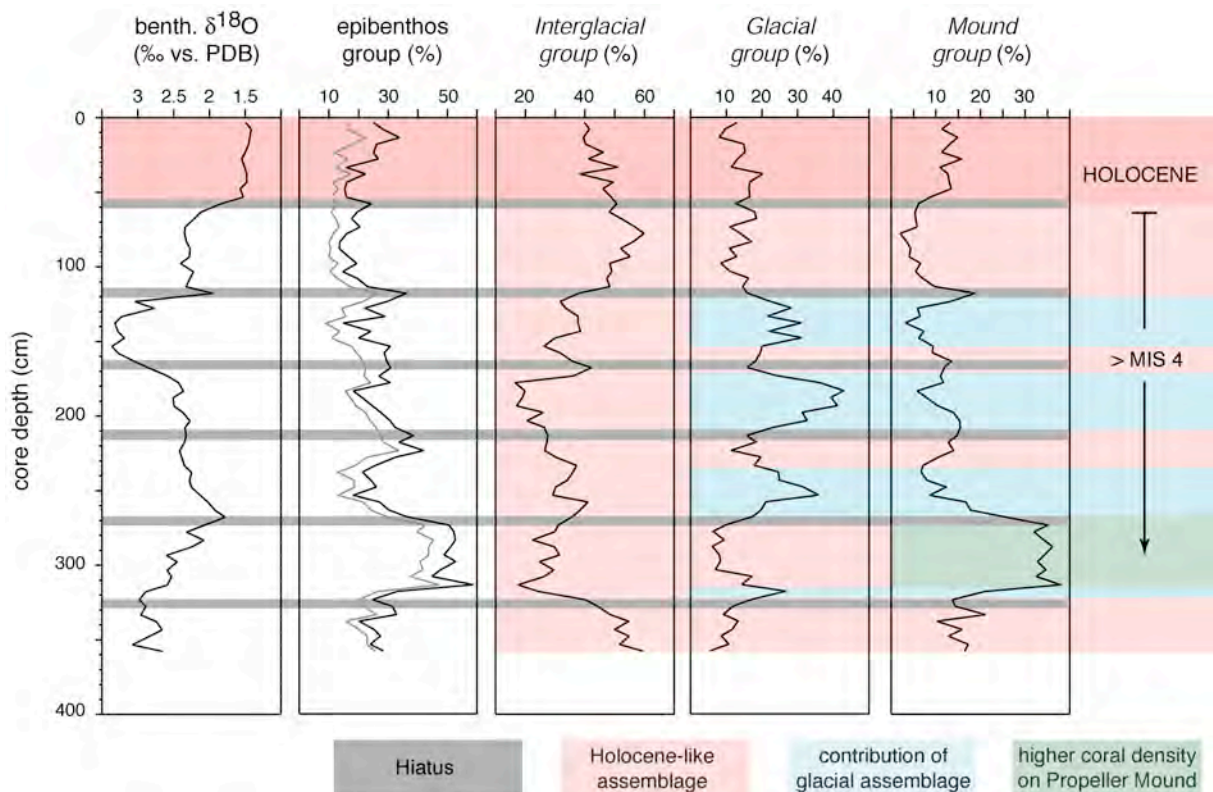


Figure 5-5. Relative abundance of the off-mound-identified *Interglacial group* and *Glacial group* transferred to on-mound core GeoB 6730-1, as well as the *Mound group* and epibenthos group. Higher abundance of each assemblage describes the different sections illustrated to the right. Epibenthic (black) and attached epibenthic species (gray) are according to Murray (1991) and Schönfeld (1997; 2002a). Dominant and subdominant species of the the *Mound group* are *D. coronata*, *G. translucens*, *C. lobatulus*, *H. sarcophaga*, *P. ariminensis*, *C. refulgens*, *T. bradyi*.

Pleistocene corresponding to the depth interval 278–323 cm (probably MIS 7; Fig. 5-5), Propeller Mound seemed to have had a much higher coral density than at present covering the entire top of the mound. This environment was favourable for species of the *Mound group* to settle and to live. The decreasing trend of this assemblage towards the Holocene is related to a decline in coral cover. First estimations of the carbonate budget in on-mound sediments show a similar feature with higher coral carbonate accumulation ~176 kyr BP.

Thus, the Late Pleistocene development of Propeller Mound displays a declining

stage with a general decrease in coral growth. If this situation persists into the future, the sediment supply from the surrounding shallow shelf areas will bury Propeller Mound, as has already occurred in the Magellan Mound province further north (Fig. 5-6).

5.4.3 The environmental control on the Late Pleistocene development of Propeller Mound

The results obtained for Propeller Mound and the closer vicinity clearly reflects the important environmental control responsible for the growth and retreat of corals,

which are steered by oceanographic and climatic factors (Freiwald, 1998; 2002; White et al., *subm.*; White, *subm.*). Under fully glacial conditions the environmental setting was beyond the habitable range of *Lophelia* corals with temperatures below 2-4°C, low current intensities supporting high sediment accumulation, and a homogenous intermediate water mass, which does not support nutrient enrichment in the depth of the carbonate mounds. Up to now for no coral from the Celtic Margin an age representing the Last Glacial Maximum has been obtained, indicating that no coral lived in this region. Thus, there also had been no skeletal framework to stabilise the fine-grained sediments deposited under such conditions.

During terminations, when the sea-level rose and the glaciers retreated from Ireland, ENAW and MOW regains its present characteristics. Enhanced currents removed the unstabilised sediments from the mound, which is expressed in several hiatuses covering glacial periods of core GeoB 6730-1. De Mol et al. (2002) and Freiwald (2002) discussed the possibility of coral larvae entering the PSB with the inflow of the MOW during the terminations, as *Lophelia* is highly abundant within the Mediterranean during the glacials but presently nearly absent (Delibrias and Taviani, 1985). With an oceanographic regime comparable to the present-day set-

ting the corals were able to (re-)colonise the elevated structure and the mound proceeded to grow.

The glacial-interglacial cycle with changing environmental conditions seems to be one mechanism driving the development of the carbonate mounds along the Celtic Margin. Interglacial/-stadial growth, glacial retreat and resettlement of corals during terminations with removal of glacial sediments are combined in a model describing the *Mound Factory* (Fig. 5-6). This model accounts for the time, when the N Atlantic experienced the Northern Hemisphere Glaciation, which started between 3.1 and 2.5 Million years BP (Shackleton et al., 1995; Haug et al., 2001). It is still under debate, which trigger was responsible for the initial mound development. The base of the Hovland-Magellan mounds is situated on an erosional surface, which is expected to be of Early Pliocene age (Huvvenne et al., 2003). The colonisation of coral larvae may have occurred on authigenic carbonates, probably related to fluid migration or gas seepage, on boulders released by rafted icebergs, or microbacterial produced carbonate crusts (e.g. Hovland et al., 1994; Henriët et al., 1998; Freiwald, 2002). However, only a deep drilling campaign through the base of such carbonate mounds will shed some light into the debate about the onset and the trigger of mound development.

5.5 Conclusions

Two different benthic foraminiferal assemblages of off-mound core GeoB 6725-1 (*Interglacial group*, *Glacial group*) indicate the environmental setting of the northern PSB during the past 31 kyr BP. These climatic and oceanographic changes are

important for the PSB and the distribution of cold-water corals on top of the mounds. The high abundances of infaunal species during the Holocene describe the present-day situation with strong bottom currents and a high supply of organic material to

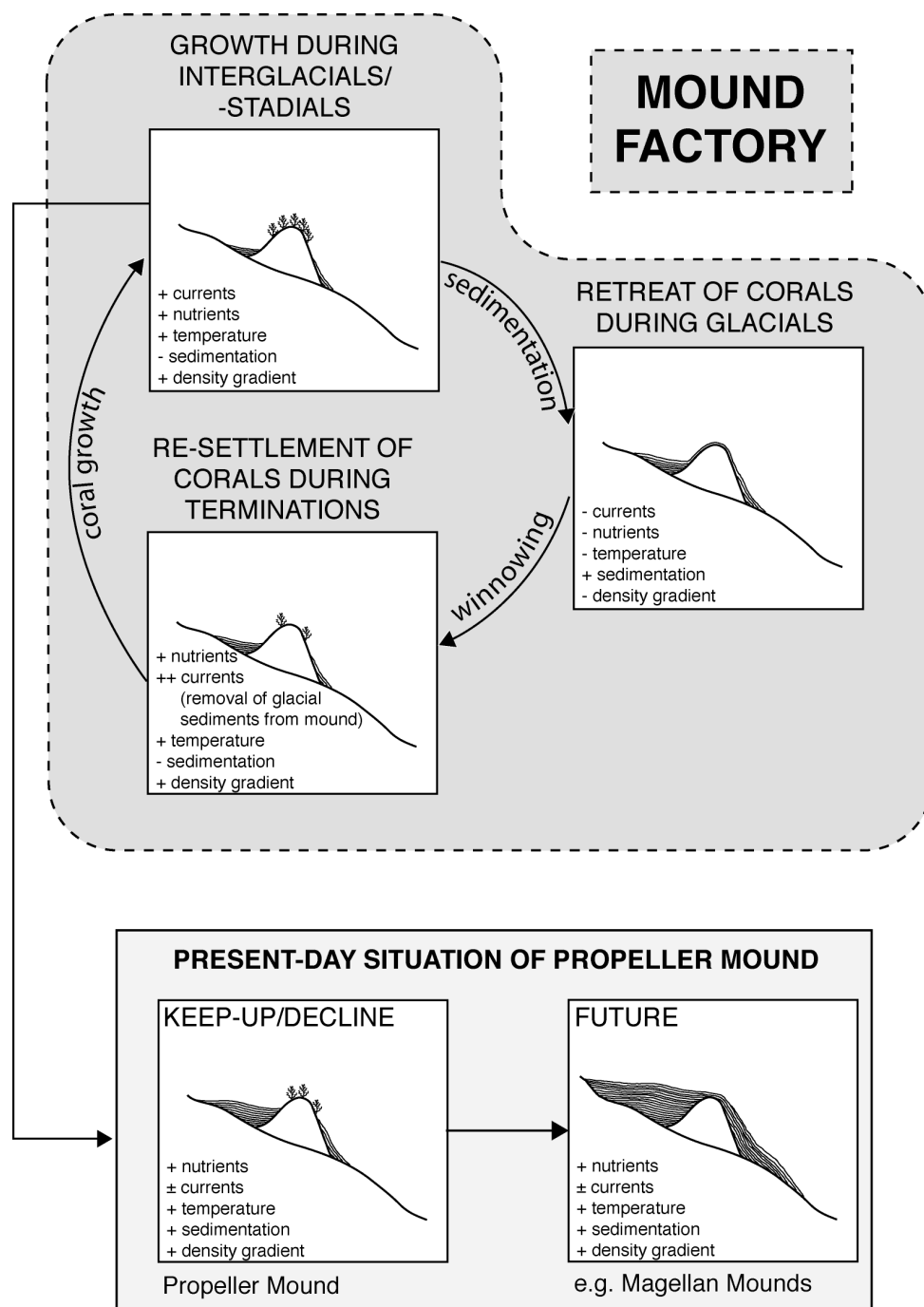


Figure 5-6. Model of the *Mound Factory* responsible for mound growth during interglacial-glacial cycles of the Pleistocene, revealed from reconstructions of the environmental setting locked in sediments on and off Propeller Mound. The *Mound Factory* follows the cycle of interglacial/-stadial mound growth, glacial retreat of corals and stagnation of mound growth, and the resettlement of corals during terminations with the introduction of the present-day oceanographic regime. Within the boxes, key factors of the environmental control are indicated (+ high/strong; – low/weak). Below, the present-day situation of Propeller Mound is indicated with the proposed future development.

the sea floor. During the Last Glacial Maximum high abundance of cassidulinid species is related to cold bottom water mass and a reduced productivity. The Late MIS 3 documents a turbidite sequence induced by a first advance of the Irish Ice Sheet. Increasing sedimentation and the occurrence of *E. excavatum* shows strong sediment erosion from surrounding shallow shelf areas.

A dominance of the *Interglacial group* is recorded throughout the entire on-mound core GeoB 6730-1, interrupted only by four sections with slightly higher abundance of the *Glacial group*. In comparison with the stable oxygen isotope record and U/Th dates, the data imply that only interglacial/stadial sediments remained on-mound and fully glacial sediments have been removed. A third assemblage with species mostly described in on-mound samples characterises the coral density on Propeller Mound. Present-day coral growth is mainly restricted to the upper flank of Propeller Mound, also evident from low abundance of the *Mound group* during the Holocene. In an earlier period this group shows higher abundances, representing a time, when the mound had a denser coral cover. Furthermore, the *Mound*

group indicates a decline of Propeller Mound, which might end in a future burial.

Finally, the model *Mound Factory* describes the external, environmental control on mound development during the (Late) Pleistocene period with changing oceanographic and climatic conditions, which monitor the controlling mechanisms (nutrients, temperature, water mass characteristic and sedimentation rates).

Acknowledgements

This study is part of the FP5-OMARC project ECOMOUND funded by the EU (Contract n°. EVK3-CT-1999-00013). We wish to thank the captains, crews and scientific shipboard parties of RV POSEIDON cruises POS 265 and POS 292. Dr. J. Schönfeld (GEOMAR, Kiel) is acknowledged for his comments and suggestions on an earlier version of this manuscript. Dr. V. Liebetrau (GEOMAR, Kiel) is acknowledged for performing U/Th datings on the deep-sea coral *Lophelia pertusa*. All colleagues of ECOMOUND, GEOMOUND and ACES are thanked for a good co-operation during the past three years.

CHAPTER 6

CONCLUSIONS AND PERSPECTIVES

This study provides the first detailed analyses of benthic foraminiferal assemblages, sedimentary structures and distribution in sediment cores located on and close to a carbonate mound in the Hovland Mound province (Porcupine Seabight, NE Atlantic). These datasets reveal insights in the paleoclimatic and paleoceanographic conditions of the near-shelf environment west off Ireland for the past ~31 kyr. The comparison between off- and on-mound sediments helped to reconstruct the Late Quaternary history of Propeller Mound. The analysis showed the mainly external control on mound development for this period.

Off-mound development

Faunal analysis of dead benthic foraminifera from an off-mound position of Propeller Mound identified two different assemblages, an *Interglacial* and a *Glacial group*. They clearly reflect the oceanographic and environmental changes over the past ~31 kyr.

The investigated sequence starts with a turbidite, which indicates mass transport of sediments from the shelf and the carbonate mound. It is slightly older than 31 kyr BP and suggests a first advance of the Irish Ice Sheet onto the Irish Mainland shelf. Strong shelf erosional processes occurred during the Late Marine Isotope Stage (MIS) 3, as deduced from high abundances of a displaced species (*Elphidium excavatum*), which usually occur in shallow marine, near-glacial environments. Between 31 and 24 kyr BP abundant gravity flows and tur-

bidity currents, as suggested by disorganised, fine-grained sediments, determines a high sediment supply into the basin, which is coherent with a decreasing sea-level of ~50 m and the further advance of glaciers.

Species of the *Glacial group* (*C. teretis*, *C. kullenbergi*, *G. subglobosa*, *C. reniforme*, *C. obtusa* and *S. wood*) occur in high abundances during Late MIS 3 and MIS 2. Their occurrence suggests an influence of a very cold intermediate water mass, as well as low nutrient availability. Sedimentation rates slightly decreased during MIS 2, even though turbidity currents and gravity flows prevailed the depositional regime.

A shift from the glaciomarine to the Holocene setting (12–10 kyr BP) is indicated by coarse-grained, carbonate-rich sediments and benthic foraminiferal species of the uppermost sediment layer draping the off-mound sea-floor. The *Interglacial group* is characterised by high abundances of infaunal species (*U. mediterranea*, *T. angulosa*, *H. balthica*, *M. barleeanum*, *B. marginata*, and *C. laevigata*) and reflects the present-day environmental setting with warm intermediate water masses (Eastern North Atlantic Water and Mediterranean Outflow Water), a strong hydrodynamic regime and a high nutrient supply to intermediate depths. This environment not only appears to be the controlling factor for the high abundance of the *Interglacial group*, but also for the cold-water coral ecosystem.

Mound development

The distribution of the off-mound assemblages in the on-mound core shows that the *Interglacial group* is relative abundant throughout the complete on-mound core. However, no clear glacial conditions are preserved in on-mound sediments, which most likely implies that glacial sediments have been removed from the mound. Additionally, the glacial environment in the northern Porcupine Seabight was not suitable for *Lophelia* to grow, as low nutrient availability, high sediment accumulation and low temperatures were beyond its habitat limits. With no corals on Propeller Mound, the unconsolidated fine-grained, terrigenous sediments can be easily removed by enhanced current speeds during termination to the present-day oceanographic regime.

The *Mound group*, only found in on-mound sediments, is dominated by attached epibenthic species (*D. coronata*, *G. translucens*, *C. lobatulus*, *C. refulgens*, *Q. vulgaris*, *H. sarcophaga*, *B. robusta*, *P. ariminensis* and *T. brady*). They prefer to live attached to elevated substrates, such as the cold-water coral *Lophelia pertusa* and characterise variations of the coral coverage on Propeller Mound. A decreasing trend of the *Mound group* for the past ~175 kyr indicates that benthic community on Propeller Mound is on a decline, which might result in final burial in the future.

Mound Factory

The results obtained for Propeller Mound and its closer vicinity indicate the important environmental control that accounts for the

growth and retreat of corals, and which are steered by oceanographic and climatic factors. Under fully glacial conditions no corals lived in this region. During terminations, ENAW and MOW regain their present characteristics. Enhanced currents removed the unstabilised sediments from the mound, which is expressed by several hiatuses covering glacial periods of core GeoB 6730-1. Coral larvae entered the PSB with the inflow of the MOW during terminations and were able to (re-)colonise the elevated structure. With an oceanographic regime comparable to the present-day setting the mound recommenced to grow.

The glacial-interglacial cycle with changing environmental conditions seems to be one mechanism driving the development of the carbonate mounds along the Celtic Margin, summarised in the model *Mound Factory*. This model accounts for the time, when the N Atlantic experienced the Northern Hemisphere Glaciation, which started between 3.1 and 2.5 Million years BP.

Perspectives

This study and the established model efficiently describes the mound growth and development covering the period of the Late Quaternary, related to external, oceanographic and climatic control mechanisms. However, factors controlling the initial mound growth and further development of the carbonate mound are still under debate and need to be specified by investigations on sediment cores penetrating the mound base. Therefore, a mound drilling campaign would ensure to resolve the speculative hypothesis for mound initiation.

REFERENCES

- Akhmetzhanov, A. M., Kenyon, N. H., Nielsen, T., Habgood, E., Ivanov, M. K., Henriot, J.-P., and Shashkin, P. (2001) Deep-sea bottom current depositional systems with active sand transport on the North-Eastern Atlantic Margin. In: *Geological Processes on Deep-Water European Margins. International Conference and 10th Anniversary Training Through Research Post-Cruise Meeting, 28 January - 3 February 2001, Moscow/Mozhenka, Russia* (Ed. by G. Akhmanov and A. Y. Suzyumov). UNESCO.
- Altenbach, A. V. (1992) Verbreitungsmuster benthischer Foraminiferen im Arktischen Ozean und in glazialen und interglazialen Sedimenten des Europäischen Nordmeeres. Habilitationsschrift, Christian-Albrechts-Universität, 95 pp.
- Altenbach, A. V., Pflaumann, U., Schiebel, R., Thies, A., Timm, S., and Trauth, M. (1999) Scaling percentages and distributional patterns of benthic foraminifera with flux rates of organic carbon. *Journal of Foraminiferal Research*, **29**(3), 173–185.
- Alve, E. (1995) Benthic foraminiferal distribution and recolonization of formerly anoxic environments in Drammensfjord, southern Norway. *Marine Micropaleontology*, **25**, 169–186.
- Alve, E., and Murray, J. W. (2001) Temporal variability in vertical distributions of live (stained) intertidal foraminifera, southern England. *Journal of Foraminiferal Research*, **31**(1), 12–24.
- Auffret, G., Zaragosi, S., Dennielou, B., Cortijo, E., Van Rooij, D., Grousset, F., Pujol, C., Eynaud, F., and Siegert, M. (2002) Terrigenous fluxes at the Celtic margin during the last glacial cycle. *Marine Geology*, **188**, 79–108.
- Austin, W. E. N., and Kroon, D. (1996) Late glacial sedimentology, foraminifera and stable isotope stratigraphy of the Hebridean Continental Shelf, northwest Scotland. In: *Late Quaternary Palaeoceanography of the North Atlantic Margin, Vol. 111* (Ed. by J. T., Andrews, W. E. N. Austin, H. Bergsten and A. E. Jennings), pp. 187–213. Geological Society Special Publication, London.
- Belanger, B. E., and Streeter, S. S. (1980) Distribution and ecology of benthic foraminifera in the Norwegian-Greenland Sea. *Marine Micropaleontology*, **5**, 401–428.
- Bergsten, H. (1994) Recent benthic foraminifera of a transect from the North Pole to the Yermak Plateau, eastern central Arctic Ocean. *Marine Micropaleontology*, **119**, 251–267.
- Bianchi, G. G., Hall, I. R., McCave, I. N., and Joseph, L. (1999) Measurements of the sortable silt current speed proxy using the Sedi-graph 5100 and Coulter Multisizer II: precision and accuracy. *Sedimentology*, **46**, 1001–1014.
- Bond, G., and Lotti, R. (1995) Iceberg discharges into the north Atlantic on millennial time scales during the last Glaciation. *Science*, **267**, 1005–1009.
- Bowen, D. Q. (1999) Only four major 100-ka glaciations during the Bruhnes Chron? *International Journal of Earth Sciences*, **88**, 276–284.
- Bowen, D. Q., Phillips, F. M., McCabe, A. M., Knutz, P. C., and Sykes, G. A. (2002) New data for the Last Glacial Maximum in Great Britain and Ireland. *Quaternary Science Review*, **21**, 89–101.
- Brüchert, V., Perez, M. E., and Lange, C. B. (2000) Coupled primary production, benthic foraminiferal assemblage, and sulfur diagenesis in organic-rich sediments of the Benguela upwelling system. *Marine Geology*, **163**, 27–40.
- Cann, J.-H., Belperio, A. P., and Murray-Wallace, C. V. (2000) Late Quaternary paleosealevels and paleoenvironments inferred from foraminifera, Northern Spencer Gulf, South Australia. *Journal of Foraminiferal Research*, **30**(1), 29–53.
- Caralp, M. H. (1985) Quaternary calcareous benthic foraminifera, Leg 80. In: *Initial Reports of the Deep Sea Drilling Project, Vol. 80* (Ed. by P. C. de Graciansky, C. W. Poag et al.), pp. 725–755. U.S. Govt. Printing Office, Washington.
- Caralp, M. H. (1989) Size and morphology of the benthic foraminifer *Melonis barleeanum*: Relationships with marine organic matter. *Journal of Foraminiferal Research*, **19**(3), 235–245.

- Cheng, H., Adkins, J., Edwards, R. L., and Boyle, E. A. (2000a) U-Th dating of deep-sea corals. *Geochimica et Cosmochimica Acta*, **64**(14), 2401–2416.
- Cheng, H., Edwards, R. L., Hoff, J., Gallup, C. D., Richards, D. A., and Asmerom, Y. (2000b) The half-lives of Uranium-234 and Thorium-230. *Chemical Geology*, **169**(1–2), 17–33.
- Clark, F. E., Patterson, R. T., and Fishbein, E. (1994) Distribution of Holocene benthic foraminifera from the tropical SW Pacific Ocean. *Journal of Foraminiferal Research*, **24**(4), 241–267.
- Clark, P. U., Alley, R. B., and Pollard, D. (1999) Northern Hemisphere Ice-Sheet Influences on Global Climate Change. *Science*, **286**, 1104–1111.
- Coles, G. P., Ainsworth, N. R., Whatley, R. C., and Jones, R. W. (1996) Foraminifera and ostracoda from Quaternary carbonate mounds associated with gas seepage in the Porcupine Basin, offshore western Ireland. *Revista Espanola de Micropaleontologia*, **28**(2), 113–151.
- Collins, L. S. (1989) Relationship of environmental gradients to morphologic variation within *Bulimina aculeata* and *Bulimina marginata*, Gulf of Maine area. *Journal of Foraminiferal Research*, **19**(3), 222–234.
- Corliss, B. H. (1991) Morphology and microhabitat preferences of benthic foraminifera from the northwest Atlantic Ocean. *Marine Micropaleontology*, **17**, 195–236.
- De Mol, B. (2002) Development of coral banks in Porcupine Seabight (SW Ireland) A multidisciplinary approach. Doctoral Thesis, Universiteit Gent, 363 pp.
- De Mol, B., Van Rensbergen, P., Pillen, S., Van Herreweghe, K., Van Rooij, D., McDonnell, A., Huvenne, V., Ivanov, M., Swennen, R., and Henriët, J. P. (2002) Large deep-water coral banks in the Porcupine Basin, southwest of Ireland. *Marine Geology*, **188**, 193–231.
- Delibrias, G., and Taviani, M. (1985) Dating the death of Mediterranean deep-sea scleractinian corals. *Marine Geology*, **62**, 175–180.
- Dons, C. (1944) Norges korallrev. *Det Kongelige Norske Videnskabers selskab, Forhandling*, **16**, 37–82.
- Doré, A. G., Lundin, E. R., Jensen, L. N., Birkeland, Ø., Eliassen, P. E., and Fichler, C. (1999) Principal tectonic events in the evolution of the northwest European Atlantic margin. In: *Petroleum Geology of Northwest Europe: Proceedings of the 5th Conference* (Ed. by A. J. Fleet and S. A. R. Boldy), pp. 41–61. Geological Society, London.
- Duplessy, J. C., Shackleton, N. J., Fairbanks, R. G., Labeyrie, L. D., Oppo, D., and Kallel, N. (1988) Deep water source variations during the last climatic cycle and their impact on global deep water circulation. *Paleoceanography*, **3**, 343–360.
- Ellet, D. J., Edwards, A., and Bowers, R. (1986) The hydrography of the Rockall Channel - an overview. *Proceedings of the Royal Society, Edinburgh B*, **88**, 61–81.
- Ellis, B. E., and Messina, A. R. (1940-1978) Catalogue of Foraminifera. American Museum of Natural History, New York.
- Elverhøi, A., and Bomstad, K. (1980) Late Weichselian glacial and glaciomarine sedimentation of the western, central Barents Sea. *Norsk Polarinstitutt Skrifter*, **29**.
- Eyles, N., and McCabe, A. M. (1989) The Late Devensian (<22,000 BP) Irish Sea Basin: The sedimentary record of a collapsed ice sheet margin. *Quaternary Science Reviews*, **8**, 307–351.
- Fairbanks, G. (1989) A 17 000-year glacio-eustatic sea level record, influence of glacial melting rates on the Younger Dryas event and deep-ocean circulation. *Nature*, **342**, 637–642.
- Feyling-Hanssen, R. W., Joergensen, J. A., Knudsen, K. L., and Andersen, A.-L. L. (1971) Late Quaternary Foraminifera from Vendysyssel, Denmark and Sandnes, Norway. *Bulletin of the Geological Society of Denmark*, **21**(2–3), 67–317.
- Filkorn, H. F. (1994) Fossil scleractinian corals from James Ross Basin, Antarctica. *Antarctica Research Series*, **65**, 1–96.
- Frederiksen, R., Jensen, A., and Westerberg, H. (1992) The distribution of the scleractinian coral *Lophelia pertusa* around the Faroe islands and the relation to internal tidal mixing. *Sarsia*, **77**, 157–171.
- Freiwald, A. (1998) Geobiology of *Lophelia pertusa* (scleractinia) reefs in the North Atlantic. Habilitationsschrift, University of Bremen, 116 pp.
- Freiwald, A. (2002) Reef-Forming Cold-Water Corals. In: *Ocean Margin Systems* (Ed. by G. Wefer, D. Billett, D. Hebbeln, B. B. Jørgensen, M. Schlüter and T. v. Weering), pp. 365–385. Springer Verlag, Berlin, Heidelberg, New York.

- Freiwald, A., and Schönfeld, J. (1996) Substrate pitting and boring pattern of *Hyrrokkina sarcophaga* Cedhagen, 1994 (Foraminifera) in a modern deep-water coral reef mound. *Marine Micropaleontology*, **28**, 199–207.
- Freiwald, A., and Wilson, J. B. (1998) Taphonomy of modern deep, cold-temperate water coral reefs. *Historical Biology*, **13**, 37–52.
- Freiwald, A., and Shipboard Party (2002) Cruise Report RV POSEIDON Cruise 292, Reykjavik - Galway, 15th July – 4th August 2002, 84 pp.
- Freiwald, A., Henrich, R., and Pätzold, J. (1997) Anatomy of a deep-water coral reef mound from Stjernsund, West Finnmark, Northern Norway. In: *Cool-Water Carbonates, Vol. 56* (Ed. by N. P. James and J. A. D. Clarke), pp. 141–162. SEPM, Tulsa, Oklahoma, U.S.A.
- Freiwald, A., Wilson, J. B., and Henrich, R. (1999) Grounding Pleistocene icebergs shape recent deep-water coral reefs. *Sedimentary Geology*, **125**, 1–8.
- Freiwald, A., Dullo, C., and Shipboard Party (2000) Cruise Report RV POSEIDON Cruise 265, Thorshavn - Galway - Kiel, 13th September – 1st October 2000, 65 pp.
- Gabel, B. (1971) Die Foraminiferen der Nordsee. *Helgoländer wissenschaftliche Meeresuntersuchungen*, **22**, 1–65.
- Games, K. P. (2001) Evidence of shallow gas above the Connemara oil accumulation, Block 26/28, Porcupine Basin. In: *The Petroleum Exploration of Ireland's Offshore Basins, Vol. 188* (Ed. by P. M. Shannon, P. D. W. Haughton and D. V. Corcoran), pp. 361–373. Geological Society Special Publications, London.
- GEBCO (1997) 1997 Edition of IOC/IHO General Bathymetric Chart of the Oceans. *GEBCO digital atlas (GDA)*. British Oceanographic Data Centre, Bidston Observatory, Merseyside.
- Gooday, A. J. (1986) Meiofaunal foraminiferans from the bathyal Porcupine Seabight (north-east Atlantic): size structure, standing stock, taxonomic composition, species diversity and vertical distribution in the sediments. *Deep-Sea Research*, **33**(10), 1345–1373.
- Gooday, A. J. (1988) A response by benthic foraminifera to the deposition of phytodetritus in the deep sea. *Nature*, **322**, 70–73.
- Gooday, A. J., and Hughes, J. A. (2002) Foraminifera associated with phytodetritus deposits at a bathyal site in the northern Rockall Trough (NE Atlantic): seasonal contrasts and a comparison of stained and dead assemblages. *Marine Micropaleontology*, **46**, 83–110.
- Grousset, F. E., Pujol, C., Labeyrie, L., Auffret, G., and Boelaert, A. (2000) Were the North Atlantic Heinrich events triggered by the behavior of the European ice sheets? *Geology*, **28**(2), 123–126.
- Gupta, A. K. (1994) Taxonomy and bathymetric distribution of Holocene deep-sea benthic foraminifera in the Indian Ocean and the Red Sea. *Micropaleontology*, **40**(4), 351–367.
- Hald, M., and Vorren, T. (1984) Modern and Holocene foraminifera and sediments on the continental shelf off Troms, North Norway. *Boreas*, **13**, 133–154.
- Hald, M., and Vorren, T. O. (1987) Foraminiferal stratigraphy and environment of Late Weichselian deposits on the continental shelf off Troms, northern Norway. *Marine Micropaleontology*, **12**, 129–160.
- Hald, M., and Steinsund, P. I. (1992) Distribution of surface sediment benthic foraminifera in the southwestern Barents Sea. *Journal of Foraminiferal Research*, **22**(4), 347–362.
- Hald, M., Steinsund, P.I., Dokken, T., Korsun, S., Polyak, L., Aspeli, R. (1994) Recent and late Quaternary distribution of *Elphidium excavatum* f. *clavatum* in the Arctic Seas. *Cushman Foundation Special Publication*, **32**, 141–153.
- Hall-Spencer, J., Allain, V., and Fosså, J. H. (2002) Trawling damage to Northeast Atlantic ancient coral reefs. *Proceedings of the Royal Society, London (B)* **269** (1490), 507–511.
- Hanken, N.-M., Bromley, R. G., and Miller, J. (1996) Plio-Pleistocene sedimentation in coastal grabens, north-east Rhodes, Greece. *Geological Journal*, **31**, 393–418.
- Haug, G. H., Tiedemann, R., Zahn, R., and Ravelo, A. C. (2001) Role of Panama uplift on oceanic freshwater balance. *Geology*, **29**(3), 207–210.
- Hebbeln, D., and Wefer, G. (1991) Effects of ice coverage and ice-rafted material on sedimentation in Fram Strait. *Nature*, **350**, 409–411.
- Henriet, J. P., De Mol, B., Pillen, S., Vanneste, M., Van Rooij, D., Versteeg, W., Croker, P. F., Shannon, P. M., Unnithan, V., Bouriak, S., and Chachkine, P. (1998) Gas hydrate crystals may help build reefs. *Nature*, **391**, 648–649.

- Henriet, J. P., Guidard, S., and Team, O. P. (2002) Carbonate Mounds as a Possible Example for Microbial Activity in Geological Processes. In: *Ocean Margin Systems* (Ed. by G. Wefer, D. Billett, D. Hebbeln, B. B. Jørgensen, M. Schlüter and T. v. Weering), pp. 437–455. Springer Verlag, Berlin, Heidelberg, New York.
- Heß, S. (1998) Rezente benthische Foraminiferen in Sedimenten des Schelfes und oberen Kontinentalhanges im Golf von Guinea (Westafrika), Geologisch-Paläontologisches Institut, Christian-Albrechts-Universität, Kiel, 173 pp.
- Hill, A. E., and Mitchelson-Jacob, E. G. (1993) Observations of a poleward-flowing saline core on the continental slope west of Scotland. *Deep Sea Research I*, **40**(7), 1521–1527.
- Hodell, D. A., Curtis, J. H., Sierro, F. J., and Raymo, M. E. (2001) Correlation of late Miocene to early Pliocene sequences between the Mediterranean and North Atlantic. *Paleoceanography*, **16**(2), 164–178.
- Holbourn, A. E., and Henderson, A. S. (2002) Re-illustration and revised taxonomy for selected deep-sea benthic foraminifers. *Palaeontologica Electronica*, **4**(2), 34 pp.
- Hovland, M. (1990) Do carbonate reefs form due to fluid seepage? *Terra Nova*, **2**, 8–18.
- Hovland, M., and Mortensen, P. B. (1999) *Norske korallrev og prosesser i havbunnen*. John Grieg Forlag, Bergen, 155 pp.
- Hovland, M., Croker, P. F., and Martin, M. (1994) Fault-associated seabed mounds (carbonate knolls?) off western Ireland and north-west Australia. *Marine and Petroleum Geology*, **11**(2), 232–246.
- Höppner, R., and Henrich, R. (1999) Kornsortierungsprozesse am Argentinischen Kontinentalhang anhand von Siltkorn-Analysen. *Zentralblatt der Geologie und Paläontologie, Teil I*, **1997**(H. 7–9), 897–905.
- Huthnance, J. M. (1986) The Rockall slope current and shelf-edge processes. *Proceedings of the Royal Society, Edinburgh B*, **88**, 83–101.
- Huthnance, J. M. (1995) Circulation, exchange and water masses at the ocean margin: the role of physical processes at the shelf edge. *Progress in Oceanography*, **35**, 353–431.
- Huthnance, J. M., and Gould, W. J. (1989) On the Northeast Atlantic slope current. In: *Poleward flows along eastern ocean boundaries, Vol. 34* (Ed. by S. J. Neshyba), pp. 76–81. Coastal and Estuarine Studies.
- Huvenne, V. A. I., Croker, P. F., and Henriët, J.-P. (2002) A refreshing 3D view of an ancient sediment collapse and slope failure. *Terra Nova*, **14**, 33–40.
- Huvenne, V., De Mol, B., and Henriët, J.-P. (2003) A 3D seismic study of the morphology and spatial distribution of buried coral banks in the Porcupine Basin, SW of Ireland. *Marine Geology*, **198**, 5–25.
- Jaffey, A. H., Flynn, K. F., Glendenin, L. E., Bentley, W. C., and Essling, A. M. (1971) Precession measurements of half-lives and specific activities of ^{235}U and ^{238}U . *Physical Reviews*, **C 4**, 1889–1906.
- Jansen, J. H. F., Van der Gaast, S. J., Koster, B., and Vaars, A. J. (1998) CORTEX, a ship-board XRF-scanner for element analyses in split sediment cores. *Marine Geology*, **151**, 143–153.
- Japsen, P. (1997) Regional Neogene exhumation of Britain and the western North Sea. *Journal of the Geological Society, London*, **154**, 239–247.
- Jennings, A. E., and Helgadottir, G. (1994) Foraminiferal assemblages from the Fjords and shelf of Eastern Greenland. *Journal of Foraminiferal Research*, **24**(2), 123–144.
- Jennings, A. E., Tedesco, K. A., Andrews, J. T., and Kirby, M. E. (1996) Shelf erosion and glacial ice proximity in the Labrador Sea during and after Heinrich events (H-3 or 4 to H-0) as shown by foraminifera. In: *Late Quaternary Palaeoceanography of the North Atlantic Margin, Vol. 111* (Ed. by J. T. Andrews, W. E. N. Austin, H. Bergsten and A. E. Jennings), pp. 29–49. Geological Society Special Publication, London.
- Johnston, S., Doré, A. G., and Spencer, A. M. (2001) The Mesozoic evolution of the southern North Atlantic region and its relationship to basin development in the south Porcupine Basin, offshore Ireland. In: *The Petroleum Exploration of Ireland's Offshore Basins, Vol. 188* (Ed. by P. M. Shannon, P. D. W. Houghton and D. V. Corcoran), pp. 237–263. Geological Society Special Publications, London.
- Joint, I., Wollast, R., Chou, L., Batten, S., Elskens, M., Edwards, E., Hirst, A., Burkill, P., Groom, S., Gibb, S., Miller, A., Hydes, D., Dehairs, F., Antia, A., Barlow, R., Rees, A., Pomroy, A., Brockmann, U., Cummings, D., Lampitt, R., Loijens, M., Mantoura, F., Miller, P., Raabe, T., Alvarez-Salgado, X., Stelfox, C., and Woolfenden, J. (2001)

- Pelagic production at the Celtic Sea shelf break. *Deep-Sea Research II*, **48**, 3049–3081.
- Jones, R. L., and Keen, D. H. (1993) *Pleistocene Environments in the British Isles*, Chapman and Hall, London, 346 pp.
- Joubin, L. (1922) Distribution géographique de quelques coraux abyssaux dans les mers occidentales européennes. *Comptes Rendus, Académie des Sciences de Paris*, **175**, 930–933.
- Kaiho, K. (1994) Benthic foraminiferal dissolved-oxygen index and dissolved-oxygen levels in the modern ocean. *Geology*, **22**, 719–722.
- Kenyon, N. H., Akhmetzhanov, A. M., Wheeler, A. J., van Weering, T. C. E., de Hass, H., and Ivanov, M. K. (2003) Giant carbonate mud mounds in the southern Rockall Trough. *Marine Geology*, **195**, 5–30.
- Knott, S. D., Burchell, M. T., Jolley, E. J., and Fraser, A. J. (1998) Mesozoic to Cenozoic plate reconstructions of the North Atlantic Margin. In: *Petroleum Geology of Northwest Europe: Proceedings of the 4th Conference* (Ed. by J. R. Parker), pp. 953–974. Geological Society, London.
- Knutz, P. C., Austin, W. E. N., and Jones, E. J. W. (2001) Millennial-scale depositional cycles related to British Ice Sheet variability and North Atlantic paleocirculation since 45 kyr B.P., Barra Fan, U.K. margin. *Paleoceanography*, **16**(1), 53–64.
- Konert, M., and Vandenberghe, J. (1997) Comparison of laser grain size analysis with pipette and sieve analysis: a solution for the underestimation of the clay fraction. *Sedimentology*, **44**, 523–535.
- Korsun, S. A., and Polyak, L. V. (1989) Distribution of benthic foraminiferal morphogroups in the Barents Sea. *Oceanology*, **29**(5), 838–844.
- Korsun, S., and Hald, M. (2000) Seasonal dynamics of benthic foraminifera in a glacially fed fjord of Svalbard, European Arctic. *Journal of Foraminiferal Research*, **30**, 251–271.
- Labeyrie, L. D., Duplessy, J.-C., and Blanc, P. L. (1987) Variations in mode of formation and temperature of oceanic deep-waters over the past 125 000 years. *Nature*, **327**, 477–482.
- Lambeck, K., Yokohama, Y., and Purcell, T. (2002) Into and out of the Last Glacial Maximum: sea-level change during Oxygen Isotope Stages 3 and 2. *Quaternary Science Reviews*, **21**, 343–360.
- Lambshead, P. J. D., and Gooday, A. J. (1990) The impact of seasonally deposited phytodetritus on epifaunal and shallow infaunal benthic foraminiferal populations in the bathyal northeast Atlantic: the assemblage response. *Deep-Sea Research*, **37**(8), 1263–1283.
- Lehman, S. J., and Keigwin, L. D. (1992) Sudden changes in North Atlantic circulation during the last deglaciation. *Nature*, **356**, 757–762.
- Linke, P., and Lutze, G. F. (1993) Microhabitat preferences of benthic foraminifera - a static concept or a dynamic adaptation to optimize food acquisition? *Marine Micropaleontology*, **20**, 215–234.
- Loubere, P. (1991) Deep-sea benthic foraminiferal assemblage response to a surface ocean productivity gradient: a test. *Paleoceanography*, **6**(2), 193–204.
- Lutze, G. F. (1980) Depth distribution of benthic foraminifera on the continental margin off NW Africa. "METEOR" *Research Results*, **32**(C), 31–80.
- Lutze, G. F., and Thiel, H. (1989) Epibenthic foraminifera from elevated microhabitats: *Cibicides wuellerstorfi* and *Planulina ariminensis*. *Journal of Foraminiferal Research*, **19**(2), 153–158.
- Mackensen, A., and Hald, M. (1988) *Cassidulina teretis* TAPPAN and *C. laevigata* d'ORBIGNY: Their modern and late quaternary distribution in Northern seas. *Journal of Foraminiferal Research*, **18**(1), 16–24.
- Mackensen, A., Sejrup, H., and Jansen, E. (1985) The distribution of living benthic foraminifera on the continental slope and rise off Southwest Norway. In: *Marine Micropaleontology, Vol. 9*, pp. 275–306.
- Mackensen, A., Grobe, H., Kuhn, G., and Fütterer, D. K. (1990) Benthic foraminiferal assemblages from the eastern Weddell Sea between 68 and 73°S: Distribution, ecology and fossilization potential. *Marine Micropaleontology*, **16**, 241–283.
- Mackensen, A., Fütterer, D. K., Grobe, H., and Schmiedl, G. (1993) Benthic foraminiferal assemblages from the eastern South Atlantic Polar Front region between 35° and 57°S: Distribution, ecology and fossilization potential. *Marine Micropaleontology*, **22**, 33–69.
- Mackensen, A., Schmidl, G., Harloff, J., and Giese, M. (1995) Deep-sea foraminifera in the South Atlantic Ocean: ecology and as-

- semblage generation. *Micropaleontology*, **41**(4), 342–358.
- Manighetti, B., and McCave, I. N. (1995) Late glacial and Holocene palaeocurrents around Rockall Bank, NE Atlantic Ocean. *Paleoceanography*, **10**(3), 611–626.
- Martinson, D. G., Pisias, N. G., Hays, J. D., Imbrie, J., Moore Jr., T. C., and Shackleton, N. J. (1987) Age dating and the orbital theory of the ice ages: development of a high resolution 0 to 300 000-year chronostratigraphy. *Quaternary Research*, **27**, 1–29.
- Masson, D. G., Bett, B. J., Billett, D. S. M., Jacobs, C. L., Wheeler, A. J., and Wynn, R. B. (2003) The origin of deep-water, coral-topped mounds in the northern Rockall Trough, Northeast Atlantic. *Marine Geology*, **194**, 159–180.
- McCabe, A. M. (1987) Quaternary deposits and glacial stratigraphy in Ireland. *Quaternary Science Reviews*, **6**, 259–299.
- McCabe, A. M., and Clark, P. U. (1998) Ice-sheet variability around the North Atlantic Ocean during the last deglaciation. *Nature*, **392**, 373–377.
- McCann, T., Shannon, P.M., and Moore, J.G. (1995) Fault patterns in the Cretaceous and Tertiary (end syn-rift, thermal subsidence) succession of the Porcupine Basin, offshore Ireland. *Journal of Structural Geology*, **17**(2), 201–214.
- McCartney, M. S., and Mauritzen, C. (2001) On the origin of the warm inflow to the Nordic Seas. *Progress in Oceanography*, **51**, 125–214.
- McCave, I. N. (2002) Sedimentary Settings on Continental Margins - an Overview. In: *Ocean Margin Systems* (Ed. by G. Wefer, D. Billett, D. Hebbeln, B. B. Jørgensen, M. Schlüter and T. v. Weering). pp. 1–14. Springer Verlag, Berlin, Heidelberg, New York.
- McCave, I. N., Manighetti, B., and Robinson, S. G. (1995) Sortable silt and fine sediment size/composition slicing: Parameters for paleocurrent speed and paleoceanography. *Paleoceanography*, **10**(3), 593–610.
- McCave, I. N., Hall, I. R., Antia, A. N., Chou, L., Dehairs, F., Lampitt, R. S., Thomsen, L., van Weering, T. C. E., and Wollast, R. (2001) Distribution, composition and flux of particulate material over the European margin at 47°–50°N. *Deep-Sea Research II*, **48**, 3107–3139.
- McDonnell, A., and Shannon, P. M. (2001) Comparative Tertiary stratigraphic evolution of the Porcupine and Rockall basins. In: *Petroleum Exploration of Ireland's Offshore Basins, Vol. 188* (Ed. by P. M. Shannon, P. Haughton and D. Corcoran), pp. 323–344. Geological Society of London Special Publications, London.
- Mohn, C. (2000) Über Wassermassen und Strömungen im Bereich des europäischen Kontinentalrandes westlich von Irland. PhD, Hamburg, 122 pp.
- Mohn, C., Bartsch, J., and Meincke, J. (2002) Observations of the mass and flow field at Porcupine Bank. *ICES Journal of Marine Science*, **59**, 380–392.
- Mortensen, P. B., Hovland, M., Brattegard, T., and Farestveit, R. (1995) Deep water bioherms of coral *Lophelia pertusa* (L.) at 64 degrees on the Norwegian shelf: structure and associated megafauna. *Sarsia*, **80**, 145–158.
- Mullins, H. T., Thompson, J. B., McDougall, K., and Vercoutere, T. L. (1985) Oxygen minimum zone edge effect: evidence from the Central California coastal upwelling system. *Geology*, **13**, 491–494.
- Murray, J. W. (1991) *Ecology and Palaeoecology of Benthic Foraminifera*. Longman Scientific and Technical, Essex, 397 pp.
- Murray, J. W. (2003) An illustrated guide to the benthic foraminifera of the Hebridean Shelf, west of Scotland, with notes on their mode of life. *Palaeontologica Electronica*, **5**(1), 31 pp.
- Nadeau, M. J., Schleicher, M., Grootes, P., Erlenkeuser, H., Gottolung, A., Mous, D.J.W., Sarthein, M., and Willkomm, N. (1997) The Leibnitz-Labor AMS Facility at the Christian-Albrechts-University, Kiel, Germany. *Nuclear Instrumental Methods in Physical Research*, **123**, 22–30.
- Nagy, Y. (1965) Foraminifera in some bottom samples from shallow waters in Vestspitsbergen. *Norsk Polarinstitutt Årbeitt*, **1963**, 109–125.
- Nelson, C. H., Twichell, D. C., Schwab, W. C., Lee, H. J., and Kenyon, N. H. (1992) Upper Pleistocene turbidite sand beds and chaotic silt beds in the channelized, distal, outer-fan lobes of the Mississippi fan. *Geology*, **20**, 693–696.
- New, A. L., Jia, Y., Coulibaly, M., and Dengg, J. (2001) On the role of the Azores Current in the ventilation of the North Atlantic Ocean.

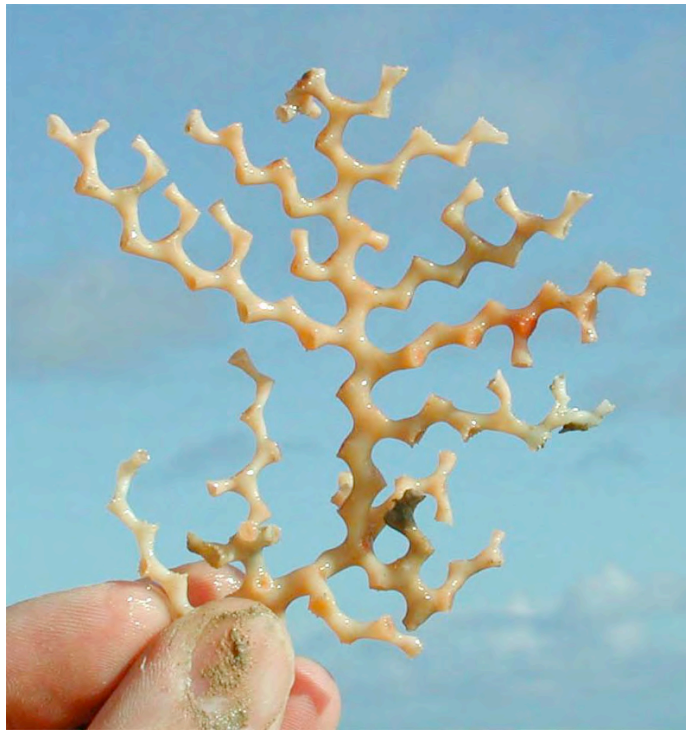
- Progress in Oceanography*, **48**, 163–194.
- Ohkushi, K., Thomas, E., and Kawahata, H. (2000) Abyssal benthic foraminifera from the northwestern Pacific (Shatsky Rise) during the last 298 kyr. *Marine Micropaleontology*, **38**, 119–147.
- Oki, K. (1989) Ecological Analysis of Benthic Foraminifera in Kagoshima Bay, South Kyushu, Japan. *South Pacific Studies*, **10**(1), 1–191.
- Oppo, D., and Lehman, S. (1993) Mid-depth circulation of the sub-polar North Atlantic during the last glacial maximum. *Science*, **259**, 1148–1152.
- Østebø, K. L., and Nagy, J. (1982) Foraminiferal distribution in the western Barents Sea, Recent and Quaternary. *Polar Research*, **1**, 53–95.
- Pingree, R. D. (1993) Flow of waters to the west of the British Isles and in the Bay of Biscay. *Deep Sea Research II*, **40**(1-2), 369–388.
- Pingree, R. D., and LeCann, B. (1989) Celtic and American slope and shelf residual currents. *Progress in Oceanography*, **23**, 303–338.
- Pingree, R. D., and LeCann, B. (1990) Structure, strength and seasonality of the slope currents in the Bay of Biscay region. *Journal of the Marine Biological Association of the UK*, **70**, 857–885.
- Pingree, R. D., and New, A. L. (1991) Abyssal penetration and bottom reflection of internal tidal energy in the Bay of Biscay. *Journal of Physical Oceanography*, **21**, 28–39.
- Pollard, R. T., Griffiths, M. J., Cunningham, S. A., Read, J. F., Perez, F. F., and Rios, A. F. (1996) Vivaldi 1991 - a study of the formation, circulation and ventilation of Eastern North Atlantic Water. *Progress in Oceanography*, **37**, 167–192.
- Pujos, M. (1971) Quelques exemples de distribution des foraminifères benthiques profonds du Golfe de Gascogne: Relation entre Microfaune et environnement. *Cahiers Oceanographique*, **13**, 445–453.
- Quilty, P. G., Gillieson, D., Burgess, J., Gardiner, G., Spate, A., and Pidgeon, R. (1990) *Ammoelphidiella* from the Pliocene of Larsemann Hills, East Antarctica. *Journal of Foraminiferal Research*, **20**(1), 1–7.
- Rasmussen, T. L., Thomsen, E., van Weering, T. C. E., and Labeyrie, L. (1996) Rapid changes in surface and deep water conditions at the Faeroe Margin during the last 58,000 years. *Paleoceanography*, **11**(6), 757–771.
- Rasmussen, T. L., Thomsen, E., Troelstra, S. R., Kuijpers, A., and Prins, M. A. (2002a) Millennial-scale glacial variability versus Holocene stability: changes in planktic and benthic foraminifera faunas and ocean circulation in the North Atlantic during the last 60 000 years. *Marine Micropaleontology*, **47**, 143–176.
- Rasmussen, T. L., Bäckström, D., Heinemeier, J., Klitgaard-Kristensen, D., Knutz, P. C., Kuijpers, A., Lassen, S., Thomsen, E., Troelstra, S. R., and van Weering, T. C. E. (2002b) The Faroe-Shetland Gateway: Late Quaternary water mass exchange between the Nordic seas and the northeastern Atlantic. *Marine Geology*, **188**, 165–192.
- Rice, A. L., Thurston, M. H., and New, A. L. (1990) Dense aggregations of the hexactinellid sponge, *Phoronema carpenteri*, in the Porcupine Seabight (northeast Atlantic Ocean), and possible causes. *Progress in Oceanography*, **24**, 179–196.
- Richter, T. O., Lassen, S., van Weering, T. C. E., and de Haas, H. (2001) Magnetic susceptibility patterns and provenance of ice-rafted material at Feni Drift, Rockall Trough: implications for the history of the British-Irish ice sheet. *Marine Geology*, **173**, 37–54.
- Rogers, A. D. (1999) The biology of *Lophelia pertusa* (Linnaeus 1758) and other deep-water reef forming corals and impact from human activities. *International Reviews of Hydrobiology*, **84**, 315–406.
- Ruddiman, W. F., and McIntyre, A. (1981) The North Atlantic during the last deglaciation. *Palaeogeography, Palaeoclimatology, Palaeoecology*, **35**, 145–214.
- Sarnthein, M., Winn, K., Jung, S. J. A., Duplessy, J.-C., Labeyrie, L., Erlenkeuser, H., and Ganssen, G. (1994) Changes in east Atlantic deepwater circulation over the last 30,000 years: Eight time slice reconstructions. *Paleoceanography*, **9**(2), 209–267.
- Sarnthein, M., Jansen, W., Weinelt, M., Arnold, M., Duplessy, J.-C., Erlenkeuser, H., Flatøy, A., Johannessen, G., Johannessen, T., Jung, S., Koc, N., Labeyrie, L., Maslin, M., Pflaumann, U., and Schulz, H. (1995) Variations in Atlantic surface ocean paleoceanography, 50°–80°N: A time-slice record of the last 30,000 years. *Paleoceanography*, **10**(6), 1063–1094.
- Sarnthein, M., Stattegger, K., Dreger, D., Erlenkeuser, H., Grootes, P., Haupt, B. J., Jung, S., Kiefer, T., Kuhnt, W., Pflaumann, U.,

- Schäfer-Neth, C., Schulz, H., Schulz, M., Seidov, D., Simstich, J., van Kreveld, S., Vogelsang, E., Völker, A., and M., W. (2001) Fundamental Modes and Abrupt Changes in the North Atlantic Circulation and Climate over the last 60 kyr – Concepts, Reconstruction and Numerical Modeling. In: *The Northern North Atlantic: A Changing Environment* (Ed. by P. Schäfer, W. Ritzrau, M. Schlüter and J. Thiede), pp. 365–410. Springer Verlag, Berlin.
- Sarnthein, M., Pflaumann, U., and Weinelt, M. (2003) Past extent of sea ice in the northern North Atlantic inferred from foraminiferal paleotemperature estimates. *Paleoceanography*, **18**(2), 10.1029/2002PA000771.
- Sars, M. (1865) Om de i Norge forekommende fossile dyrelvinger fra Quartaerperioden. *Christiania, Universitetsprogram for forste halvaar*, **1864**, 1–164.
- Schiebel, R. (1992) Rezente benthische Foraminiferen in Sedimenten des Schelfes und oberen Kontinentalhanges im Golf von Guinea (Westafrika), pp. 179. Geologisch-Paläontologisches Institut, Christian-Albrechts-Universität, Kiel.
- Schönfeld, J. (1997) The impact of the Mediterranean Outflow Water (MOW) on benthic foraminiferal assemblages and surface sediments at the southern Portuguese continental margin. *Marine Micropaleontology*, **29**(1997), 211–236.
- Schönfeld, J. (2002a) Recent benthic foraminiferal assemblages in deep high-energy environments from the Gulf of Cadiz (Spain). *Marine Micropaleontology*, **44**, 141–162.
- Schönfeld, J. (2002b) A new benthic foraminiferal proxy for near-bottom current velocities in the Gulf of Cadiz, northeastern Atlantic Ocean. *Deep-Sea Research I*, **49**, 1853–1875.
- Schönfeld, J., and Zahn, R. (2000) Late Glacial to Holocene history of the Mediterranean Outflow. Evidence from benthic foraminiferal assemblages and stable isotopes at the Portuguese margin. *Palaeogeography, Palaeoclimatology, Palaeoecology*, **159**, 85–111.
- Schröder-Adams, C. J., Cole, F. E., Medioli, F. S., Mudie, P. J., Scott, D. B., and Dobbin, L. (1990) Recent arctic shelf foraminifera: seasonally ice covered vs. perennially ice covered areas. *Journal of Foraminiferal Research*, **20**(1), 8–36.
- Scoffin, T. P., and Bowes, G. E. (1988) The facies distribution of carbonate sediments on Porcupine Bank, northeast Atlantic. *Sedimentary Geology*, **60**, 125–134.
- Seidenkrantz, M.-S., Kouwenhoven, T. J., Jorissen, F. J., Shackleton, N. J., and Van der Zwaan, G. J. (2000) Benthic foraminifera as indicators of changing Mediterranean-Atlantic water exchange in the late Miocene. *Marine Geology*, **163**, 387–407.
- Sejrup, H. P., Fjæran, T., Hald, M., Beck, L., Hagen, J., Miljeteig, I., Morvik, I., and Norvik, O. (1981) Benthic foraminifera in surface samples from the norwegian continental margin between 62°N and 65°N. *Journal of Foraminiferal Research*, **11**, 277–295.
- Shackleton, N. J., Hall, M., and Pate, D. (1995) Pliocene stable isotope stratigraphy of Site 846. In: *Proceedings of the Ocean Drilling Program, Scientific Results, Vol. 138*, pp. 337–357. Ocean Drilling Program, College Station, Texas.
- Siddall, M., Rohling, E. J., Almogi-Labin, A., Hemleben, C., Meischner, D., Schmelzer, I., and Smeed, D. A. (2003) Sea-level fluctuations during the last glacial cycle. *Nature*, **423**, 853–858.
- Siegert, M. J., and Dowdeswell, J. A. (2002) Late Weichselian iceberg, surface-melt and sediment production from the Eurasian Ice Sheet: results from numerical ice-sheet modelling. *Marine Geology*, **188**, 109–127.
- Smart, C. W., and Gooday, A. J. (1997) Recent benthic foraminifera in the abyssal northeast Atlantic Ocean: Relation to phytodetrital input. *Journal of Foraminiferal Research*, **27**, 85–92.
- Smith, R. (1989) Poleward flows along eastern boundaries: An introduction and historical review. In: *Poleward flows along eastern ocean boundaries* (Ed. by S. J. Neshyba, C. N. K. Mooers, R. L. Smith and R. T. Barber), pp. 17–25. Springer Verlag.
- Squires, D. F. (1957) New species of caryophylliid corals from the Gulf Coast Tertiary. *Journal of Paleontology*, **31**, 992–996.
- Squires, D. F. (1964) Fossil coral thickets in Wairarapa, New Zealand. *Journal of Paleontology*, **38**, 904–915.
- Stanley, G. D., and Cairns, S. D. (1988) Constructional azooxanthellate coral communities: an overview with implications for the fossil record. *Palaios*, **3**, 233–242.
- Steinsund, P. I., and Hald, M. (1994) Recent calcium carbonate dissolution in the Barents

- Sea; Paleogeographic applications. *Marine Geology*, **117**, 303–316.
- Stoker, M. S. (1997) A Mid- to Late Cenozoic sedimentation on the continental margin off NW Britain. *Journal of the Geological Society, London*, **154**, 509–515.
- Stoker, M. S., van Weering, T. C. E., and Svaerdborg, T. (2001) A mid- to late Cenozoic tectonostratigraphic framework for the Rockall Trough. In: *Petroleum Exploration of Ireland's Offshore Basins, Vol. 188* (Ed. by P. M. Shannon, P. Haughton and D. Corcoran), pp. 411–438. Geol. Soc. London Spec. Publ., London.
- Stow, D. V. A., Howell, D. G., and Nelson, H. C. (1985) Sedimentary, tectonic, and sea-level controls. In: *Submarine Fans and Related Turbidite Systems* (Ed. by A. H. Bouma, W. R. Normark and N. E. Barnes), pp. 15–22. Springer Verlag, New York.
- Stow, D. A. V., Reading, H. G., and Collinson, J. D. (1996) Deep seas. In: *Sedimentary environments: Processes, Facies and Stratigraphy* (Ed. by H. G. Reading), pp. 385–453. Blackwell Science, Oxford.
- Struck, U. (1992) Zur Paläo-Ökologie benthischer Foraminiferen im Europäischen Nordmeer während der letzten 600.000 Jahre, Vol. 38, Berichte aus dem Sonderforschungsbereich 313, Kiel, 129 pp.
- Stuiver, M., and Reimer, P. J. (1993) Extended ^{14}C data base and revised CALIB 3.0 ^{14}C age calibration program. *Radiocarbon*, **35**, 215–230.
- Stuiver, M., Reimer, P. J., and Braziunas, T. F. (1998) (revised dataset). *Radiocarbon*, **40**, 1127–1151.
- Teichert, C. (1958) Cold- and deep-water coral banks. *AAPG Bulletin*, **42**(5), 1064–1082.
- Thies, A. (1991) Die Benthosforaminiferen im Europäischen Nordmeer, Vol. 31, Berichte aus dem Sonderforschungsbereich 313, Kiel 97 pp.
- Thomas, F. C., Medioli, F. S., and Scott, D. B. (1990) Holocene and latest Wisconsinan benthic foraminiferal assemblages and paleocirculation history, Lower Scotian slope and rise. *Journal of Foraminiferal Research*, **20**(3), 212–245.
- Thomas, E., Booth, L., Maslin, M., and Shackleton, N. J. (1995) Northeastern Atlantic benthic foraminifera during the last 45,000 years: Changes in productivity seen from the bottom up. *Paleoceanography*, **10**(3), 545–562.
- Thorpe, S. A., and White, M. (1988) A deep intermediate nepheloid layer. *Deep Sea Research Part A. Oceanographic Research Paper*, **35**(9), 1665–1671.
- Timm, S. (1992) Rezente Tiefsee-Benthosforaminiferen aus Oberflächensedimenten des Golfes von Guinea (Westafrika) - Taxonomie, Verbreitung, Ökologie und Korngrößenfraktionen, pp. 192. Geologische-Paläontologisches Institut, Christian-Albrechts-Universität, Kiel.
- van Aken, H. M. (2000) The hydrography of the mid-latitude northeast Atlantic Ocean II: The intermediate water masses. *Deep-Sea Research I*, **47**, 789–824.
- van Morkhoven, F. P. C. M., Berggren, W. A., and Edwards, A. S. (1986) *Cenozoic cosmopolitan deep-water benthic foraminifera*, 434 pp.
- Van Rooij, D., De Mol, B., Huvenne, V., Ivanov, M., and Henriot, J.-P. (2003) Seismic evidence of current-controlled sedimentation in the Belgica mound province, upper Porcupine slope, southwest of Ireland. *Marine Geology*, **195**, 31–53.
- Vella, P. (1964) Foraminifera and other fossils from Late Tertiary deep-water coral thickets, Wairarapa, New Zealand. *Journal of Paleontology*, **38**, 916–928.
- Veum, T., Jansen, E., Arnold, M., Beyer, I., and Duplessy, J.-C. (1992) Water mass exchange between the North Atlantic and the Norwegian Sea during the past 28,000 years. *Nature*, **356**, 783–785.
- Voelker, A. H. L., Sarnthein, M., Grootes, P.M., Erlenkeuser, H., Laj, C., Mazaud, A., Nadeau, M.-J., and Scelicher, M. (1998) Correlation of marine ^{14}C ages from the Nordic Seas with the GISP2 isotope record: Implications for radiocarbon calibration beyond 25 ka BP. *Radiocarbon*, **40**(1,2), 517–534.
- Weinelt, M., Kuhnt, W., Sarnthein, M., Altenbach, A., Costello, O., Erlenkeuser, H., Pflaumann, U., Simstich, J., Struck, U., Thies, A., Trauth, M. H., and Vogelsang, E. (2001) Paleoceanographic Proxies in the Northern North Atlantic. In: *The Northern North Atlantic: A Changing Environment* (Ed. by P. Schäfer, W. Ritzrau, M. Schlüter and J. Thiede), pp. 319–352. Springer Verlag, Berlin.
- Weston, J. F. (1985) Comparison between Recent benthic foraminiferal faunas of the Porcupine Seabight and Western Approaches Continental Slope. *Journal of Micropalae-*

- ontology*, **4**(2), 165–183.
- Wheeler, A. J., Beyer, A., Freiwald, A., de Haas, H., Huvenne, V. A. I., Kozachenko, M., and Olu-Le Roy, K. (subm.) Morphology and Environment of Deep-water Coral Mounds on the NW European Margin. In: *Modern Carbonate Mound System: A Window to Earth History* (Ed. by J.-P. Henriot and W.-C. Dullo). Springer Verlag, Berlin.
- White, M. (2001) Hydrography and Physical Dynamics at the NE Atlantic Margin that influence the Deep Water Cold Coral Reef Ecosystem, 31pp. Department of Oceanography, NUI, Galway.
- White, M. (subm.) The hydrography of the Porcupine Bank and Sea Bight and associated carbonate mounds. In: *Modern Carbonate Mound System: A Window to Earth History* (Ed. by J.-P. Henriot and W.-C. Dullo). Springer Verlag, Berlin.
- White, M., and Bowyer, P. (1997) The shelf-edge current north-west of Ireland. *Annales Geophysicae*, **15**, 1076–1083.
- White, M., Mohn, C., and Orren, M. J. (1998) Nutrient distribution across the Porcupine Bank. *ICES Journal of Marine Science*, **55**(6), 1082–1094.
- White, M., de Stigter, H., de Haas, H., and van Weering, T. (subm.) Hydrography of the carbonate mound of the Rockall Trough. *Progress in Oceanography*.
- Wilson, J. B. (1979) "Patch" development of the deep-water coral *Lophelia pertusa* (L.) on Rockall Bank. *Journal of Marine Biological Association, U.K.*, **59**, 149–164.
- Wollenburg, J. E., and Mackensen, A. (1998) Living benthic foraminiferas from the central Arctic Ocean: faunal composition, standing stock and diversity. *Marine Micropaleontology*, **34**, 153–185.
- Wunsch, C. (1975) Internal tides in the ocean. *Reviews of Geophysics and Space Physics*, **13**, 167–182.
- Zaragosi, S., Auffret, G. A., Faugeres, J.-C., Garlan, T., Pujol, C., and Cortijo, E. (2000) Physiography and recent sediment distribution of the Celtic Deep-Sea Fan, Bay of Biscay. *Marine Geology*, **169**, 207–237.
- Zenk, W. (1971) Zur Schichtung des Mittelmeerwassers westlich von Gibraltar. *'Meteor' Forschungs-Ergebnisse*, **A9**, 1–30.
- Zenk, W. (1975) On the origin of the intermediate double-maxima in T/S profiles from the North Atlantic. *'Meteor' Forschungs-Ergebnisse*, **A 16**, 35–43.
- Zenk, W., and Armi, L. (1990) The complex spreading pattern of mediterranean water off the portuguese continental slope. *Deep-Sea Research*, **37**, 1805–1823.
- Zenk, W., Schultz-Tokos, K., and Boebel, O. (1992) New observations of meddy movement south of the Tejo plateau. *Geophysical Research Letters*, **19**, 2389–2392.

APPENDIX



APPENDIX 1

Faunal reference list of benthic foraminiferal species considered in this thesis (in alphabetical order)

Agglutinated tube fragments, this group covers fragments of tubes of agglutinated species of different size and shape, which only can be related to the genera as *Astorhiza* sp., *Rhabdammina* sp. and *Saccorhiza* sp.

Amphicoryna scalaris (BATSCH) = *Nautilus (Othoceras) scalaris* BATSCH, 1791. Oki (1989, pl.6, figs. 3a-b).

Bolivina robusta BRADY – *B. robusta* BRADY, 1881. Oki (1989, pl. 10, fig. 1).

Bolivina subspinescens CUSHMAN = *B. subspinescens* CUSHMAN, 1922. Ellis and Messina (1940-1978, <http://www.micropress.org/micropress/eandm/index.php3>).

Bulimina marginata d'ORBIGNY = *B. marginata* d'ORBIGNY, 1826. Feyling-Hanssen et al. (1971, pl. 6, fig. 17-20), Oki (1989, pl. 11, fig. 3), Collins (1989, pl. 1, fig. 4).

Cassidulina laevigata d'ORBIGNY = *C. laevigata* d'ORBIGNY, 1826. Feyling-Hanssen et al. (1971, pl. 7, figs. 20-21, pl. 18, fig. 12), Mackensen and Hald (1988, pl. 1, figs. 1-7), Schiebel (1992, pl. 2, fig. 11), Heß (1998, pl. 13, fig. 8).

Cassidulina obtusa WILLIAMSON = *C. obtusa* WILLIAMSON, 1858. Hald and Steinsund (1992, pl. 2, fig.3), Gooday and Hughes (2002, pl. 2, fig. d).

Cassidulina reniforme NØRVANG = *C. reniforme* NØRVANG, 1945. Thomas et al. (1990, pl. 4, figs. 13, 14, pl. 10, fig. 10).

Cassidulina teretis TAPPAN = *C. teretis* TAPPAN, 1951. Mackensen and Hald (1988, pl. 1, figs. 8-15), Gooday and Hughes (2002, pl. 2, fig. e).

Cibicides lobatulus (WALKER & JACOB) = *Nautilus lobatulus* WALKER & JACOB, 1798. Feyling-Hanssen et al. (1971, pl. 9, figs. 9-14), Thies (1991, pl. 17, fig. 4, pl. 18, figs. 1-20), Struck (1992, pl. 5, fig. 1), Schönfeld (2002b, pl.1, figs. 2-3).

Cibicides refulgens MONTFORT = *C. refulgens* MONTFORT, 1808. Schönfeld (2002b, pl.1, figs. 11-12), Weston (1985, pl. 2, fig. 8).

Cibicidoides kullenbergi (PARKER) = *Cibicides kullenbergi* PARKER, 1953. Caralp (1985, pl. 6, figs. 8-11), Clark et al. (1994, pl. 1, figs. 1-3).

Cibicidoides wuellerstorfi (SCHWAGER) = *Anomalina wuellerstorfi* SCHWAGER, 1866. Holbourn and Henderson (2002, pl. 5, figs. 6-8, as *Planulina wuellerstorfi*, as they follow generic assignation of van Morkhoven et al. (1986)).

Cornuspira involvens (REUSS) = *Operculina involvens* REUSS 1850. Murray (2003, pl. 4, fig. 5).

Dentalina frobisherensis LOEBLICH and TAPPAN = *D. frobisherensis* LOEBLICH and TAPPAN, 1953. Feyling-Hanssen et al. (1971, pl. 3, fig. 2), Schröder-Adams et al. (1990, pl. 4, fig. 10).

Discanomalina coronata (PARKER and JONES) = *Anomalina coronata* PARKER and JONES, 1857. Schönfeld (2002b, pl.1, fig. 14).

Elphidium excavatum (TERQUEM) = *Polystomella excavata* TERQUEM, 1875. Thomas et al. (1990, pl. 4, figs. 5-7, pl. 7, figs. 1-3, pl. 9, figs. 19-22), Thies (1991, pl. 19, fig. 5), Alve and Murray (2001, pl. 1, fig. 3), Jennings and Helgadottir (1994, pl. 2, fig. 14), Lloyd (2000, pl. 2, fig. g).

Elphidium incertum (WILLIAMSON) = *Polystomella umbilicatula* var. *incerta* WILLIAMSON, 1858. Feyling-Hanssen et al. (1971, pl. 21, figs. 8-9).

Epistominella exigua (BRADY) = *Pulvinulina exigua* BRADY, 1884. Gupta (1994, pl. 4, figs. 18-19), Mackensen et al. (1990, pl. VII, figs. 1-2).

- Fissurina laevigata* REUSS = *F. laevigata* REUSS, 1850. Oki (1989, pl. 8, figs. 2a-b), Quilty et al. (1990, pl. 1, fig. 3).
- Fissurina marginata* (MONTAGU) = *Vermiculum marginatum* MONTAGU, 1803. Murray (2003, pl. 5, figs. 3-4), Gabel (1971, pl. 15, figs. 36-37).
- Gaudryina nitida* HAQUE = *G. nitida* HAQUE, 1956. Oki (1989, pl. 4, fig. 4).
- Gavelinopsis translucens* PHLEGER & PARKER = *G. translucens* PHLEGER & PARKER, 1951. Gooday and Hughes (2002, pl. 1, fig. A), Heß (1998, pl. 15, figs. 1-2), Timm (1992, pl. 7, fig. 12), Schiebel (1992, pl. 4, fig. 5).
- Globocassidulina subglobosa* (BRADY) = *Cassidulina subglobosa* BRADY, 1881. Struck (1992, pl. 3, fig. 2), Timm (1992, pl. 6, fig. 20), Heß (1998, pl. 13, fig. 14), Ohkushi et al. (2000, pl. 2, fig. 8).
- Globulina* sp.1 = *Globulina* 633 of Lutze collection, Institute of Micropaleontology, University of Kiel.
- Gyroidina neosoldanii* BROTZEN = *G. neosoldanii* BROTZEN, 1936. Ellis and Messina (1940-1978, <http://www.micropress.org/micropress/eandm/index.php3>).
- Hoeglundina elegans* d'ORBIGNY = *Rotalia (Turbinulina) elegans* d'ORBIGNY, 1826. Oki (1989, pl. 22, figs. 7a-c), Gupta (1994, pl. 2, figs. 7-8).
- Hyalinea balthica* (SCHRÖTER) = *Nautilus balthicus* SCHRÖTER, 1783. Oki (1989, pl. 17, fig. 6).
- Hyrrokin sarcophaga* CEDHAGEN = *H. sarcophaga* CEDHAGEN, 1994. Freiwald and Schönfeld (1996, p. 202, fig. 2a; p. 205, fig. 5a)
- Islandiella norcrossi* (CUSHMAN) = *Cassidulina norcrossi* CUSHMAN, 1933. Feyling-Hanssen et al. (1971, pl. 8, figs. 1-2), Jennings and Helgadottir (1994, pl. 2, fig. 5).
- Melonis barleeana* (WILLIAMSON) = *Nonionina barleeana* WILLIAMSON, 1858. Struck (1992, pl. 4, fig. 6), Timm (1992, pl. 6, fig. 6), Heß (1998, pl. 13, fig. 5).
- Nonion depressulus* (WALKER & JACOB) = *Nautilus depressulus* WALKER & JACOB, 1858. Thomas et al. (1990, pl. 10, fig. 11).
- Nonion pauperatum* (WALKER & WRIGHT) = *Nonionina pauperatum* WALKER & WRIGHT, 1885. Murray (2003, pl. 9, fig. 1).
- Nonionella auricula* HERON-ALLEN and EARLAND = *N. auricula* HERON-ALLEN and EARLAND, 1930. Feyling-Hanssen et al. (1971, pl. 10, fig. 7-9).
- Nonionellina labradorica* (DAWSON) = *Nonionina labradorica* DAWSON, 1860. Jennings and Helgadottir (1994, pl. 2, fig. 8), Thomas et al. (1990, pl. 10, fig. 14).
- Oolina hexagona* (WILLIAMSON) = *Entosolenia squamosa* (MONTAGU) var. *hexagona* WILLIAMSON, 1858. Oki (1989, pl. 7, fig. 10), Feyling-Hanssen et al. (1971, pl. 17, fig. 6).
- Oolina striata* d'ORBIGNY = *O. striata* d'ORBIGNY, 1839. Ellis and Messina (1940-1978, <http://www.micropress.org/micropress/eandm/index.php3>).
- Oolina williamsoni* (ALCOCK) = *Entosolenia williamsoni* ALCOCK, 1865. Gabel (1971, pl. 11, fig. 6), Feyling-Hanssen et al. (1971, pl. 18, fig. 1-2).
- Patellina corrugata* WILLIAMSON = *P. corrugata* WILLIAMSON, 1858. Schröder-Adams et al. (1990, pl. 6, fig. 3).
- Planopulvinulina dispansa* (BRADY) = *Pulvinulina dispansa* BRADY, 1884. Ellis and Messina (1940-1978, <http://www.micropress.org/micropress/eandm/index.php3>).
- Planulina ariminensis* d'ORBIGNY = *P. ariminensis* d'ORBIGNY, 1826. Feyling-Hanssen et al. (1971, pl. 9, fig. 4-6), Heß (1998, pl. 16, fig. 8).
- Praeglobobulimina pupoides* (d'ORBIGNY) = *Bulimina pupoides* d'ORBIGNY 1846. Gabel (1971, pl. 14, fig. 18).
- Psammosphaera fusca* SCHULZE = *P. fusca* SCHULZE, 1875. Schröder-Adams et al. (1990, pl. 3, fig. 3).

- Pullenia bulloides* (d'ORBIGNY) = *Nonionina bulloides* d'ORBIGNY, 1826. Feyling-Hanssen et al. (1971, pl. 10, figs. 13-14).
- Pullenia quinqueloba* (REUSS) = *Nonionina quinqueloba* REUSS, 1851. Oki (1989, pl. 20, figs. 7a-c).
- Pyrgo rotalaria* LOEBLICH & TAPPAN = *P. rotalaria* LOEBLICH & TAPPAN, 1953. Thies (1991, pl. 14, fig. 4; pl. 15, figs. 1-21), Struck (1992, pl. 3, fig. 1).
- Quinqueloculina seminulum* (LINNÉ) = *Serpula seminulum* LINNÉ, 1758. Feyling-Hanssen et al. (1971, pl. 1, figs. 18-20), Jennings and Helgadottir (1994, pl. 1, fig. 14).
- Quinqueloculina vulgaris* d'ORBIGNY = *Q. vulgaris* d'ORBIGNY, 1826. Oki (1989, pl. 5, fig. 6).
- Rosalina vilardeboana* d'ORBIGNY = *R. vilardeboana* d'ORBIGNY, 1839. Gabel (1971, pl. 16, fig. 1-3).
- Sigmoilopsis schlumbergeri* (SILVESTRI) = *Sigmoilina schlumbergeri* SILVESTRI, 1904. Oki (1989, pl. 5, figs. 7a-b), Feyling-Hanssen et al. (1971, pl. 2, figs. 17, 18).
- Sigmoilopsis woodi* ATKINSON = *S. woodi* ATKINSON, 1968. Ellis and Messina (1940-1978, <http://www.micropress.org/micropress/eandm/index.php3>).
- Spiroloculina depressa* d'ORBIGNY = *S. depressa* d'ORBIGNY, 1826. Oki (1989, pl. 4, figs. 11a-b)
- Trifarina angulosa* (WILLIAMSON) = *Uvigerina angulosa* WILLIAMSON, 1858. Oki (1989, pl. 12, fig. 10), Schiebel (1992, pl. 3, fig. 1), Timm (1992, pl. 6, fig. 5).
- Trifarina bradyi* CUSHMAN = *T. bradyi* CUSHMAN, 1923. Weston (1985, pl. 1, fig. 5), Heß (1998, pl. 10, fig. 14).
- Triloculina oblonga* MONTAGU = *T. oblonga* MONTAGU, 1803. Cann et al. (2000, pl. 4, fig. p-s), .
- Triloculina rotunda* d'ORBIGNY = *T. rotunda* d'ORBIGNY, 1893. Gabel (1971, pl. 7, figs. 7-9), Ellis and Messina (1940-1978, <http://www.micropress.org/micropress/eandm/index.php3>).
- Uvigerina mediterranea* HOFKER = *U. mediterranea* HOFKER, 1932. Thies (1991, pl. 17, fig. 3), Schiebel (1992, pl. 3, fig. 7).
- Uvigerina peregrina* CUSHMAN = *U. peregrina* CUSHMAN, 1923. Feyling-Hanssen et al. (1971, pl. 7, figs. 9-11), Timm (1992, pl. 6, fig. 2), Heß (1998, pl. 11, figs. 2-3), Ohkushi et al. (2000, pl. 2, fig. 4).

PLATE 1

1. *Bolivina robusta* BRADY, 1881.
Sample: GeoB 6730-1, 18 cm, fraction 125-250 μm .
2. *Bulimina marginata* d'ORBIGNY, 1826.
Sample: GeoB 6725-1, 368 cm, fraction 250-500 μm .
3. *Bolivina subspinescens* CUSHMAN, 1922.
Sample: GeoB 6725-1, 338 cm, fraction 250-500 μm .
4. *Cassidulina laevigata* d'ORBIGNY, 1826.
Sample: GeoB 6725-1, 253 cm, fraction 125-250 μm .
5. *Cibicides lobatulus* (WALKER & JACOB, 1798).
Sample: GeoB 6725-1, 58 cm, fraction 500-1000 μm .
6. *Cibicides lobatulus* (WALKER & JACOB, 1798).
Sample: GeoB 6725-1, 58 cm, fraction 500-1000 μm .
7. *Cibicidoides kullenbergi* (PARKER, 1953).
Sample: GeoB 6725-1, 338 cm, fraction 250-500 μm .
8. *Cibicidoides wuellerstorfi* (SCHWAGER, 1866).
Sample: GeoB 6725-1, 368 cm, fraction 250-500 μm .
9. *Discanomalin coronata* (PARKER & JONES, 1857).
Sample: GeoB 6730-1, 3 cm, fraction 500-1000 μm .
10. *Discanomalin coronata* (PARKER & JONES, 1857).
Sample: GeoB 6730-1, 3 cm, fraction 500-1000 μm .
11. *Elphidium excavatum* (TERQUEM, 1875).
Sample: GeoB 6725-1, 338 cm, fraction 250-500 μm .
12. *Elphidium incertum* (WILLIAMSON, 1858).
Sample: GeoB 6725-1, 338 cm, fraction 250-500 μm .
13. *Epistominella exigua* (BRADY, 1884).
Sample: GeoB 6725-1, 313 cm, fraction 125-250 μm .

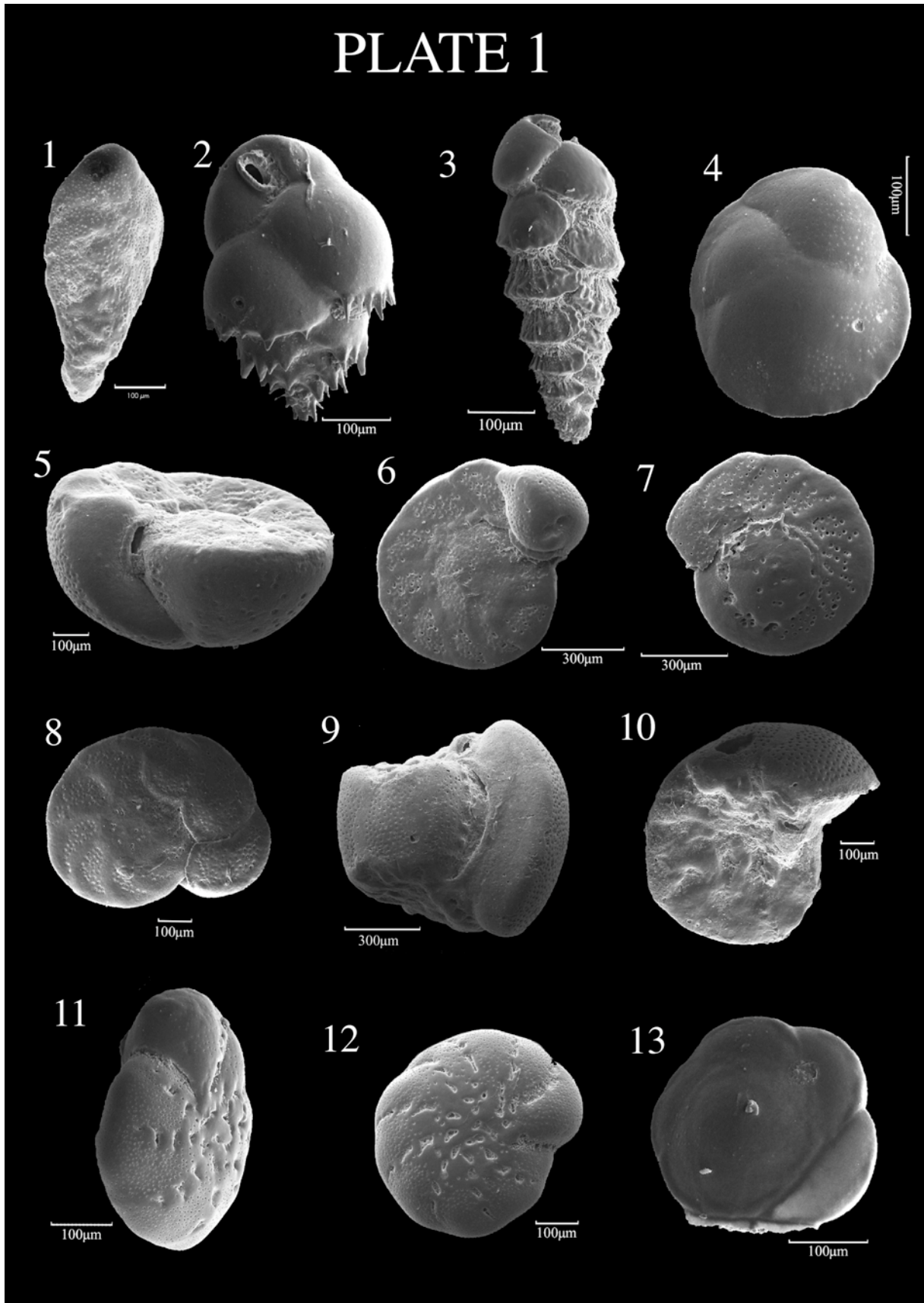
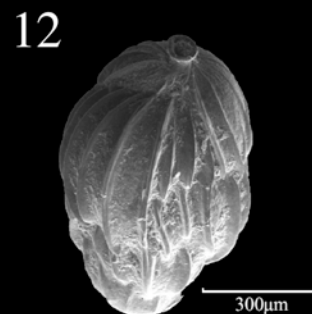
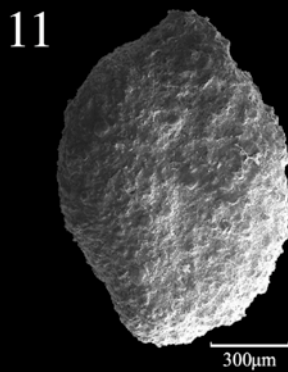
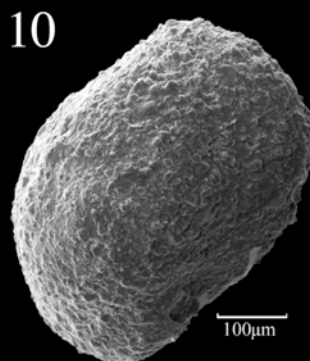
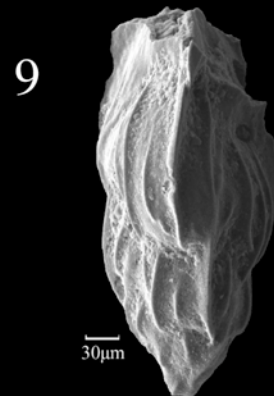
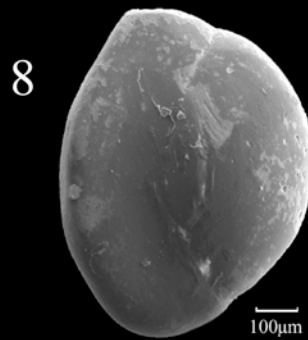
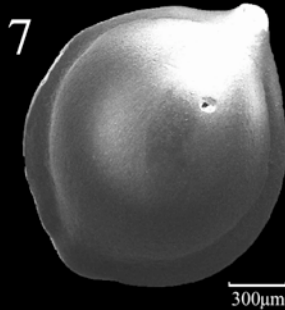
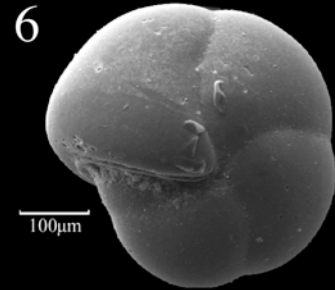
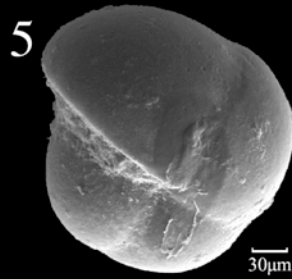
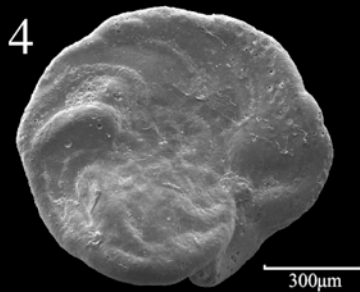
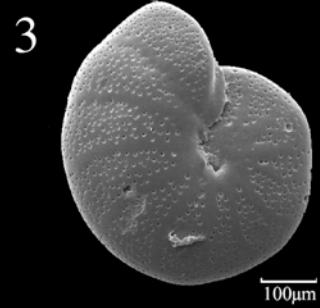
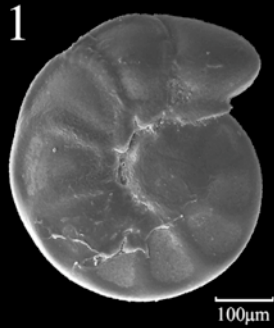


PLATE 2

1. *Hyalinea balthica* (SCHRÖTER, 1783).
Sample: GeoB 6725-1, 13 cm, fraction 250-500 μm .
2. *Hyrrokin sarcophaga* CEDHAGEN, 1994.
Sample: GeoB 6730-1, 3 cm, fraction >1000 μm .
3. *Melonis barleeanum* (WILLIAMSON, 1858).
Sample: GeoB 6725-1, 338 cm, fraction 250-500 μm .
4. *Planulina ariminensis* d'ORBIGNY, 1826.
Sample: GeoB 6730-1, 3 cm, fraction 500-1000 μm .
5. *Pullenia bulloides* (d'ORBIGNY, 1826).
Sample: GeoB 6730-1, 148 cm, fraction 125-250 μm .
6. *Pullenia quinqueloba* (REUSS, 1851).
Sample: GeoB 6730-1, 3 cm, fraction 250-500 μm .
7. *Pyrgo rotalaria* LOEBLICH & TAPPAN, 1953.
Sample: GeoB 6730-1, 3 cm, fraction >1000 μm .
8. *Quinqueloculina seminulum* (LINNÉ, 1758).
Sample: GeoB 6730-1, 3 cm, fraction 500-1000 μm .
9. *Trifarina angulosa* (WILLIAMSON, 1858).
Sample: GeoB 6725-1, 23 cm, fraction 250-500 μm .
10. *Sigmoilopsis woodi* ATKINSON, 1968.
Sample: GeoB 6730-1, 3 cm, fraction 500-1000 μm .
11. *Sigmoilopsis woodi* ATKINSON, 1968.
Sample: GeoB 6730-1, 3 cm, fraction 500-1000 μm .
12. *Uvigerina mediterranea* HOFKER, 1932.
Sample: GeoB 6725-1, 23 cm, fraction 250-500 μm .

PLATE 2



APPENDIX 2.1

Relative abundances (%)
of
benthic foraminiferal species (> 2 %)

Off-mound core GeoB 6725-1

APPENDIX 2.2

Relative abundances (%)
of
benthic foraminiferal species (> 2 %)

On-mound core GeoB 6730-1

APPENDIX 3.1

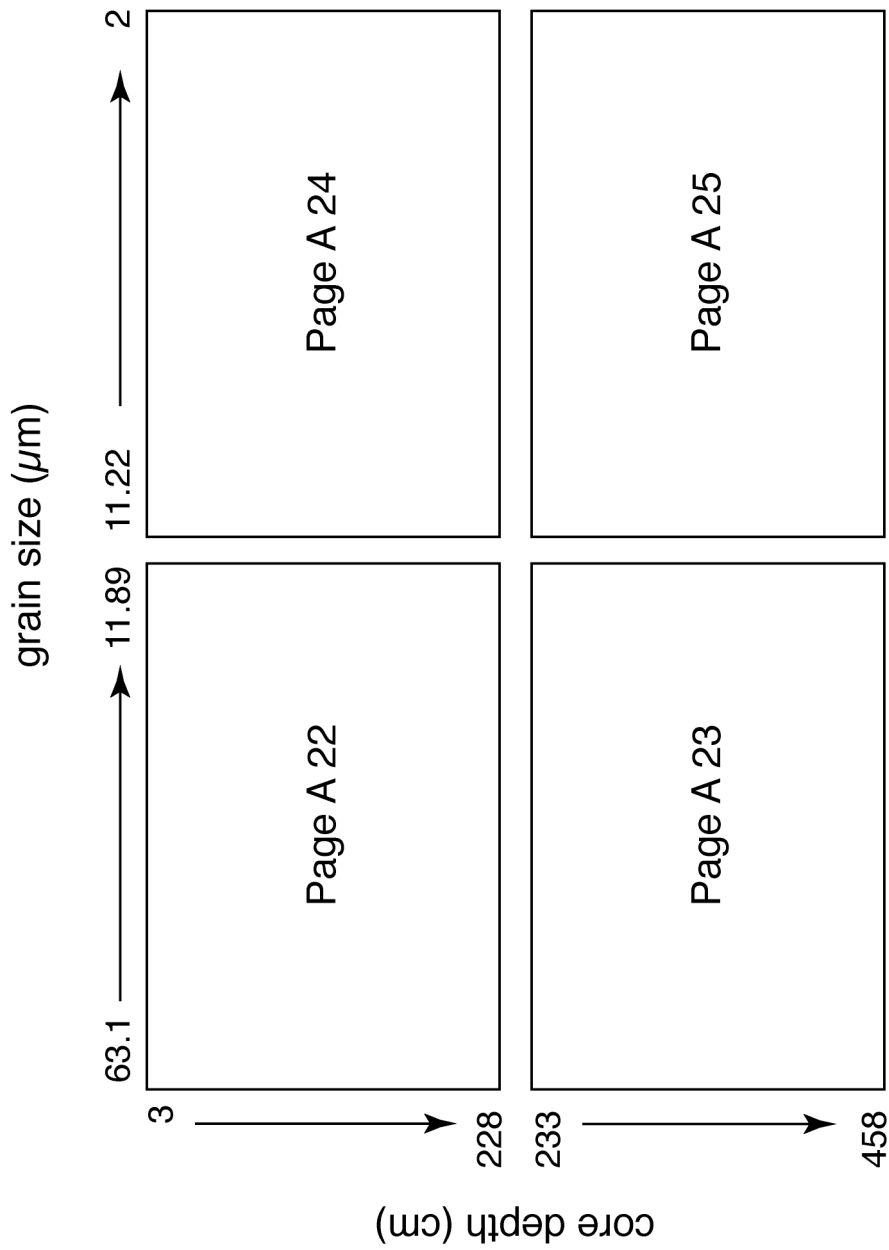
Grain size data:
Sand ($> 63 \mu\text{m}$), silt ($2-63 \mu\text{m}$) and clay ($< 2 \mu\text{m}$) content

depth (cm)	GeoB 6718-2			GeoB 6725-1			GeoB 6727-2		
	$> 63 \mu\text{m}$ (g)	$2-63 \mu\text{m}$ (g)	$< 2 \mu\text{m}$ (g)	$> 63 \mu\text{m}$ (g)	$2-63 \mu\text{m}$ (g)	$< 2 \mu\text{m}$ (g)	$> 63 \mu\text{m}$ (g)	$2-63 \mu\text{m}$ (g)	$< 2 \mu\text{m}$ (g)
3	9.09	7.08	2.01	6.78	4.68	2.09	5.49	3.94	1.55
8	9.51	6.97	2.54	7.88	5.47	2.41	6.47	4.66	1.81
13	9.60	6.80	2.80	7.31	4.98	2.33	6.72	4.60	2.12
18	9.37	6.58	2.79	8.32	4.94	3.38	7.75	4.10	3.65
23	10.08	7.14	2.93	9.48	4.86	4.62	9.02	4.70	4.32
28	10.75	7.82	2.93	9.63	4.95	4.68	9.69	4.40	5.29
33	10.28	7.52	2.77	9.66	4.63	5.03	9.21	4.47	4.74
38	11.18	8.52	2.66	9.67	4.47	5.20	9.85	4.69	5.16
43	10.28	7.88	2.39	7.53	3.88	3.64	9.89	4.99	4.89
48	10.00	7.52	2.48	7.80	3.67	4.13	9.34	4.67	4.67
53	10.03	7.64	2.39	9.15	4.04	5.10	8.99	4.91	4.08
58	9.77	7.37	2.39	9.36	3.97	5.39	9.21	4.96	4.26
63	9.20	6.86	2.35	9.27	4.19	5.08	9.75	5.49	4.26
68	8.65	6.41	2.24	7.82	4.05	3.77	9.70	5.30	4.41
73	8.70	6.62	2.08	7.79	4.46	3.33	9.90	5.73	4.17
78	8.00	5.42	2.58	9.84	5.20	4.65	9.75	5.31	4.45
83	9.43	5.95	3.48	9.32	5.10	4.22	10.58	5.63	4.95
88	8.53	5.47	3.06	9.75	4.92	4.82	9.44	5.08	4.36
93	8.64	5.45	3.19	9.34	4.34	5.00	9.42	5.10	4.32
98	8.88	4.65	4.23	9.00	3.81	5.20	9.48	5.01	4.48
103	8.56	4.99	3.57	8.76	3.65	5.11	9.42	4.94	4.48
108	8.30	4.43	3.87	8.83	4.04	4.79	9.14	4.98	4.16
113	8.06	3.81	4.26	9.04	4.25	4.79	9.44	5.13	4.30
118	8.35	3.75	4.60	9.13	4.15	4.99	8.72	4.57	4.15
123	8.40	3.70	4.71	9.78	4.85	4.93	9.39	4.88	4.52
128	8.48	3.78	4.70	9.34	4.76	4.58	9.45	4.79	4.66
133	7.91	3.46	4.45	9.63	4.69	4.94	9.62	5.13	4.49
138	7.77	3.22	4.56	9.72	4.98	4.75	9.66	5.25	4.40
143	7.91	3.66	4.25	9.60	5.05	4.55	9.84	5.29	4.56
148	9.14	4.67	4.47	9.46	5.00	4.46	10.31	5.64	4.67
153	7.74	3.50	4.24	9.27	5.00	4.27	9.92	5.61	4.30
158	8.60	3.68	4.92	9.58	5.15	4.43	10.18	5.94	4.25
163	9.04	4.44	4.60	10.04	5.66	4.38	10.85	6.42	4.43
168	8.41	4.15	4.25	10.25	6.00	4.26	11.26	7.05	4.21
173	8.93	4.28	4.66	10.09	5.40	4.69	10.40	6.19	4.21
178	8.47	4.06	4.41	10.50	5.70	4.80	10.50	6.29	4.21
183	8.57	4.64	3.92	9.65	5.26	4.39	9.64	5.85	3.79
188	9.00	4.47	4.53	10.34	5.31	5.02	9.77	5.76	4.02
193	8.45	4.40	4.05	9.77	5.26	4.52	9.56	5.91	3.65
198	8.07	4.05	4.02	10.10	5.60	4.49	9.46	5.73	3.73
203	8.11	3.72	4.39	10.70	6.12	4.58	9.43	5.94	3.49
208	8.32	4.06	4.26	10.21	5.98	4.23	9.77	6.03	3.74
213	8.08	3.75	4.33	10.08	5.29	4.79	10.14	6.25	3.89
218	8.30	3.54	4.77	10.00	5.49	4.51	9.54	5.48	4.06
223	8.20	3.43	4.77	9.85	5.19	4.66	10.04	5.54	4.50
228	8.66	3.69	4.97	9.75	5.17	4.58	9.89	5.83	4.07
233	8.45	3.85	4.61	9.50	5.43	4.07	8.56	5.70	2.86
238	8.29	3.73	4.56	9.46	5.37	4.09	8.91	5.46	3.45
243	9.12	4.71	4.41	9.60	5.21	4.39	7.40	4.73	2.67
248	9.53	5.30	4.23	9.60	5.51	4.09	6.43	4.13	2.29
253	9.20	4.60	4.60	9.45	5.39	4.05	6.51	4.33	2.18

depth (cm)	GeoB 6718-2			GeoB 6725-1			GeoB 6727-2		
	> 63 μm (g)	2-63 μm (g)	< 2 μm (g)	> 63 μm (g)	2-63 μm (g)	< 2 μm (g)	> 63 μm (g)	2-63 μm (g)	< 2 μm (g)
258	9.22	4.40	4.82	10.09	6.07	4.02	6.68	4.28	2.40
263	9.28	4.11	5.17	9.93	5.55	4.38	6.31	3.86	2.45
268	9.30	4.11	5.19	9.75	5.20	4.55	9.73	4.52	5.20
273	9.41	4.20	5.21	10.18	5.75	4.43	10.45	5.04	5.41
278	9.70	4.27	5.43	10.85	6.24	4.61	10.62	4.84	5.78
283	9.96	4.43	5.53	10.57	6.24	4.33	10.19	5.28	4.91
288	9.78	4.35	5.43	11.05	6.58	4.48	10.03	4.75	5.29
293	9.84	4.51	5.33	11.14	6.92	4.22	10.09	4.53	5.56
298	9.72	4.65	5.07	11.76	7.33	4.44	10.60	4.86	5.75
303	10.16	4.82	5.35	11.74	7.31	4.43	10.37	4.86	5.51
308	10.68	5.16	5.52	12.44	7.77	4.66	10.70	5.13	5.57
313	9.93	5.05	4.87	12.24	7.50	4.74	10.34	5.06	5.29
318	10.05	5.22	4.82	11.65	6.83	4.82	9.76	4.13	5.63
323	9.45	4.99	4.46	11.29	6.74	4.55	9.58	4.05	5.53
328	9.73	5.20	4.52	10.54	6.65	3.89	9.89	5.08	4.80
333	9.83	5.33	4.50	10.58	6.34	4.24	9.04	4.35	4.69
338	8.41	4.60	3.81	10.31	6.34	3.97	9.87	5.04	4.83
343	9.31	5.02	4.29	10.21	6.13	4.07	9.07	4.34	4.73
348	11.78	6.46	5.33	9.79	6.12	3.67	9.37	4.61	4.76
353	10.92	5.68	5.24	11.61	6.87	4.74	9.08	3.92	5.16
358	10.30	5.19	5.11	10.58	6.59	3.99	9.23	3.87	5.36
363	10.12	5.45	4.66	10.68	6.41	4.27	9.62	4.50	5.12
368	9.93	5.22	4.70	10.62	6.12	4.50	9.64	4.43	5.20
373	9.69	5.19	4.49	10.56	6.04	4.52	9.33	4.31	5.02
378	9.64	5.09	4.55	10.85	6.03	4.82	9.50	4.06	5.44
383	10.14	5.75	4.39	10.58	5.74	4.85	9.66	4.22	5.44
388	10.16	6.04	4.11	10.84	5.58	5.26	9.70	4.65	5.06
393	10.27	5.95	4.32	10.90	6.21	4.69	9.61	4.45	5.16
398	10.85	6.74	4.11	11.04	6.34	4.70	9.96	4.79	5.17
403	10.97	6.82	4.15	11.50	6.56	4.95	8.99	3.45	5.54
408	12.08	7.56	4.52	10.47	6.61	3.85	9.51	4.03	5.48
413	11.95	7.21	4.75	9.22	6.30	2.92	9.24	3.78	5.46
418	11.23	6.56	4.67	7.85	5.27	2.57	8.94	3.75	5.19
423	10.99	6.39	4.59	8.80	5.47	3.34	9.78	4.76	5.01
428	10.32	6.71	3.61	10.71	6.39	4.31	10.52	5.28	5.24
433	11.16	7.04	4.12	9.16	5.58	3.58	10.91	5.76	5.15
438	10.97	7.05	3.91	8.92	5.85	3.07	11.14	6.10	5.03
443	11.66	7.21	4.44	6.03	4.48	1.55	11.19	6.20	4.99
448				6.01	4.48	1.53	7.47	3.69	3.78
453				7.37	4.89	2.48	9.76	4.63	5.12
458				7.66	4.79	2.86	10.46	5.51	4.95
463				8.23	5.68	2.55			

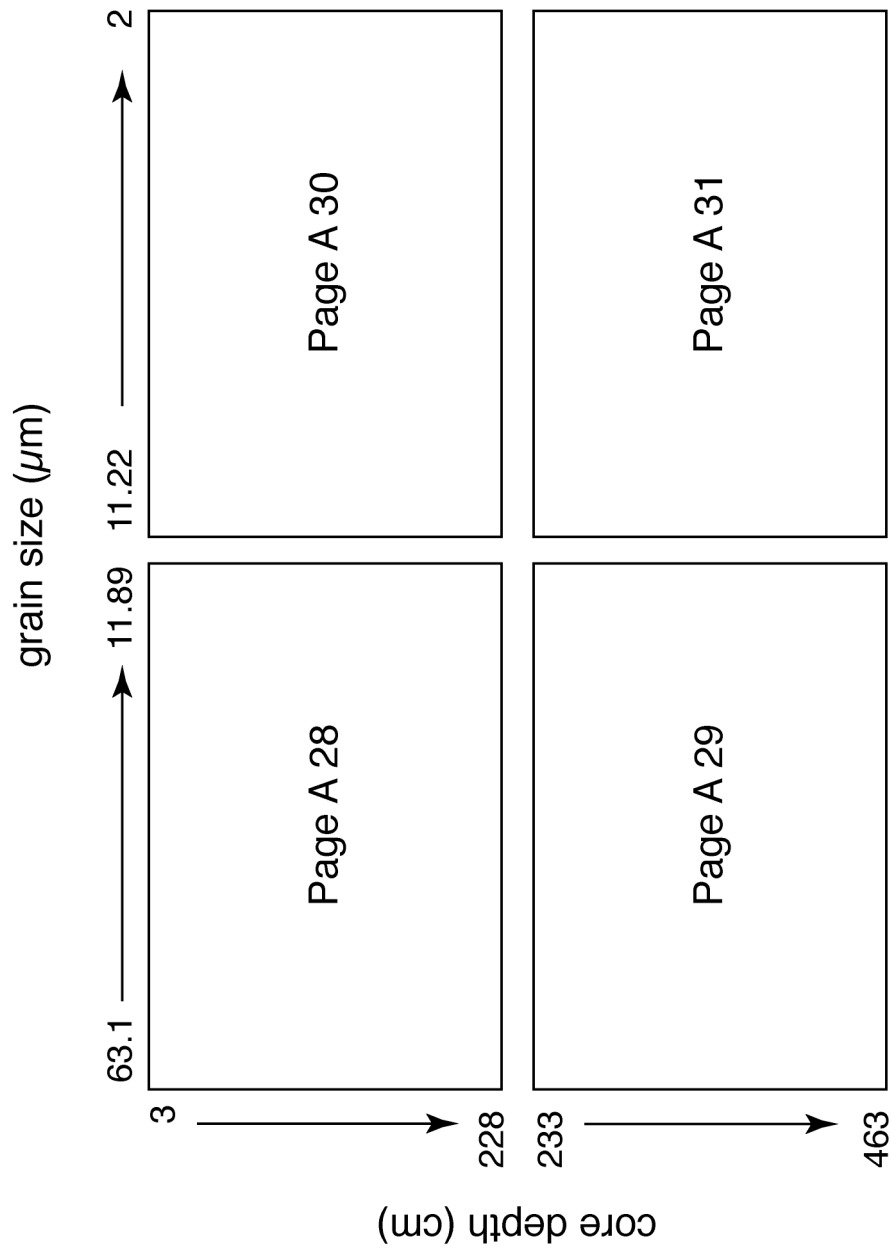
APPENDIX 3.2

Silt fraction of core GeoB 6718-2
(in mass-%, orig. Sedigraph output data)



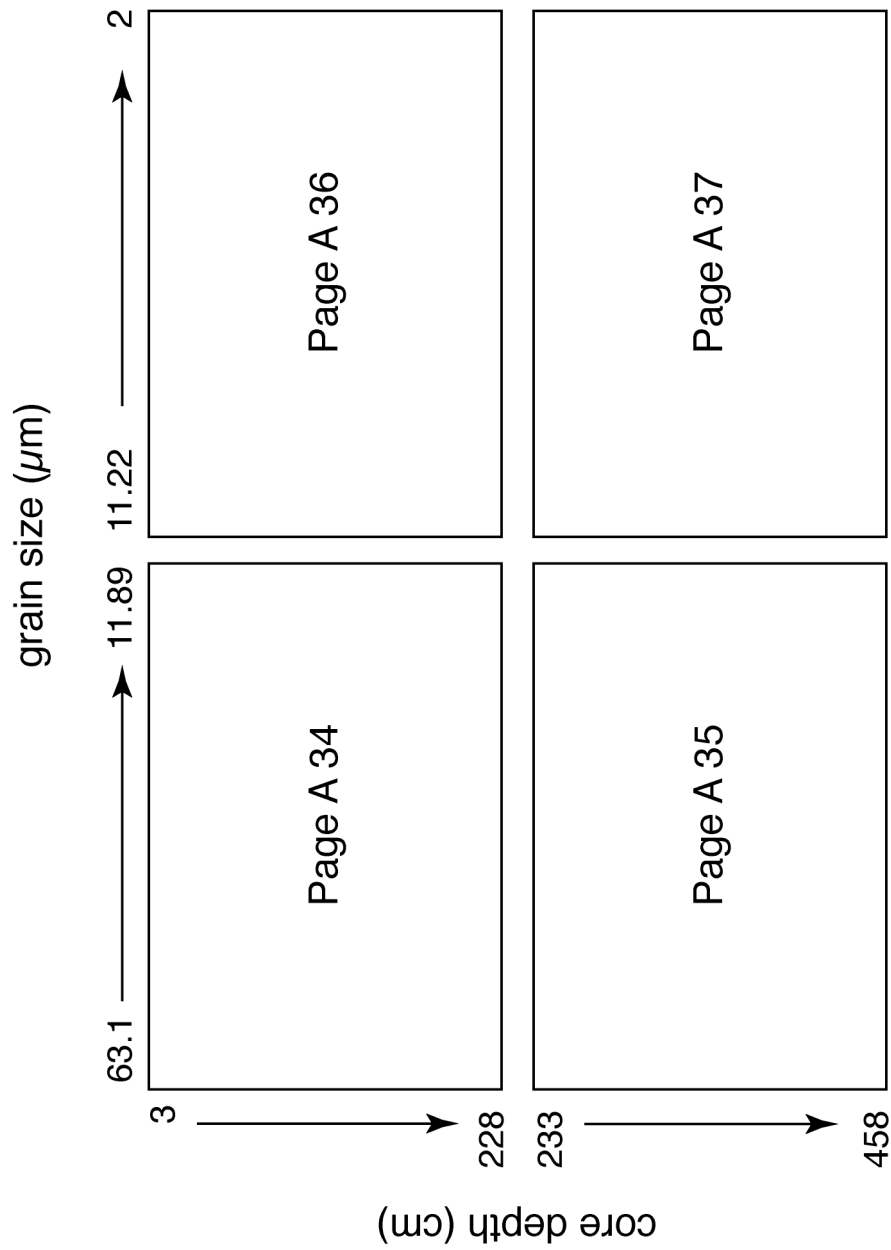
APPENDIX 3.2

Silt fraction of core GeoB 6725-1
(in mass-%, orig. Sedigraph output data)



APPENDIX 3.2

Silt fraction of core GeoB 6727-2
(in mass-%, orig. Sedigraph output data)



APPENDIX 4

Carbonate (Carb) and total organic carbon (Corg) content

depth (cm)	GeoB 6718-2		GeoB 6719-1		GeoB 6725-1		GeoB 6727-2		GeoB 6730-1	
	Corg (%)	Carb (%)	Corg (%)	Carb (%)	Corg (%)	Carb (%)	Corg (%)	Carb (%)	Corg (%)	Carb (%)
3	0.62	38.11	—	36.50	0.43	33.29	0.35	38.38	0.47	63.95
8	0.54	38.67	—	39.81	0.39	34.56	0.32	42.41	0.39	53.36
13	0.52	40.35	—	39.27	0.28	35.51	0.36	40.57	0.31	58.31
18	0.49	39.72	—	33.14	0.36	29.65	0.26	22.24	0.40	55.62
23	0.54	39.38	—	37.31	0.36	32.09	0.31	24.42	0.37	54.61
28	0.49	35.97	—	28.56	0.33	22.45	0.28	20.68	0.38	48.41
33	0.47	36.10	—	23.05	0.35	23.34	0.31	19.94	0.37	50.00
38	0.47	35.12	—	25.79	0.27	30.41	0.26	18.61	0.37	50.81
43	0.43	35.27	—	24.05	0.36	20.58	0.24	18.99	0.40	50.41
48	0.41	34.45	—	22.81	0.33	19.35	0.31	19.40	0.32	45.26
53	0.42	36.13	—	21.45	0.34	21.61	0.23	21.79	0.36	45.61
58	0.40	37.36	—	21.59	0.27	25.96	0.25	20.91	0.33	53.14
63	0.33	34.55	—	20.95	0.27	24.14	0.26	21.51	0.29	62.33
68	0.37	33.67	—	21.21	0.31	19.93	0.25	22.86	0.25	66.24
73	0.31	31.59	—	21.06	0.20	25.93	0.31	23.28	0.25	64.80
78	0.29	28.65	—	21.09	0.24	19.78	0.28	19.24	0.37	58.46
83	0.29	22.66	—	22.02	0.34	21.35	0.24	23.31	0.41	56.19
88	0.33	24.45	—	19.03	0.31	22.71	0.24	21.58	0.40	53.92
93	0.45	25.52	—	22.90	0.30	21.13	0.31	19.37	0.45	52.91
98	0.28	35.46	—	19.18	0.37	18.38	0.33	19.63	0.46	53.49
103	0.43	19.94	—	19.69	0.33	15.99	0.31	18.57	0.42	52.89
108	0.45	17.74	—	19.74	0.32	16.53	0.30	20.21	0.40	52.72
113	0.45	17.41	—	20.19	0.34	15.88	0.32	18.95	0.34	55.85
118	0.38	19.48	—	21.36	0.28	16.22	0.34	19.05	0.20	58.93
123	0.36	18.27	—	20.39	0.27	16.55	0.35	17.82	0.14	51.90
128	0.38	17.68	—	22.81	0.30	17.53	0.33	17.82	0.22	47.03
133	0.37	16.63	—	34.22	0.27	17.16	0.30	18.59	0.28	47.80
138	0.40	14.77	—	25.87	0.28	18.66	0.31	18.90	0.31	43.97
143	0.33	18.29	—	22.35	0.27	18.42	0.23	19.10	0.31	44.48
148	0.33	19.18	—	24.81	0.25	18.18	0.24	19.19	0.36	39.14
153	0.34	16.35	—	26.22	0.25	19.16	0.21	17.91	0.39	34.53
158	0.32	17.19	—	21.86	0.28	18.85	0.25	17.93	0.25	43.62
163	0.36	18.98	—	20.13	0.26	20.06	0.24	18.90	0.35	39.89
168	0.32	16.86	—	20.52	0.25	21.05	0.19	18.34	0.27	45.14
173	0.39	17.26	—	19.91	0.31	20.56	0.21	21.60	0.30	31.38
178	0.42	17.12	—	20.35	0.36	19.66	0.23	21.06	0.28	41.05
183	0.45	17.52	—	20.87	0.35	17.35	0.23	22.64	0.38	40.84
188	0.50	16.09	—	20.18	0.32	17.57	0.24	23.54	0.25	41.98
193	0.49	15.86	—	19.54	0.37	16.67	0.22	23.76	0.19	46.36
198	0.52	15.54	—	19.98	0.24	17.45	0.25	23.47	0.22	45.03
203	0.55	15.94	—	20.19	0.25	20.53	0.22	25.81	0.26	41.88
208	0.41	16.15	—	19.64	0.26	19.78	0.23	28.13	0.30	41.34
213	0.33	16.92	—	20.64	0.33	18.86	0.27	26.64	0.22	39.54
218	0.40	16.39	—	22.19	0.32	18.14	0.19	25.13	0.17	30.45
223	0.29	17.18	—	23.14	0.30	21.55	0.18	24.84	0.19	39.09
228	0.29	16.91	—	23.85	0.33	17.90	0.23	30.44	0.10	62.56
233	0.33	17.18	—	24.15	0.31	20.40	0.24	38.91	0.16	57.21
238	0.30	18.96	—	24.88	0.33	18.32	0.21	32.63	0.14	67.04
243	0.28	20.52	—	26.06	0.36	17.87	0.20	33.96	0.13	59.21
248	0.28	21.26	—	26.63	0.35	17.60	0.39	36.94	0.14	62.65

depth (cm)	GeoB 6718-2		GeoB 6719-1		GeoB 6725-1		GeoB 6727-2		GeoB 6730-1	
	Corg (%)	Carb (%)	Corg (%)	Carb (%)	Corg (%)	Carb (%)	Corg (%)	Carb (%)	Corg (%)	Carb (%)
253	0.27	19.77	—	26.12	0.34	17.74	0.15	54.24	0.17	58.41
258	0.30	17.93	—	24.46	0.32	18.55	0.18	48.78	0.13	63.26
263	0.33	15.98	—	26.22	0.26	18.20	0.11	49.93	0.17	60.31
268	0.31	16.96	—	28.46	0.26	17.85	0.15	35.21	0.14	63.74
273	0.33	16.64	—	33.06	0.23	18.22	0.10	17.14	0.10	70.37
278	0.31	16.57	—	34.82	0.25	17.84	0.24	25.16	0.21	66.70
283	0.29	17.04	—	33.20	0.23	18.52	0.16	17.20	0.17	65.65
288	0.28	17.37	—	33.31	0.23	17.85	0.23	17.22	0.15	66.21
293	0.28	17.08	—	31.80	0.20	17.06	0.20	17.40	0.13	63.46
298	0.29	17.32	—	36.73	0.20	18.83	0.23	15.24	0.10	59.91
303	0.25	18.31	—	28.94	0.22	18.98	0.30	15.30	0.08	49.18
308	0.36	17.80	—	26.18	0.26	20.37	0.33	15.54	0.10	41.15
313	0.27	18.65	—	21.31	0.27	20.39	0.34	16.04	0.14	51.11
318	0.27	19.01	—	21.39	0.28	20.67	0.37	16.14	0.16	23.80
323	0.25	18.89	—	21.90	0.27	21.49	0.42	14.94	0.25	31.87
328	0.25	18.95	—	25.81	0.27	20.90	0.48	14.73	0.45	23.59
333	0.28	19.53	—	29.99	0.24	23.06	0.49	14.61	0.14	40.31
338	0.23	19.70	—	36.21	0.22	23.44	0.47	15.02	0.15	33.26
343	0.24	21.57	—	49.39	0.27	23.22	0.56	15.34	0.14	34.38
348	0.27	21.05	—	56.80	0.26	23.85	0.51	15.61	0.13	39.63
353	0.26	22.54	—	56.04	0.27	21.09	0.47	14.64	0.15	39.02
358	0.29	18.37	—	61.64	0.30	25.64	0.46	14.94	0.16	47.83
363	0.32	21.22	—	59.83	0.23	27.64	0.45	16.35		
368	0.27	18.85	—	57.22	0.35	22.33	0.44	15.77		
373	0.26	19.15	—	57.17	0.29	20.12	0.47	14.30		
378	0.25	20.21	—	54.65	0.27	22.30	0.47	16.26		
383	0.23	19.28	—	27.58	0.29	22.49	0.39	15.91		
388	0.22	19.21	—	25.42	0.29	22.04	0.40	13.86		
393	0.22	19.15	—	28.47	0.31	23.55	0.42	15.45		
398	0.20	18.53	—	45.71	0.33	25.83	0.45	14.81		
403	0.19	16.18	—	22.04	0.33	23.16	0.42	14.06		
408	0.24	20.85	—	24.64	0.34	28.75	0.46	16.02		
413	0.25	21.68	—	19.76	0.34	29.71	0.42	14.49		
418	0.24	23.17	—	20	0.21	27.44	0.36	14.23		
423	0.25	23.27	—	19.19	0.31	27.62	0.19	15.95		
428	0.24	23.36	—	19.23	0.29	21.46	0.16	16.20		
433	0.26	25.42	—	19.05	0.28	23.62	0.23	16.81		
438	0.25	25.69	—	18.49	0.24	27.67	0.20	16.71		
443	0.26	25.94	—	18.73	0.24	40.25	0.15	21.70		
448			—	18.54	0.25	48.74	0.16	34.80		
453			—	18.57	0.24	50.78	0.14	23.65		
458			—	18.33	0.19	41.59	0.17	31.24		
463			—	17.98	0.38	23.23				

APPENDIX 5

Stable oxygen isotopes

depth (cm)	GeoB 6718-2 $\delta^{18}\text{O}$ (‰)	GeoB 6719-1 $\delta^{18}\text{O}$ (‰)	GeoB 6725-1 $\delta^{18}\text{O}$ (‰)	GeoB 6727-2 $\delta^{18}\text{O}$ (‰)	GeoB 6730-1 $\delta^{18}\text{O}$ (‰)
3	2.60	3.55	3.58	2.88	1.49
8	—	3.16	3.59	3.86	1.42
13	1.90	3.53	3.60	3.68	1.44
18	3.22	3.65	3.59	3.78	1.45
23	3.25	3.62	3.63	3.84	1.50
28	2.68	3.42	3.60	3.84	1.55
33	1.69*	3.60	3.68	3.78	1.51
38	2.91	3.73	3.71	3.81	1.48
43	2.78	3.73	3.68	3.72	1.48
48	3.29	3.58	3.71	3.69	1.57
53	2.14	—	3.67	3.66	1.53
58	1.85	3.77	3.64	3.73	1.84
63	1.86*	3.66	3.71	—	2.12
68	1.83*	3.67	3.66	3.63	2.21
73	2.00*	3.77	3.59	3.51	2.34
78	2.80*	3.74	3.63	3.60	2.35
83	3.16	3.65	3.78	3.57	2.32
88	3.26	3.70	3.62	3.14	2.27
93	3.23	3.59	3.54	3.78	2.28
98	3.42	3.54	3.52	3.80	2.40
103	3.50	3.56	3.55	3.66	2.22
108	3.37	3.62	3.61	3.75	2.27
113	3.33	3.64	3.51	3.59	2.33
118	3.45	3.39	—	3.68	1.95
123	3.51	3.54	3.62	3.64	3.04
128	3.63	3.47	—	3.72	2.77
133	3.53	3.28	3.59	3.58	3.22
138	3.47	3.47	3.55	3.62	3.32
143	3.61	3.48	—	3.60	3.28
148	3.14	3.53	3.59	3.72	3.19
153	3.62	3.49	3.49	3.84	3.36
158	3.84	3.53	3.54	3.61	3.28
163	3.86	3.45	3.99	3.59	3.05
168	3.87	3.51	3.61	3.66	2.85
173	3.57	3.50	3.61	3.56	2.58
178	4.00	3.47	3.39	3.68	2.43
183	—	3.51	3.23	3.62	2.36
188	3.83	3.26	3.20	3.68	2.51
193	3.88	3.42	3.35	3.79	2.49
198	3.87	3.53	3.42	3.61	2.37
203	4.17	3.35	3.29	3.63	2.27
208	4.10	3.41	3.56	3.61	2.34
213	3.88	3.46	3.60	3.51	2.33
218	3.84	3.55	3.64	3.10	2.35
223	3.89	3.44	3.62	3.44	2.42
228	3.73	3.58	3.71	3.33	2.35
233	3.58	3.48	3.49	3.22	2.25
238	3.71	3.68	3.61	3.24	2.28
243	3.83	3.28	3.68	3.41	2.25
248	3.83	3.40	3.54	3.59	2.02
253	3.83	3.37	3.37	2.82	1.92
258	3.90	3.18	3.57	2.62	1.78

depth (cm)	GeoB 6718-2 δ ¹⁸ O (‰)	GeoB 6719-1 δ ¹⁸ O (‰)	GeoB 6725-1 δ ¹⁸ O (‰)	GeoB 6727-2 δ ¹⁸ O (‰)	GeoB 6730-1 δ ¹⁸ O (‰)
263	3.83	—	3.39	2.53	2.32
268	3.78	3.28	3.48	3.10*	2.08
273	3.69	3.13	3.57	2.90*	2.25
278	3.71	3.15	3.47	3.01*	2.60
283	3.71	3.36	3.55	3.28*	2.45
288	3.69	3.25	3.53	3.34*	2.59
293	3.70	3.34	3.42	3.20°	2.53
298	3.62	3.30	3.60	2.81°	2.59
303	—	3.17	3.51	3.02°	2.89
308	—	3.09	3.44	3.07°	2.98
313	3.64	—	3.43	2.97°	2.89
318	3.52	3.02	3.54	—	2.96
323	3.70	2.97	3.73	—	2.74
328	3.63	3.46	3.66	—	2.66
333	3.58	3.58	3.39	—	3.08
338	3.63	3.47	3.44	—	2.65
343	3.48	3.57	3.40	—	
348	3.34	3.57	3.40	—	
353	3.58	3.60	3.48	—	
358	3.73	—	3.35	—	
363	3.65	2.54	3.17	—	
368	3.71	2.42	3.11	—	
373	3.45	3.11	3.28	—	
378	3.57	2.41	3.28	—	
383	3.68	2.60	3.11	—	
388	3.59	2.45	3.31	—	
393	3.59	2.29	3.25	—	
398	3.62	2.30	3.22	—	
403	3.79	2.85	3.11	—	
408	3.56	1.16	2.79	—	
413	3.57	—	3.09	—	
418	3.66	2.83	2.82	—	
423	3.73	—	3.34	—	
428	3.68	—	3.61	—	
433	3.67	—	3.64	—	
438	3.63	—	3.22	—	
443	3.47	—	2.80	—	
448	—	—	2.37	—	
453	—	—	2.46	—	
458	—	—	2.33	—	
463	—	—	2.96	—	

All values correspond to measurements on tests of *Cibicoides kullenbergi*, except * = *Cibicoides wuellerstorfi*, and ° = *Cibicoides* spp., — = no data.

APPENDIX 6

Computer tomographic images

Off-mound cores

GeoB 6718-2 (section 1-3).....A 44
(section 4-5).....A 45

GeoB 6725-1 (section 1-3).....A 46
(section 4-5).....A 47

GeoB 6727-2 (section 1-3).....A 48
(section 4-5).....A 49

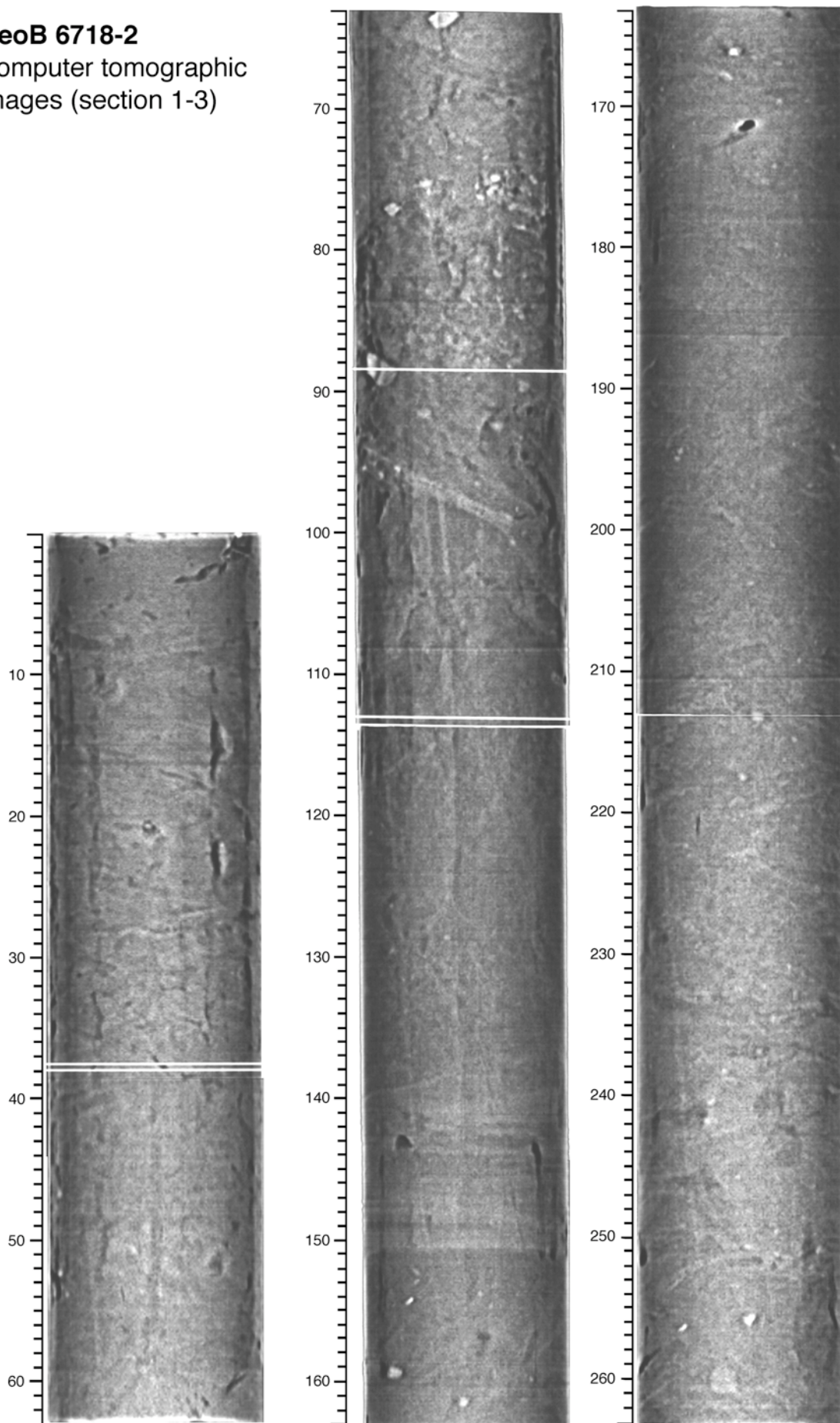
On-mound cores

GeoB 6728-2 (section 1-3).....A 50
(section 4-5).....A 51

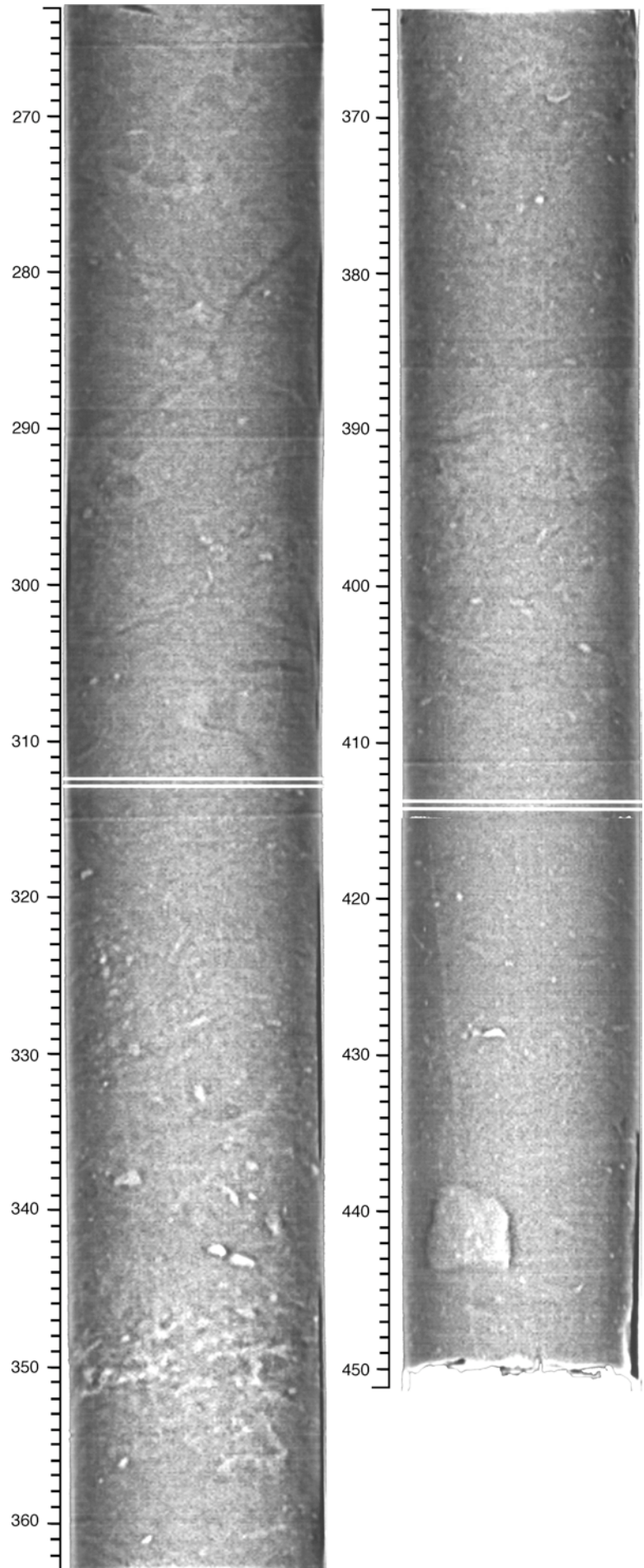
GeoB 6729-1 (section 1-3).....A 52
(section 4-5).....A 53

GeoB 6730-1 (section 1-3).....A 54
(section 4-5).....A 55

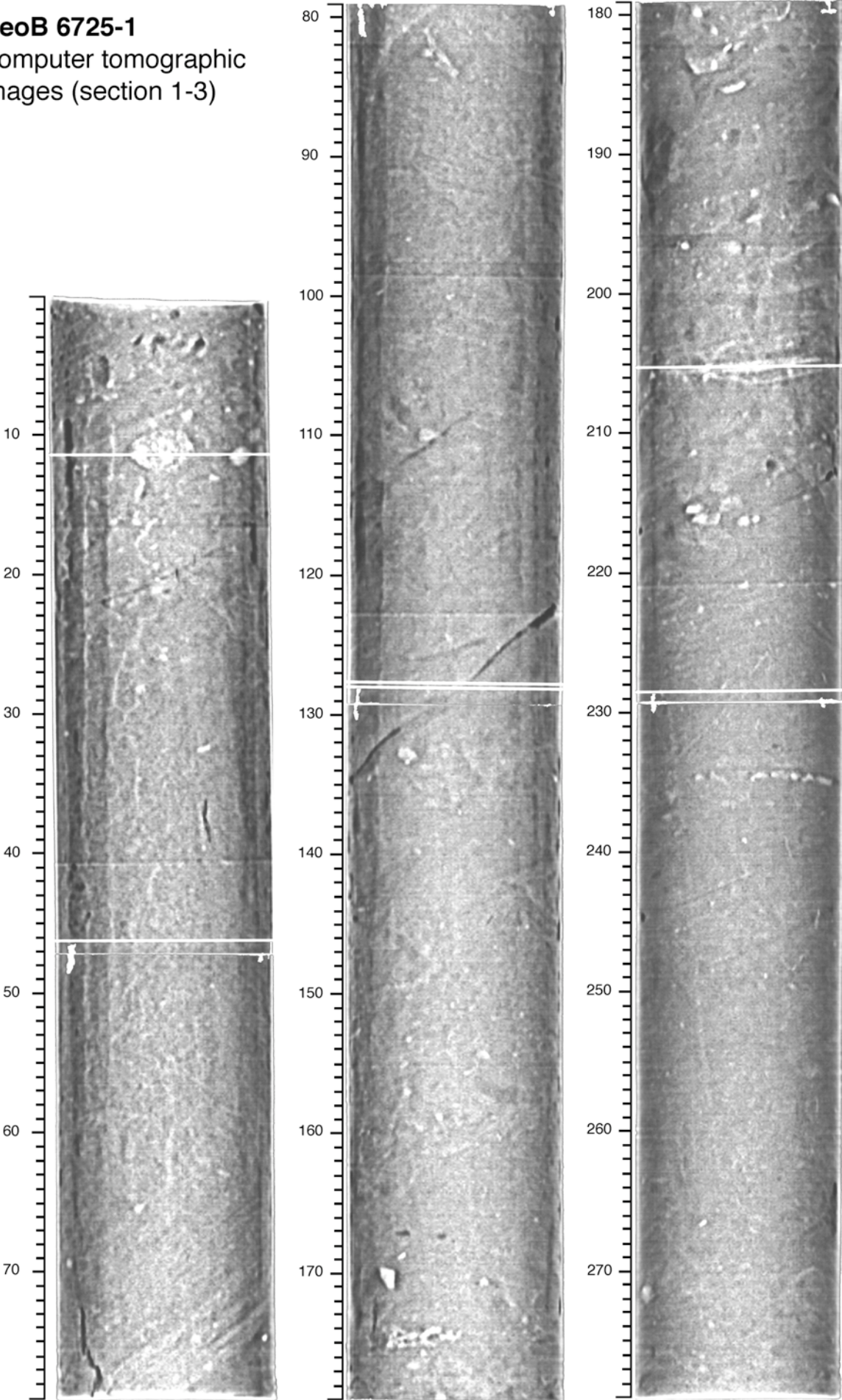
GeoB 6718-2
Computer tomographic
images (section 1-3)



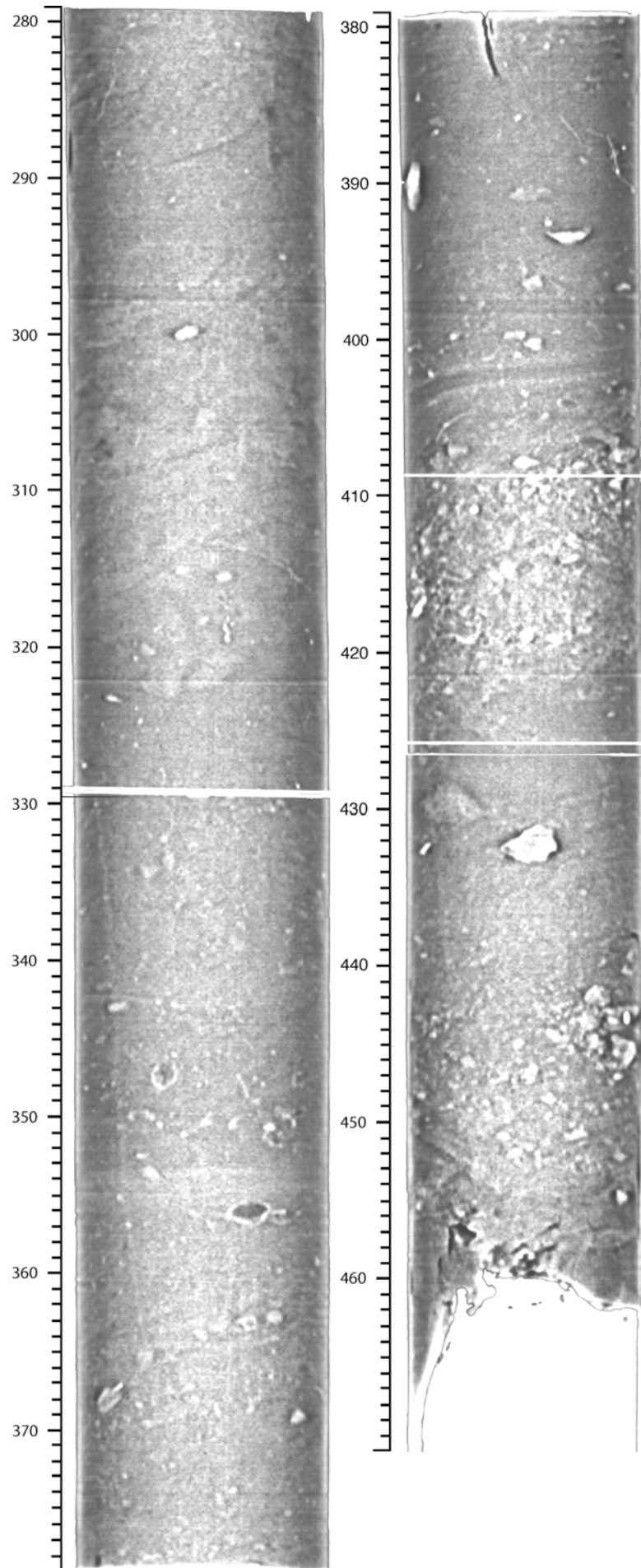
GeoB 6718-2
Computer tomographic
images (section 4-5)



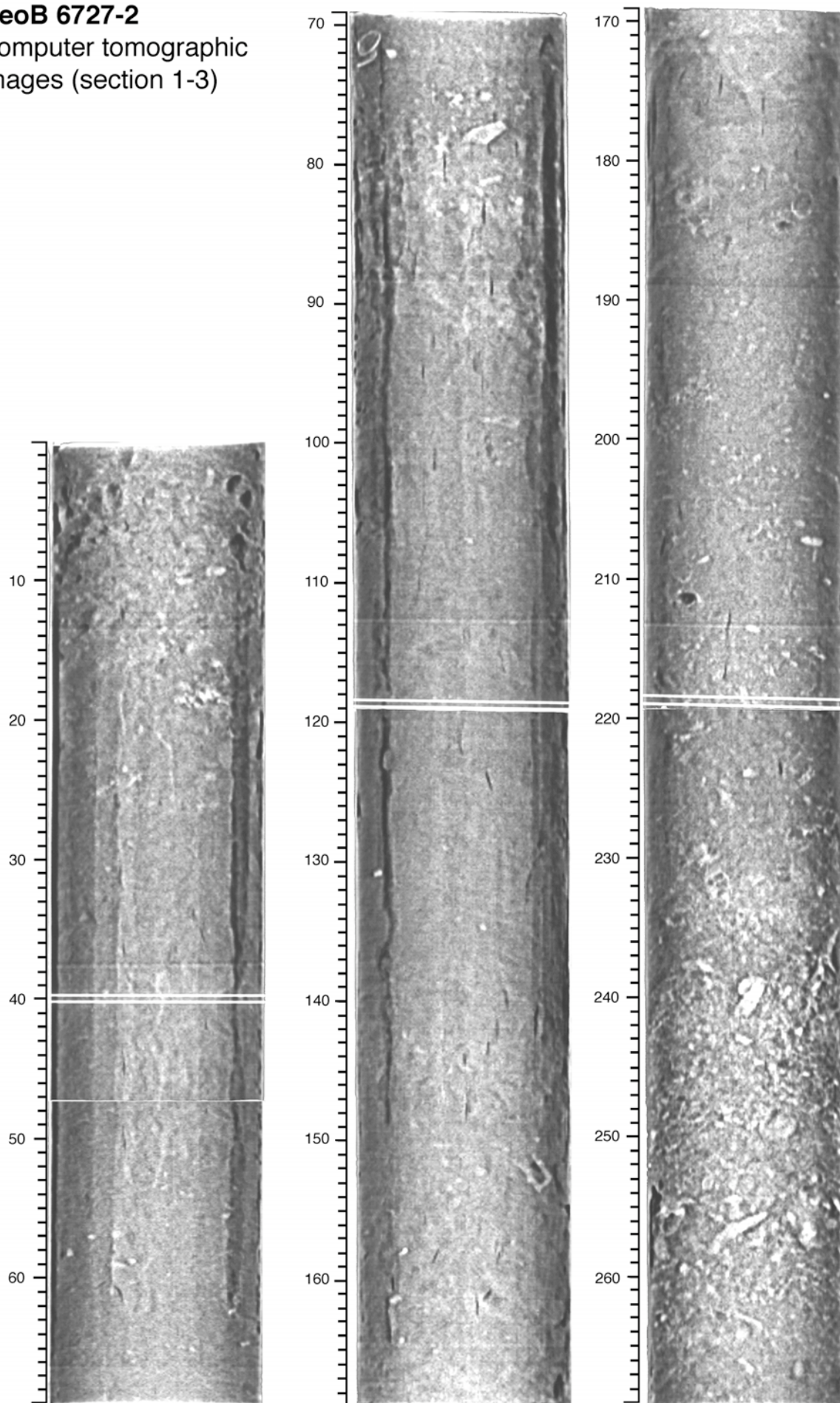
GeoB 6725-1
Computer tomographic
images (section 1-3)



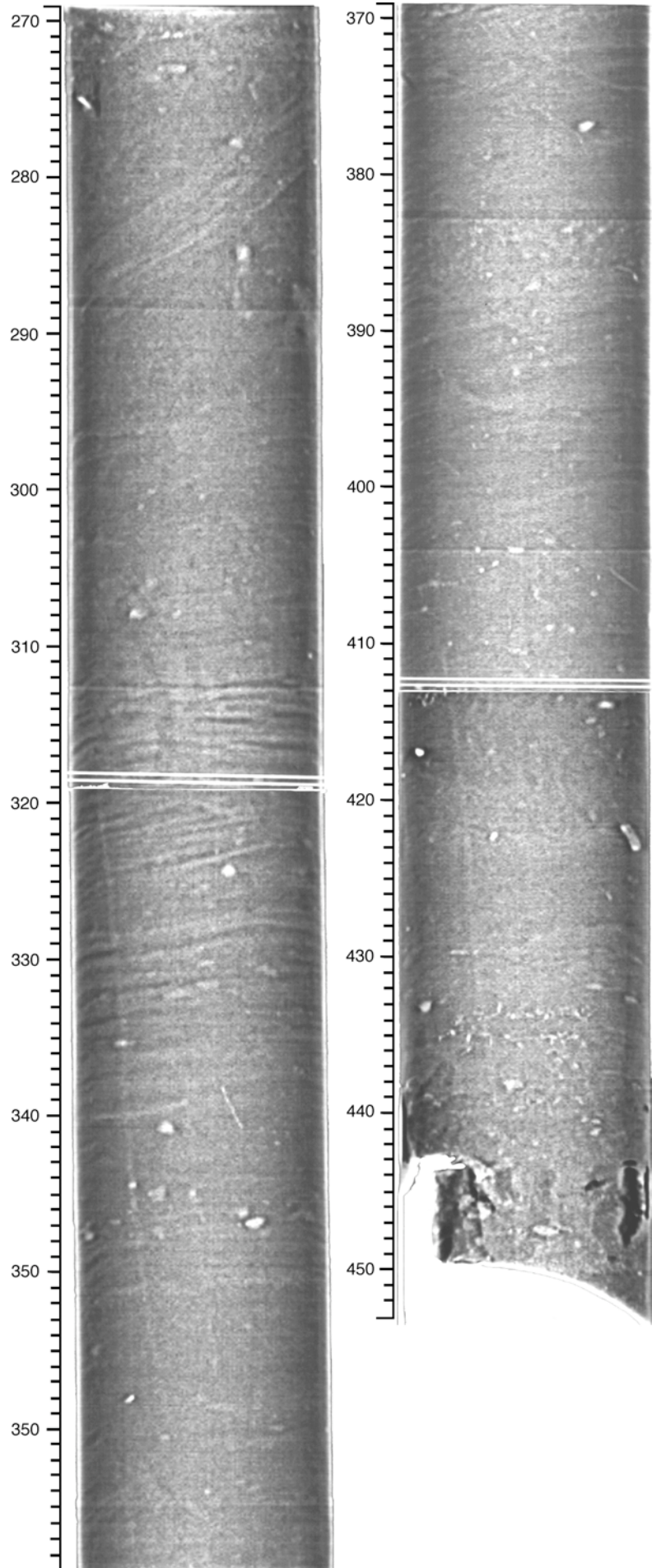
GeoB 6725-1
Computer tomographic
images (section 4-5)



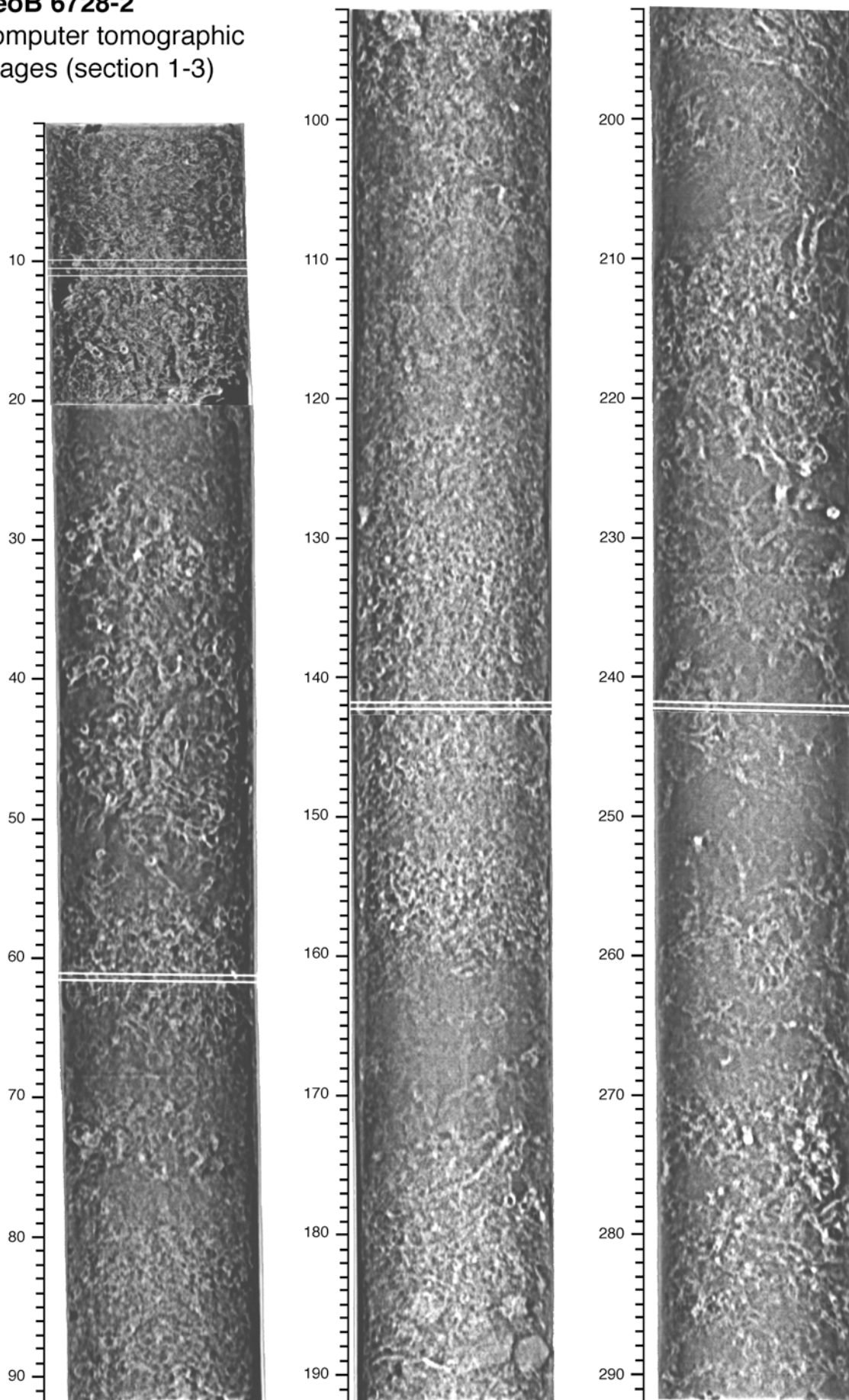
GeoB 6727-2
Computer tomographic
images (section 1-3)



GeoB 6727-2
Computer tomographic
images (section 4-5)

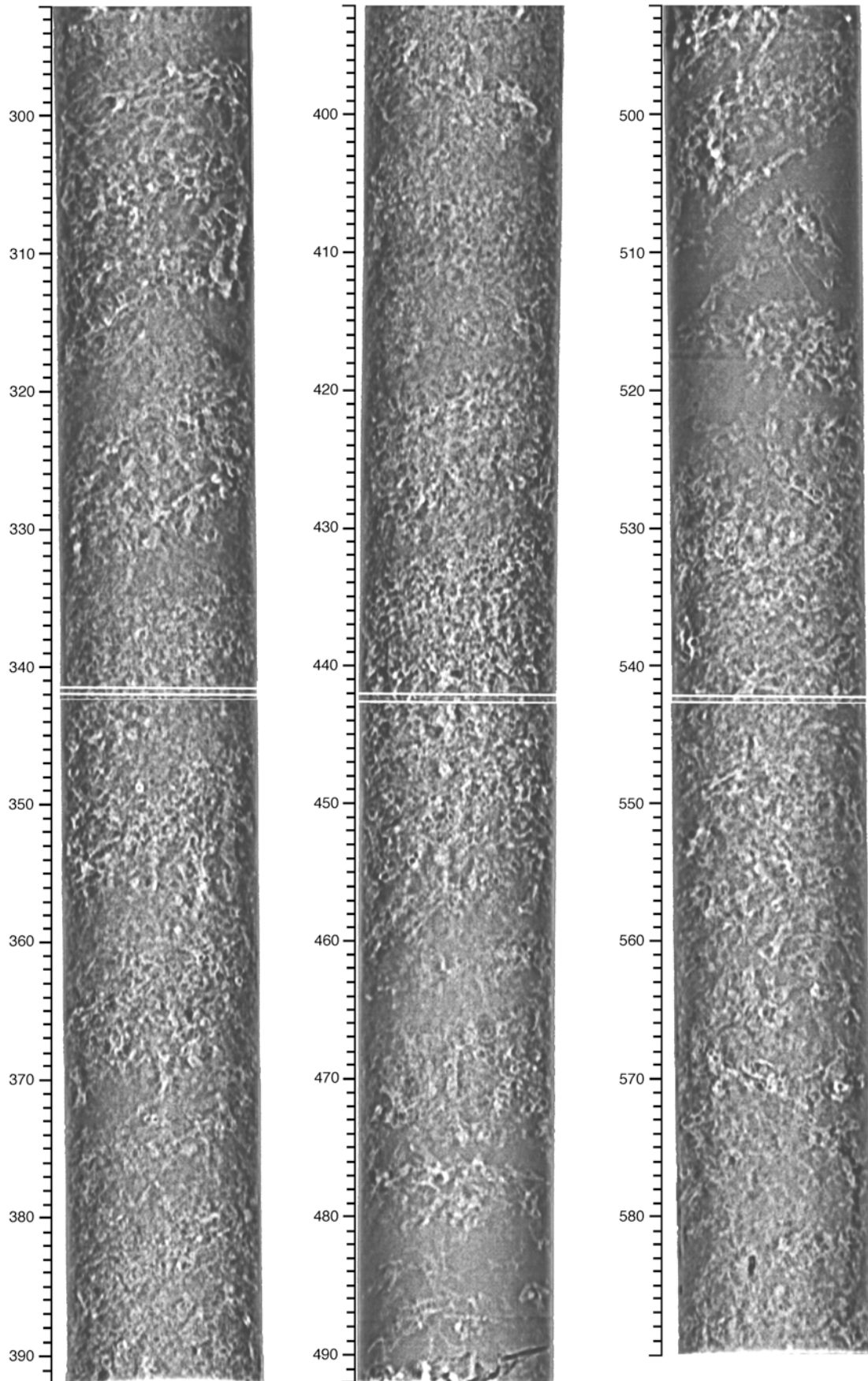


GeoB 6728-2
Computer tomographic
images (section 1-3)

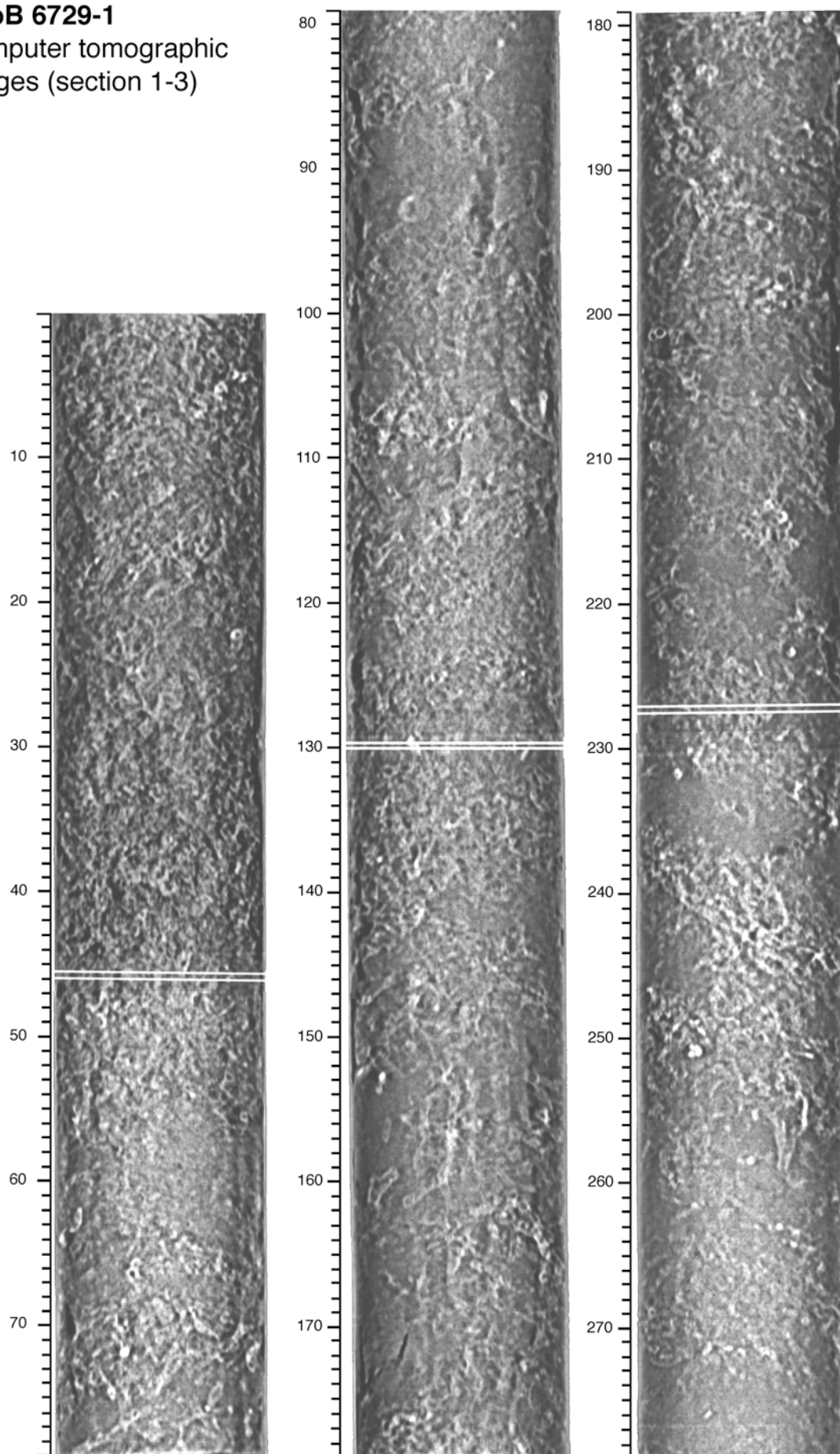


GeoB 6728-2

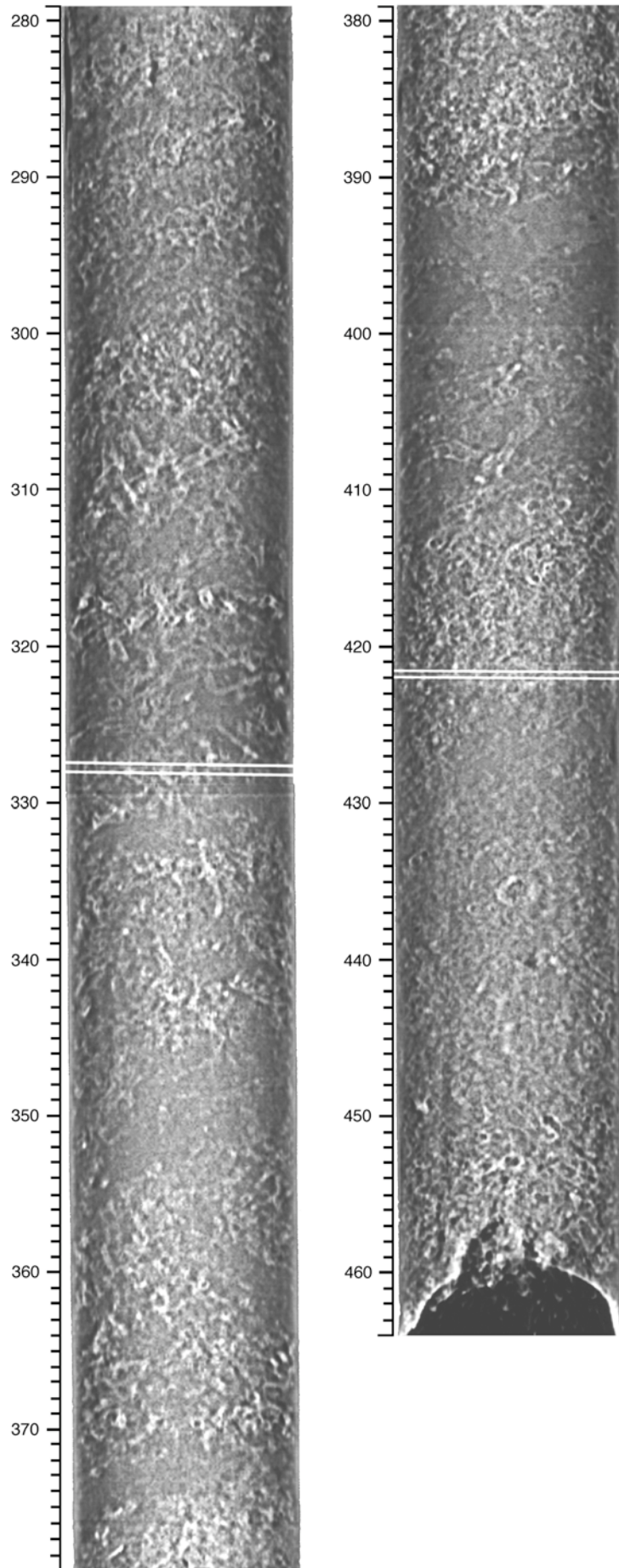
Computer tomographic images (section 4-6)



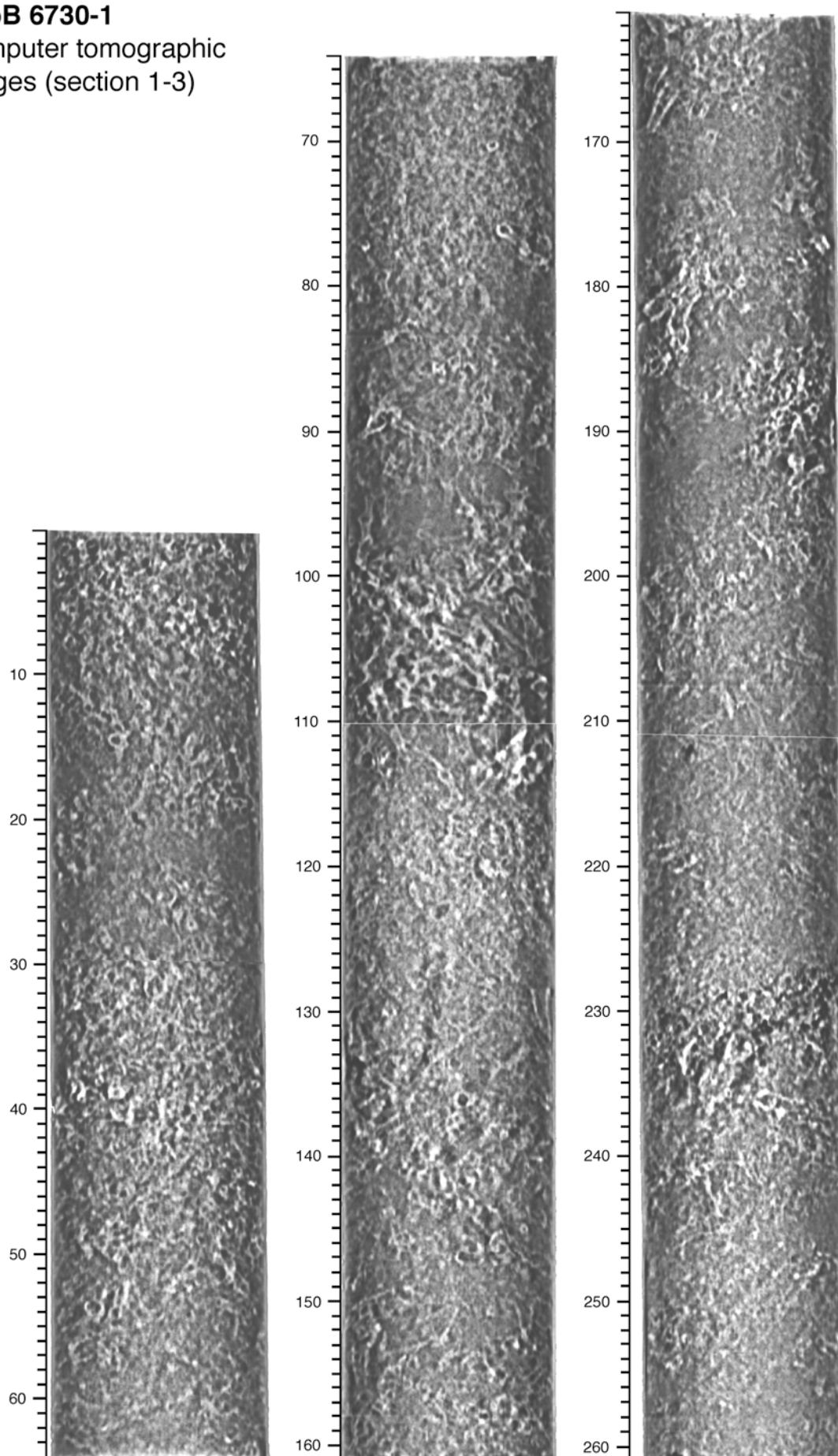
GeoB 6729-1
Computer tomographic
images (section 1-3)



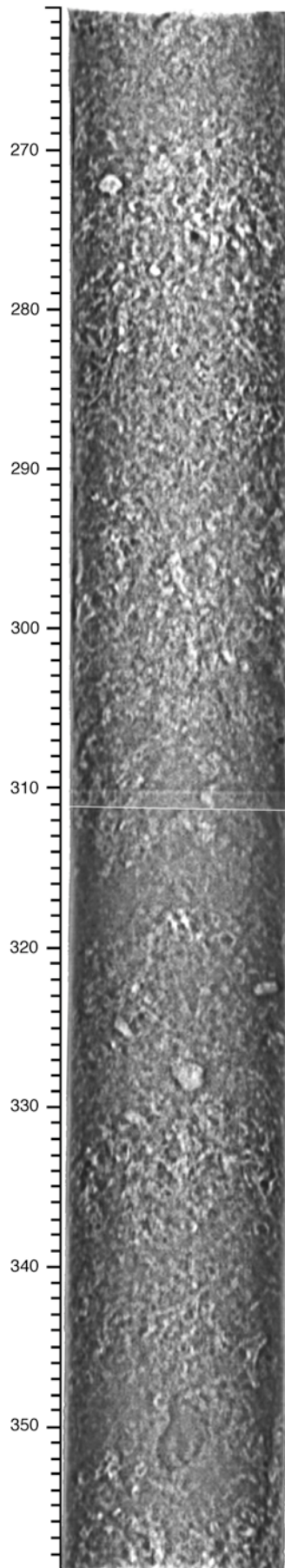
GeoB 6729-1
Computer tomographic
images (section 4-5)



GeoB 6730-1
Computer tomographic
images (section 1-3)



GeoB 6730-1
Computer tomographic
images (section 4)



APPENDIX 7

CARBONATE BUDGET OF A COLD-WATER CORAL CARBONATE MOUND: PROPELLER MOUND, PORCUPINE SEABIGHT

Boris Dorschel¹, Dierk Hebbeln¹, Andres Rüggeberg², Christian Dullo²,

¹ Department of Geology, University of Bremen. Postbox 330440, D-28334 Bremen, Germany

² GEOMAR Research Center for Marine Geosciences, Wischhofstraße 1-3, D-24148 Kiel, Germany,

Abstract

High resolution studies from the Propeller Mound, a cold water coral carbonate mound in the NE Atlantic, show that this mound consists to >50% of carbonate justifying the name “carbonate mound”. Through the last ~300,000 years approximately one third of the carbonate has been contributed by cold water corals, namely by the species *Lophelia pertusa* and *Madrepora oculata*. This coral bound contribution to the carbonate budget of Propeller Mound is probably accompanied by an unknown portion of sediments buffered from suspension by the corals. However, extended hiatuses on Propeller Mound only allow the calculation of a netto carbonate accumulation based on the preserved sediments. Thus, netto carbonate accumulation for the last 175 kyr accounts for only <0.3 g/cm²*kyr, which is even less than for the “normal” sedimentation off the mound. These data imply, that Propeller Mound faces burial by hemipelagic sediments as it happened to numerous buried carbonate mounds found slightly to the north of the investigated area.

corresponding author:
Boris Dorschel
Adr.
Tel.0049-(0)421-2182764
Fax0049-(0)421-218
e-mail: dorschel@uni-bremen.de

1. Introduction

Cold water corals have been found all along the European margin from the Gulf of Cádiz south of Spain (Somoza et al., 2002) to northern Norway (Lindberg et al., *subm.*) and often these are found on sea-floor elevations called carbonate mounds (Freiwald, 2002). On and around these structures complex interactions of geological, biological and hydrological processes develop, while one of the key processes in the formation of the carbonate mounds most likely is the growth of cold water corals, namely of the two common species *Lophelia pertusa* and *Madrepora oculata*. Such carbonate mounds are especially common along the Celtic margin in the Porcupine Seabight and in the Rockall region. There numerous types of carbonate mounds occur as single conical structures or as more complex composite mounds ranging in height above the sea-floor from <1 m to >150 m, with a substantial part of the mounds being below the sea-floor (De Mol et al., 2002; Van Rooij et al., 2003). Thus, these carbonate mounds represent a significant volume within the sedimentary system of the Celtic margin.

As the growth rates of these aphotic cold water corals can be as high as 25 mm/yr (Freiwald et al., 1997), what is comparable to those of reef forming corals in the oligotrophic shallow water reefs of the lower latitudes, the question arises to what extent the cold water corals and the carbonate mounds contribute to the global carbonate budget. Due to the volume of the carbonate mounds along the Celtic margin together with the neritic shallow water carbonates of the Norwegian margin (Mortensen et al., 1995; Freiwald et al., 1997) the common idea that calcium carbonate is mainly accumulated within the

lower latitudes has already been challenged. The wide distribution of the cold water coral carbonate mounds has only recently being discovered and year by year new mound provinces are found (P. Croker, *pers. comm.*). Therefore, up to now the carbonate stored in these mounds has not been considered in any global carbonate budget or any global model of the distribution of the greenhouse gas carbon dioxide.

To provide some background information about the carbonate budget of such carbonate mounds, a case study is presented here focusing on a particular mound: Propeller Mound. It is situated in the Porcupine Seabight, where three distinct mound provinces exist, each consisting of numerous carbonate mounds. The densest coral cover has been observed on mounds in the Belgica Mound province on the eastern side of the Porcupine Seabight. Less well developed coral thickets have been reported from the Hovland Mound province in the northern Porcupine Seabight. Slightly further to the north is the Magellan Mound province, which largely consists of buried mounds only detectable by seismic observations (Henriet et al., 1998; De Mol et al., 2002).

Propeller Mound belongs to the Hovland Mound province, where the carbonate mounds are associated with moats, which indicate strong bottom currents in the area (Hovland et al., 1994; De Mol et al., 2002). It is located in 850 m water depth. Its three lobate structure extends ca. 2 km in latitudinal and 0.7 km in longitudinal direction. With a maximum elevation of 140 m it is one of the bigger composite mounds. Box corer sampling and ROV observations revealed patchy *L. pertusa* dominated thickets covering the upper

slopes of Propeller Mound, which gradually change into a coral rubble facies mixed with hemipelagic sediments towards the lower slopes (Freiwald et al., 2000; Freiwald, 2002).

By comparing sediment records from Propeller Mound itself and from the surrounding “normal” hemipelagic sediments the specific settings in terms of carbonate sedimentation for this carbonate mound will be assessed. Due to the complex

stratigraphic record of Propeller Mound, marked by numerous hiatuses, a quantitative carbonate budget is restricted to a netto budget with respect to the preserved sediments. However, differences in contemporaneous sedimentation between the two settings were only possibly in a qualitative way, showing that due to the corals sedimentation on the carbonate mounds is enhanced by >15-20%.

2. Materials and Methods

This study focuses on six gravity cores from the Propeller Mound and the adjacent areas taken during a sampling campaign by the German RV POSEIDON in the NE Atlantic in September 2000 (Freiwald et al., 2000; Table A1). The coring locations from the neighbourhood of Propeller Mound were

taken along a transect from 1.2 km NE of Propeller Mound (core GeoB 6718-2), 0.9 km N of the mound at the adjacent moat (core GeoB 6725-1) and at the lower slope of the mound between its two northerly lobes (core GeoB 6719-1) (Fig. A1).

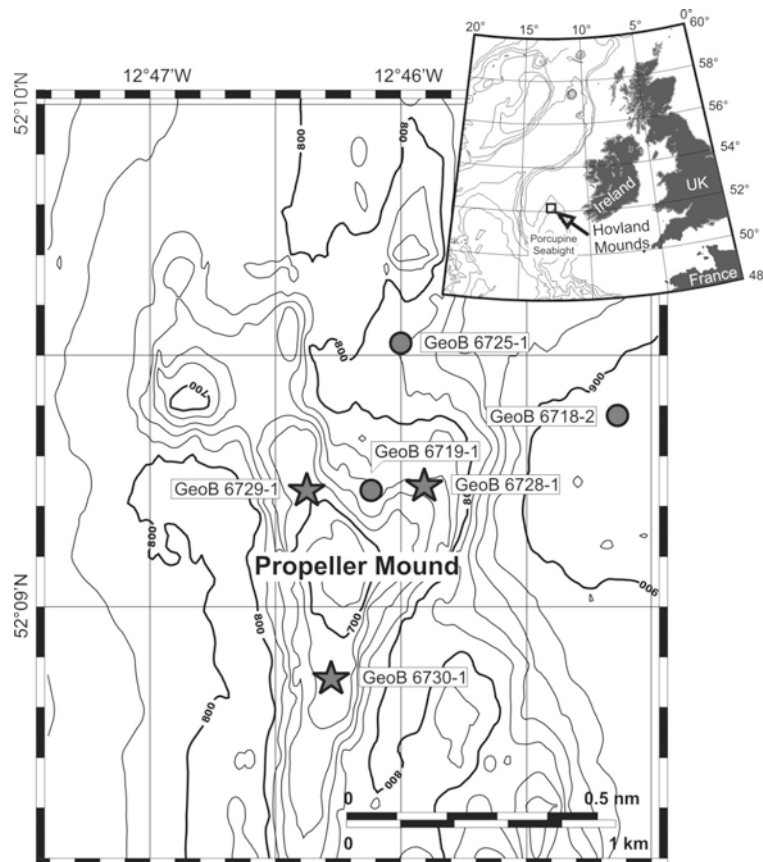


Figure A1. Overview and morphological setting of the coring sites in the Propeller Mound area, Hovland Mound province, Porcupine Seabight. The stars indicate the on-mound cores, while the dots show the off-mound cores.

Table A1. Overview about the coring locations.

Station #	latitude °N	longitude °W	water depth (m)	recovery (cm)
off-mound				
GeoB 6718-2	52°09,379N	12°45,158W	900	450
GeoB 6719-1	52°09,233N	12°46,127W	758	480
GeoB 6725-1	52°09,520N	12°46,010W	820	450
on-mound				
GeoB 6728-1	52°09,240N	12°45,920W	749	590
GeoB 6729-1	52°09,231N	12°46,380W	711	460
GeoB 6730-1	52°08,861N	12°46,282W	704	360

These cores are between 4 and 5 m long and consisted mainly of hemipelagic sediments. In the following these cores are termed the off-mound cores.

The cores GeoB 6728-1, GeoB 6729-1 and GeoB 6730-1 were recovered within a ~0.5 km radius from the three different lobes of Propeller mound (Fig. A1). These on-mound cores are 3.4 to 6 m long and contain coral fragments embedded in a fine grained matrix (Fig. A2). The coral fragments with up to 30 cm in length built a loose uncemented framework in these cores and occurred with changing concentrations at all depths, with some intervals are distinctively enriched in corals. These cores were opened while frozen using a diamond bladed circular saw. Cutting fluid and the uppermost surface were removed immediately after opening. This procedure preserved a maximum of sedimentary structures, kept the corals in place and provided an excellent surface of the split cores for further scanning analyses.

2.1. Carbonate analyses

Discrete samples for carbonate analyses were taken every five centimetre. Analyses were carried out with a CARLO ERBA Elemental Analyzer at the GEOMAR in Kiel following standard procedures (for

details see Chapter 2). The standard deviation for the data presented here is <2%.

2.2. XRF-measurements for high resolution Ca and Fe analyses

In addition to the discrete carbonate analyses carried out in five centimetre intervals, high resolution calcium (Ca) determinations were done with the CORTEX-XRF scanner (Jansen et al., 1998) at the University of Bremen. It is a non-destructive analysis system for scanning the surface of split sediment cores. Its central sensor unit consists of a molybdenum X-ray source (3-50kV), a Peltier-cooled PSI detector (KEVEXTM) with 125 μ m beryllium window and a multichannel analyser with a 20 eV spectral resolution. The system configuration (X-ray tube energy, detector sensibility) at the University of Bremen allows the analyses of elements from K (atomic no.19) to Sr (atomic no. 38) (X-ray tube voltage: 20 kV).

For this study element intensities for Ca were analysed in 1 cm intervals, with each measurement taken over an area of 1 cm². To obtain statistically significant data 30 second count time were used with an X-ray current of 0.087 mA. The acquired XRF spectrum for each measurement was processed by the KEVEXTM software

Toolbox©. Background subtraction, sum-peak and escape-peak correction, deconvolution, and peak integration were successively applied. The resulting data are element intensities in counts per second (cps) and are used as a proxy for the carbonate content.

2.3. Image analysis for the quantification of corals

As both methods for the determination of the carbonate content do not allow differentiating between carbonate from corals and carbonate from other sources, an image analysis was carried out in order to quantify the coral content in the cores. The coral fragments are easily to distinguish from the matrix of hemipelagic sediments as it becomes obvious from Fig. A2.

For the image analyses calibrated digital pictures were taken from the coral bearing cores with the GEOTEK colour scanner at the University of Bremen.

The scans were transformed into grey-scale images (0 equals black, 255 equals white) and gridded with grid-intervals of one pixel. In a first step the grids were squared to increase the contrast. In the next steps a 7x7 pixel median filter and a 3x3 pixel structural filter were used on the images smoothing the background and eroding single pixel with a high contrast. After these preparations data were collected separately for every square centimetre over the full width of the split core. To detect the corals a threshold for each sampling interval, defined by the median grey value of the particular interval and an absolute offset of 20 units was used. The floating threshold was necessary to compensate for the variations in the matrix. In a last step the values were integrated over each centimetre depth interval resulting in area percentages

of corals being present in each interval. Although this method did not differentiate between corals and e.g. molluscs or gastropods shells it still was sufficient due to the dominance of coral material relative to other carbonate particles.

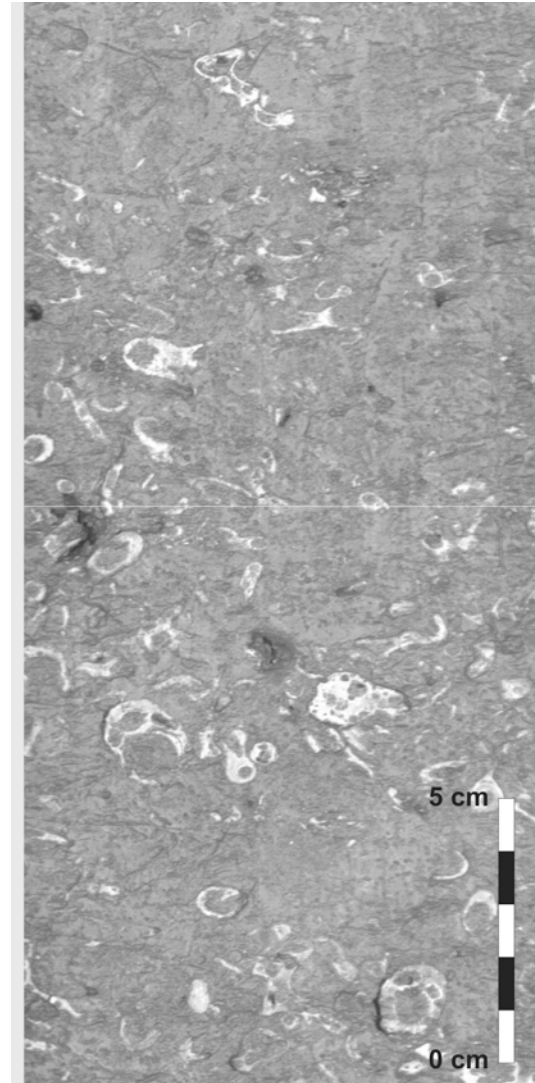


Figure A2. Image showing coral fragments in the on-mound core GeoB 6730-1 (section 20-40 cm).

For better comparison with the discrete and the XRF-scanner data sets the area percentages of the corals were transformed into weight percentages aragonite of the dry bulk sediment. The transformation was done using an average coral-density of 2.66 g/cm^3 , according to density analyses

carried out on 15 coral fragments from Propeller mound and an average dry bulk density (DBD) for the matrix of 1.19 g/cm³.

2.4. Age determinations

The stratigraphical framework of the off-mound cores and partly also of the on-mound cores is based on AMS ¹⁴C ages using mono-species samples (~10 mg) of the planktic foraminifera species *Neogloboquadrina pachderma* (either dextral or sinistral) from the fraction 125-250 μm (Table A2). The samples were analysed at the Leibniz Laboratory for Age Determinations and Isotope Research at the University of Kiel (Nadeau et al., 1997).

The data were corrected for ¹³C and the calibration to calendar years was done with the program Calib 4.3 (Stuiver and Reimer, 1993) using the marine data set of Stuiver et al., (1998), while ages greater 21 kyr BP were calibrated using the method of Voelker et al., (1998) (Table A2).

In addition, from the on-mound cores fragments of the cold water coral *L. pertusa* have been taken and dated by the U/Th method using the Finnigan MAT 262 RPQ2+ Thermal Ionisation Mass Spectrometer (TIMS) at GEOMAR Kiel. Details of the cleaning procedure of these samples are given in Chapter 5. Data information is provided in Table A3.

Table A2. AMS ¹⁴C dates of the cores GeoB 6719-1, GeoB 6725-1 and GeoB 6730-1

Laboratory number	core depth (cm)	¹⁴ C AMS age (yr BP)	+/- err. (yr)	calibrated age (cal yr BP)
Core GeoB 6719-1				
KIA 17091	18	6200	35	6640
KIA 17092	98	16100	70	18630
KIA 17093	163	21670	110	25420
KIA 17094	273	26780	180	30830
Core GeoB 6725-1				
KIA 16206	68	7135	45	7600
KIA 16202	168	20360	140	23530
Core GeoB 6730-1				
KIA 16201	23	4370	35	4500

Table A3. U/Th ages for the cores GeoB 6728-1; GeoB 6729-1 and GeoB 6730-1

Core	core depth (cm)	²³⁴ U/ ²³⁸ U (‰)	²³⁸ U (dpm/g)	²³⁰ Th (dpm/g)	²³² Th (dpm/g)	²³⁰ Th/ ²³² Th (dpm/g)	²³⁰ Th/ ²³⁴ Th (dpm/g)	age (kyr)	error (kyr)
GeoB 6728-1									
	3	86±2	2.251±0.002	1.825±0.008	0.01621±0.00002	112.6±0.5	0.741±0.003	143	1.3
	83	82±3	2.549±0.003	2.263±0.004	0.00533±0.00001	424.6±0.9	0.818±0.002	178	1.0
	218	72±2	2.495±0.003	2.323±0.009	0.01473±0.00003	157.7±0.7	0.865±0.004	207	2.6
	368	60±3	2.574±0.004	2.531±0.008	0.00929±0.00002	272.3±1.0	0.924±0.003	261	3.6
GeoB 6729-1									
	23	113±3	3.086±0.003	1.332±0.006	0.02022±0.00030	66.8±0.3	0.388±0.002	53	0.3
	73	80±3	2.416±0.003	2.095±0.007	0.01395±0.00002	151.0±0.5	0.802±0.003	170	1.4
	268	44±2	2.630±0.003	2.607±0.006	0.00678±0.00001	385.5±1.0	0.949±0.003	300	4.1
GeoB 6730-1									
	88	107±2	3.294±0.003	2.122±0.003	0.01370±0.00003	155.8±0.4	0.582±0.001	93	0.3
	158	109±4	1.994±0.003	1.526±0.006	0.03068±0.00004	50.6±0.2	0.690±0.003	124	1.0
	268	82±7	2.673±0.008	2.357±0.007	0.01040±0.00001	226.5±0.7	0.815±0.003	176	1.8
	358	62±3	3.184±0.005	2.891±0.011	0.02652±0.00004	109.9±0.5	0.855±0.004	207	2.5

3. Results

In order to use the Ca intensities derived from the XRF scanning to increase the resolution of the carbonate content determinations, the XRF data have been correlated to the discrete carbonate content measurements for those core depths the latter are available. For the off-mound cores all data plot with $r^2 = 0.77$ (Fig. A3a), disregarding the turbiditic samples at the base of cores GeoB 6719-1 and GeoB 6725-1 (see below). With the resulting linear regression the Ca intensities have been transformed to carbonate contents (Fig. A4). The same procedure has been employed for the on-mound cores. However, the relation ($r^2 = 0.59$) between Ca intensities and discrete carbonate measurements has a slightly lower slope (Fig. A3b), which is most likely due to a different composition of the cores induced by their coral content.

The carbonate contents in the off-mound cores are marked by high values ($>30\%$) in the uppermost core sections (Fig. A4). Cores GeoB 6719-1 and GeoB 6725-1 also have comparable or even higher values at the base of the core. Below the maximum close

to the core tops all three cores have an extended core section with rather low ($<23\%$) carbonate contents. However, in all three cores a significant double peak occurs in the middle of the low carbonate section (Fig. A4).

In the on-mound cores the carbonate contents are significantly higher than in the off-mound cores. They display some variation and range mostly between 30% and 70% and do not show any similarities neither to the off-mound cores nor to each other (Fig. A5). Among these cores the average carbonate contents are rather constant ranging from 53% (GeoB 6730-1) to 56% (GeoB 6728-1) to finally 57% (GeoB 6729-1). The coral carbonate contents range between almost 0% and maximum values of $\sim 40\%$, with the coral carbonate content in core GeoB 6730-1 (on average 17%) being almost three times as high as in the two other cores (on average 5%) (Fig. A6). There seems to be no significant correlation between total carbonate and coral carbonate contents.

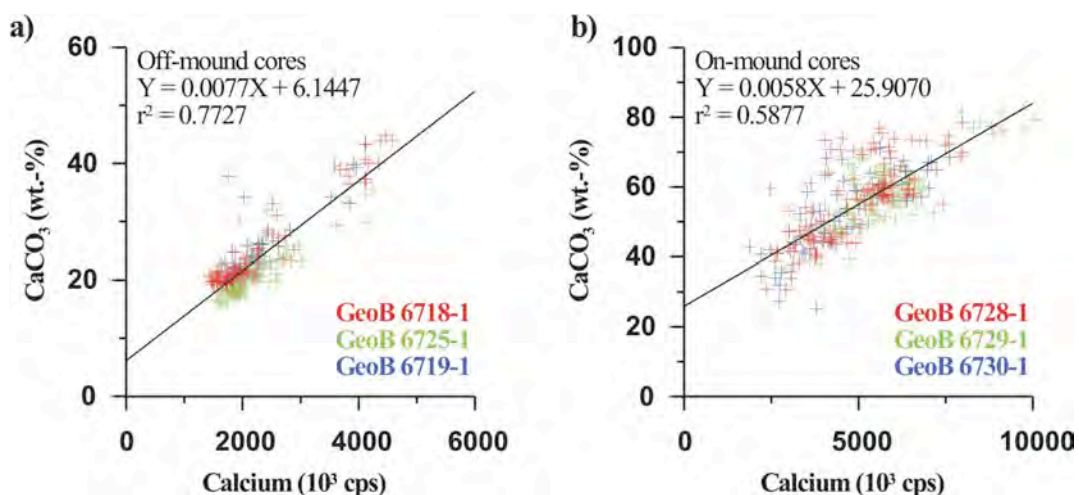


Figure A3. Calcium carbonate content versus XRF Ca counts for (a) the off-mound cores GeoB 6718-2, GeoB 6725-1 and GeoB 6719-1 and (b) the on-mound cores GeoB 6728-1, GeoB 6729-1 and GeoB 6730-1. Regressions (a) based on all off-mound data excluding the turbidite sections in GeoB 6719-1 and GeoB 6725-1. Regression (b) based on all on-mound data.

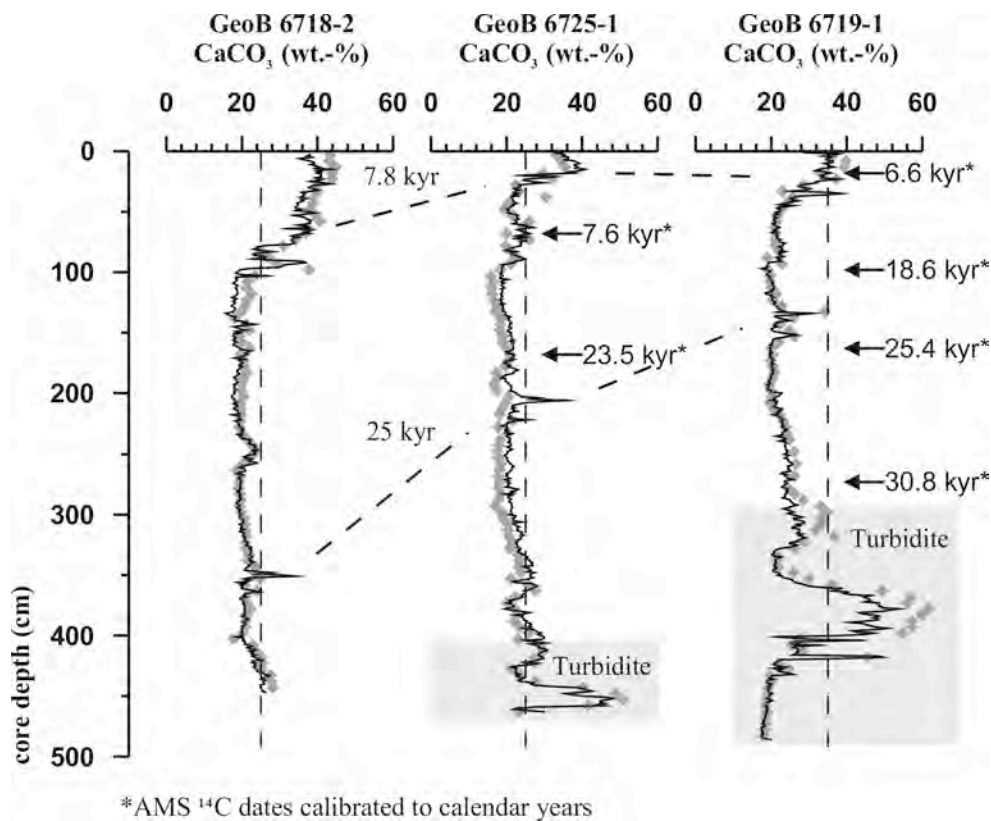


Figure A4. CaCO_3 content versus depth in the off-mound cores based on calibrated scanner data (line) and discrete samples (rectangles). The turbidite sections are marked by the shaded area and stratigraphical information is provided by AMS ^{14}C dates. Correlation horizons for budget calculations are indicated by the dashed lines.

4. Stratigraphy

According to the AMS ^{14}C ages the off-mound cores (GeoB 6718-2, GeoB 6719-1 and GeoB 6725-1) seem to contain rather continuous sediment records going back to ~30 cal kyr BP (Fig. A4), which is also corroborated by $\delta^{18}\text{O}$ data (Chapter 5, Appendix 8). In cores GeoB 6719-1 and GeoB 6725-1 the AMS ^{14}C dates reveal a regular sequence with younger ages following older ones.

The records are marked by the same major turbiditic sequence occurring at the base of cores GeoB 6719-1 (below 294 cm core depth) and GeoB 6725-1 (below 404 cm core depth). According to the oldest AMS date in core GeoB 6719-1 just above the turbidite it seems to be slightly older

than 31 cal kyr BP. Due to higher sedimentation rates in core GeoB 6718-2 the turbidite level, if present, is not reached in this core.

Besides the AMS ^{14}C dates shown in Fig. A4 an additional stratigraphic tie point is indicated by a characteristic double peak in the carbonate records in all three cores (GeoB 6718-2: 364-551 cm, GeoB 6719-1: 134-152 cm and GeoB 6725-1: 206-222 cm). Being situated between the AMS ^{14}C dates of 25.4 cal kyr BP just below (GeoB 6719-1) and 23.6 cal kyr BP just above (GeoB 6725-1), the second and higher part of this carbonate double peak is assumed to be ~25 cal kyr old. As it occurs in all three cores it provides a perfect

correlation tie point for these cores. It is probably related to the Heinrich 2 event and its European precursor event, both dated to 25.6 respectively 24 cal. kyr BP (Grousset et al., 2000).

Another stratigraphical tie point for the correlation of these off-mound cores is the significant increase in the carbonate content close to the top of the cores (Fig. A4). It is interpreted to reflect the onset of the Holocene, when drastic paleoenvironmental changes resulted in a distinct shift towards higher carbonate contents. Also this interpretation is supported by $\delta^{18}\text{O}$ measurements (Chapter 5, Appendix 8). Thus, the first sample in each of the cores in which the carbonate content started to stay on the Holocene level is set to an age of 7.8 cal kyr BP, corresponding to that date the standard oxygen isotope curve of (Martinson et al., 1987) reaches a constant Holocene level. In addition, to allow a quantitative comparison of the cores it is assumed that the core tops reflect the present-day surface sediment.

In these cores the sedimentation rates are generally higher during the glacial period compared to the Holocene. The general trend of decreasing sedimentation rates towards the Propeller Mound is assumed to be due to enhanced winnowing (Appendix 8) related to focusing of bottom currents around the mound (Guo et al., 2000). Such a mechanism has been named as the prime process generating the moats around most of the carbonate mounds in the Porcupine Seabight (De Mol et al., 2002).

According to AMS ^{14}C datings, U/Th measurements and $\delta^{18}\text{O}$ records the on-mound cores (GeoB 6728-1, GeoB 6729-1 and GeoB 6730-1) are marked by numerous hiatuses with almost no fully interglacial or fully glacial sediments being preserved

(Appendix 8). Nevertheless, the available U/Th ages provide a mean by which the netto carbonate accumulation (i.e. the preserved material) can be put into a temporal framework.

U/Th data with ages between 170 and 178 kyr available for all three cores (Fig. A5) allow a correlation of the three cores with respect to the netto sedimentation over a comparable time interval, i.e. the last ~175 kyr, which covers core intervals of 83 cm (GeoB 6729-1), 73 cm (GeoB 6728-1) and 268 cm (GeoB 6730-1). Older available U/Th dates in core GeoB 6728-1 and GeoB 6729-1 allow to determine the netto sedimentation even further back in time.

Of course, the sedimentation rates derived by this method do not reflect the actual sedimentation rate at Propeller Mound during these time intervals (Appendix 8). However, the netto sedimentation, which really contributes to the shape and size of the actual Propeller Mound is well covered and allows a comparison with the surrounding drift sediments on a Late Pleistocene time scale. Thus, the core tops again have been set to a zero age, although it is clear, e.g. from core GeoB 6728-1 with an age of 143 kyr close to the surface (Fig. A5), that this assumption is not valid in a solely stratigraphical sense. Nevertheless, for the calculation of netto accumulation rates it seems to be a proper approach.

According to an AMS ^{14}C date of 4,500 cal yrs BP (Fig. A5) and rather low $\delta^{18}\text{O}$ data (Appendix 8) core GeoB 6730-1 contains a section of Holocene sediments at its top. For a quantitative comparison with the off-mound cores it is tentatively assumed that the core section from 0 to 53 cm in core GeoB 6730-1, marked by low $\delta^{18}\text{O}$ data, corresponds to the last 7.8 kyr.

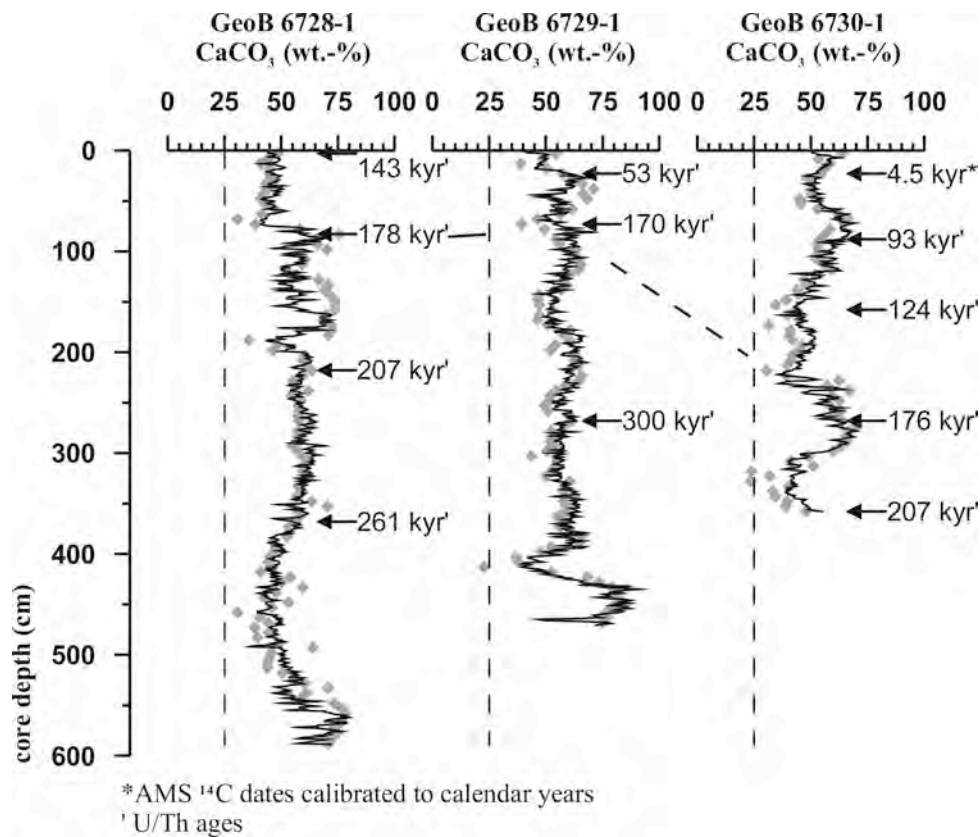


Figure A5. CaCO₃ content versus depth in the on-mound cores based on calibrated scanner data (line) and discrete samples (rectangles). Stratigraphical information is provided by AMS ¹⁴C and U/Th dates. Correlation horizons for budget calculations are indicated by the dashed lines.

5. Discussion

In order to discern the impact of a carbonate mound on the carbonate sedimentation, the sedimentological data have to be put in a wider context also including “normal” hemipelagic sediments, i.e. not affected by a carbonate mound, to assess the background sedimentation, which of course also affects the carbonate mound. In this study the background sedimentation is reflected in the off-mound cores, which can be compared on various scales with the on-mound cores representing the carbonate mound setting.

5.1 Carbonate contents

The off-mound cores can be clearly distinguished in Holocene (0 – 7.8. cal. kyr BP) and Last Glacial Maximum/Termination 1 (LGM-T1, 7.8 – 25 cal. kyr BP) sections, with the sediments of these two periods being quite different (Fig. A4). During the LGM-T1 the average carbonate contents in the three cores range between 20 and 23 wt.-%, while during the Holocene much higher values of 34 to 37 wt.-% are observed (Table A4).

As to be expected the carbonate contents on the carbonate mound are significantly higher with values below 30 wt.-% are rather rare (Fig. A5). According to the

available stratigraphical tie points those sediments of the last ~175 kyr that remained in place can be compared. They are marked by average carbonate contents between 48 and 54 wt.-% with slightly higher average values (~57 wt.-%) if also the older sediments are regarded (Table A4). Only for core GeoB 6730-1 also average Holocene carbonate contents can be described. With 53 wt.-% these are in line with the other “young” (i.e. <~175 kyr) on-mound sediments.

Comparing the two settings it appears that the carbonate contents of the on-mound sediments are on average >25wt.-% higher than those of the Holocene off-mound sediments. If the low carbonate glacial off-mound sediments are considered, the

difference is even bigger. However, as no comparable glacial sediments are preserved on the mound (Appendix 8) this comparison will focus on the Holocene off-mound sediments.

5.2 Coral contents

Despite some tiny coral fragments in the off-mound cores (Chapter 5), significant amounts of corals have only been found in the three on-mound cores. According to the image analyses the coral content in the <175 kyr section of cores GeoB 6728-1 and GeoB 6729-1 mainly ranges between 0 and <20 wt.-% and is on average rather low (3 wt.-%, Tab. A4).

Table A4. Sediment composition and accumulation of the investigated sediment cores.

	GeoB 6718-2		GeoB 6725-1		GeoB 6719-1	
	Holocene	Glacial	Holocene	Glacial	Holocene	Glacial
time interval (kyr)	0 – 7.8	7.8 – 25	0 – 7.8	7.8 – 25	0 – 7.8	7.8 – 25
depth interval (cm)	0 – 78	78 – 352	0 – 18	18 – 206	0 – 26	26 – 134
sed. rate (cm/kyr).	9.99	15.94	2.30	10.94	3.33	6.28
mean DBD (g/cm ₃)	1.19	1.06	1.31	1.17	1.29	1.17
mean CaCO ₃ (%)	37.17	20.41	37.24	21.61	34.44	22.50
Accumulation (g/cm ₃ kyr)						
bulk sediment	11.887	16.856	3.022	12.756	4.283	7.355
CaCO ₃	4.418	3.440	1.125	2.757	1.475	1.655
	GeoB 6728-1		GeoB 6729-1		GeoB 6730-1	
	last 175 kyr	older	last 175 kyr	older	Holocene	last 175 kyr
time interval (kyr)	0 – 178	0 – 261	0 – 170	0 – 300	0 – 7.8	0 – 176
depth interval (cm)	0 – 83	0 – 368	0 – 73	0 – 268	0 – 53	0 – 268
sed. rate (cm/kyr)	0.47	1.41	0.43	0.89	6.79	1.52
mean DBD (g/cm ₃)	1.23	1.28	1.24	1.26	1.42	1.45
mean CaCO ₃ (total) (%)	48.08	56.24	54.09	57.34	53.56	52.93
mean CaCO ₃ (coral) (%)	2.92	6.13	3.07	4.71	15.62	17.69
Accumulation (g/cm ₃ kyr)						
bulk sediment	0.575	1.805	0.530	1.125	9.634	2.208
total CaCO ₃	0.277	1.015	0.287	0.645	5.160	1.169
coral CaCO ₃	0.017	0.111	0.016	0.053	1.505	0.391

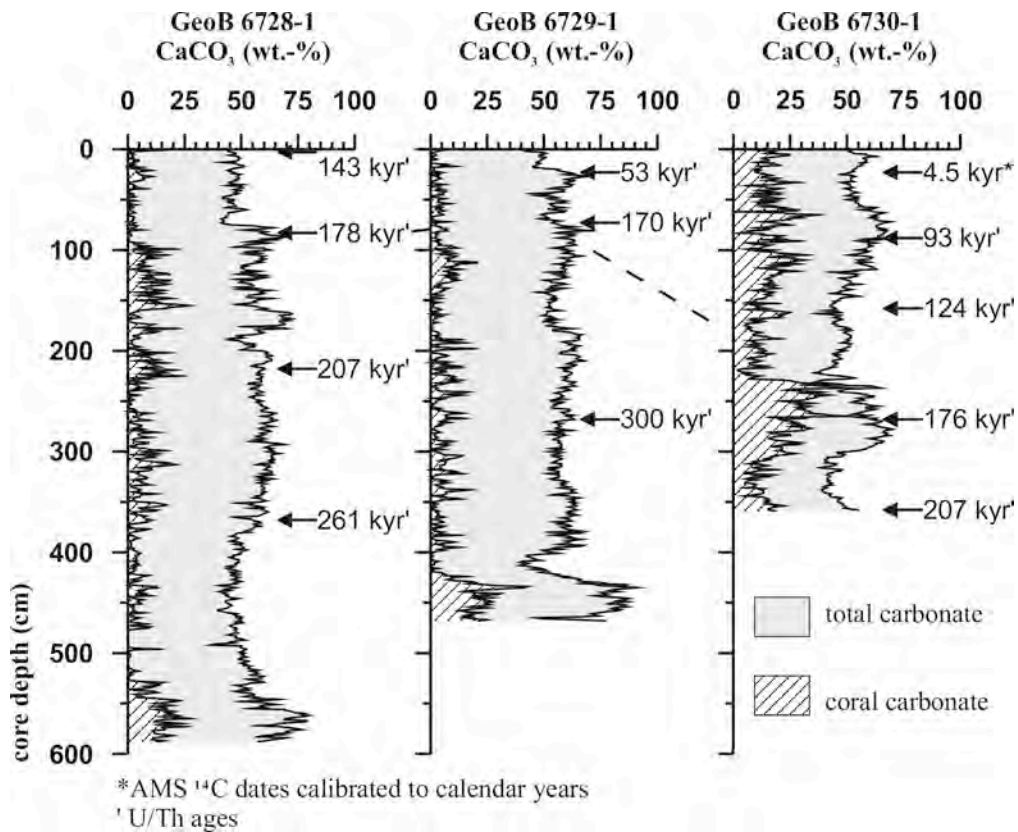


Figure A6. Total CaCO₃ content and coral derived CaCO₃, derived from image analyses, versus depth in the on-mound cores. Stratigraphical information is provided by AMS ¹⁴C and U/Th dates. Correlation horizons for budget calculations are indicated by the dashed lines.

Further downcore the average coral content can be slightly higher (4-6 wt.-%). In contrast, in core GeoB 6730-1 the average coral content (17 wt.-%) as well as the individual data points (Fig. A6) are considerably higher.

Although the coral contents differ strongly, the carbonate contents are rather similar among the three on-mound cores. Subtracting the coral content from the carbonate content in core GeoB 6730-1 yields a background carbonate content of 35 wt.-%, which is very close to the carbonate content of the Holocene off-mound sediments. Thus, for this core it can be assumed that the carbonate in the sediment consists of the normal background sedimentation (~35 wt.-%) accompanied by

~17 wt.-% coral carbonate. In this case the coral fragments in this core must be rather large assuring the detection of all coral particles by the image analysis.

Extending this observation to the other two on-mound cores reveals a different pattern. Assuming the background carbonate content (~35 wt.-%) to be comparable at all sites, these two sites have besides a coral content of ~3 wt.-% an undefined carbonate contribution of ~13 wt.-%. Together with the corals this adds up almost exactly to the coral content in core GeoB 6730-1. Thus, these 13 wt.-% of carbonate might also reflect a coral contribution. However, this coral material must be so fine grained that it is not to detect by the image analysis.

While core GeoB 6730-1 is taken close to the top of Propeller Mound at a site of recent coral growth, indicated by living corals in a near-by box core (GeoB 6722-1, (Freiwald et al., 2000), no living corals have been reported from sites close to the other two cores. If core GeoB 6730-1 contains mainly corals grown at the site, these are most likely preserved in rather large pieces, which will be detected by the image analyses. If, in contrast, the corals found in the other two cores have been transported to the core sites from fields of active coral growth further upslope the delicate coral fragments were probably subject to major destruction during the transport resulting in a shift of the coral material from the coarse into the fine fraction, i.e. out of the detection window of the image analysis.

Based on this assumption it appears that the coral content in the on-mound cores is rather constant between 15 and 20 wt.-%,

adding to a background carbonate content of ~35 wt.-%, typical for the Holocene off-mound sediments.

5.3 Carbonate accumulation rates

Along the off-mound transect the sedimentation rates decrease significantly towards the mound from 10 cm/kyr (Holocene) and 16 cm/kyr (LGM-T1) to 3.3/6.3 cm/kyr (Table A4), most likely due to winnowing induced by bottom currents focused around the mounds. Interestingly, the sediment composition with respect to the carbonate content seems to be unaffected by this process. It also becomes obvious that glacial sedimentation rates are significantly higher than those found in the Holocene (Table A4, Fig. A7).

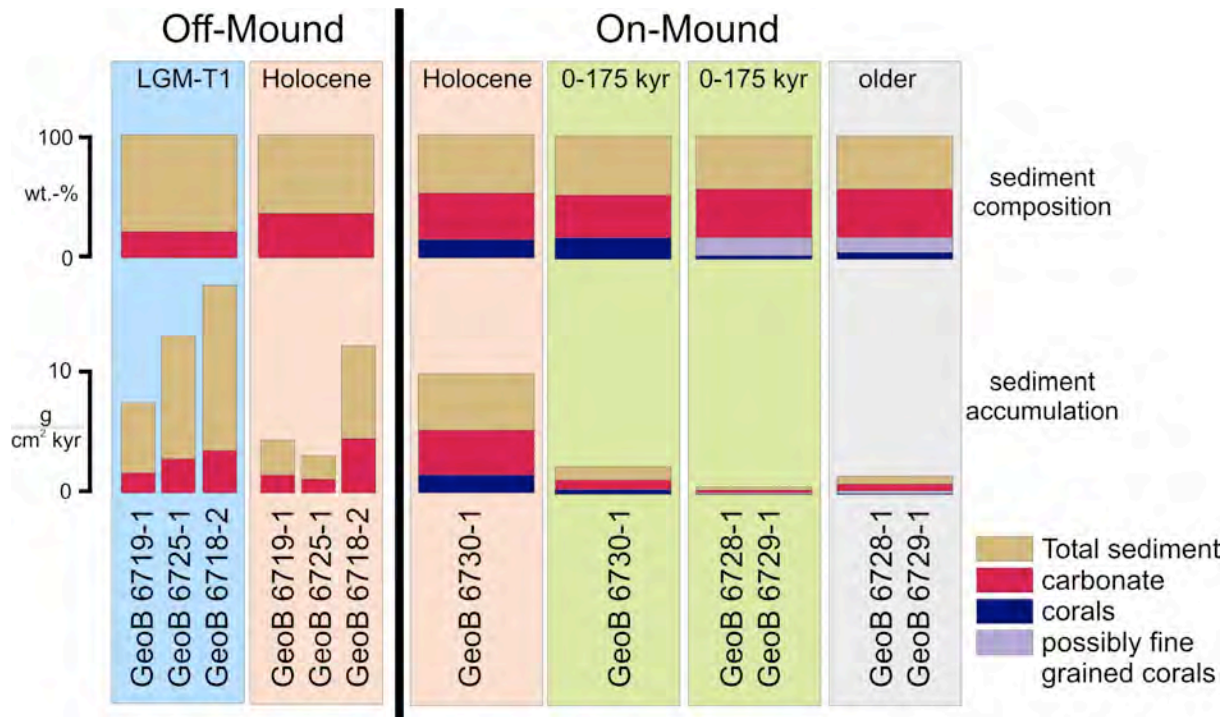


Figure A7. Sediment composition and sediment accumulation in the Propeller Mound area indicated for the intervals Last Glacial Maximum-Termination 1 (LGM-T1), Holocene for the off-mound location and Holocene, the interval 0-175 kyr and older sediments for the on-mound locations.

In terms of total and carbonate accumulation rates, which have been calculated according to (van Andel et al., 1975), a similar pattern of decreasing values towards the mound appears. For the comparison with the on-mound sediments only core GeoB 6718-2 will be considered as it is located furthest away from the mound. Being least affected by any mound-induced bottom current disturbances this core is probably the best representative of the background sedimentation in the area. On a Holocene/LGM-T1 scale its total accumulation rate (AR_{total}) and its carbonate accumulation rate ($AR_{carbonate}$) range between 11.9/16.9 g/cm²*kyr and 4.4/3.4 g/cm²*kyr, respectively (Table A4, Fig. A7).

Over the rather long time periods represented in the on-mound cores the resulting sedimentation rates (<1.5 cm/kyr), AR_{total} (<2.2 g/cm²*yr) and $AR_{carbonate}$ (<1.2 g/cm²*kyr) are rather low and partly only around 10% of the comparable off-mound values (Table A4, Fig. A7), what, of course, is due to the incompleteness of the records as mentioned above. Thus, these numbers are only netto rates over the respective time spans but they do not allow a direct comparison with the off-mound cores in terms of real sedimentation.

The only direct comparison appears to be possible for the Holocene sections of the on-mound core GeoB 6730-1 and the off-mound core GeoB 6718-2, although the completeness of these sections in a stratigraphical sense can only be assumed. AR_{total} and $AR_{carbonate}$ are quite similar in both cores, with the AR_{total} being slightly higher in the off-mound core (11.9 g/cm²*kyr vs. 9.6 g/cm²*kyr) and $AR_{carbonate}$ being slightly higher in the on-mound core (4.4 g/cm²*kyr vs. 5.1 g/cm²*kyr), reflecting the higher CaCO₃ content in this core (Fig. A7).

5.4 Carbonate budget

The establishment of a full carbonate budget for the uppermost part of the Propeller Mound is hampered by the incompleteness of the sediment record. Based on the preserved sediments the netto carbonate accumulation through the last 175 kyr is between 0.5 kg/cm² (GeoB 6728-1 and GeoB 6729-1) and 2.1 kg/cm² (GeoB 6730-1), with approximately 1/3 of this values can be attributed to coral carbonate. These values are rather low and the total accumulation rates are even lower than in the off-mound sediments.

This observation sheds some light on Propeller Mound as an individual mound but not on the sedimentation on carbonate mounds in general. The comparison of off-mound and on-mound sediment accumulation in the Propeller Mound area indicates that on a Late Pleistocene time scale the mound is even shrinking relative to the surrounding sediments, what is most likely due to ongoing erosion on the mound. However, there must have been a different setting in the history of Propeller Mound, otherwise it would not be a mound.

Coral growth on a mound is assumed to increase also the sedimentation of allochthonous material by creating a low-energy micro environment among the corals enhancing the deposition of suspended material brought along by bottom currents (Freiwald and Shipboard Party, 2002). Indeed, the sediments deposited under such conditions are noticeably finer grained than those deposited in areas barren of corals (Dorschel, unpubl. data). Thus, by the contribution of coral material and an enhanced amount of fine sediments, coral growth on a carbonate mound should significantly enhance total accumulation.

Seismic investigations in the near-by Belgica Mound province in the eastern Porcupine Seabight show that the carbonate mounds must have grown extremely fast during their initial stages, as it is indicated by onlap and moat structures in the surrounding sediments (Van Rooij et al., 2003). Later during their development the growth rate seems to have decreased. Slightly to the north of the Hovland Mound province, to which also the Propeller Mound belongs, the final stage of carbonate mound development can be seen. There in the Magellan Mound province a huge amount of carbonate mounds totally buried by

sediments has been detected in seismic surveys (Henriet et al., 1998; De Mol et al., 2002; Huvenne et al., 2002).

In such a scenario also Propeller Mound might fit in as it possibly represents a carbonate mound at the turn from a (slow) growing carbonate mound to a mound in the stage of getting buried by hemipelagic sediments. The lower accumulation compared to the off-mound sediments supports the conclusion that Propeller Mound already entered the stage of decline and if this development continues into the future Propeller Mound will follow the fate of the already buried Magellan Mounds.

6. Conclusion

Extrapolating the results from Propeller Mound, which has a carbonate content of >50% with the carbonate to a significant amount consisting of fragments of the cold-water corals *L. pertusa* and *M. oculata*, to other sea-floor structures called mounds in the Porcupine Seabight and in the adjacent regions, the term cold-water coral carbonate mounds, or simply carbonate mounds, seems to be well justified. Unfortunately, the complex sedimentation and erosion pattern on Propeller Mound prevent the establishment of a quantitative carbonate budget. However, some qualitative conclusions can be drawn. It is obvious that

the ~20% of coral carbonate found on the mound are unique to these kind of structures compared to the “normal” sea-floor around them. In addition, it is very likely that the corals act as a sediment buffer, thereby adding another portion to the hemipelagic background sedimentation. Thus, based on the available data the netto effect of coral growth on the accumulation of carbonate mounds can be given with 15% + X. Future analyses on carbonate mounds still being in the growing phase will help to better quantify their carbonate and their overall sediment budget

7. References

- De Mol B., Van Rensbergen P., Pillen S., De Mol, B., Van Rensbergen, P., Pillen, S., Van Herreweghe, K., Van Rooij, D., McDonnell, A., Huvenne, V., Ivanov, M., Swennen, R., and Henriet, J.P. (2002) Large deep-water coral banks in the Porcupine Basin, southwest of Ireland: *Marine Geology*, v. **188**, p. 193-231.
- Freiwald, A., Henrich, R., and Pätzold, J. (1997) Anatomy of a deep-water coral reef mound from Stjernsund, West Finnmark, Northern Norway. *In: James, N.P., and Clarke, J.A.D., eds., Cool-Water Carbonates*, Volume **56**: Tulsa, Oklahoma, U.S.A., SEPM, p. 141-162.
- Freiwald, A., Dullo, C., and Shipboard Party (2000) Cruise Report RV POSEIDON Cruise 265, Thorshavn - Galway - Kiel, 13th September - 1st October 2000, p. 65.
- Freiwald, A. (2002) Reef-Forming Cold-Water

- Corals. In: Wefer, G., Billett, D., Hebbeln, D., Jørgensen, B.B., Schlüter, M., and Weering, T.v., eds., *Ocean Margin Systems*. Berlin, Heidelberg, New York, Springer Verlag, p. 365-385.
- Freiwald, A., and Shipboard Party (2002) Cruise Report RV POSEIDON Cruise 292, Reykjavik - Galway, 15th July - 4th August 2002, p. 84.
- Grousset, F.E., Pujol, C., Labeyrie, L., Auffret, G., and Boelaert, A. (2000) Were the North Atlantic Heinrich events triggered by the behavior of the European ice sheets?: *Geology*, v. **28**, p. 123-126.
- Guo, Y., Davies, P.A., Cavatelli, A., and Jacobs, P. (2000) Topography and stratification effects on shelf edge flows: *Dynamics of Atmosphere and Oceans*, v. **31**, p. 73-116.
- Henriet, J.P., De Mol, B., Pillen, S., Vanneste, M., Van Rooij, D., Versteeg, W., Croker, P.F., Shannon, P.M., Unnithan, V., Bouriak, S., and Chachkine, P. (1998) Gas hydrate crystals may help build reefs: *Nature*, v. **391**, p. 648-649.
- Henriet, J.P., Guidard, S., and Team, O.P. (2002) Carbonate Mounds as a Possible Example for Microbial Activity in Geological Processes. In: Wefer, G., Billett, D., Hebbeln, D., Jørgensen, B.B., Schlüter, M., and Weering, T.v., eds., *Ocean Margin Systems*: Berlin, Heidelberg, New York, Springer Verlag, p. 437-455.
- Hovland, M., Croker, P.F., and Martin, M. (1994) Fault-associated seabed mounds (carbonate knolls?) off western Ireland and north-west Australia: *Marine and Petroleum Geology*, v. **11**, p. 232-246.
- Huvenne, V.A.I., Blondel, Ph., Henriët, J.-P. (2002) Textural analyses of sidescan sonar imagery from two mound provinces in the Porcupine Seabight: *Marine Geology*, v. **189**, p. 323-341.
- Jansen, J.H.F., Van der Gaast, S.J., Koster, B., and Vaars, A.J. (1998) CORTEX, a shipboard XRF-scanner for element analyses in split sediment cores: *Marine Geology*, v. **151**, p. 143-153.
- Lindberg, B., Berndt, C., and Mienert, J. (subm.) The Fugløy Reefs on the Norwegian-Barents Continental Margin: Cold-water Corals at 70°N, their acoustic signature, geologic, geomorphologic and oceanographic setting. In: Henriët, J.-P., and Dullo, W.-C., eds., *Modern Carbonate Mound Systems: A window to Earth History*: Berlin, Heidelberg, New York, Springer.
- Martinson, D.G., Pisias, N.G., Hays, J.D., Imbrie, J., Moore Jr., T.C., and Shackleton, N.J. (1987) Age dating and the orbital theory of the ice ages: development of a high resolution 0 to 300 000-year chronostratigraphy: *Quaternary Research*, v. **27**, p. 1-29.
- Mortensen, P.B., Hovland, M., Brattegard, T., and Farestveit, R. (1995) Deep water bioherms of coral *Lophelia pertusa* (L.) at 64 degrees on the Norwegian shelf: structure and associated megafauna: *Sarsia*, v. **80**, p. 145-158.
- Nadeau, M.J., Schleicher, M., Grootes, P., Erlenkeuser, H., Gottolong, A., Mous, D.J.W., Sarnthein, M., and Willkomm, N. (1997) The Leibnitz-Labor AMS Facility at the Christian-Albrechts University, Kiel, Germany: *Nucl. Instrum. Methods Phys. Res.*, v. **123**, p. 22-30.
- Somoza, L., Gardner, J.N., Díaz-del-Río, V., Vázquez, J.T., Pinheiro, L.M., Hernández-Molina, F.J., and TASYO/ANASTASYA Shipboard Scientific Parties. (2002) Numerous Methane Gas-related Sea Floor Structures Identified in Gulf of Cádiz: *EOS*, v. **83**, p. 541+549.
- Stuiver, M., and Reimer, P.J. (1993) Extended ¹⁴C data base and revised CALIB 3.0 ¹⁴C age calibration program: *Radiocarbon*, v. **35**, p. 215-230.
- Stuiver, M., and Reimer, P.J. (1998) (revised dataset): *Radiocarbon*, v. **40**, p. 1127-1151.
- van Andel, T.H., Heath, G.R., and M, T.C. (1975) Cenozoic history and paleoceanography of the central equatorial Pacific Ocean: *Geol. Soc. Am. Mem.*, v. **143**, p. 134.
- Van Rooij, D., De Mol, B., Huvenne, V., Ivanov, M., and Henriët, J.-P. (2003) Seismic evidence of current-controlled sedimentation in the Belgica mound province, upper Porcupine slope, southwest of Ireland: *Marine Geology*, v. **195**, p. 31-53.
- Voelker, A.H.L., Sarnthein, M., Grootes, P.M., Erlenkeuser, H., Laj, C., Mazaud, A., Nadeau, M.-J., and Schleicher, M. (1998) Correlation of marine ¹⁴C ages from the Nordic Seas with the GISP2 isotope record: Implications for radiocarbon calibration beyond 25 ka BP: *Radiocarbon*, v. **40**, p. 517-534.

APPENDIX 8

DEGLACIAL SWEEPING OF A DEEP-WATER CARBONATE MOUND

Boris Dorschel ¹⁾, Dierk Hebbeln ²⁾, Andres Rüggeberg ³⁾, Wolf-Christian Dullo ³⁾
and André Freiwald ⁴⁾

¹⁾ *Dept. of Geosciences, Bremen University, 28359 Bremen, Germany*

²⁾ *MARUM – Center for Marine Environmental Studies, Bremen University, 28359 Bremen, Germany*

³⁾ *GEOMAR Research Center for Marine Geosciences, Wischhofstr. 1-3, 24148 Kiel, Germany*

⁴⁾ *Institute of Paleontology, Erlangen University, 91054 Erlangen, Germany*

submitted to

Nature

Abstract

Since their first detailed scientific description in 1994 (Hovland et al., 1994) the deep-water carbonate mounds at the Celtic continental slope off Ireland received considerable scientific interest (Henriet et al., 1998; Kenyon et al., 2002; van Weering et al., 2003; De Mol et al., 2002). The almost exclusive occurrence of these mounds in hydrocarbon exploration areas raised the question to what extent these mounds are related to escaping fluids or gases from the sediments (Hovland et al., 1994; Henriet et al., 1998). An alternative hypothesis relates these mounds, which rise up a few hundred meters above the surrounding seafloor (Kenyon et al., 2002; De Mol et al., 2002), solely to environmental forcing, that supports the rich deep-water coral ecosystems thriving on top of the mounds (Freiwald, 2002). Analyses of these carbonate mounds were so far mainly based on seismo-acoustic studies (Henriet et al., 1998; Hovland et al., 1994; van Rooij et al., 2003; Huvenne et al., 2003; van Weering et al., 2003), with only a limited number of sediment samples being available (De Mol et al., 2002; Coles et al. 1996). Here we present the first detailed stratigraphic analysis of Late Quaternary sediments recovered from a carbonate mound in the Porcupine Seabight (Fig. A8) indicating that its top sediment sequence is characterised by numerous hiatuses. These are most likely related to sweeping of the mound in turn with the re-establishment of interglacial circulation patterns and strongly point to environmental forcing as the dominant mechanism shaping deep-water carbonate mounds during the Late Quaternary.

Here we focus on Propeller Mound which belongs to the Hovland Mound Province, one of the three mound provinces found in the Porcupine Seabight (Van Rooij et al., 2003) (Fig. A8). While the Belgica Mounds in the eastern and the Hovland Mounds in the northern Porcupine Seabight form large conical or composite elevations above the seafloor, the Magellan Mounds found slightly northward of the Hovland Mounds are totally buried by sediments (De Mol et al., 2002). Propeller Mound has been sam-

pled with three so-called on-mound sediment cores, while an additional off-mound sediment core has been collected from a reference site at the normal seafloor in the neighbourhood of Propeller Mound. (Fig. A8). While the off-mound core consists of typical hemipelagic sediments reflecting the background sedimentation, the on-mound cores additionally contain on average 5-18 % of coral fragments, with core sections totally barren of corals being very rare (Appendix 7).

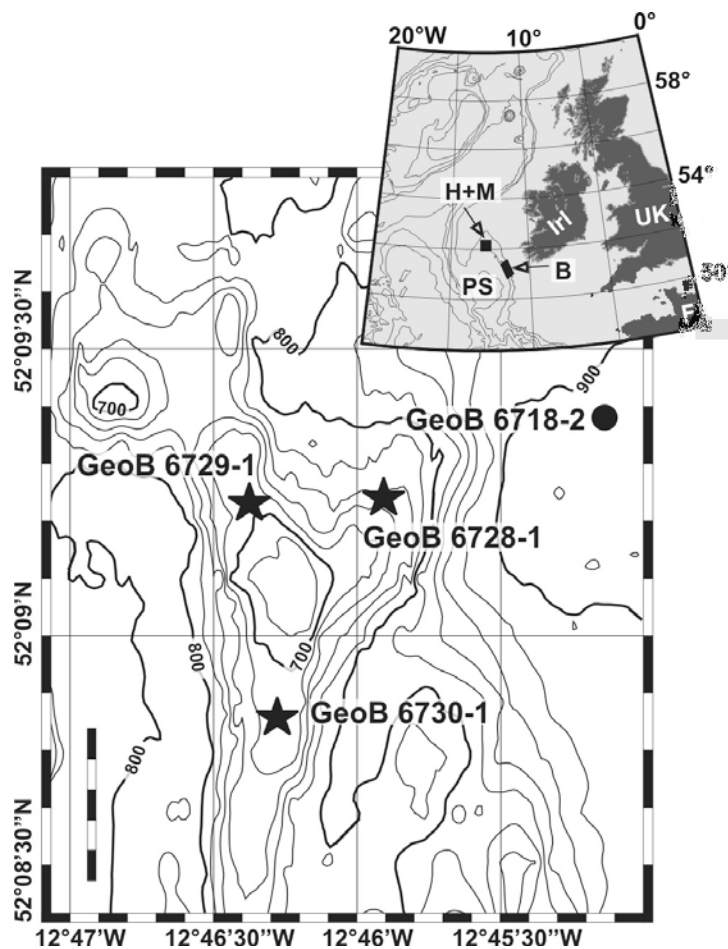


Figure A8. Overview map showing the area of Propeller Mound, a deep-sea carbonate mound, in the Hovland mound province. The positions of the investigated on-mound sediment cores (stars) and the off-mound core (dot) are indicated. The total length of the scale bar corresponds to 500 m and the depth contours are given in meters. The inset shows the position of the Hovland (H), the Magellan (M) and the Belgica (B) mound provinces in the Porcupine Seabight (PS) in the North Atlantic off Ireland.

For the off-mound core stable oxygen isotope data, obtained on the benthic foraminifera *Cibicides sp.*, display a typical record reaching slightly further back than the last glacial maximum (Fig. A9). This interpretation is corroborated by a detailed correlation using Ca-records to two nearby cores dated by ^{14}C (Appendix 7) indicating that the off-mound core represents a rather continuous paleoenvironmental record covering the last ~27 kyr. According to extensive AMS ^{14}C and U/Th dating the on-mound sediments reach back to >250 kyrs (Fig. A9), thereby only providing strongly condensed or fragmentary sections compared to the off-mound setting. The different

ages at the top of the on-mound cores as well as the varying and comparatively low inferred sedimentation rates of the individual core sections point to the presence of numerous hiatuses in these records. As such hiatuses occur in all three on-mound cores, they seem to be typical for Propeller Mound and probably also for other carbonate mounds. Thus, the key to understand the long-term development of Propeller Mound in particular and of similar carbonate mounds in general through the last several 100 kyrs is to unravel the processes causing these hiatuses.

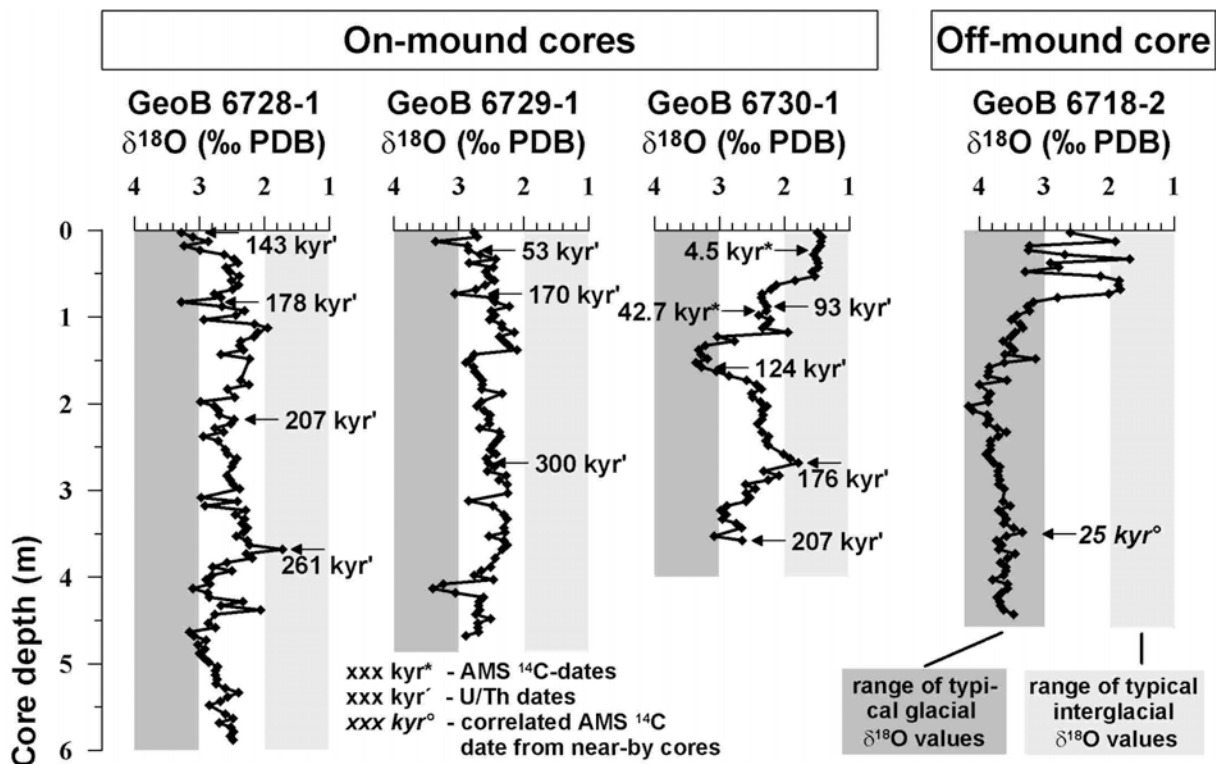


Figure A9. Stable oxygen isotope ($\delta^{18}\text{O}$) data from the on-mound and off-mound sediment cores from the Propeller Mound area, northern Porcupine Seabight. The $\delta^{18}\text{O}$ data have been analysed on ~5 individuals of the benthic foraminifera *Cibicides sp.* following standard procedures (Hebbeln et al. 2002). The age assignments have been taken from Dorschel et al. (Appendix 7). Dark and light shaded signatures indicate the range of typical glacial (>3 ‰ PDB) and interglacial (<2 ‰ PDB) $\delta^{18}\text{O}$ values, respectively.

A closer look at the on-mound core GeoB 6730-1 reveals that these hiatuses, most of them indicated by sudden shifts in the $\delta^{18}\text{O}$ data, are characterized by distinct peaks of coarse ($>250\ \mu\text{m}$) lithic grains (Fig. A10). In the Porcupine Seabight such coarse grains almost exclusively reach the sea-floor as ice rafted detritus (IRD) during glacial times, as

indicated by the continuous presence of IRD in the glacial section ($>1.4\ \text{m}$ core depth) of the off-mound core GeoB 6718-2 (Fig. A10). The concentration of this coarse material in distinct layers in the on-mound core GeoB 6730-1 points to winnowing as an important factor contributing to the generation of the hiatuses.

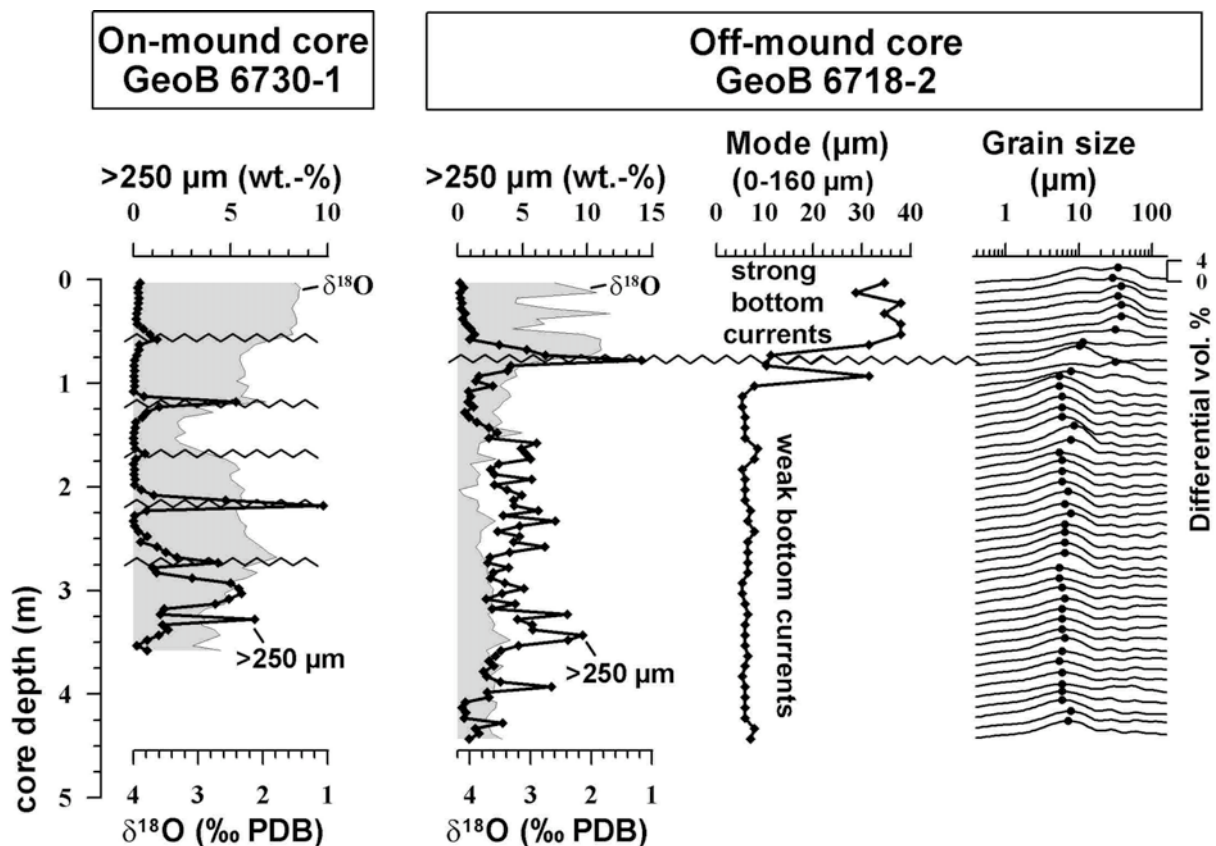


Figure A10. Grain size and $\delta^{18}\text{O}$ from an on-mound and an off-mound sediment core from the Propeller Mound area, northern Porcupine Seabight. Grain-size analyses revealed that peaks in the $>250\ \mu\text{m}$ fraction, sieved from a decalcified sample, are often associated with jumps in the $\delta^{18}\text{O}$ records (shaded curves). These peaks are interpreted to reflect hiatuses, indicated by the wavy line. Continuously high proportions of the $>250\ \mu\text{m}$ fraction, as found in the glacial section of off-mound core GeoB 6718-2, are typical for IRD-bearing sediments. The mode of the $0\text{--}160\ \mu\text{m}$ fraction, obtained by standard procedures using a Coulter laser particle sizer (Van den Bergh et al., 2003), has been determined for the terrigenous, carbonate-free portion of the sediments. High modes are assumed to reflect strong bottom currents and vice versa. As not all individual samples have a clear unimodal grain size distribution also the whole grain size spectra ($0\text{--}160\ \mu\text{m}$) for the samples are shown with the respective modes are indicated by black dots.

Another hint to the processes causing the hiatuses is provided by the $\delta^{18}\text{O}$ data. The off-mound core shows that in the northern Porcupine Seabight full-glacial sediments are characterized by $\delta^{18}\text{O}$ values >3.5 ‰ PDB, while Holocene interglacial $\delta^{18}\text{O}$ values are below a threshold of <2 ‰ PDB (Fig. A9). The two excursions to heavy values in the Holocene sequence of GeoB 6718-2 are most certainly due to bioturbation, transferring the dominantly glacial foraminifer *C. kullenbergi* into the Holocene sequences (Chapter 3).

Using the $\delta^{18}\text{O}$ boundaries defined by the off-mound core (interglacial <2 ‰ PDB; glacial >3.5 ‰ PDB), the preserved on-mound sediment intervals show that hardly any full-glacial nor full-interglacial signals are preserved on Propeller Mound (Fig. A9). Only in core GeoB 6730-1 the top 53 cm are characterised by a clearly interglacial signal (<1.6 ‰ PDB) and the interval 133–163 cm reveals slightly heavier, glacial values (3.0–3.4 ‰ PDB). Thus, at all three on-mound sites almost only interstadial sequences with $\delta^{18}\text{O}$ values mostly between 2 and 3 ‰ PDB are preserved and almost all full-glacial and full-interglacial sediments either have not been deposited or must have been removed after deposition.

Under recent – interglacial – conditions, the dominant water mass interfering with the carbonate mounds in the Porcupine Seabight is the contour-following branch of the Mediterranean Outflow Water (MOW) (White, *subm.*). Among the carbonate mounds in the Porcupine Seabight rather high current velocities of > 20 cm s⁻¹ (D.H., *unpubl. data*) are reflected in typical bedforms associated with strong bottom currents as e.g. dunes, sand waves and gravel ridges, which prevail around the carbonate mounds in large parts of the Porcupine

Seabight (Akhmetzhanov et al. 2001, Beyer et al., 2003; Kenyon et al., 1998).

In an extensive study of cold water coral occurrences along the entire Atlantic margin of Europe Freiwald (2002) concluded that most cold water corals in this region are confined to the MOW. This environment is probably associated with a relatively good food supply for these corals (Freiwald, 2002) which might be related to an accumulation of sinking particles on the pycnocline between the dense MOW and the overlying Eastern North Atlantic Water (ENAW, White, *subm.*). In addition, internal tidal currents, trapped waves and baroclinic motions intensified at the pycnocline reported from this region (White, *subm.*) might further increase food availability for the corals by repeated pumping of particles through the coral thickets.

However, under glacial conditions with a sea-level lowered by ~ 120 m the exchange between the Atlantic and the Mediterranean through the narrow Strait of Gibraltar was significantly reduced. The density-defined flow path of the MOW was quite different under the conditions of the Last Glacial Maximum (LGM) and it did not reach further north than 40°N (Schönfeld and Zahn, 2000).

The absence of the MOW in the Porcupine Seabight during glacial times changed the whole environmental setting in the mound provinces. Detailed analyses of the grain-size distribution of the <160 μm fraction, which is already highly susceptible to bottom current strengths of >20 cm s⁻¹, in the off-mound core revealed much finer sediments under glacial conditions compared to the prevailing interglacial (Fig. A10), implying that the bottom currents in the mound provinces were much weaker, i.e. slower, ~ 20 kyr ago than today.

Enhanced deposition of fine-grained terrigenous material (associated with some IRD) as well as reduced bottom current activity result in a rather unfavourable setting for the corals (Freiwald, 2002).

In addition, due to the replacement of the MOW and the ENAW by a homogenous water mass termed Glacial North Atlantic Intermediate Water (GNAIW) (Manighetti and McCave, 1995) the pycnocline supporting the food supply for the corals was absent. Thus, these oceanographic changes had a profound impact on the living conditions for the cold water corals and on the sedimentary setting on the carbonate mounds. Actually, up to now for no coral fragment from the Celtic margin an LGM age has been obtained, indicating that under fully glacial conditions no corals lived in this region. Thus, there also have been no coral fragments to stabilise the fine-grained sediments deposited under such conditions (Fig. A11).

In the course of deglaciation, in turn with the rising sea-level, the MOW regains its present characteristics and begins to sweep the mound provinces in the Porcupine Seabight. Especially on the carbonate mounds, where the currents are focused as indicated by numerous moats around the mounds (Van Rooij et al., 2003, De Mol et al., 2002), the unstabilised fine-grained sediments deposited under glacial conditions were easily winnowed (Fig. A11). Depending on the current strength only parts of the sediments can be winnowed with especially the coarsest material being accumulated as a lag sediment. At Propeller Mound these lag sediments, characterised by high amounts of coarse fragments (Fig. A10), indicate the position of the hiatuses attributed to the re-establishment of the regional MOW circulation. Actually, also the off-mound sediments

seem to have experienced some winnowing during the last deglaciation, as indicated by a hiatus in our off-mound core at the respective core depth (Fig. A10).

Moreover, outcropping hardgrounds at the flanks of Propeller and other mounds observed during dives of remotely operated vehicles (ROVs) provide clear evidence for flank erosion. It is assumed that this flank erosion can result in slope failure and subsequent mass wasting (Fig. A11), which is indicated by (a) the high spatial variability of the mound sediments hampering any correlation among the on-mound cores, (b) the rather old ages at the top of the two flank on-mound cores GeoB 6728-1 and 6729-1, and (c) the rare occurrence of dropstones on the mounds compared to the dropstone pavement found at their base (A.F., unpubl. data).

After the removal of glacial sediments from the mounds down to a level where corals again stabilised the sediments, the continuous presence of a strong interglacial MOW hampered the deposition of fine interglacial sediments at most parts of the mound, while coral growth was supported (Fig. A11). Baffling of some fine material among the corals may have taken place under such conditions, but continuous deposition of fine material was mostly restricted to interstadials, as indicated by the $\delta^{18}\text{O}$ data. Thus, the best conditions for real mound growth probably existed during interstadials, when the interplay between bottom current strength, availability of coral framework and probably some coral growth and hemipelagic sedimentation produced those sediment sequences still preserved at Propeller Mound.

Through the last 300.000 years the netto sedimentation on Propeller Mound is by far lower compared to the surrounding off-

mound sediments. Thus, at least over this time span the mound is shrinking relative to the seafloor around it and if this development continues into the future, Propeller

Mound will get buried and follow the fate of the already buried near-by Magellan Mounds.

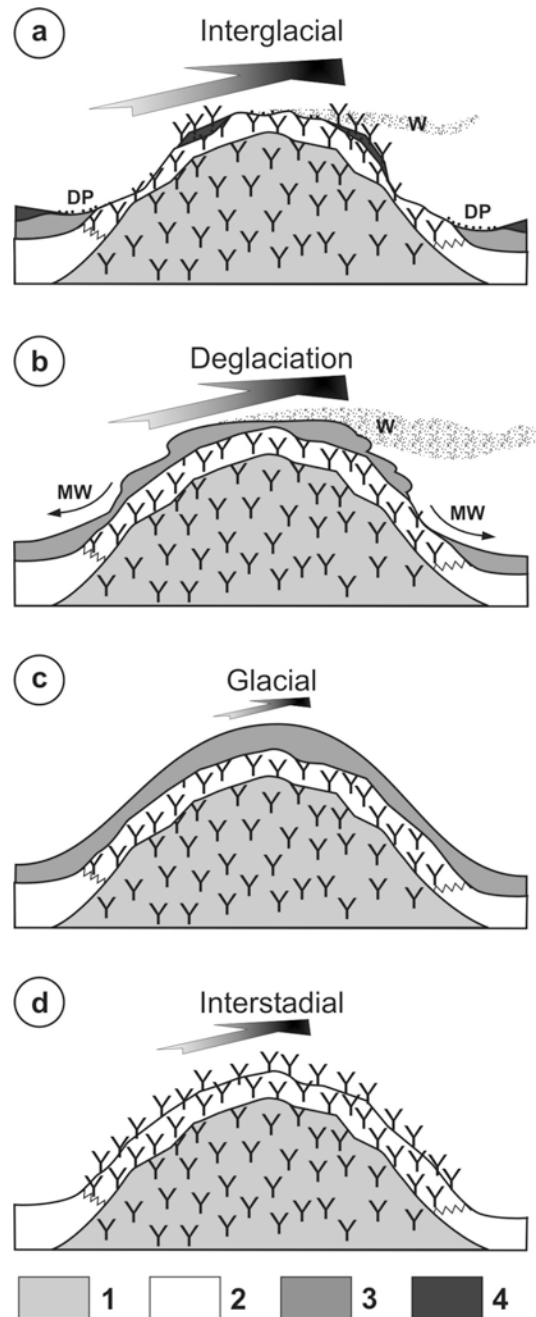


Figure A11. Model for the Late Quaternary development of Propeller Mound and probably other deep-water carbonate mounds in the NE-Atlantic. The four stages (a-d) describe the temporal sequence of different settings mainly forced by the presence/absence of the Mediterranean Outflow Water and the resulting variations in bottom current strengths, indicated by the arrow size. Y – corals, W – winnowing, MW – mass wasting, DP – drop stone pavements in the moats, 1 – carbonate mound at begin of the sequence, 2 – interstadial sediments, 3 – glacial sediments, 4 – interglacial sediments.

In addition, these results also shed some light on the long-term development of the deep-sea carbonate mounds. A recent model (Henriet et al. 2002) for the development of such carbonate mounds differentiates between (a) a trigger stage, during which a solid substratum for the initial settling of coral larvae is formed, (b) a booster stage, representing a period of fast mound growth as indicated by on-lapping sediment layers in the surrounding drift sediments (Van Rooij et al. 2002), (c) a coral bank stage reflecting a mature carbonate mound and (d) a burial stage, when mound growth cannot keep pace with hemipelagic sedimentation around the mound. The pure size of the carbonate mounds testifies a phase of rapid

growth (i.e. the booster stage), while the results obtained from Propeller Mound indicate this mound to be a prime example for a carbonate mound at the turn from the coral bank stage to the burial stage, thereby providing support for the mound development model described above.

Finally, our data clearly show the dominance of environmental forcing in shaping the carbonate mounds – at least for their youngest history in the Late Quaternary. However, as long as the base of carbonate mounds has not been sampled, what can only be done by drilling, the question if hydrocarbon seeping is involved in the initial formation of these mounds has to remain unanswered.

References

- Akhmetzhanov A. M., Kenyon N. H., Nielsen T., Habgood E., Ivanov M. K., Henriet J.-P., and Shashkin P. (2001) Deep-sea bottom current depositional systems with active sand transport on the North-Eastern Atlantic Margin. In *Geological Processes on Deep-Water European Margins. International Conference and 10th Anniversary Training Through Research Post-Cruise Meeting, 28 January - 3 February 2001, Moscow/Mozhenka, Russia* (ed. G. Akhmetzhanov and A. Y. Suzyumov). UNESCO.
- Beyer A., Schenke H. W., Klenke M., and Niederjasser F. (2003) High resolution bathymetry of the eastern slope of the Porcupine Seabight. *Marine Geology* **198**, 27-54.
- Coles G. P., Ainsworth N. R., Whatley R. C., and Jones R. W. (1996) Foraminifera and ostracoda from Quaternary carbonate mounds associated with gas seepage in the Porcupine Basin, offshore western Ireland. *Revista Espanola de Micropaleontologia* **28**(2), 113-151.
- De Mol B., Van Rensbergen P., Pillen S., Van Herreweghe K., Van Rooij D., McDonnell A., Huvenne V., Ivanov M., Swennen R., and Henriet J. P. (2002) Large deep-water coral banks in the Porcupine Basin, southwest of Ireland. *Marine Geology* **188**, 193-231.
- Freiwald A. (2002) Reef-Forming Cold-Water Corals. In *Ocean Margin Systems* (ed. G. Wefer, D. Billett, D. Hebbeln, B. B. Jørgensen, M. Schlüter, and T. v. Weering), pp. 365-385. Springer Verlag.
- Hebbeln D., Marchant M., Wefer G. (2002) Paleoproductivity in the southern Peru-Chile Current through the last 33 000 yr. *Marine Geology* **186**, 487-504.
- Henriet J. P., De Mol B., Pillen S., Vanneeste M., Van Rooij D., Versteeg W., Croker P. F., Shannon P. M., Unnithan V., Bouriak S., and Chachkine P. (1998) Gas hydrate crystals may help build reefs. *Nature* **391**, 648-649.
- Henriet J. P., Guidard S., and Team O. P. (2002) Carbonate Mounds as a Possible Example for Microbial Activity in Geological Processes. In *Ocean Margin Systems* (ed. G. Wefer, D. Billett, D. Hebbeln, B. B. Jørgensen, M. Schlüter,

- and T. v. Weering), pp. 437-455. Springer Verlag.
- Hovland M., Croker P. F., and Martin M. (1994) Fault-associated seabed mounds (carbonate knolls?) off western Ireland and north-west Australia. *Marine and Petroleum Geology* **11**(2), 232-246.
- Huvenne V., De Mol B., and Henriët J.-P. (2003) A 3D seismic study of the morphology and spatial distribution of buried coral banks in the Porcupine Basin, SW of Ireland. *Marine Geology* **198**, 5-25.
- Kenyon N. H., Ivanov M. K., and Akhmetzhanov A. M. (1998) *Cold water carbonate mounds and sediment transport on the NE Atlantic Margin*. UNESCO.
- Kenyon N. H., Akhmetzhanov A. M., Wheeler A. J., van Weering T. C. E., de Haas H., and Ivanov M. K. (2003) Giant carbonate mud mounds in the southern Rockall Trough. *Marine Geology* **195**, 5-30.
- Manighetti B. and McCave I. N. (1995) Late glacial and Holocene palaeocurrents around Rockall Bank, NE Atlantic Ocean. *Paleoceanography* **10**(3), 611-626.
- Schönfeld J. and Zahn R. (2000) Late Glacial to Holocene history of the Mediterranean Outflow. Evidence from benthic foraminiferal assemblages and stable isotopes at the Portuguese margin. *Palaeogeography, Palaeoclimatology, Palaeoecology* **159**, 85-111.
- Van den Bergh G. D., Boer W., de Haas H., van Weering T. C. E., and van Wijk R. (2003) Shallow marine tsunami deposits in Teluk Bantan (NW Java, Indonesia), generated by the 1883 Krakatoa eruption. *Marine Geology* **197**, 13-34.
- Van Rooij D., De Mol B., Huvenne V., Ivanov M., and Henriët J.-P. (2003) Seismic evidence of current-controlled sedimentation in the Belgica mound province, upper Porcupine slope, southwest of Ireland. *Marine Geology* **195**, 31-53.
- van Weering T. C. E., de Haas H., de Stigter H. C., Lykke-Anderson H., and Kouvaev I. (2003) Structure and development of giant carbonate mounds at the SW and SE Rockall Trough margins, NE Atlantic Ocean. *Marine Geology* **198**, 67-81.
- White M. (subm.) The hydrography of the Porcupine Bank and Sea Bight and associated carbonate mounds. In *Modern Carbonate Mound System: A Window to Earth History* (ed. J.-P. Henriët and W.-C. Dullo). Springer Verlag.

VITA AND PUBLICATION LIST

Dipl.-Geol. Andres Rüggeberg
GEOMAR
Research Center for Marine Geosciences
Wischhofstr. 1-3
24148 Kiel, Germany
Tel.: +49 431 600 2843
Fax.: +49 431 600 2941
E-Mail: arueggeberg@geomar.de



Academic Education

2000 – present

Current doctoral within ECOMOUND Project: Reconstruction of environmental processes controlling the build up of carbonate mounds along the European continental margin and their sedimentary settings

1997 - 2000

Diploma (MSc) in Geology and Palaeontology with main courses in Marine Geology and Oceanography at Christian-Albrechts-Universität zu Kiel.

Diploma theses:

Late Quaternary Paleooceanography in the South Tasman Region: Implications of Benthic Foraminifers and Grain Size Analysis.

Field work: Geologische Kartierung des Gebietes E' von Genicera, Provinz Castilla y León (NW Spanien).

1994 – 1997

BSc at Geologisch-Paläontologisches Institut der Technische Hochschule Darmstadt (today: Technische Universität Darmstadt)

Research Interests

Deep-water corals, carbonate mounds, benthic foraminifera, grain-size analysis, paleoclimatology, paleooceanography with special focus of past interglacial-glacial cycles in the NE Atlantic sector.

Cruises

2002

FS POSEIDON POS292 “ECOMOUND / ACES”, Reykjavik (Iceland) – Galway (Ireland); 15.07.2002 - 04.08.2002

2001

RV JAN MAYEN “ECOMOUND”, Tromsø - Tromsø (Norway); 21.11. - 30.11.2001

2000

FS POSEIDON POS265 “ECOMOUND / ACES”, Thórshavn (Faeroe) – Galway (Ireland) - Kiel; 13.09. - 01.10.2000

1998

FS SONNE SO136 “TASQWA”, Wellington (New Zealand) – Hobart (Tasmania); 16.10. - 12.11.1998

Publications and conference contributions

- Roth, S., and Rüggeberg, A.(Eds.) (2001) 2001 MARGINS Meeting. Schriftenreihe, Nr. 14, S. 251. Deutsche Geologische Gesellschaft, Hannover.
- Rüggeberg, A. (2000) Late Quaternary Paleoceanography in the South Tasman Region: Implications of Benthic Foraminifers and Grain Size Analysis. Unpubl. Diploma thesis, Christian-Albrechts-Universität, Kiel.
- Rüggeberg, A. (2000) Geologische Kartierung des Gebietes E' von Genicera, Provinz Castilla y Leon (NW-Spanien). Unpubl. Diploma thesis, Christian-Albrechts-Universität, Kiel.

Poster presentations

- A. Rüggeberg, C. Dullo, B. Dorschel, D. Hebbeln (2003) Ecological signals in mounds: an example from Propeller Mound. Ocean Margin Research Conference, September 15-17, 2003, Paris, France.
- A. Rüggeberg, B. Dorschel, C. Dullo, D. Hebbeln, A. Freiwald (2003) Benthic foraminiferal assemblages help to understand carbonate mound evolution. In: Geophysical Research Abstracts, Vol. 5, EGS-AGU-EUG Joint Assembly, Nice, France.
- B. Dorschel, D. Hebbeln, A. Rüggeberg, C. Dullo (2003) A cold-water coral carbonate mound on the decline: Propeller Mound, northern Porcupine Seabight. In: Geophysical Research Abstracts, Vol. 5, EGS-AGU-EUG Joint Assembly, Nice, France.
- Rüggeberg, A., Dorschel, B.& W.-C. Dullo (2002) Using benthic foraminiferal assemblages and grain size analysis for paleoceanographic reconstructions from a cool-water carbonate mound in the Porcupine Seabight. In: GEO 2002, Vol. 21 (Ed. by B. Nierbuhr). Schriftenreihe der Deutschen Geologischen Gesellschaft.
- Rüggeberg, A., Dorschel, B., Dullo, W.-Chr. (2002) Reconstruction of the paleoenvironment of a carbonate mound in the Porcupine Seabight, west off Ireland. EGS XXVII General Assembly, Nice, France.
- Dorschel, B., Rüggeberg, A., Hebbeln, D., Dullo, C., Freiwald, A. (2002) Temporal evolution of a carbonate mound in the NE Atlantic. EGS XXVII General Assembly, Nice, France.
- Rüggeberg, A., Dorschel, B., Dullo, W.-Chr., Freiwald, A. (2001) "On-" and "off-mound" sediment cores from Propeller Mound, Porcupine Seabight. In: 2001 Margins Meeting, Vol. 14 (Ed. by Sven Roth and Andres Rüggeberg). Schriftenreihe der Deutschen Geologischen Gesellschaft, Kiel, Germany.
- Dorschel, B., Rüggeberg, A., Hebbeln, D., Freiwald, A., Dullo, W.-Chr. (2001) Developing the carbonate budget of a carbonate mound in the NE Atlantic. In: 2001 Margins Meeting, Vol. 14 (Ed. by Sven Roth and Andres Rüggeberg). Schriftenreihe der Deutschen Geologischen Gesellschaft, Kiel, Germany.
- Rüggeberg, A., Dorschel, B., Hebbeln, D., Dullo, W.-Chr., Freiwald, A. (2001) X-ray Computer Tomographic Analysis of Sediment Cores from Propeller Mound (Porcupine Seabight). In: EUG XI, Strasbourg (France), Journal of Conference Abstracts 6, Cambridge Publications.
- Dorschel, B., Rüggeberg, A., Hebbeln, D., Freiwald, A, Dullo, W.-Chr. (2001) Sediment Distribution on a Carbonate Mound in the Porcupine Seabight. In: EUG XI, Strasbourg (France), Journal of Conference Abstracts 6, Cambridge Publications.
- Roth, S., Rüggeberg, A., Überall, S., Nees, S., Reijmer, J. J. G. (1999) Sedimentologische und Karbonatmineralogische Untersuchungen an zwei Kernen in der südlichen Tasman See (SW-Pazifik). In: Terra Nostra, Vol. 99. Alfred-Wegener-Stiftung, Bremen, Germany.
- Rüggeberg, A., Überall, S., Roth, S. (1999) Hochauflösende Untersuchungen an spätquartären benthischen Foraminiferengemeinschaften des Südpolarmeeres (australisch-neusee-

ländischer Sektor) - Ein Beitrag zu Klimarekonstruktion in einem ozeanischen Schlüsselgebiet. In: Terra Nostra, Vol. 99. Alfred-Wegener-Stiftung, Bremen, Germany.

Oral presentations

- Rüggeberg, A., Dorschel, B., Dullo, W.-Chr., Hebbeln, D., Liebetrau, V. (2003) Benthic foraminiferal assemblages and grain-size analysis help to reconstruct the history of a cold-water carbonate mound. GEO2003, Gemeinschaftstagung der Deutschen Mineralogischen Gesellschaft zusammen mit der Geologischen Vereinigung und der Deutschen Geophysikalischen Gesellschaft, 22.-25. September 2003, Bochum, Germany.
- Rüggeberg, A., Dorschel, B., Dullo, W.-Chr., Hebbeln, D. (2003) Environmental control on Propeller Mound (Hovland Mound province) during the past interglacial-glacial cycles. 2nd International Symposium on Deep Sea Corals, Sept. 9 – 12, 2003, Erlangen, Germany.
- Rüggeberg, A., Dorschel, B., Dullo, W.-Chr. (2002) Paläozeanographie eines Kaltwasser-Karbonat-Hügels westlich von Irland. In: Sediment 2002, Vol. 17 (Ed. by H. Hüssner, M. Hinderer, A. E. Götz and R. Petschick). Schriftenreihe der Deutschen Geologischen Gesellschaft, Frankfurt a. M. - Darmstadt, Germany.

ERKLÄRUNG

Hiermit erkläre ich, daß ich erstmalig an einem Promotionsverfahren teilnehme. Ausserdem versichere ich, daß die vorliegende Dissertation nach Inhalt und Form, abgesehen von den von mir angegebenen Quellen und Hilfsmitteln, sowie der Beratung durch meine akademischen Lehrer, meine eigene Arbeit ist.

Kiel, im September 2003

.....

